SUBDIVISIONS AND CONNECTIONS OF AUDITORY CORTEX IN MARMOSET

MONKEYS

By

Lisa Anne de la Mothe

Dissertation

Submitted to the Faculty of the

Graduate School of Vanderbilt University

in partial fulfillment of the requirements

for the degree of

DOCTOR OF PHILOSOPHY

in

Psychology

December, 2008

Nashville, Tennessee

Approved:

Jon Kaas

Troy Hackett

Jo-Anne Bachorowski

Ford Ebner

To my husband, Dave,

for his unwavering love and support.

ACKNOWLEDGEMENTS

I would first like to thank Troy Hackett, who has been a wonderful mentor and has been instrumental throughout every phase of my graduate work. Regardless of the various aspects of my training Troy has always been supportive and encouraging. I am extremely grateful for the foundation that he has provided me, the many conversations that have inspired me and the investment that he has made in me. I know I will be a better scientist because of his guidance.

I am also grateful to Jon Kaas, who is responsible for bringing me here to Vanderbilt and has generously allowed me to work with Troy in the auditory system. In addition to bringing me into his lab in the psychology department, Jon has served as the chair of my committee and has been continually supportive of my decisions as a graduate student. I am also grateful to Jo-Anne Bachorowski and Ford Ebner, the additional members of my committee, who have provided insightful comments and criticisms that improved the quality of this dissertation.

I would like to thank the members of the auditory group who have been unbelievably generous with their time and support throughout my graduate studies. Suzanne Blumell who shared an office with me for a number of years, was my guide when I started in the lab, and who assisted with surgeries and histology; Yoshi Kajikawa who also assisted on the surgeries and was responsible for the physiology side of the experiments; Bill D'Angelo and Susanne Sterbing-D'Angelo who were constant sources of insight into the auditory system and were extremely willing to share their knowledge with me; and Corrie Camalier who has shared many hours of productive and challenging

conversations in the office over the final stages of this dissertation, and who's supportive and thoughtful comments have made the work and this journey that much better. Thank you all for the many ways in which you have helped me reach this point, the laughter, the memories and your friendship.

I would also like to thank the members of the Kaas Laboratory both past and present (Mary Baldwin, Charnese Bowes, Mark Burish, Christina Cerkevich, Christine Collins, Reuben Fan, Peichun Fang, Omar Gharbawie, Peter Kaskan, Hui-Xin Qi, Mike Remple, Iwona Stepniewska, Toru Takahata, Peiyan Wong, Laura Trice, and Mary Varghese) who have all in their own way supported me through this journey as well as Mary Feurtado for technical assistance with experiments. I would especially like to thank Jamie Reed from the Kaas lab, who also shared an office space with me for a number of years, and has continued to provide helpful comments, shown patience with my endless revisions and been a supportive friend.

I am deeply indebted to my undergraduate advisor, Jeremy Tuner, who is initially responsible for fostering my interest in auditory research and encouraging me to pursue this path of graduate school.

Most importantly I need to thank my family for their unwavering support. My parents, who have always had faith in me and worked extremely hard to provide and support the various opportunities that have been presented to me. My siblings, Laura, Linda, and Mike, who from our childhood to today have loved and supported me in all of my endeavors and have been great sources of strength throughout this journey. The family I had the great fortune of marrying into (Elaine, Ronnie, and Cheryl), and most importantly Dave, my husband, who more than anyone has traveled this journey with me.

iv

I am so grateful for all of the sacrifices he has made, the love and support he has shown and the stability he has provided through all of this.

TABLE OF CONTENTS

LIST OF TABLES

LIST OF FIGURES

LIST OF ABBREVIATIONS

A1   Auditory area 1 (core)
A11   Secondary auditory cortex
A1L   Auditory area 1, lateral division
A1M   Auditory area 1, medial division
AAF   Anterior auditory field
AChE   Acetylcholinesterase
AD   Medial geniculate complex, anterodorsal division
AL   Anterolateral area (belt)
A-m   Anteromedial auditory field
AS   Arcuate sulcus
BA   Basal Amygdala
BDA   Biotinylated dextran amine (tracer)
BIC   Brachium of the inferior colliculus
BrSC   Brachium of the superior colliculus
Caud   Caudate nucleus
CG   Central Grey
CIC   Commissure of the inferior colliculus
Cis   Circular sulcus
CL   Caudolateral area (belt)
Cla   Claustrum
CM   Caudomedial area (belt)
CMd   Centromedian
CO   Cytochrome oxidase
CPB   Caudal parabelt area (parabelt)
CS   Central sulcus
CTB   Cholera toxin, subunit B (tracer)
dc   Dorsal cortex of the inferior colliculus
dm   Dorsomedial portion of the inferior colliculus
Ent   Entorhinal cortex
FB   Fast Blue (tracer)
FE   Fluoroemerald (tracer)
FR   Fluororuby (tracer)
Hb   Habenular nucleus
IC   Inferior Colliculus
ICc   Central nucleus of the inferior colliculus
Ins   Insula
IPS   Intraparietal sulcus
ITG   Inferior temporal gyrs
LA   Lateral amygdala
LGN   Lateral geniculate nucleus
Lim   Limitans nucleus
ln   Lateral nucleus of the inferior colliculus

LS   Lateral sulcus
LuS   Lunate sulcus
M   Medial geniculate complex, magnocellular division
MD   Medial dorsal nucleus
MF   Myelinated fibers
MGad   Medial geniculate complex, anterodorsal division
MGC   Medial geniculate complex
MGd   Medial geniculate complex, dorsal division
MGm   Medial geniculate complex, magnocellular division
MGpd   Medial geniculate complex, posterodorsal division
MGv   Medial geniculate complex, ventral division
ML   Middle lateral area (belt)
MT   Middle temporal area
PA   Anterior (oral) pulvinar
Pa   Posterior auditory area
paAc   Caudal parakoniocortex area
PAF   Posterior auditory field
PD   Medial geniculate complex, posterodorsal division
PI   Inferior pulvinar
PIc   Inferior pulvinar, central division
PIm   Inferior pulvinar, medial division
PIp   Inferior pulvinar, posterior division
PL   Lateral pulvinar
PM   Medial pulvinar
P-m   Posteromedial auditory field
Po   Posterior nucleus
PPN   Peripeduncular nucleus
Pro   Proisocortical area
proA   Prokoniocortex area
PS   Pricipal sulcus
Put   Putamen
PV   Parietoventral area
R   Rostral area (core)
Ri   Retroinsular area
RM   Rostromedial area (belt)
RPB   Rostral parabelt area (parabelt)
RT   Rostrotemporal area (core)
RTL   Rostrotemporal lateral area (belt)
RTM   Rostrotemporal medial area (belt)
S2   Somatosensory area 2
SC   Superior Colliculus
Sg   Suprageniculate nucleus
SN   Sustantia Nigra
STG   Supeior temporal gyrus
STS   Superior temporal sulcus
T   Thalamus

Tpt   Temporal parietotemporal area
VPAF Ventroposterior auditory field
ZI   Zonus intermedius

CHAPTER I

INTRODUCTION

Within the last number of years there has been an increase in both the number of

studies conducted and the amount of information discovered about the auditory cortex of

primates. By incorporating the results from these studies in various primate species, a

working model of auditory cortex has emerged that includes a primary core region,

surrounded by a secondary belt region, with a third level of processing, the parabelt,

located lateral to the belt (Hackett, 2002; Hackett and Kaas, 2002; Kaas et al., 1999; Kaas

and Hackett, 2000) (Fig. 1). Despite the comprehensive appearance of the model, the

model itself is incomplete, in that not all of the proposed features have been tested. The

medial belt in particular has been the least studied area of auditory cortex, due in part to

its deep location within the lateral sulcus that makes access difficult. While recent

neurophysiological studies suggest that the medial belt areas may have unique functional

roles, such as multisensory properties (Foxe et al., 2002; Fu et al. 2003; Kayser et al.,

2005; Robinson and Burton, 1980a,b; Schroeder and Foxe, 2002; Schroeder et al. 2001,

2003), little is known about the anatomical connectional patterns. Connectional data that

is available on these medial belt areas has been identified indirectly, through

neuroanatomical injections into other areas of auditory cortex. The examination of tracer

injections into the medial belt and throughout auditory cortex will provide the

opportunity to refine and extend the working model, allowing direct descriptions of the

connections of the medial belt region.
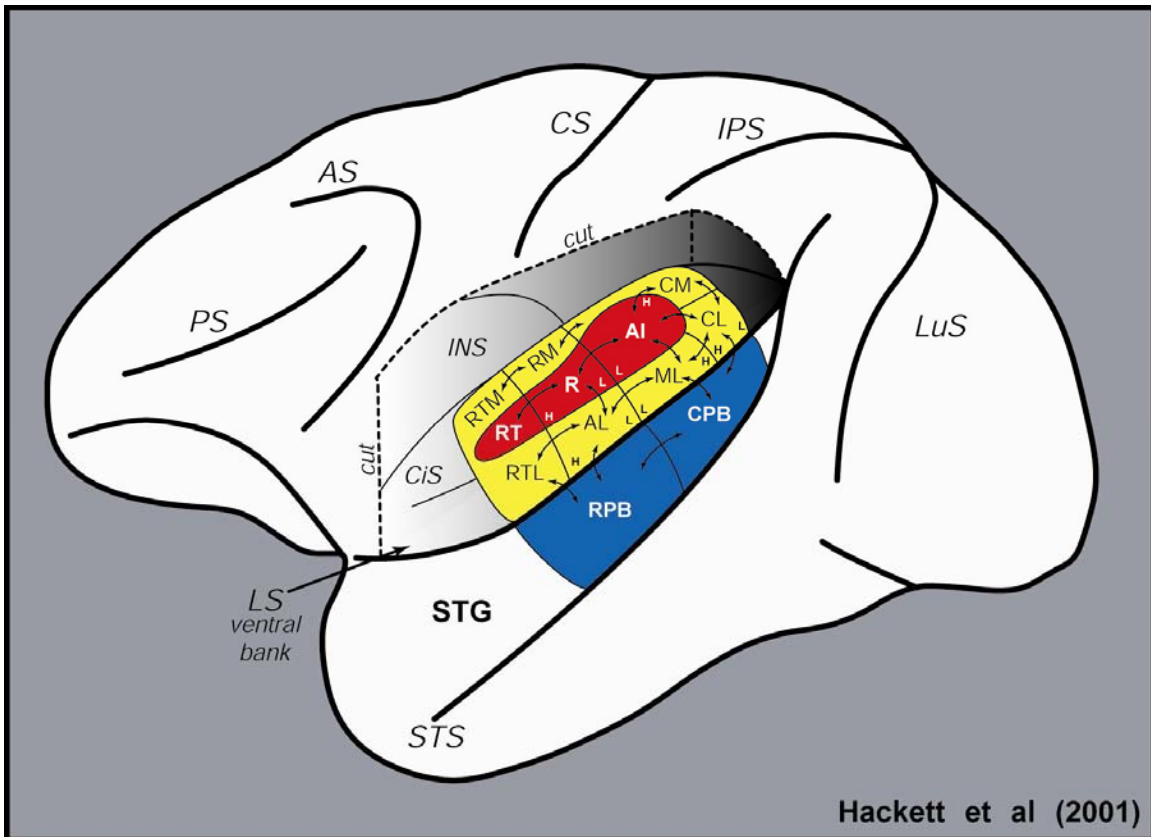
Figure 1. Current working model of primate auditory cortex as illustrated by Hackett et al. 2001. Red shading identifies core areas, yellow shading belt areas, blue shading parabelt areas. Some tonotopic and connectional relations are shown.

As mentioned, the model has been pieced together based on previous research in various species. While this has proven useful in the construction of the model itself, the model remains to be validated in any one species. Although much of the development of the current model has come from data in the macaque monkey, attention has also turned to the use of the marmoset monkey in recent physiological experiments, due in part to the fact that it is a highly vocal animal (Bendor and Wang, 2005; Kajikawa and Hackett, 2005; Kajikawa et al., 2005, Lu and Wang, 2004; Philbert et al., 2005; Wang et al. 1995). In addition, access to the auditory cortex of the marmoset makes it an appealing species for study as it has a large portion of auditory cortex exposed on the gyral surface and a

shallow lateral sulcus. Determining the congruency between the marmoset monkey and the general primate model would provide a basis for utilizing this species for future studies. Work by Hackett et al. (2001) demonstrated that similar architectonic characteristics exist in the auditory areas of macaques, chimpanzees and humans. Even though the primate model relies heavily on the findings from non-human primates the possibility remains that these findings may be applicable to humans. The purpose of this thesis is to examine in detail the architecture and connections of the auditory cortex in the marmoset monkey with emphasis on the medial belt, to compare those findings to the current working model, and to provide a framework for future studies of the auditory cortex in this species.

<div align="center">Organization of the Primate Auditory Cortex</div>

What is auditory cortex? One of the defining characteristics of auditory cortex is that it receives its main input from the medial geniculate complex (MGC) of the thalamus. While additional areas may demonstrate auditory properties (i.e. responses to auditory stimuli) areas that do not receive this significant input from the MGC are identified as auditory-related cortex. The current working model divides auditory cortex into three regions of processing (core, belt and parabelt), all of which are preferential targets of the medial geniculate complex (MGC) (Fig. 1). The core, comprised of three subdivisions (A1, R, and RT) is the first level of cortical processing and receives input from the ventral division of the medial geniculate complex (MGv). The core region is surrounded by a secondary level of processing, the belt, which flanks both the medial and lateral sides. The belt, which is sometimes distinguished as medial and lateral regions, is

subdivided into 7-8 areas (Lateral: CL, ML, AL and RTL; Medial: CM, MM?, RM, RTM). The third level of processing is the parabelt, located lateral to the lateral belt and is divided into caudal and rostral areas (CPB, RPB). Both the belt and parabelt receive input from the dorsal division of the medial geniculate (MGd).

Auditory Pathways

Most of what is known about the subcortical structures of the mammalian auditory system comes from species other than primates (specifically cat, bat and rodents) as studies in primates are scarce. While there is an overall lack of primate data, based on the consistency of the available data with previous studies in other species, it has become common to generalize these findings to all mammals. In the auditory pathway there are a number of connections, both major and minor, between the subcortical nuclei. The main inputs and projections are described below and illustrated in figure 2.

When sound enters the ear it passes through the cochlea and the eighth cranial nerve (CN VIII, also known as the vestibulocochlear nerve) before ascending through five subcortical nuclei, the first being the cochlear nucleus which is divided into ventral and dorsal divisions (VCN, DCN) (Cant, 1992). After this point in the pathway information that enters each ear is crossed so that input from both ears is available to both sides of the brain. The VCN, which can be further subdivided into anteroventral (AVCN) and posteroventral (PVCN), projects to both the contralateral and ipsilateral Superior Olivary Complex (SOC) (Schwartz, 1992). The SOC, which has three subdivisions: lateral (LSO), medial (MSO), and medial nucleus of the trapezoid body (MNTB),

4

Figure 2. The major ascending auditory pathways from the cochlea (C) to auditory cortex (AC). Major pathways and projections are indicated by thick lines. Divisions of subcortical nuclei and minor pathways are not shown. Adapted from Hackett and Kaas, 2003.

CORPUS CALLOSUM

AC

AC

MGC

MGC

COMMISSURE OF
INFERIOR COLLICULUS

IC

IC

COMMISSURE
OF PROBST

NLL

NLL

SOC

SOC

CN

CN

C

C
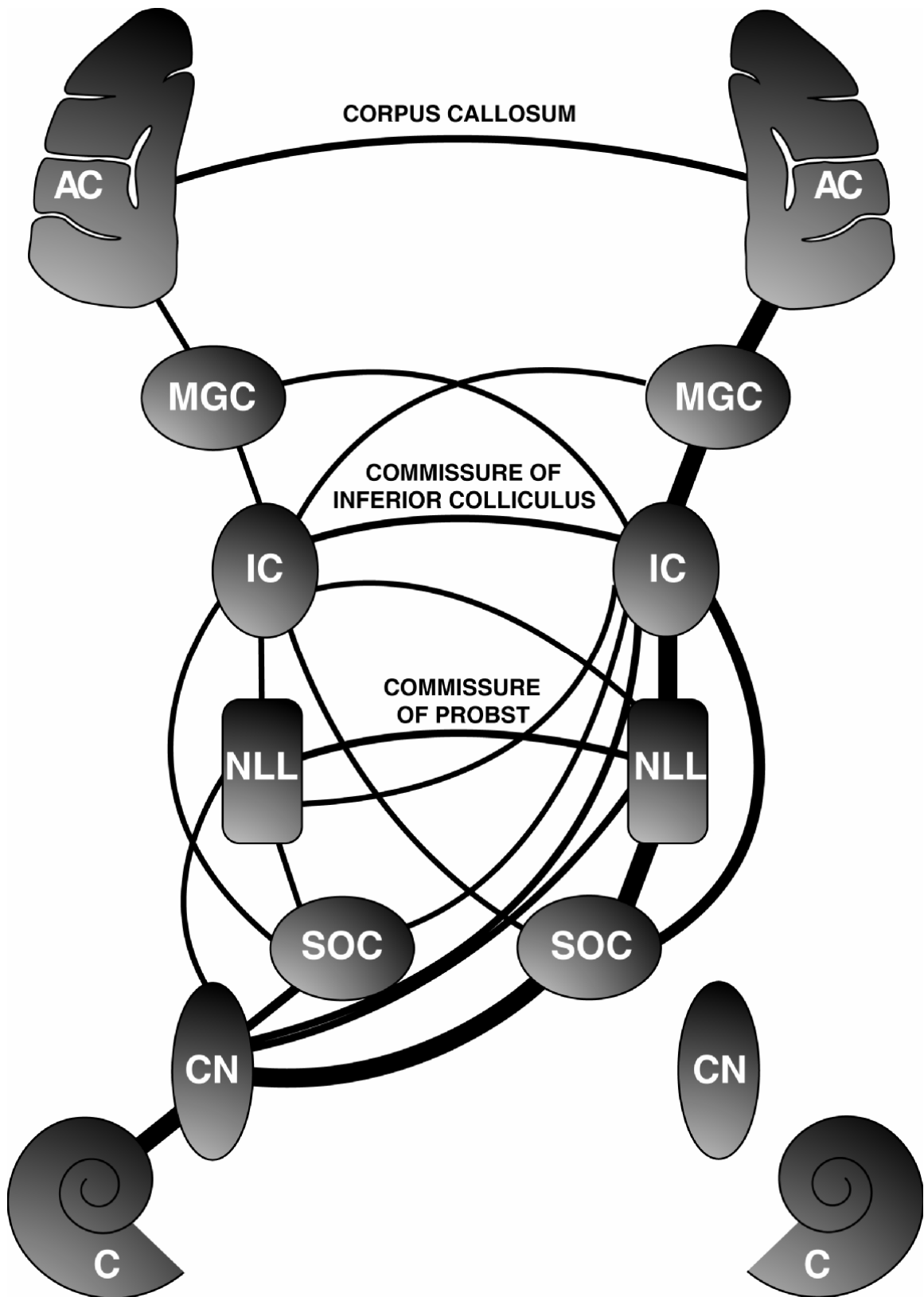
receives its main input from the contralateral AVCN (Schwartz, 1992). The lateral

lemniscus (LL) is the principal fiber tract between the SOC and the inferior colliculus

(IC) and has two subnuclei: ventral nucleus of the LL (VNLL) and dorsal nucleus of the

LL (DNLL). The nuclei of LL receives inputs mainly from the LSO and MSO (Henkel

& Spangler, 1983) and both nuclei of the LL project to the ipsilateral IC (Brunso-

Bechtold et al., 1981; Coleman & Clerici, 1987; Covey & Casseday, 1986; Kudo, 1981)

with a contralateral IC projection coming from DNLL (Brunso-Bechtold et al., 1981;

Coleman & Clerici, 1987; Covey & Casseday, 1986; Glendenning & Masterton, 1983;

Kudo, 1981; Merchan et al., 1994). In addition to projecting to nuclei of the LL, the SOC

also has a major projection to the ipsilateral IC (Brunso-Bechtold et al., 1981; Covey &

Casseday, 1986; Glendenning & Masterton, 1983; Henkel & Brunso-Bechtold, 1993).

The IC is commonly divided into three nuclei: central (ICc), external (ICx), and

pericentral (ICp) or dorsal cortex (ICdc) and serves as the principal source of input to the

MGC, projecting to both the ipsilateral and contralateral MGC. The MGC is an

obligatory and final stage of subcortical processing and is comprised of ventral (MGV),

dorsal (MGd: anterodorsal (MGad) and posterodorsal (MGpd)), and medial or

magnocellular (MGm) subdivisions (Burton and Jones, 1976; Fitzpatrick and Imig,

1978). The MGv receives its main input from the ipsilateral ICc (Anderson et al., 1980;

Calford & Aitkin, 1983; Kudo & Niimi, 1980) and projects to primary auditory cortex,

the core region ((Burton and Jones, 1976; Fitzpatrick and Imig, 1978; Luethke et al.,

1989; Morel and Kaas, 1992; Morel et al., 1993; Pandya et al., 1994; Molinari et al.,

1995). The dorsal division receives input mainly from the ICp (Andersen et al., 1980;

Calford & Aitkin, 1983; Kudo & Niimi, 1980) and projects to non-primary areas of

auditory cortex, the belt and parabelt regions (Burton and Jones, 1976; Hackett et al., 1998b, 2007a; Molinari et al., 1995; Morel and Kaas, 1992; Pandya et al., 1994). The inputs to MGm are less known but may include a principal input from ICx (Calford & Aitkin, 1983; Kudo & Niimi, 1980), and this division projects to all areas of auditory cortex (Burton and Jones, 1976; Hashikawa et al., 1995).

Tonotopic, non-tonotopic, and multisensory pathways

As stated above, a defining characteristic of auditory cortex is that it receives preferential input from the medial geniculate complex. In accordance with that definition three separate pathways have been identified in the auditory system, each passing through one of the major subdivisions of the MGC (Fig. 3). The first, the tonotopic pathway, is so named because the frequency representation from the cochlea is maintained throughout this pathway (Andersen et al., 1980; Calford and Aitkin, 1983; Rouillier et al., 1989). The MGv receives input from the ICc and projects onto the core (primary) areas of auditory cortex, each of which has a tonotopic representation (Andersen et al., 1980; Calford and Aitkin, 1983). These frequency representations are reversed at the borders such that A1 and R share a low frequency border (Aitkin et al. 1986; Bendor and Wang, 2005; 2008; Imig et al. 1977; Kajikawa et al. 2005; Kosaki et al. 1997; Merzenich and Brugge, 1973; Morel and Kaas, 1992; Morel et al. 1993; Petkov et al., 2006; Philibert et al., 2005; Rauschecker et al. 1995; 1997; Recanzone et al. 2000a) and R and RT share a common high frequency border (Bendor and Wang, 2005; 2008; Petkov et al., 2006). This pathway is also referred to as the lemniscal or primary pathway since it involves the primary areas of auditory cortex.

Figure 3. Schematic of three pathway model for primate auditory processing based on the model widely adopted in the cat.

Tonotopic Pathway

Non-tonotopic Pathway

Multisensory Pathway

10
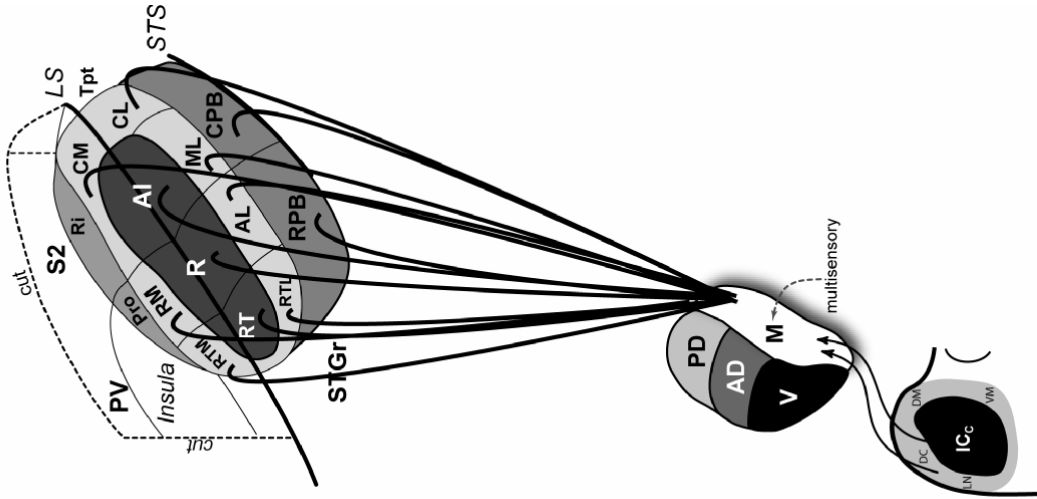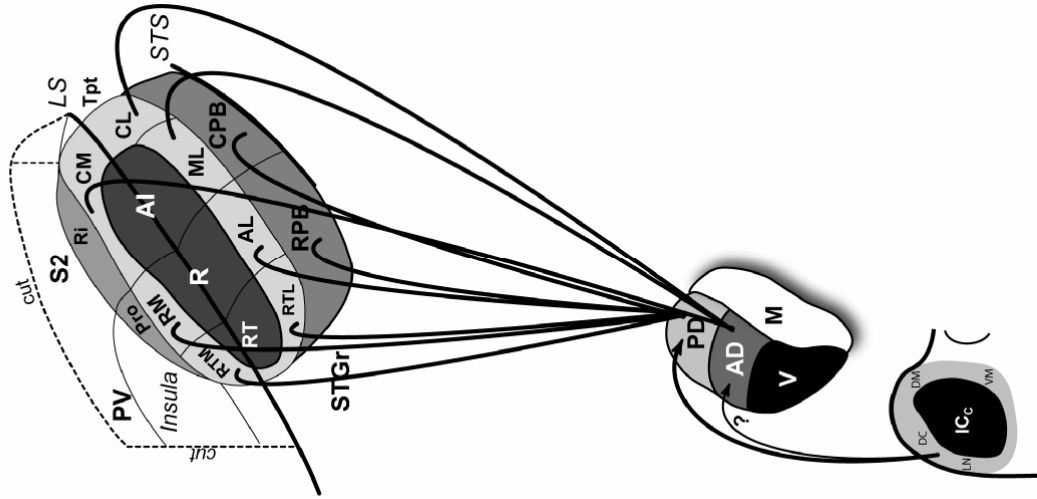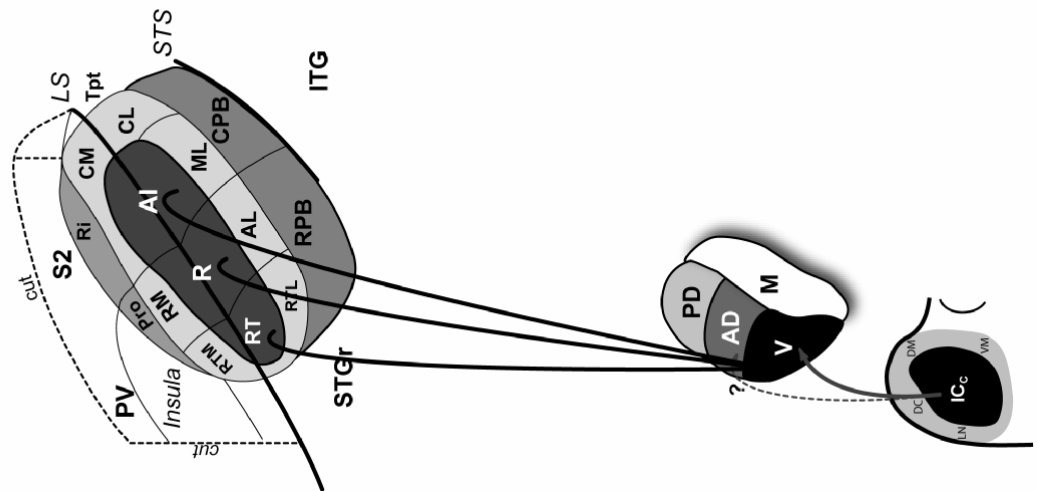
A second pathway, the non-tonotopic or diffuse pathway, is not tonotopically organized and involves the dorsal division of the MGC which receives inputs from the ICp (Andersen et al., 1980; Calford and Aitkin, 1983; Rouillier et al., 1989). This pathway, also referred to as the non-lemniscal pathway, involves non-primary areas of auditory cortex with the MGd projecting to the belt and parabelt areas. In several primate studies two divisions have been identified in MGd: anterodorsal (MGad) and posterodorsal (MGpd) (Burton and Jones, 1976, de la Mothe et al., 2006b; Hashikawa et al., 1995; Hackett et al., 2007a; Jones, 2007; Jones et al., 1995; Jones and Burton 1976; Molinari et al., 1995) although this distinction has not been consistent throughout the literature. The grouping of the anterior and posterior divisions of the MGd in some early studies may have been responsible for the general notion that the MGd projects to all belt and parabelt areas and thus both divisions are considered part of the non-lemniscal pathway. Jones and colleagues however, have suggested that MGad may actually be part of the lemniscal, primary pathway in that it also receives input from the central IC, and has a similar expression of parvalbumin (Pv) (Jones, 2003; Jones et al., 1995; Molinari et al., 1995). From this observation they have proposed the idea that there may be a parvalbumin-immunoreactive pathway (which includes both the MGv and the MGad) and a calbindin-immunoreactive pathway that projects more diffusely (Jones, 2003; Jones et al., 1995; Molinari et al., 1995).

The third pathway involves the magnocellular division of the MGC (MGm) which receives input preferentially from the ICx (Calford and Aitkin, 1983; Rouillier et al., 1989). The MGm projects to all areas of auditory cortex and is referred to as the multisensory, or polysensory pathway since the neurons in MGm respond to several

11

different sensory stimuli including auditory, somatosensory and visual (Calford and

Aitkin, 1983; Rouillier et al., 1989).

Response properties such as short response latencies, sharp frequency tuning, and

low response thresholds are characteristic throughout the tonotopic system and appear to

be common to neurons in primary areas (Imig et al., 1977; Kosaki et al., 1997; Morel and

Kaas, 1992; Morel et al., 1993; Rauschecker et al., 1997; Recanzone et al., 2000a). The

diffuse pathway appears to have slower latencies, broader tuning, and higher thresholds,

as evidenced by the response properties of neurons in the MGd and belt areas (Imig et al.,

1977; Merzenich and Brugge, 1973; Rauschecker and Tian, 2004; Rauschecker et al.,

1995; 1997; Recanzone et al., 2000a,b). The MGm has more variety in its response

properties with fast, medium and long latencies, all found within the division (Calford

&Aitkin, 1983). It is functionally unique in that it is multisensory both in neuron

response properties and varied sensory inputs (Rouilier et al., 1989), and projects to all

areas of auditory cortex, covering the tonotopic and diffuse pathways.

While the 3 pathway model is based mainly on data from cats, the primate data, in

general, fit well into this scheme. Core areas have bee identified as receiving input

predominantly from MGv, belt and parabelt areas from either of the divisions of MGd

(MGad, MGpd), and MGm had been reported to project to all areas of auditory cortex.

Thus based on anatomical findings the thalamic projection patterns from the primate data

are consistent with the 3 pathways model. While functional data from studies in primates

is consistent with the tonotopic and non-tonotopic pathways, the multisensory pathway in

primates remains underdeveloped.

Identification of Auditory Cortical Areas

Cortical auditory areas can be identified based on a number of different criteria such as; neuron response properties, connection patterns, and comparison of architectonic features. The main architectonic categories include cytoarchitecture (arrangement and types of neurons), myeloarchitecture (orientation and density of myelinated axons), and chemoarchitecture (distribution and expression of proteins, enzymes, and other substances within neurons or neuropil). For the purpose of this thesis auditory areas were identified using architectonic criteria previously established in other primates as a guide (Galaburda and Pandya, 1983; Hackett et al., 2001; Hackett et al., 1998a; Imig et al., 1977; Jones et al., 1995; Luethke et al., 1989; Morel et al., 1993; Morel and Kaas, 1992).

Core region

Core areas can be identified based on similar architecture that includes a densely packed population of small granule cells especially in layers III and IV, a broad layer IV, and a cell-sparse layer V, as well as astriate myelination (inner and outer bands of Baillarger in layers IV and Vb not visible due to high density of myelinated axons) and dense expression of acetylcholinesterase (AChE), cytochrome oxidase (CO), and parvalbumin (Pv) (Galaburda and Pandya, 1983; Imig et al., 1977; Hackett et al., 1998a, 2001; Leuthke et al., 1989; Morel et al., 1993; Morel and Kaas, 1992; Pandya and Sanides, 1973). There appears to be a gradient within the core areas in which features are more pronounced caudally with a decrease in overall myelin density, as well as dense expression of Co, AchE, and Pv rostrally (Leuthke et al., 1989; Morel and Kaas, 1992; Pandya and Sanides, 1973). The core area RT, consistent with its most rostral location,

exhibits muted core features, and has been described as the least certain area of the core (Morel and Kaas, 1992; Pandya and Sanides, 1973) However, it is more densely myelinated than the surrounding belt areas, consistent with its inclusion in the core region (Morel and Kaas, 1992; Pandya and Sanides, 1973).

Input into auditory cortex from the thalamus is an important characteristic in defining cortical areas. Areas of the core which are part of a tonotopic pathway (Roullier et al. 1991) receive input from MGv and MGm (Burton and Jones, 1976; Jones and Burton, 1976; Fitzpatrick and Imig, 1978; Hashikawa et al., 1995; Luethke et al., 1989; Morel and Kaas, 1992; Morel et al., 1993; Pandya et al., 1994; Molinari et al., 1995). which results in complete or partial frequency maps in all areas of the core (Aitkin et al., 1986; Bendor and Wang, 2005; Imig et al., 1977; Kajikawa et al., 2005; Kosaki et al., 1997; Merzenich and Brugge, 1973; Morel and Kaas, 1992; Morel et al., 1993; Rauschecker et al., 1995; 1997; Recanzone et al., 2000a). Information in auditory cortex is thought to be processed both serially and in parallel. Evidence for serial processing comes from anatomical and physiological studies (Hackett et al., 1998a; Rauschecker et al., 1997) in which the belt both relies on the core for activation and serves as an intermediate stage between the core and the parabelt. Thus, the core areas (A1, R and RT) receive information in parallel from the MGv and project serially onto the belt areas, the second level of cortical processing (Hackett and Kaas, 2004; Kaas and Hackett, 1998; Kaas et al., 1999; Rauschecker , 1998).

Neuronal response properties can also be used to identify core areas. The tonotopic gradients, which are created by the maintenance of frequency representation from the cochlea, are reversed at each of the borders within the core, providing a means

not only for identifying core areas, but the subdivisions within. Early on, this important

characteristic was advanced by Merzenich and Brugge (1973) in which they mapped

monkey auditory cortex and provided initial physiological evidence for multiple fields.

Recently tonotopic reversals have been revealed in most of the core and belt areas of the

macaque monkey using functional magnetic resonance imaging (fMRI) (Petkov et al.,

2006), confirming the results of the physiological studies and providing another

technique through which to identify auditory areas. Although tonotopic organization is a

key feature of core areas, that by itself is not enough to identify an auditory area.

additional neuron response properties used to identify areas include frequency tuning and

threshold levels. The narrower the frequency range to which a neuron responds, the

sharper the neuron is considered to be tuned. Conversely the larger the frequency range

to which a neuron responds the more broadly tuned the neuron is considered to be. With

regard to response threshold, the lower the intensity required from an auditory stimulus to

elicit a neuronal response, the lower the threshold that neuron is considered to have.

Neurons found in the core, in addition to being tonotopically organized are generally

sharply tuned with lower thresholds (Imig et al., 1977; Kosaki et al., 1997; Morel and

Kaas, 1992; Morel et al., 1993; Rauschecker et al., 1997; Recanzone et al., 2000a). Areas

outside of the core have also been revealed to be tonotopically organized and thus these

additional features are important in differentiating the core areas from the surrounding

belt areas.

Belt region

Belt areas surround the core both medially and laterally and can be identified

based on architectonic criteria that includes large pyramidal cells in lower layer III, a bistriate pattern of myelination (inner and outer bands of Baillarger are visible due to lighter myelination in layer Va and VI), and decreased expression of AChE, CO, and Pv in layers IIIb/IV compared to that of the core (Galaburda and Pandya, 1983; Imig et al., 1977; Hackett et al., 1998a, 2001; Jones et al., 1995; Morel et al., 1993; Morel and Kaas, 1992; Pandya and Sanides, 1973). Similar to the core region there appears to be a gradient of these architectonic features with systematic changes in the cytoarchitecure, decreasing in the overall myelin density and a reduction in Pv, CO, and AchE expression from caudal to rostral in the belt (Galaburda and Pandya, 1983; Imig et al., 1977; Hackett et al., 1998a; Morel et al., 1993).

Belt areas receive inputs mainly from MGad, MGpd and MGm (Burton and Jones, 1976; Hackett and Kaas, 2002; Kaas et al., 1999; Molinari et al., 1995; Morel and Kaas, 1992; Pandya et al., 1994). The grouping of the anterior and posterior divisions of the MGd in some early studies may have been responsible for the general notion that the MGd projects to all belt and parabelt areas. Separation of this nucleus into anterior and posterior divisions (Burton and Jones, 1976, Hashikawa et al., 1995; Hackett et al., 2007a; Jones et al., 1995; Jones and Burton 1976; Molinari et al., 1995) reveals a topographic pattern in which MGad projects preferentially to caudal areas and MGpd projects preferentially to rostral areas (Hackett et al., 2007a; Molinari et al., 1995). While the medial and lateral belt areas combine to form the more general belt region, Galaburda and Pandya (1983) identified these as distinct regions. The areas medial to the core were identified as the root fields and those lateral to the core were identified as the belt fields (Galaburda and Pandya, 1983; Pandya et al., 1994). Differences between the

medial and lateral belt areas have been reported in the thalamic connections with stronger

projections from Sg to the medial belt (Burton and Jones, 1976; Pandya et al., 1994) and

it has been proposed that the root (medial belt) areas may play a multisensory role

(Pandya et al., 1994).

With regard to neuron response properties, neurons in the belt areas are more

broadly tuned, with higher thresholds than those of the core areas (Imig et al., 1977;

Merzenich and Brugge, 1973; Rauschecker and Tian, 2004; Rauschecker et al., 1995;

1997; Recanzone et al., 2000a, b), and tonotopic organization in the belt tends to parallel

that of the core (Kosaki et al., 1997; Merzenich and Brugge, 1973; Rauschecker and Tian,

2004; Rauschecker et al., 1995). Like the core, the tonotopic organization of the

surrounding belt areas has been revealed using fMRI (Petkov et al., 2006), confirming the

findings of previous studies. Since the belt areas have been described as part of the non-

tonotopic or non-lemniscal pathway (Roullier et al., 1991) in which no cochlear

representation is maintained, tonotopic representation in the belt is most likely inherited

through the connections with the core. This reliance of the belt on the core for its

tonotopic input supports the notion of serial processing and the belt as a secondary stage

in that hierarchy (Kaas and Hackett, 2000; Rauscecker et al., 1997; Recanzone et al.,

2000a, b). Attention has turned recently to a specific area of the belt, CM, due in part to

the uncharacteristic mix of both core-like and belt-like responses revealed in this area.

Neurons in CM are tonotopically organized with short latencies comparable to those in

A1 for both tones and noise (Bieser and Muller-Preuss, 1996; Kajikawa et al., 2005;

Lakatos et al., 2005; Recanzone et al. 2000a), but are broadly tuned similar to belt areas

(Aitkin et al. 1986; Fu et al. 2003; Imig et al. 1977; Kosaki et al. 1997; Luethke et al.

1989; Merzenich and Brugge, 1973; Rauschecker et al. 1997; Recanzone et al. 2000a).

These features challenge the notion of a strict serial relationship between A1 and CM. In

addition, interest in this area has come from functional studies in which CM was found to

be responsive to both auditory and somatosensory (Foxe et al., 2002; Fu et al. 2003;

Kayser et al., 2005; Robinson and Burton, 1980a,b; Schroeder and Foxe, 2002; Schroeder

et al. 2001, 2003). Responses to somatosensory stimulation at such a low level of

processing in the auditory system introduces the question of where the somatosensory

input originates? The present study will address this question.

Parabelt Region

Parabelt areas are found lateral to the lateral belt and can be identified based on

architecture that includes a general decrease in the overall myelin density and reduced

expression of AChE, CO, and Pv compared to the adjacent belt region, as well as more

pronounced columnar organization of the cells (long narrow columns of pyramidal cells)

(Hackett et al., 1998a; Pandya and Sanides, 1973). The parabelt, similar to the core and

belt regions, exhibits a reduction in myelin density and expression of AchE and Pv from

caudal to rostral (Hackett et al., 1998a).

Similar to the belt areas, the parabelt is part of the diffuse pathway (Roullier et al.,

1991) and receives strong input from the MGd (MGad, MGpd) (Hackett et al., 1998b;

Kaas and Hackett, 2000). Since it does not receive input from the core, it relies on the

belt areas for its activation, suggesting serial processing, and is considered a third level of

auditory processing (Hackett and Kaas, 2004; Hackett et al., 1998a; Kaas et al., 1999;

Kaas and Hackett, 2000). Inputs to the various levels of auditory cortex include

additional nuclei of the thalamus, such as the MGm, which projects to all auditory areas

(Burton and Jones, 1976; Hashikawa et al. 1995), yet inputs from the MGv and the MGd

provide a means of determining generally if an area is part of the core (MGv) or the

belt/parabelt (MGd). The parabelt region also receives a strong input from the medial

pulvinar (PM), which projects to higher order areas of cortex (i.e. prefrontal), consistent

with the notion that of the parabelt as a later stage in hierarchical processing. This strong

PM projection to the parabelt, which is not present in the belt, provides a means of

distinguishing belt areas from parabelt areas. Studies of the neuron response properties

in the parabelt are lacking and is an area in need of further study.

General corticocortical connections

Based on the general pattern of connections in auditory cortex appears to have

both serial and parallel processing components. While the core areas project to the

surrounding belt region (considered a second level of processing), they do not project to

the parabelt and in turn must rely on the belt areas to project onto the parabelt. This is

consistent with a serial flow of information from the core, to the belt, and then the

parabelt. In addition, there is a parallel processing component where areas within a

region receive parallel inputs. Fore example, the three areas of the core (A1, R, RT)

receive inputs from the MGv. In addition there appears to be a general rostrocaudal

pattern of connections within the auditory cortex so that more rostral areas have stronger

connections with other rostral areas, and caudal areas with other caudal areas (Galaburda

and Pandya, 1983; Hackett et al., 1998a; Hackett and Kaas, 2002; Kaas and Hackett,

1998, 2000; Morel and Kaas, 1992). An exception to this may be area RM, which is

diffusely connected with both rostral and caudal divisions of the parabelt in one study

(Hackett et al., 1998a). This divergence or strengthening along rostrocaudal domains

continues with the prefrontal projections of auditory cortex. Rostral areas of the belt and

parabelt connect with rostral and orbital prefrontal cortex (PFC) (areas 10,12,13 and

rostral 46). Caudal areas of the belt and parabelt connect with caudal prefrontal regions

(areas 8a, 12 and caudal 46) (Hackett et al., 1999; Romanski et al., 1999a). This

rostrocaudal topography is not explicit; as there is some overlap between the streams and

some PFC areas receive projections from both the rostral and caudal areas. Romanski et

al. (1999a) concluded that it is within the auditory belt that the two streams diverge.

Rostral medial belt areas RTM and RM, as well as the rostral lateral areas (RTL and AL),

send smaller projections to the rostral areas of PFC (anterior and orbital PFC) and send a

stronger projection to rostral parabelt. In turn, the rostral parabelt projects strongly to the

rostral PFC. The caudal medial belt area CM, as well as the caudal lateral areas (CL and

ML), segregate into the caudal stream, sending smaller projections to the PFC, the dorsal

arcuate region, caudal principalis, ventrolateral PFC, and may relay in the posterior

parietal cortex which has dense connections with the caudal PFC. They send stronger

projections to the caudal parabelt, which in turn projects densely to the previously

mentioned areas. This divergence has spawned debate over a dual streams hypothesis in

the auditory system: a rostral "what" stream for processing non-spatial information and a

caudal "where" stream for processing spatial information (Alain et al. 2001; Clarke et al.

2002; Colombo et al., 1996; Kaas and Hackett, 1999; Rauschecker and Tian, 2000;

Romanski et al. 1999b; Tian et al. 2001), similar to what has been proposed in the visual

system (Mishkin et al., 1983; Ungerleider and Mishkin, 1982). Support for this

hypothesis has been suggested from additional studies such as those revealing a higher propensity for spatially selective neurons in CM than the core (Rauschecker et al., 1997; Recanzone, 2000b, Woods et al., 2006), a rostral lateral belt preference for identification versus a caudal lateral belt preference for spatial selectivity (Tian et al., 2001), as well as somatosensory responses in CM (Foxe et al., 2002; Fu et al. 2003; Kayser et al., 2005; Robinson and Burton, 1980a,b; Schroeder and Foxe, 2002; Schroeder et al. 2001, 2003). Imaging studies have also revealed distinct regions of activation for neurons responding to spatial location and pitch perception within posterior and anterior auditory cortex respectively (Barrett and Hall, 2006). Evidence has also been reported, however, that the streams are not necessarily completely segregated and that interaction between the two does occur (Kaas and Hackett, 1999; Zatorre et al., 2002). Further study is needed to address this issue.

Research Rationale

While the primate model of auditory cortex is one that has become widely adopted over the last number of years, it also remains largely untested. The areas of the medial belt in particular have not been well studied, and represent a large void in the anatomical organization of the primate model and are therefore the emphasis of the current thesis. Developed from incomplete studies of both New World and Old World monkeys, the model has yet to be systematically studied in even one species. That is, the extent to which the model is valid for any one species of primate is unknown. Providing basic connectional patterns and architecture of the auditory cortex in marmosets will

allow comparison and testing of the current primate model as well as provide a

foundation for species-specific auditory studies.

Species Rationale

In the present studies we chose to examine the auditory cortical areas of the

marmoset monkey. There are several reasons for selecting this species. The marmoset

(*Callithrix jacchus jacchus*) is an arboreal, diurnal New World monkey. It is native to

northeast and central Brazil and has the capacity for abundant reproduction which makes

them ideal for research colonies. The litters range in size from 1-4 (although usually

twins), and the average weight of an adult (12 months or older) is 400g. One reason we

chose the marmoset for study is that the marmoset has a smooth brain with few sulci and

provides easier access to the medial belt areas due to the shallow lateral sulcus. This

facilitates access to the medial belt for direct injections (one of the specific aims of this

project). Second, since marmosets have a range of vocalizations and are able to

recognize and discriminate between familiar and non-familiar calls (Clarke, 1994), they

have become increasingly used in neurophysiological studies of audition; thus

constructing an anatomical framework for this species may aid in future experiments.

Specific Aims

The following outlines the purpose of the present thesis:

1) Connection patterns of the medial belt cortex with other areas of auditory cortex will

be examined by direct injection of tracers into the medial belt. In addition, injections will

also be made in the core, lateral belt and parabelt areas at both rostral and caudal levels

for comparison not only between regions of auditory cortex (e.g. core and medial belt) but also within regions of auditory cortex (CM and RM). We hypothesize that the medial belt will show a distinct connectional pattern from the lateral belt, core and parabelt regions.

2)Architectonic criteria for the identification of areas and borders within the marmoset auditory cortex will be determined for each region. By using histological treatments in adjacent sections, borders between and within regions of auditory cortex can be identified. We hypothesize that the areas of auditory cortex contained in the model will be identifiable in marmoset auditory cortex using architectonic criteria established in other primates.

3) Thalamic inputs to auditory cortex of the marmoset monkey will be established via the retrograde label from injections into auditory cortex. The architecture of the thalamus will also be examined in order to identify its major nuclei and the borders between them. We hypothesize that the medial belt will have distinct inputs from the thalamus compared with other regions of auditory cortex.

4) The organization of the marmoset monkey auditory cortex will be compared to the current working model of primate auditory cortex. The combination of the injections into various areas of auditory cortex and identification of the architectonic areas together, will permit the examination of the overall organization of the auditory cortex of the marmoset monkey and thus provide a framework for this comparison. We hypothesize that the

marmoset auditory cortex will follow the organization of the current primate model of

auditory cortex.

CHAPTER II

CORTICAL CONNECTIONS OF AUDITORY CORTEX IN MARMOSET MONKEYS:
CORE AND MEDIAL BELT REGIONS

Introduction

In recent years we have adopted a model of auditory cortical organization in

primates based on findings compiled from both Old and New World primates (for

reviews, see Kaas & Hackett, 1998; Kaas et al., 1999; 2000; Hackett, 2002; Jones, 2003;

Pandya, 1995; Rauschecker, 1998). The model defines *auditory cortex* as the corpus of

cortical areas that are the preferential targets of neurons in either the ventral (MGv) or

dorsal (MGd) divisions of the medial geniculate complex (MGC). By this definition,

three regions of the superior temporal cortex comprise the auditory cortex in primates:

core, belt, and parabelt (Fig. 4). Numerous cortical regions outside the boundaries of

auditory cortex also process auditory information. These include areas in the rostral

superior temporal gyrus (STGr), temporal pole, superior temporal sulcus (STS), posterior

parietal, and prefrontal cortex. Since these areas generally do not receive significant

inputs from the MGC, and auditory activation is largely dependent on corticocortical

inputs from some portion of auditory cortex, they are referred to as *auditory-related*

cortex.

One major feature of the model is that the core, belt, and parabelt regions

represent successive stages in the processing of auditory information in cortex. This

hierarchy was introduced to account for patterns of connections between areas and related

physiological observations in primates (Kaas and Hackett, 1998; Rauschecker, 1998).
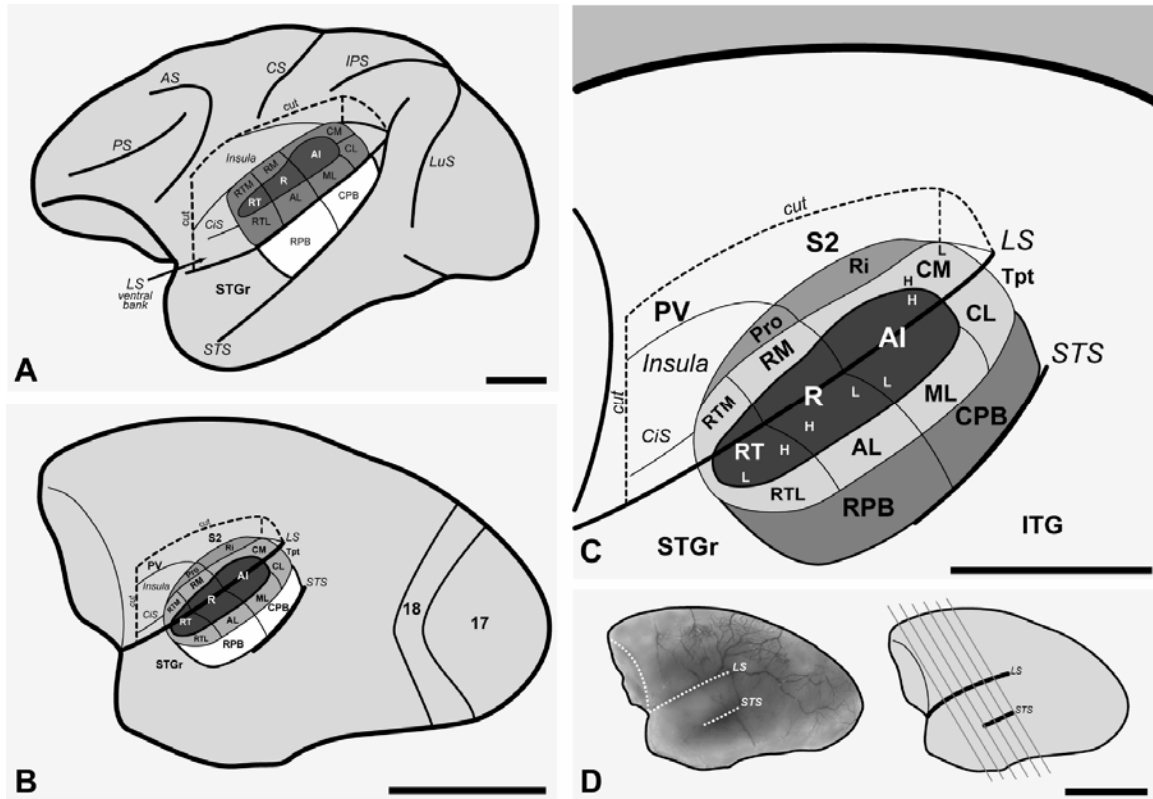
Figure 4. Schematic models of macaque (A) and marmoset (B - D) monkey auditory cortex. The lateral sulcus (LS) of the left hemisphere was graphically opened (cut) to reveal the locations of auditory cortical areas on its lower bank. The circular sulcus (CiS) was flattened to show the position of the rostromedial (RM) and rostrotemporal medial (RTM) areas that occupy its lateral wall. The upper bank of the LS was partly opened (cut) to show the locations of the retroinsular area (Ri) in the fundus, second (S2) and parietoventral (PV) somatosensory areas on the upper bank, and insula (Ins). The three areas that comprise the core region of auditory cortex (dark shading) are located on the lower bank (A1, auditory area 1; R, rostral; RT, rostrotemporal). The core is surrounded by seven or eight areas that belong to the belt region (light shading) (CM, caudomedial; CL, caudolateral; ML, middle lateral; RM, rostromedial; AL, anterolateral; RTM, rostrotemporal medial; RTL, rostrotemporal lateral). The proisocortex area (Pro) is a putative addition to the medial belt. The core and lateral belt regions are mostly contained within the lateral sulcus in macaques, but extend onto the superior temporal gyrus (STG) in the marmoset. On the surface of the STG are two areas that make up the parabelt region (medium shading) (RPB and CPB, rostral and caudal parabelt). The rostral part of the STG (STGr) extends to the temporal pole. The temporal parietotemporal area (Tpt) occupies the caudal end of the STG and extends onto the supratemporal plane within the LS. Tonotopic gradients within areas are indicated by H (high frequency) and L (low frequency). Other sulci shown include the arcuate sulcus (AS), central sulcus (CS), intraparietal sulcus (IPS), and superior temporal sulcus (STS). (D) Photographic image of the marmoset left hemisphere and schematic showing the plane of section (diagonal lines) used in the present study for histological processing. Scale bars (A, B, D), 10 mm; (C), 5 mm.

Key anatomical support for a hierarchy is that that the core region projects to the belt, but not the parabelt region (Hackett et al., 1998a; Morel et al., 1993; Morel and Kaas, 1992). Physiological evidence of progressive spectral and temporal integration in the belt areas (Kajikawa et al., 2005; Rauschecker et al., 1995; Rauschecker, 2004; Recanzone et al., 2000a) , as well as evidence that neuronal activity in CM is at least partly dependent on intact inputs from A1 (Rauschecker et al., 1997).

A second feature of the model is that each of the three major auditory cortical regions consists of two or more areas, or subdivisions (e.g., AI-R-RT, AL-ML-CL), in which thalamic and cortical inputs are processed in parallel. Since the establishment of individual subdivisions depends on the identification of subsets of unique anatomical and physiological features, this component of the model is in the greatest need of refinement and validation. The areas within core region, especially A1, have been intensively studied, while several other subdivisions were established from minimal anatomical or physiological data. This is especially true of the belt region, where as many as seven distinct areas have been proposed (Fig. 4), but only a few studied in much detail, as described below.

The current model groups all of the belt areas together within a single region representing the second stage of auditory cortical processing. This probably represents an oversimplification, as several lines of evidence suggest that the belt is structurally and functionally heterogeneous. First, the architectonic features of the belt region are not uniform. The parainsular (medial belt) cortex, positioned between the core and insula, has always been considered architectonically distinct from cortex lateral to the core in humans (Beck, 1928; Brodmann, 1909; Galaburda and Sanides, 1980; Hopf, 1954; Vogt

and Vogt, 1919; von Economo and Koskinas, 1925) and nonhuman primates (Galaburda and Pandya, 1983; Imig et al., 1977; Jones and Burton, 1976; Jones et al., 1995; Morel et al., 1993; Morel and Kaas, 1992; Pandya and Sanides, 1973; Sanides and Krishnamurti, 1967). Pandya & Sanides (1973) distinguished a medial belt of areas (i.e., *root* areas) from those lateral to the core (i.e., *belt* areas) in macaque monkeys, a distinction that was maintained in subsequent revisions of that scheme (Cipolloni and Pandya, 1989; Galaburda and Pandya, 1983). Second, the thalamic inputs to the belt differ between areas. The main source of input is the dorsal division (MGd) of the medial geniculate complex (MGC), which has anterior (MGad) and posterior (MGpd) subdivisions. The belt areas appear to differ with respect to the balance of inputs from these divisions, as well as other nuclei in the posterior thalamus (Burton and Jones, 1976; de la Mothe et al., 2006b; Hackett et al., 1998b; Jones, 2003; Molinari et al., 1995; Rauschecker et al., 1997). Third, the rostral and caudal belt areas are connected with distinct areas of prefrontal and posterior parietal cortex (Lewis and Van Essen, 2000; Romanski et al., 1999a; Romanski et al., 1999b). Fourth, area CM and several of the lateral belt areas have been distinguished by auditory response properties, including reversals in tonotopic organization, FM rate preferences, and preferences for spatial and nonspatial stimuli (Imig et al., 1977; Kajikawa et al., 2005; Kosaki et al., 1997; Merzenich and Brugge, 1973; Rauschecker and Tian, 2000; Rauschecker and Tian, 2004; Rauschecker et al., 1995; Recanzone et al., 2000a; Romanski et al., 1999b; Tian and Rauschecker, 2004; Tian et al., 2001). Fifth, recent studies indicate that neurons in the caudomedial belt area, CM, are responsive to both auditory and somatosensory stimulation (Fu et al., 2003; Schroeder et al., 2001), confirming limited observations in earlier studies of

somatosensory areas in the caudal lateral sulcus (Robinson and Burton, 1980a; Robinson and Burton, 1980b; Robinson and Burton, 1980c). Known connectivity suggests that the belt areas are likely to differ with respect to multisensory activity. Thus, the areas that comprise the belt region appear to be both structurally and functionally heterogeneous in ways that are gradually being revealed, but not yet firmly established.

The most poorly studied areas of the belt region are those medial to the core, hereafter referred to as the medial belt. At least three areas comprise this region: caudomedial, CM; rostromedial; RM; and rostrotemporal medial, RTM (Fig. 4). The lack of data is partly a consequence of their location deep within the lateral sulcus of all primates. Thus, their connections are known mostly from tracer injections of more accessible auditory and auditory-related cortical areas. Physiological properties, recordings have mainly focused on CM.

In the present study and its companion (de la Mothe et al., 2006b), the cortical and thalamic connections of RM and CM were compared with adjacent core areas, R and A1, following tracer injections into these target areas. The main goal of these experiments was to refine and extend our working model of the primate auditory cortex, with special emphasis on the organization of the medial belt region. More specifically, the following predictions of the model were tested: (1) RM and CM are anatomically-distinct areas of auditory cortex and of the medial belt region; (2) RM and CM receive direct projections from the core, consistent with their position in the processing hierarchy; (3) The auditory cortical connections of the medial belt areas are distinct from those of the core; (4) RM and CM receive inputs from somatosensory cortex. A secondary goal of these experiments was to begin to define the anatomical organization of the marmoset auditory

29

cortex and determine how closely it approximates that of other primates. Our knowledge of the anatomical organization of auditory cortex in this species is limited to connections of the core (Aitkin et al., 1988; Luethke et al., 1989), yet marmosets have increasingly become an important neurophysiological model for the study of the primate auditory cortex (see Discussion). To establish the anatomical features of auditory cortex in the marmoset would facilitate ongoing and future studies of audition in this vocal primate species, and also reveal the extent to which auditory cortex organization may be conserved across taxa. A preliminary report of these findings appeared in abstract form (de la Mothe et al., 2002).

Materials and Methods

Animal subjects

All experimental procedures were conducted in marmoset monkeys (*Callithrix jacchus jacchus*) in accordance with NIH Guidelines for the Use of Laboratory Animals under a protocol approved by the Vanderbilt University Institutional Animal Care and Use Committee. Eight adult marmosets served as animal subjects in the present study. The experimental history of each animal is included in Table 1.

General surgical procedures

Aseptic techniques were employed during all surgical procedures. Animals were premedicated with cefazolin (25 mg/kg), dexamethasone (2 mg/kg), cimetidine HCl (5 mg/kg), and robinul (0.015 mg/kg). Anesthesia was induced by intramuscular injection of ketamine hydrochloride (10 mg/kg) then maintained by intravenous administration of

Table 1. Experimental history of animal subjects. Areas of tracer injections (A1, auditory core area 1; R, rostral core; RM, rostromedial belt; CM, caudomedial belt; CPB, caudal parabelt; CL, caudolateral belt; AL, anterolateral belt; PP, posterior parietal cortex). Neuroanatomical tracers (CTB, cholera toxin subunit B; BDA, biotinylated dextran amine; FB, fast blue; FE, fluoroemerald; FR, fluororuby), aqueous concentration and volume injected are listed for each tracer. [1]Cell plot reconstructions not illustrated for this case. [2] Tracer injection not analyzed for inclusion in the present study.

Case	Sex	Areas Injected	Tracer	%	Volume (μl)
1 (01-37)	M	RM	BDA	10	0.4
		R	FR	10	0.3
		R	FE	10	0.4
		AL/ML[2]	FB	10	0.25
2 (01-118)	M	RM	BDA	10	0.4
		R	FR	10	0.3
		CL[2]	FB	10	0.2
3 (02-17)	M	CM	CTB	1	0.4
		PP	BDA	10	0.4
4 (02-51)	M	A1	CTB	1	0.4
		R	FR	10	0.3
5 (02-60)	M	A1	FR	10	0.3
		CPB[2]	FB	10	0.2
6 (04-51)	M	CM	CTB	1	0.4
		AL[2]	FR	10	0.3
7 (01-89)[1]	M	CM	CTB	1	0.4
8 (04-40)[1]	M	CM	BDA	10	0.4

ketamine hydrochloride (10 mg/kg) supplemented by intramuscular injections of xylazine

(0.4 mg/kg) or by isoflurane inhalation (2 – 3%). Body temperature was kept at 37°C

with a water circulating heating pad. Heart rate, expiratory CO_2, and O_2 saturation were

continuously monitored throughout the surgery and used to adjust anesthetic depth.

Oxygen was delivered passively through an endotracheal tube at a rate of 1 liter/minute.

The head was held by hollow ear bars affixed to a stereotaxic frame (David Kopf

Instruments, Tujunga, CA). A midline incision was made exposing the skull, followed by

retraction of the temporal muscle. A craniotomy was performed exposing the left dorsal

superior temporal gyrus, lateral fissure, and overlying parietal cortex. After retraction of

the dura, warm silicone was applied to the brain to prevent desiccation of the cortex.

Photographs of the exposed cortical surface were taken for recording the locations of

electrode penetrations in relation to blood vessels and the lateral sulcus.

Retraction of the parietal operculum and neuroanatomical tracer injections

Tracer injections were made into target areas through a pulled glass pipette

affixed to a 1 µl Hamilton syringe. The pipette was advanced into cortex under stereo

microscopic observation to a depth of 1000 µm using a stereotaxic micromanipulator.

After manual pressure injection of the tracer volume (Table 1), the syringe was held in

place for 10 minutes under continuous observation to maximize uptake and minimize

leakage. Injections of the core areas (A1, R) were made directly into the lateral surface of

the superior temporal gyrus (STG) after removal of the dura (see Fig. 4b-c). Injections of

medial belt targets within the lateral fissure were achieved in one of two ways. In cases 1,

3, and 7 BDA or CTB were injected into RM or CM by passing the syringe through the

overlying parietal cortex. Depth was controlled by stereotaxic measurements and verified

by recordings made using a tungsten microelectrode affixed to the syringe. In all other

cases, access to injection targets within the lateral fissure was achieved by retraction of

the banks of the lateral fissure, as recently described (Hackett et al., 2005). This was done

to gain direct access to target areas without tissue resection, as connections with

somatosensory areas would have been lost. Briefly, after microdissection of the arachnoid

membrane around blood vessels at the edge of the lateral sulcus, the upper bank was

gently retracted using a stereotaxic arm and blunt dissection of arachnoid within the

sulcus. Once the desired opening was achieved, tracer injections were made directly into target areas relative to gross anatomical landmarks and blood vessel patterns.

Auditory stimulation and recordings

For most of the cases included in this report, detailed recordings were obtained seven days after tracer injections during a terminal experiment that averaged 24 hours in duration. The recording sites were concentrated in A1 and CM using a battery of stimuli, including tones, broad band noise, frequency modulated tones, and marmoset vocalizations. The tonotopic maps derived from these recordings were marked by electrolytic lesions and aided the reconstructions of architecture and connections, primarily at the borders of A1 and CM. The physiological results of these experiments and methodological details are reported elsewhere (Kajikawa et al., 2005; Kajikawa and Hackett, 2005; Kajikawa et al., 2008) and while complimentary, are not the focus of the present work. The tonotopic maps derived from these studies were marked with electrolytic lesions to facilitate later reconstruction of the map. In one case (01-37) a map was obtained following injections. In one case (case 1) the left hemisphere was mapped prior to tracer injections into the same hemisphere and the reversal of tonotopic organization at the A1/R border was useful in corroborating the border defined by architecture and connections. However, because neuronal responses could be abolished or otherwise altered by nearby tracer injections, post-injection recordings were generally confined to the opposite hemisphere.

Perfusion and histology

At the end of the terminal recording experiment a lethal dose of pentobarbital was administered intravenously. Just after cardiac arrest the animal was perfused through the heart with cold (4° C) saline, followed by cold (4° C) 4% paraformaldehyde dissolved in 0.1 M phosphate buffer (pH 7.4). Immediately following perfusion the brains were removed and photographed. The cerebral hemispheres were separated from the thalamus and brainstem, blocked, and placed in 30% sucrose for 1 to 3 days. The cerebral hemispheres were cut perpendicular to the lateral sulcus in the caudal to rostral direction at 40 µm, as shown in Fig. 1d. In each series of sections every sixth section was processed for the following set of histochemical markers: (i) fluorescent microscopy; (ii) biotinylated dextran amine (BDA) or cholera toxin subunit B (CTB); (iii) myelinated fibers (MF) (Gallyas, 1979); (iv) acetylcholinesterase (AChE) (Geneser-Jensen and Blackstad, 1971); (v) stained for Nissl substance with thionin; (vi) cytochrome oxidase (CO) (Wong-Riley, 1979); or (vii) parvalbumin immunohistochemistry (PV).

Architectonic identification of cortical areas

A full architectonic analysis was necessary since a complete parcellation of the marmoset auditory cortex has not been previously published. The architectonic criteria used to identify areas of auditory cortex in other primates were used to guide identification of corresponding areas in marmosets (Galaburda and Pandya, 1983; Hackett et al., 2001; Hackett et al., 1998a; Imig et al., 1977; Jones et al., 1995; Luethke et al., 1989; Morel et al., 1993; Morel and Kaas, 1992). The combined use of multiple markers improved the reliability of border identification and was especially useful when

borders between areas were ambiguous in one stain, or another. Of particular importance in this context was the plane of section. A standard coronal plane was not ideal for visualization of auditory cortex since cell and fiber columns were then cross-cut at an angle of about 30 degrees relative to the orientation of the lateral sulcus. To minimize these distortions, all brains were cut perpendicular to the long axis of the lateral sulcus after removal of the thalamus and brainstem, as shown in the inset of figure 4d. Columnar orientation also has implications for the approach angle chosen for microelectrode recordings, as radial orientation varied between cortical areas, and cell columns were often curved. Digital images were acquired using a Nikon DXM1200F digital camera and Nikon E800S microscope. These images were cropped, adjusted for brightness and contrast using Adobe Photoshop 7.0 software, but were otherwise unaltered. Final figures containing images and line drawings were made using Canvas 8.0 software (Deneba Systems, Inc., Miami, FL) and Adobe Illustrator 10.0 (Adobe Systems, Inc.).

Analysis and reconstruction of connections

The X-Y locations of cell somata labeled by retrograde axonal transport of each tracer were plotted using a Neurolucida system (MicroBright Field, Inc., Williston VT). Auditory areas were identified in sections stained for the histochemical markers listed above, according to architectonic features described in the Results. For each histochemical marker, the borders of individual areas and patches of anterograde terminal labeling were drawn onto plots of labeled cells by alignment of blood vessels and common architectonic features using a drawing tube affixed to a Zeiss Axioscope. These drawings were used to create the reconstructions (e.g., Fig. 12). In most figures, every

other section was chosen for illustration. For each tracer injection, the percent of total labeled cells was derived for each by dividing total cell counts for each area by the total number of cells in the auditory cortex labeled by that injection. Labeled cells in areas outside of the auditory cortex were counted separately and not factored into the percent total calculations. Values were tabulated separately for ipsilateral and contralateral hemispheres. Multiple tracers were used in this study to maximize the information gained from each experiment. Because sensitivity varies between tracers, greater numbers of labeled cells were observed in some cases. CTB was the most sensitive retrograde tracer used and labeled the most cells per case. BDA and FR typically labeled fewer cells per case, but BDA was the most sensitive anterograde tracer. In the analysis and interpretation of results, it was assumed that the proportion of labeled cells found in each area was maintained, while absolute cell counts differed between tracers. Therefore, the percent of total labeled cells was used to reflect connection magnitude, rather than total cell number. A second important factor affected cell counts in the diffusion zone in and around injection sites. Due to high tracer density and tissue damage in these zones, cell counts for one or more tracers were lower than normal. The potential error was reflected in the histograms by using a white bar in the column associated with the injected area.

Results

Architectonic identification of auditory areas

The architecture of the marmoset auditory cortex was illustrated at different levels of magnification over several figures to show the relative locations of individual areas (e.g., Figs. 5, 6), and the structural details of each (Figs. 7 – 11). The auditory areas

occupied most of the superior temporal lobe between the fundus of the lateral sulcus (LS)

and upper bank of the superior temporal sulcus (STS), as shown in figures 4 and 5. The

greatest source of variation between animals stemmed from the depth of STS, which

ranged from about 2.5 mm (Figs 5a, 6) to not more than a mild depression (Fig. 5b, 8),

and typically reached maximum depth in the caudal half of the temporal lobe. In animals
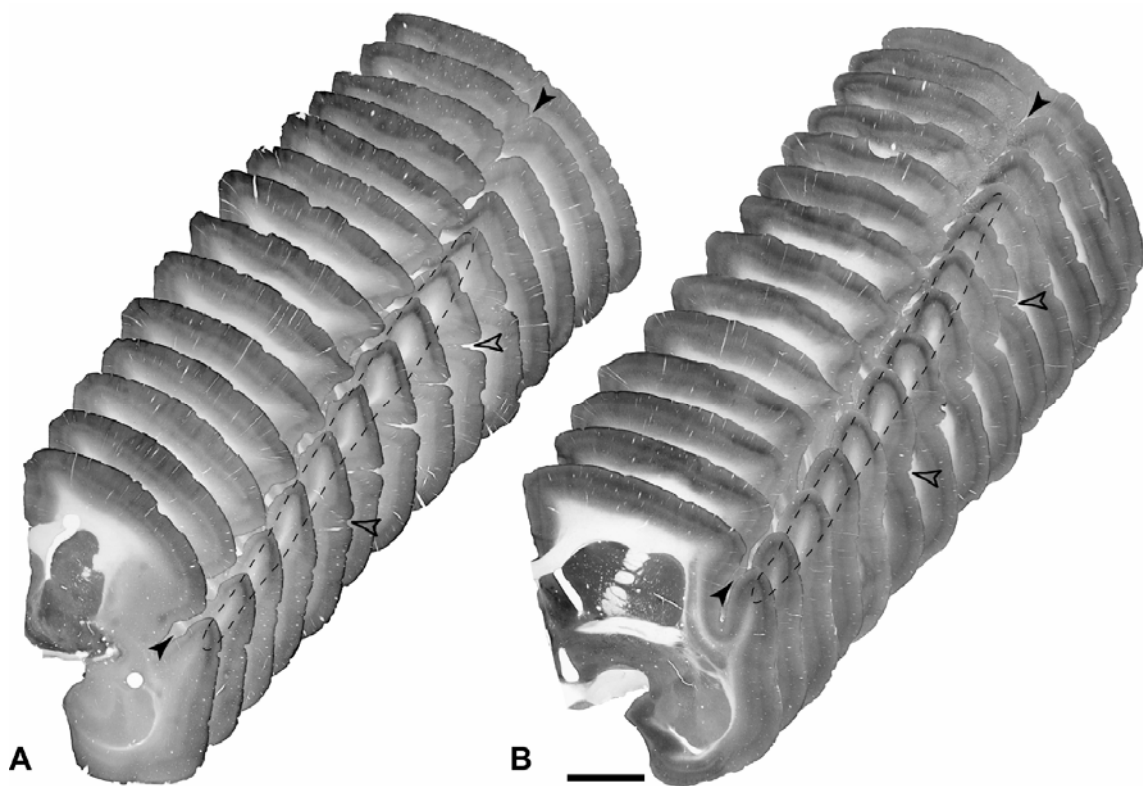
Figure 5. Marmoset monkey left hemisphere. Series of sections from the left hemisphere of two animals (A, B) stained for cytochrome oxidase (CO) to show the gross anatomy of the temporal lobe. The location of the core region is outlined by dashed lines which encompass the band of dense CO staining centered on layer IV of the core. Rostral is at the bottom-left of each panel. Solid arrows, lateral sulcus. Open arrows, superior temporal sulcus. Scale, 4 mm.

with a prominent STS, the parabelt region usually occupied the lateral portion of its upper

bank, bordering a weakly-myelinated zone in the fundus (Fig. 6f, g). In animals with a

Figure 6. Architecture of the marmoset auditory cortex at low magnification. (A - D) Thionin stain for Nissl; (E - H) Myelin stain; (I - L) Cytochrome oxidase; (M - P) Acetylcholinesterase. Columns are arranged from caudal (left) to rostral (right). Dashed black lines mark boundaries between areas. Dashed white line denotes subareal border between the medial ($A1_M$) and lateral ($A1_L$) divisions of A1. Filled arrowhead denotes lateral sulcus (LS). Open arrowhead marks superior temporal sulcus (STS). AL, anterolateral belt area; Caud, caudate nucleus; Cla, claustrum; CL, caudolateral area; CM, caudomedial area; CPB, caudal parabelt area; Ent, entorhinal cortex; Hip, hippocampus; ML; middle lateral belt area; MT, middle temporal area; Pro, proisocortical area; RM, rostromedial belt area; RPB, rostral parabelt area; Ri retroinsular area; S2, somatosensory area 2. Scale bar = 1mm.
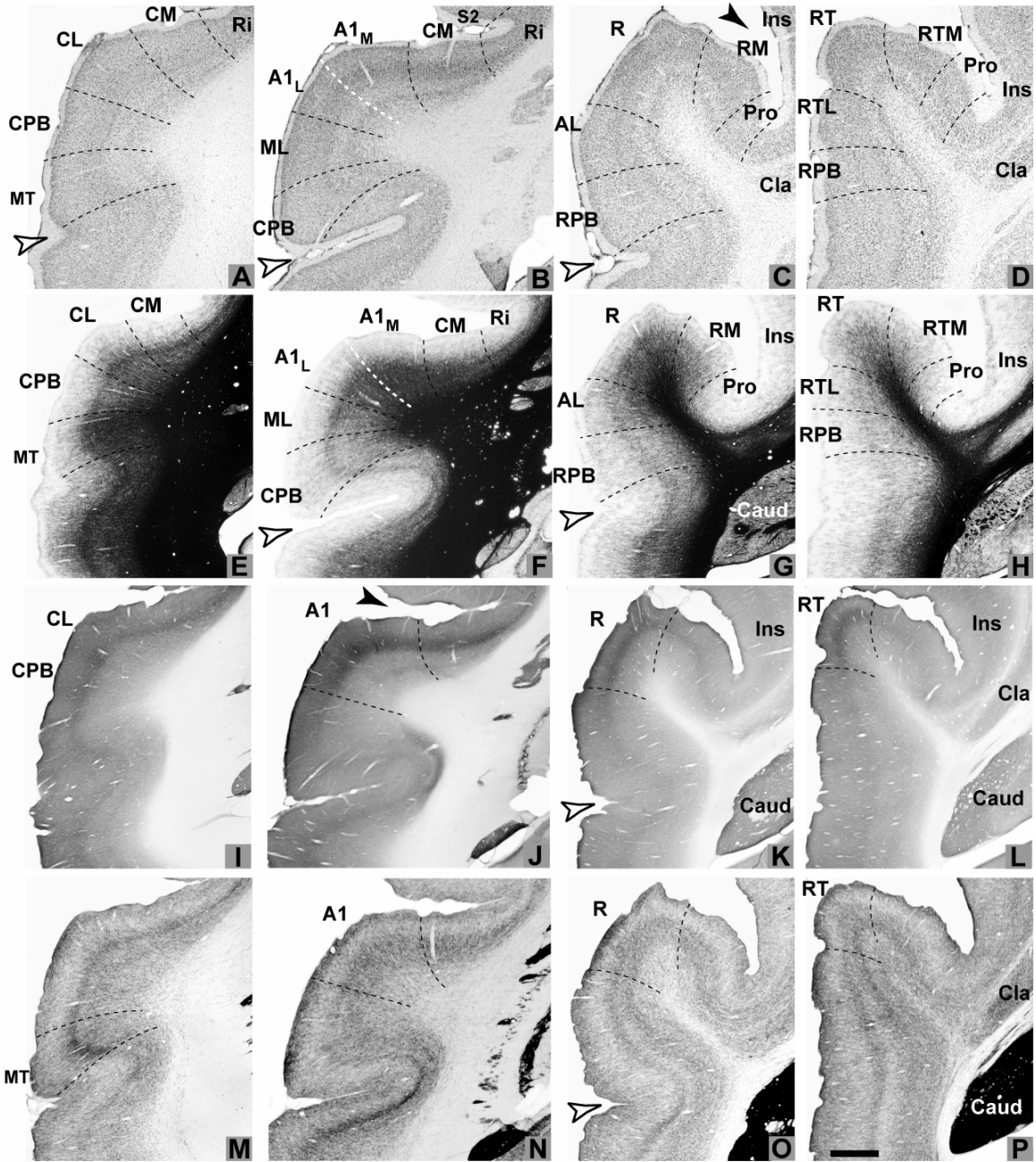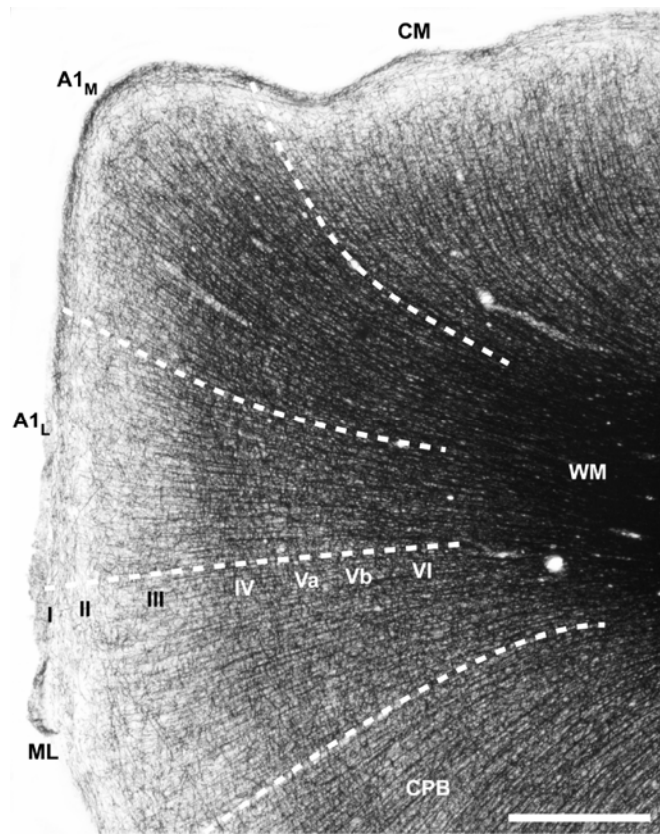
Figure 7. Myeloarchitecture of marmoset auditory cortex. Myelin stain through A1(case 8) to show medial (A1$_M$) and lateral (A1$_L$) subdivisions of A1 in relation to CM and ML. Dense myelination across laminae in A1$_M$ is reduced in layers III and Va of A1$_L$. Cortical layers indicated by Roman numerals I - VI. WM, white matter. Scale bar, 500 μm.

shallow fissure, the weakly-myelinated zone usually straddled the banks of the STS, shifting the ventral border of the parabelt onto the surface of the STG (Fig. 6). Variations in the gross anatomical configuration of the superior temporal lobe varied between animals, as can be seen in figures throughout this report, and may relate to variability previously observed in this species (Aitkin et al., 1986).
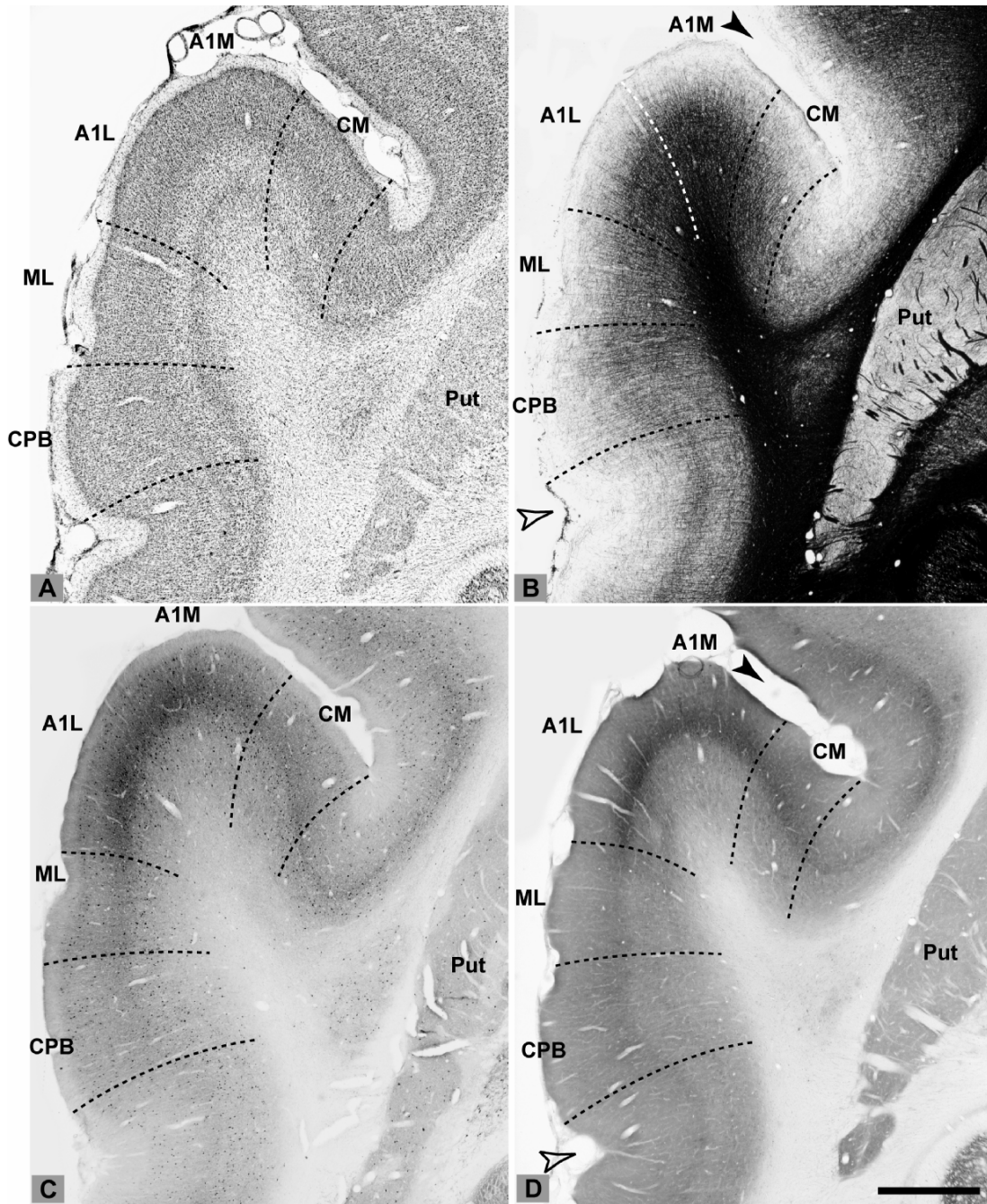
Figure 8. Architecture of marmoset auditory cortex through rostral A1. (A) thionin stain for Nissl; (B) myelin stain; (C) parvalbumin immunohistochemistry; (D) cytochrome oxidase stain. Note correspondence of dense myelin, parvalbumin, and cytochrome oxidase in the layer III/IV band of A1. Layer III/IV expression was moderately dense in CM and less dense in ML and CPB. Parvalbumin expression was weakest in CPB. Solid arrowheads mark lateral sulcus. Open arrowheads mark the location of the STS, which was very shallow in this animal (compare to Fig. 5). Scale bar = 1 mm.

Cytoarchitecture of the core region

The core region was easily identified in all cases, and typically straddled the edge of the lateral sulcus along most of its length from caudal to rostral, with roughly two-thirds of its area on the surface of the STG (Fig. 4b, c). Its location could be approximated at low magnification due to dense expression of cytochrome oxidase in the middle cortical layers (Fig. 5). The cytoarchitecture of the core areas was koniocellular, as typified by a cell-sparse layer V, broad granular layer IV, and high density of small pyramidal cells in layer III (Figs. 8a, 9a-d). No clear differences were noted between $A1_M$ and $A1_L$ other than an increase in cortical thickness where $A1_M$ wrapped over the edge of the lower bank. Key distinctions between A1 and the rostral core areas (R and RT) were a reduction in cortical thickness, most obvious in layers III and IV, and an increase in layer V cell density. In comparing R and RT, granular cell density in layers III - IV was slightly greater in R, consistent with greater fiber density in R, as described below.

Myeloarchitecture of the core region

Myelin density was higher in the core compared to neighboring belt areas (Figs. 6f-h, 7, 8b). The main exception was area CM, which was also myelin-dense across laminae. Within A1 a division between its medial ($A1_M$) and lateral ($A1_L$) halves was consistently noted. Whereas the myelination pattern in $A1_M$ was astriate, due to high density across layers III – VI, layer IV could be more clearly resolved in $A1_L$ due to a reduction of myelin density in layers III and Va (Figs. 8b, 9e-f). This pattern has also been observed in macaques, chimpanzees, and humans (Hackett et al., 2001; Hackett et al., 1998a; Pandya and Sanides, 1973), and therefore appears to be conserved across taxa. We highlight the

Figure 9. Cytoarchitecture and myeloarchitecture of marmoset auditory cortex, core region. *Top*, thionin stain for Nissl. *Bottom*, corresponding section, myelin stain. (A, E) area $A1_M$; (B, F) area $A1_L$; (C, G) area R; (D, H) area RT. Cortical layers indicated by Roman numerals I - VI. WM, white matter. Scale, 250 µm.
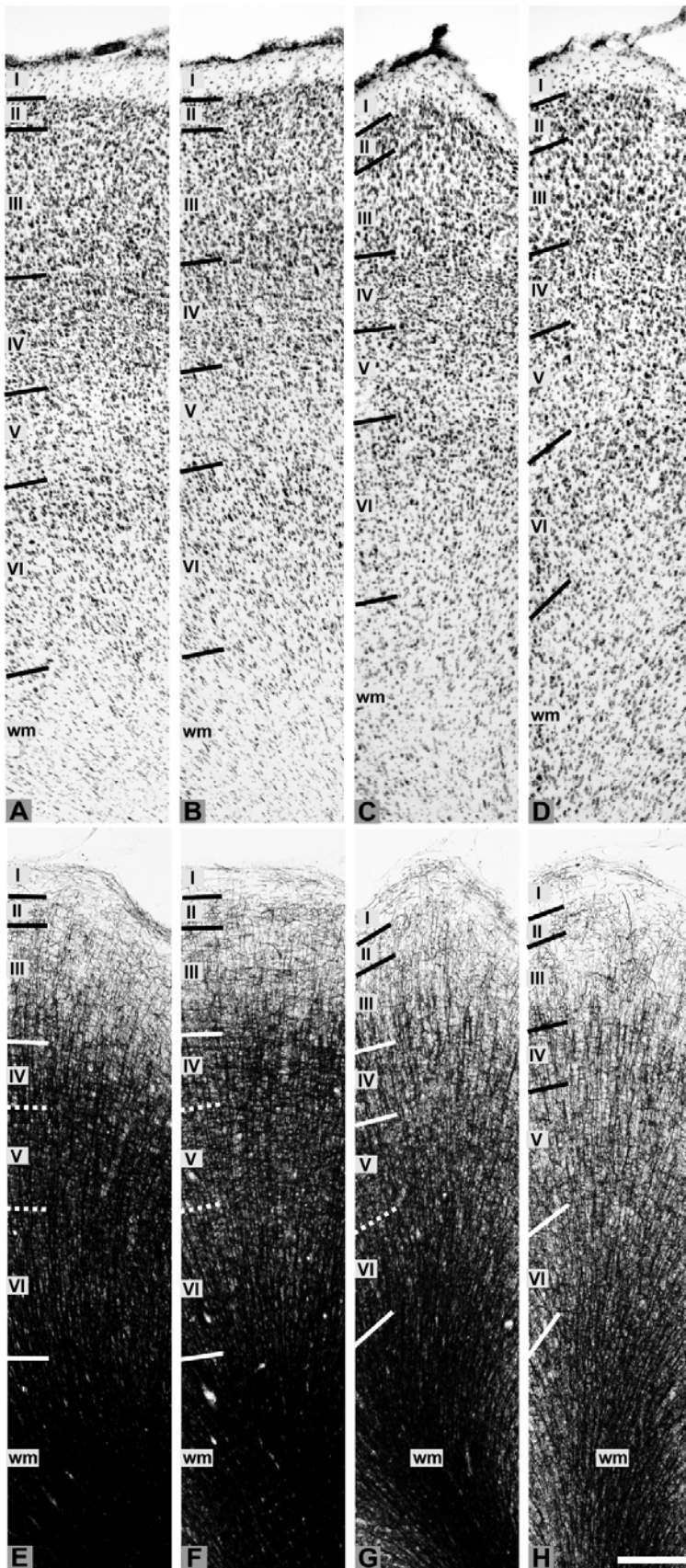
distinction here because the connections of the medial belt areas varied with respect to the lateral and medial halves of the core. While myelin density was greatest in A1, myelin density decreased rostrally in the core, reaching a minimum in RT (Fig. 6e-h, 9e-h). This density shift mainly reflected a reduction of horizontal axons in layers III – V of R and RT (Fig. 9e-h). Accordingly, R and RT had a stronger radial appearance compared to A1, where horizontal and radial fibers formed a dense astriate matrix. Compared to the lateral belt areas, however, the inner and outer horizontal striae in layers IV and Vb were not prominent in any of the core areas.

Chemoarchitecture of the core region

Within the core region, the metabolic enzyme, cytochrome oxidase (CO) was densely expressed in a horizontal band involving layer IV and the lower half of layer III (Figs. 5, 6i-l, 8d). This band was slightly narrower in R and RT, but prominent throughout the core by comparison to the belt and parabelt areas (Fig. 5). One exception to this pattern concerned area CM, in which the density of the layer III/IV band was comparable to $A1_M$ (Figs. 6j, 8d). Acetylcholinesterase (AChE) was most densely expressed in the layer III/IV band and layer Vb, corresponding to the most prominent inner and outer bands of myelinated fibers. While AChE expression was slightly more intense in the core, its distribution across all three regions was rather uniform (Fig. 6m-p). This result was unexpected since dense AChE expression in the layer III/IV band has been a key marker of the core in other primates. It was not clear whether the present results reflected a species difference in AChE expression or histological incompatibility. The latter seemed more likely, given dense coexpression of CO and parvalbumin in the

45

layer III/IV band (Fig. 8c-d). In any event, the observation was reliable using the same protocol in twelve cases over four years with variable incubation times.

Cytoarchitecture of the lateral belt and parabelt regions

A key cytoarchitectonic feature of the lateral belt and parabelt areas was the prominent radial orientation of generously spaced cell columns, especially in the granular and supragranular layers (Fig. 10a-f). This contrasted with dense columns of smaller cells in the core. Other features included narrowing of layer IV, and the appearance of larger pyramidal cells in lower layer III and layer Va. Area CL, located caudal to A1 and lateral to CM, had a broad layer III and dense columns of granule cells in layer IV. This contrasted with the adjacent belt area ML, which had a relatively narrow layer III and broader columnar spacing in layer V. The cytoarchitecture of AL resembled ML, but columnar spacing was slightly more generous in layer III and overall cortical thickness was reduced. This trend continued rostrally into RTL, where layers IV and VI became less distinct. The cytoarchitectonic border between the lateral belt and parabelt regions was generally not robust, except for the following features. Layer III was typically broader in the parabelt and characterized by prominent radial alignment of granular and pyramidal cells. The orderly spacing and orientation of cells in these columns extended across most of the cortical mantle from layers VI through III, giving the CPB and RPB a striking radial appearance (Fig. 10e-f).

Figure 10. Cytoarchitecture and myeloarchitecture of marmoset auditory cortex, lateral belt and parabelt regions. *Top*, thionin stain for Nissl. *Bottom*, corresponding section, myelin stain. (A, G) area CL; (B, H) area ML; (C, I) area AL; (D, J) area RTL; (E, K) area CPB; (F, L) area RPB. Cortical layers indicated by Roman numerals I - VI. WM, white matter. Scale, 250 µm.
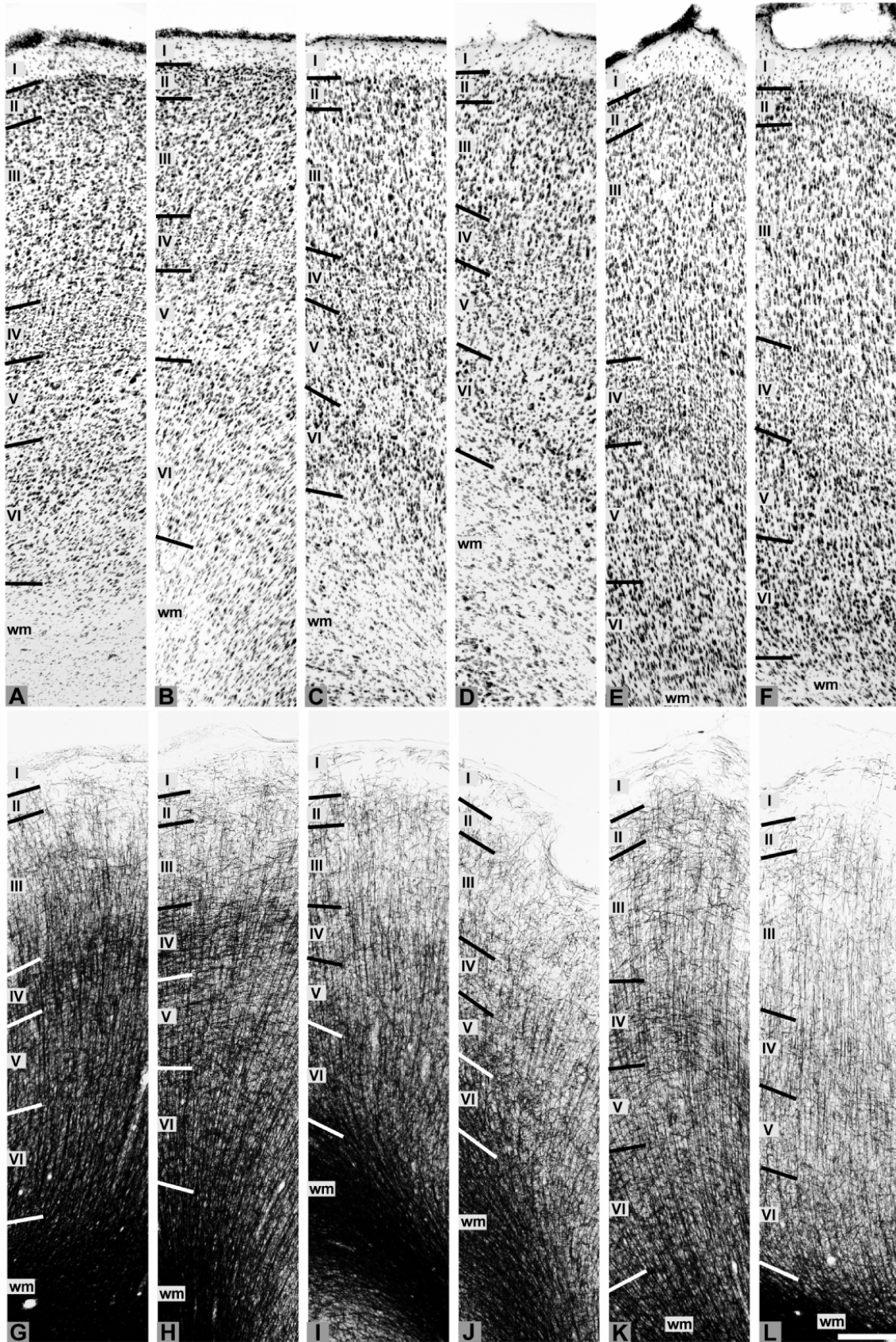
Myeloarchitecture of the lateral belt and parabelt regions

Compared to the core, myelin density in the lateral belt and parabelt regions was relatively weak in layers III and Va, revealing a prominent band of horizontal fibers in layer IV, and a weaker band in layer Vb (Figs. 6e-h, 7, 10g-l). Like the core and medial belt regions, myelin density decreased from caudal to rostral in both the lateral belt (Fig. 10g-j) and parabelt (Fig. 10k-l). In CL, the outer horizontal stria in layer IV was prominent against dense radial fibers that extended well into layer III. A secondary horizontal band in Vb was also apparent, but less prominent due to a dense network of fibers in the infragranular layers. In ML, the density of myelinated fibers was reduced overall, but the layer IV band remained prominent. In AL, horizontal fiber density was greatly reduced compared to CL and ML, along with greater spacing between radial fascicles. This reduction continued into RTL, which had very weak fiber organization in layer III. In the parabelt, the radial appearance noted in the cytoarchitecture was matched by the strong radial orientation of myelinated fibers that extended from layer VI through layer III and into layer II (Fig. 10k-l). Horizontal fibers formed clear bands in layer IV of the CPB, compared to weak horizontal organization in RPB.

Chemoarchitecture of the lateral belt and parabelt regions

The main finding in the lateral belt and parabelt areas was a dramatic reduction in the expression of CO and parvalbumin in the layer III/IV band compared to the adjacent core areas (Figs. 5, 6i-j, 8c-d). The expression of CO in this band diminished rostrally in both regions. Parvalbumin expression was weaker in the parabelt than lateral belt (Fig. 8).

Otherwise, there were no clear differences between or within the lateral belt and parabelt regions with respect to these markers.

Cytoarchitecture of the medial belt region

The cytoarchitecture of the medial belt region and adjoining fields varied reliably between areas. The most distinctive area was CM, which bordered A1 medially and caudomedially, occupying most of the superior temporal plane caudal to A1 (Fig. 4b-c). CM was characterized by a population of medium-sized pyramidal cells with poor radial alignment concentrated in the lower half of layer III (Fig. 11a). Layer III was broad compared to layers IV through VI, but cortical thickness was reduced relative to $A1_M$. Layer IV was narrow compared to A1, and populated by stacks of granule cells arranged in broad columns. Layer V was densely populated by small to medium-sized cells. The cytoarchitecture of the rostral medial belt areas was more like the lateral belt areas than CM (Fig. 11b-c). Area RM was located medial to area R and rostral to the narrow extension of CM medial to A1, while RTM was medial to RT (Fig. 4c-d). Layer IV was reduced in width compared to the neighboring core areas, highlighted by thin strings of granule cells arranged in broadly-spaced columns. Layer III was populated by orderly columns of small to medium sized pyramidal cells that contrasted sharply with their disorganized counterparts in CM. The broader columnar spacing in RM and RTM was a key feature in their distinction from R and RT. Cell spacing in RTM was slightly greater than RM. Medial to CM was the retroinsular area (Ri), which occupied the fundus of the lateral sulcus. It extended onto the lower bank of the medial LS for about 0.5 mm and bordered the second somatosensory area, S2, on the upper bank (Fig. 4c-d, 6a-b). In the
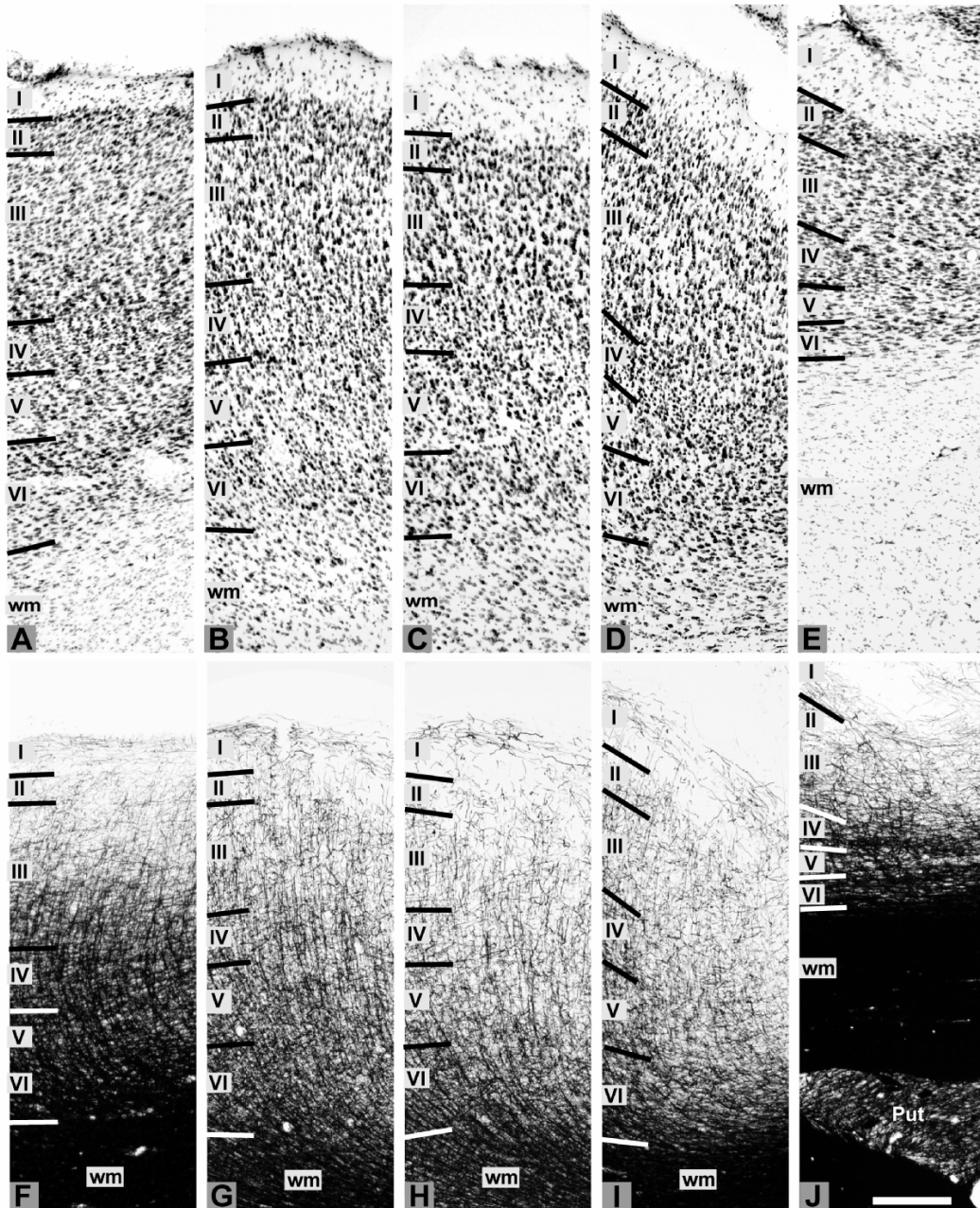
Figure 11. Cytoarchitecture and myeloarchitecture of marmoset auditory cortex, medial belt region and adjoining areas. *Top*, thionin stain for Nissl. *Bottom*, corresponding section, myelin stain. (A, F) area CM; (B, G) area RM; (C, H) area RTM; (D, I) area Pro; (E, J) area Ri. Cortical layers indicated by Roman numerals I - VI. WM, white matter. Scale, 250 μm.

mapping experiments involving this same group of animals, we often observed robust

responses to cutaneous somatosensory and vibratory (Pacinian-like) stimulation in Ri, but

no clear auditory responses (Kajikawa et al., 2005). The cytoarchitecture of Ri was characterized by a dramatic reduction in cortical width reflecting compression across laminae (Fig. 11e). Columnar spacing in Ri was greater than in CM. Layer III contained a uniform distribution of pyramidal cells, and a narrow layer IV contained broad stacks of granule cells. Layer V was somewhat cell-sparse, and layer VI contained numerous cells with horizontally-oriented dendrites. RTM may wrap around the rostral end of RT to join RTL on the lateral surface of the STG, but at this level the architecture of the temporal polar region was quite uniform, and so this observation remains tentative. Medial to RM and RTM was another area that separated these areas from the insular cortex (Fig 3d, 5c-d). We adopted the name "Pro", since it appeared to correspond to a similar field identified in macaque monkeys (Galaburda and Pandya, 1983). Compared to RM and RTM, cell density was reduced in Pro overall. Layers IV and V became very narrow in their transition toward the insula (Fig. 10d). Pro was consistently labeled by injections of core and medial belt areas in this study, and may therefore comprise part of the auditory cortex.

Myeloarchitecture of the medial belt region

The myeloarchitecture of CM complemented its cytoarchitecture. Thick radial fascicles ran between cell columns, crossed by a dense plexus of horizontal fibers from layer VI to the middle of layer III (Figs. 7, 11f). The density of this nearly astriate pattern was only slightly reduced compared to A1. However, reduced density in the upper part of layer III, reduced cortical thickness, and coarse appearance of the broadly-spaced radial fibers allowed for reliable identification of CM. Medial to CM, area Ri was dominated by

horizontal fibers, especially in layers IV and VI (Fig. 11j). These bands were crossed by broadly-spaced thick radial fascicles that extended into layer III. Rostral to CM, myelin density in the medial belt was greatly diminished (Fig. 6e-h). In RM and RTM radial fibers were broadly-spaced, and horizontal fiber organization was greatly reduced compared to CM and R or RT (Fig. 11g-h). Myelin density was weakest in RTM due to broad columnar spacing and sparse horizontal fibers. These features were even weaker in Pro (Figs. 6g-h, 11i).

Chemoarchitecture of the medial belt region

As briefly noted above, CO expression was comparable in the layer III/IV band of both $A1_M$ and CM (Figs. 5, 6i-j, 8d), thus reliable identification of CM depended mainly on analysis of the cyto- and myeloarchitecture. Parvalbumin expression was also moderately dense in CM (Fig. 8c). Rostrally, in RM and RTM, CO expression was relatively weak, comparable to that of the lateral belt areas. AChE and parvalbumin expression in the layer III/IV band was also similar to the lateral belt and parabelt areas. By comparison to RM and RTM, therefore, CM was rather primary-like due to dense myelination and expression of CO and parvalbumin.

Connections of medial belt and core areas

Ipsilateral connections of CM

In case 3 the CTB injection was made into the part of CM that caps A1 caudally (Fig. 12). In the most caudal sections (#165 – 177) labeled cells and terminals were concentrated in the supragranular and infragranular layers of CM, while in Ri, there was

53

Figure 12. Ipsilateral cortical connections of area CM, case 3. Series of serial sections are arranged from caudal (upper left) to rostral (lower right), and continue onto the next page. Labeled cells (filled circles) and terminals (shading) are drawn onto each section, showing borders between areas identified by architectonic criteria. *Inset*, schematic of marmoset auditory cortex showing location of CTB injection in caudal CM.

Figure 12 (continued)

no clear evidence of anterograde projections to any layer. Labeling in CL was

concentrated in layer II. The distribution of labeling did not extend beyond Ri dorsally

into S2, but stopped cleanly at the border. With the emergence of A1 (#189 – 201),

labeled cells and terminals spanned supragranular and infragranular layers of Ri, CM,

ML, and A1. Further rostrally (#213 – 255), connections with A1 weakened significantly,

especially with A1$_M$, while connections with CM, Ri, ML, and CPB remained strong. In

ML and CPB, labeling was concentrated in columnar patches where strong anterograde

projections overlapped clusters of retrogradely labeled somata. A column of terminals

and cells also overlapped in A1$_L$ over part of this range. The absence of connections with

A1$_M$ formed a prominent gap between the lateral and medial belt regions, as viewed in

the coronal plane (Fig. 13). Variants of this pattern characterized all medial belt
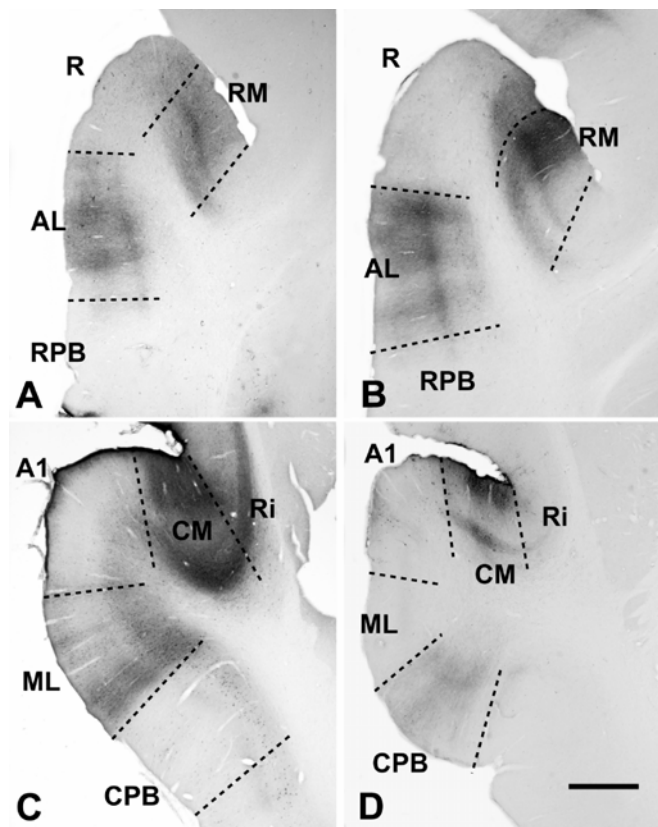
Figure 13. Columns of labeled cells and terminals overlap in the medial and lateral belt regions after BDA injections of RM and CM. Labeling in the intervening core region is absent or greatly attenuated forming a continuous gap that spans the rostrocaudal axis of auditory cortex. (A) CTB-labeling in RM and AL rostral to RM injection. Note dense focus of anterograde label in layer IV of RM. Case 2, #263. (B) CTB-labeling in RM and AL just rostral to RM injection. Dense anterograde projections to layer IV are visible in RM and AL. Case 1, #69. (C) CTB-labeling in CM, Ri, and ML after large CM injection. Label in A1 and CPB is mostly infragranular. Case 7, #129. (D) BDA-labeling in CM and CPB after CM injection. Weak labeling is visible in A1L. Case 8, #176. Scale bar, 1 mm.

injections in this study, as described below. Near the border of A1 and R (#255), labeling in ML and CPB weakened and was concentrated in the infragranular layers. Labeled cells were dense in Ri, whereas only scattered cells remained in A1 and CM. Rostrally, at the level of R and RT (#267 – 327), the core and lateral belt areas were mostly devoid of labeled elements. Labeling in RM did not persist beyond the A1/R border region. Labeled cells were consistently observed in Pro over this range, and became increasingly infragranular. In RPB, labeled cells were also confined to the infragranular layers over this entire range. Outside of auditory cortex, cells were found ventral to RPB in the STS. Labeled cells in the lower layers of the entorhinal cortex (Fig. 14a) were distributed in a continuous band in sections rostral to the A1/R border (#267 – 327). Additional connections were revealed with parietal cortex caudal to the lateral sulcus. Labeled cells and terminals from a BDA injection not illustrated in the reconstructions of this case were concentrated in supragranular CM, as well as in Ri, and CL (Fig. 14b). Label was also found distributed lightly throughout the posterior belt and parabelt areas in this case, suggesting the caudal auditory cortex has significant connections with posterior parietal areas (Lewis and Van Essen, 2000).

In cases 6, 7, and 8 the injection was made along the narrow extension of CM that borders A1 medially. In case 6, the injection was made directly into medial CM just caudal to its border with RM (#128) while the upper bank was retracted (Fig. 15). The injection was fairly well confined to CM on the lower bank between Ri and A1$_M$. Unfortunately, a small amount of tracer appears to have diffused into the upper bank after the sulcus was allowed to close, leading to some labeling in the part of S2 opposing the injection site. Therefore, we cannot be certain whether the labeling observed in S2 in this
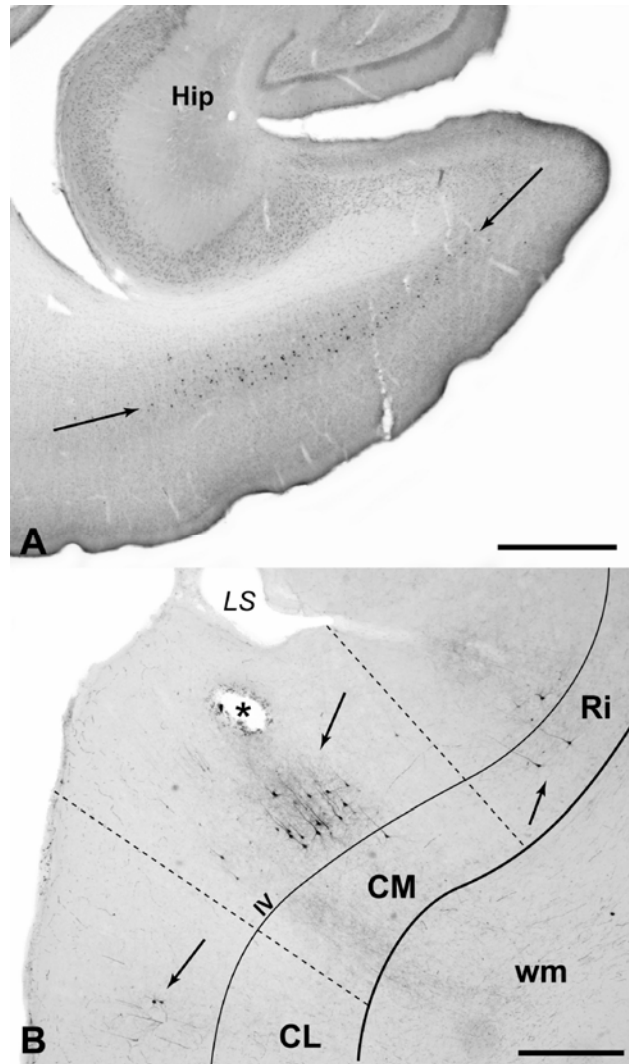
Figure 14. CM connections outside auditory cortex. (A) CTB-labeled cells (between arrows) in the lower layers of entorhinal cortex from CM injection. Cells were distributed in this region along most of the rostrocaudal axis of the auditory cortex after CM injections (see Figs. 9, 12). Injections of RM did not label cells in entorhinal cortex. Scale bar, 1mm. (B) Patches of BDA-labeled cells and terminals in Ri, CM, and CL (arrows) after an injection into posterior parietal cortex just caudal to the end of the lateral sulcus (LS). The concentration of cells and terminals in layer III of CM coincide with the CTB injection of CM (see case 3, #177). Asterisk marks the pipette track made by that CTB injection. IV, layer IV (thin line); wm, white matter. Dashed lines, borders between areas. Scale bar, 500 µm.
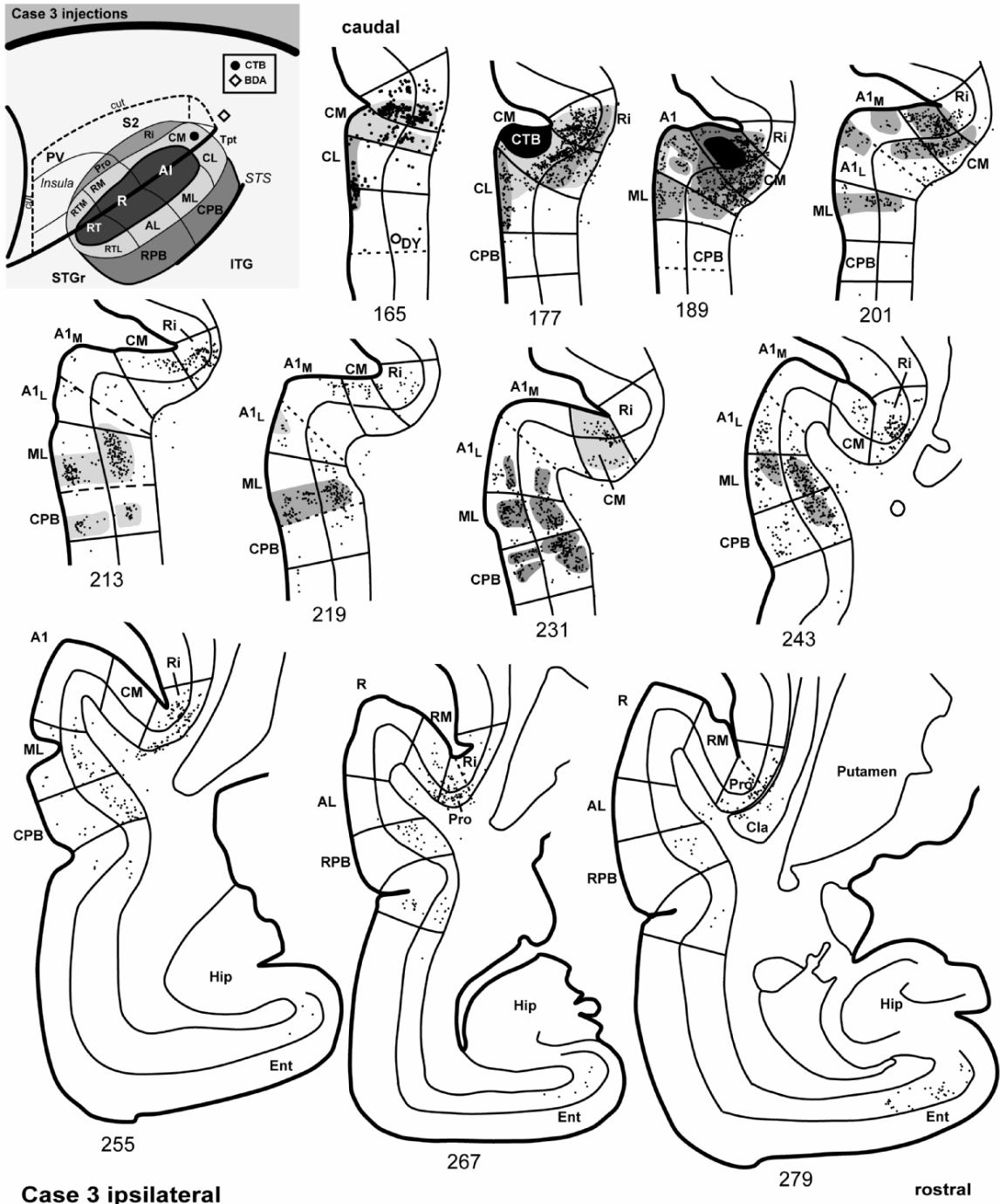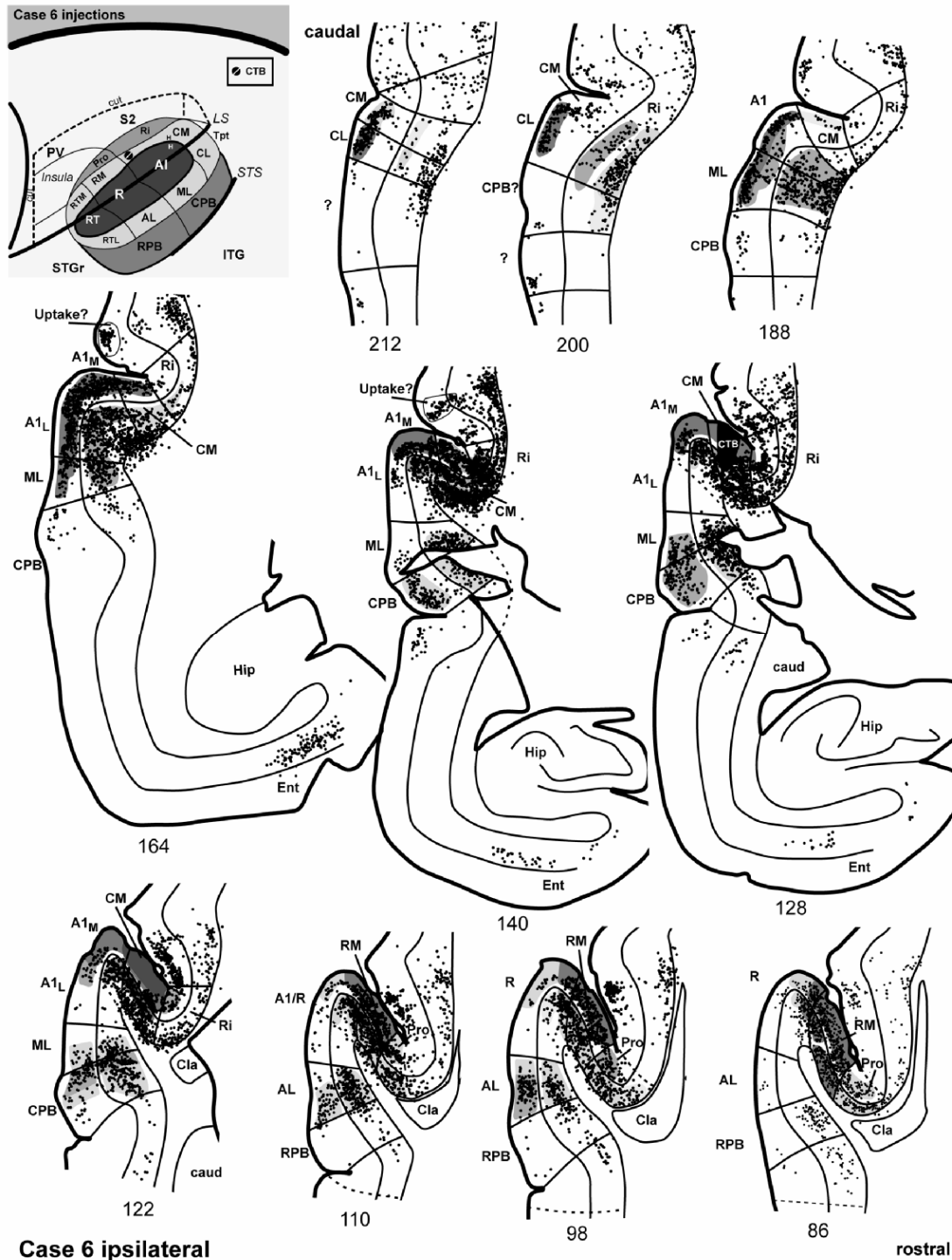
Figure 15. Ipsilateral cortical connections of area CM, case 6. Series of serial sections are arranged from caudal (upper left) to rostral (lower right), and continue onto the next page. Labeled cells (filled circles) and terminals (shading) are drawn onto each section, showing borders between areas identified by architectonic criteria. *Inset*, schematic of marmoset auditory cortex showing location of CTB injection in rostral CM.
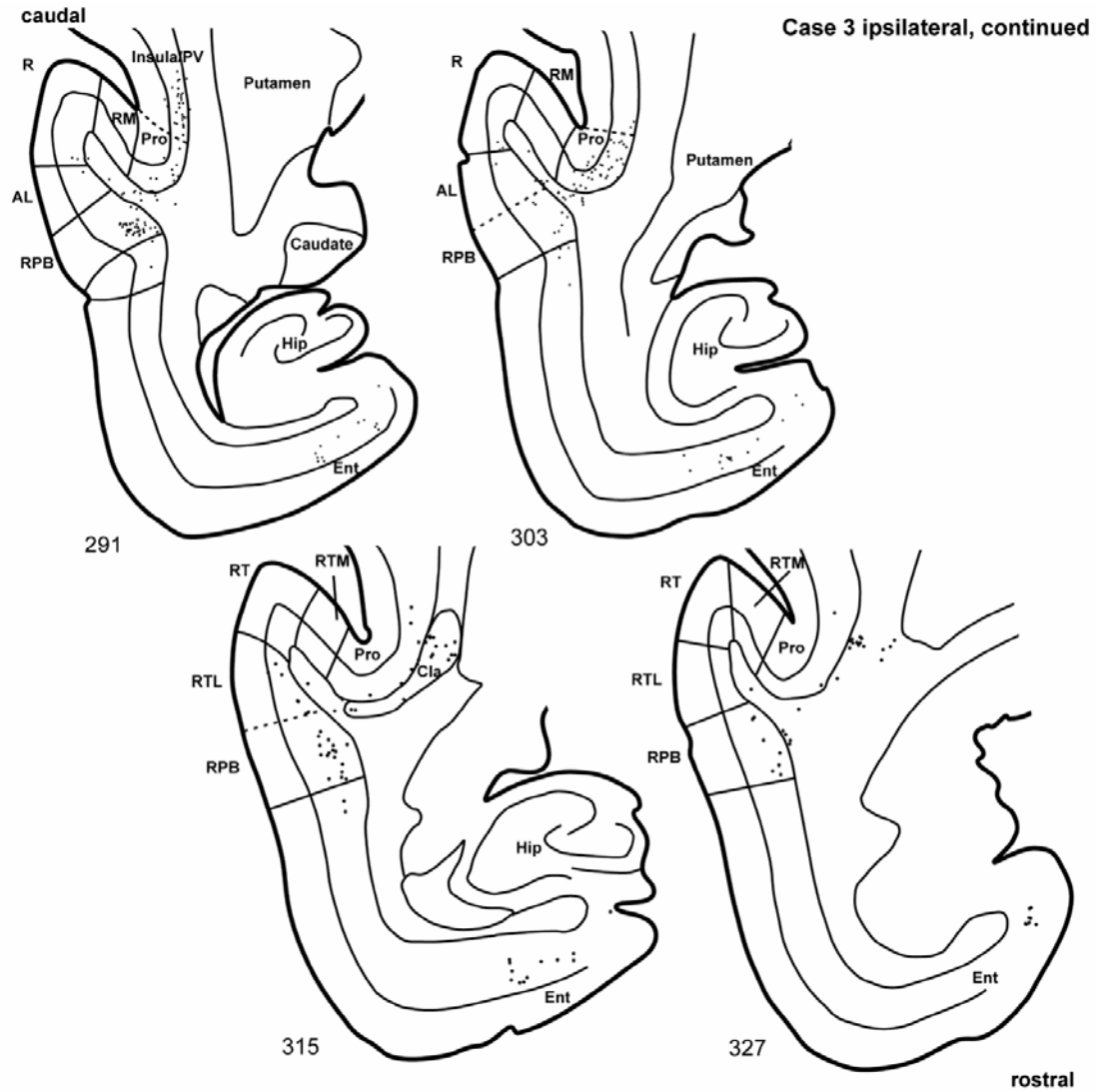
Figure 15 (continued)

case was due to the CM injection, diffusion across the sulcus, or both. In the most caudal

sections (#212 – 200) labeled cells and terminals were concentrated in CL and CM.

Distinct bands of dense anterograde labeling overlapped the labeled cells in layers II, III,

V, and VI, but avoided layer IV and the lower part of III. Cells were also found in Ri and

dorsally onto the surface of posterior parietal cortex. CL was bordered ventrally by a

region characterized by dense astriate myelination, possibly corresponding to the middle

temporal area, MT. While some labeling extended into this region, it did not appear to

coincide with CPB. At the level of A1 (#188 – 152), dense labeling was found in

supragranular and infragranular layers of A1, CM, and ML. Labeled cells in Ri and CPB

were less numerous caudally, but increased in numbers rostrally over this range closer to

the injection site. In this range (#152 – 122) the greatest concentration of labeled cells

and terminals was centered on CM and extended into Ri and $A1_M$, with secondary

labeling in CPB and ventrally in STS. By contrast, labeling in ML and especially $A1_L$

were greatly diminished, forming a notable gap between $A1_M$ and CPB (Fig. 8). With the

60

emergence of R (#110 – 74), dense labeling continued into RM and extended medially in to Pro. Labeling in R was moderate medially, but the lateral portion of R was nearly devoid of label. While this is reminiscent of the division of $A1_M$ and $A1_L$, an architectonic division of R was not obvious in most sections. In AL, labeled cells and terminals overlapped in supragranular and infragranular layers for most of its range, forming a gap comprising the lateral part of R. Labeling in RPB was mostly infragranular, as was labeling in the STS. Rostrally, labeling rapidly diminished in RTM and labeled cells in Pro were mostly infragranular. Labeling was moderate in RTL and RPB, favoring the lower layers. Weak labeling in RT (#62 – 50) maintained the gap between medial and lateral belts. Rostral to known areas of auditory cortex (not illustrated), scattered labeled cells persisted in the lower layers along the lateral STGr. Also outside of auditory cortex, labeled cells were broadly distributed in the lower layers of entorhinal cortex (#176 - 98), as in case 3 and with all CM injections.

In cases 7 and 8, injections of CM medial to A1 (reconstructions not illustrated) produced similar patterns to case 6. In case 7, the pattern of labeling was almost identical to case 6 (see Fig. 13c). However, the injection was made through overlying parietal cortex and labeled even larger numbers of cells in S2 and other posterior parietal areas on the lateral surface of the brain. In case 8, BDA was injected directly into CM after sulcus retraction. The injection was confined to the lower bank of the lateral sulcus with no diffusion into the upper bank. Despite a shortened survival time (3 days) in this case, labeled cells and terminals were distributed broadly throughout the auditory cortex in patterns that also matched case 6 (see Fig. 13d). By contrast, there were almost no labeled

cells beyond the borders of Ri or S2 in this case, suggesting that the labeling in S2 in

cases 6 and 7 was the result of diffusion of CTB into the upper bank.

Interhemispheric connections of CM

In case 3 the CTB injection into caudal CM was mirrored in the opposite

hemisphere in the most caudal sections (#195 – 171), where a dense focus of label was

centered in layer III of CM, with secondary labeling in the adjacent areas, Ri and CL

(Fig. 16). With the emergence of A1 (#171 – 159) rostrally, labeled cells were found in
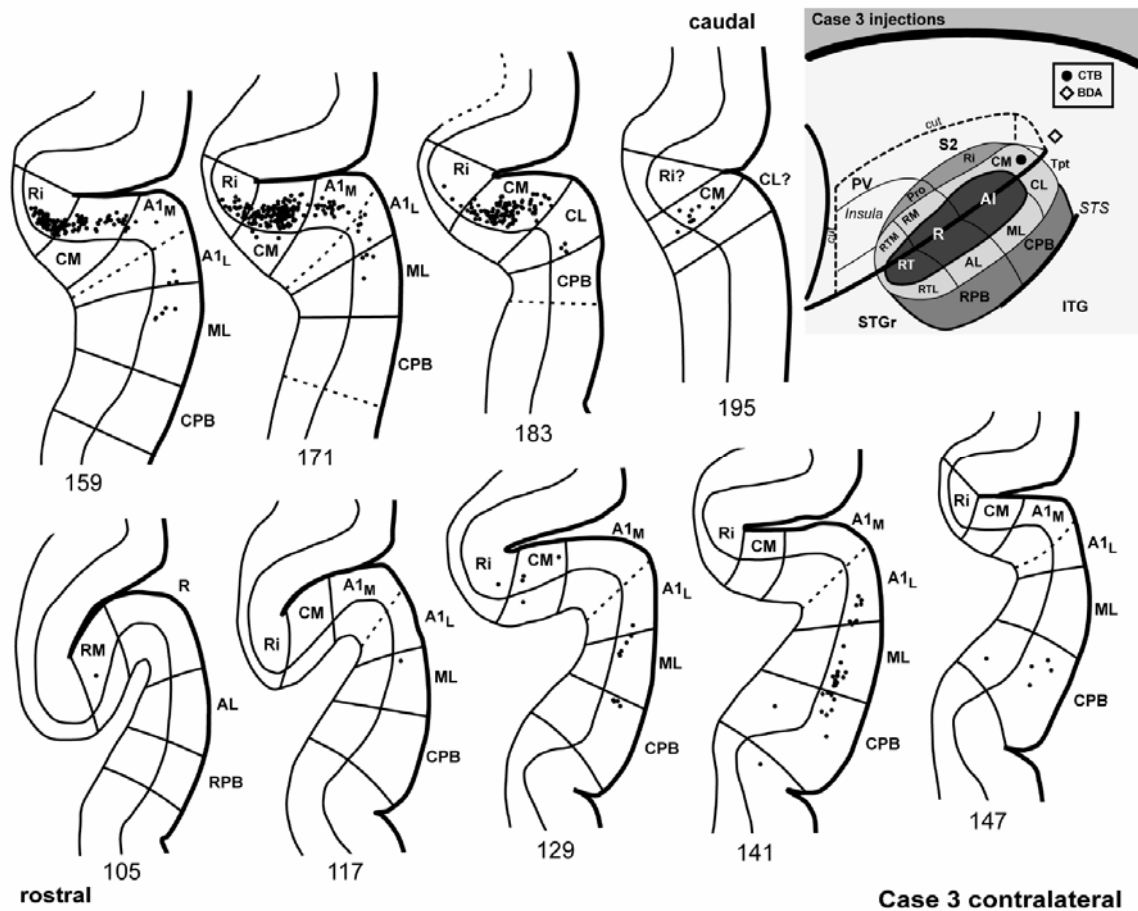
Figure 16. Interhemispheric cortical connections of area CM, case 3. Series of serial sections are arranged from caudal (upper right) to rostral (lower left). Labeled cells (filled circles) and terminals (shading) are drawn onto each section, showing borders between areas identified by architectonic criteria. *Inset*, schematic of marmoset auditory cortex showing location of CTB injection in caudal CM in the contralateral hemisphere.

A1 and ML, but remained concentrated in CM and Ri. Further rostral (#147 – 117) labeled cells were distributed widely across A1$_L$, ML and CPB, but dropped to almost zero in Ri and CM. Labeling stopped abruptly rostral to the A1/R border (#105).

In case 6 few labeled cells were found in contralateral CM, CL, and Ri of the most caudal sections (#206 – 164), reflecting the more rostral placement of the injection within CM in the opposite hemisphere (Fig. 17). Instead, overlapping cells and terminals were concentrated more laterally in layer III of CM and A1. Nearer the homotopic location of the injection site at section (#128), labeled cells became more numerous in CM and Ri, but diminished in A1 (#152 – 140). Rostrally, at the border of A1 and R, labeling continued to dominate in CM, extending into RM, with additional cells appearing in Pro (#116 – 104). Thereafter, the number of labeled cells in RM tapered off until no more cells were found (#92 – 80). An example of overlapping cell and terminal labeling in the contralateral hemisphere is shown in figure 18, associated with the CTB injection in this case. Anterograde banding extended from layer III into layer I across some columns in CM. A cell-sparse band of terminal labeling distinguished layer V of CM in this section. Terminal labeling in A1 and Ri was relatively light.

Summary of CM connections

Injections into CM caudal to A1 and CM medial to A1 revealed similar patterns of connections overall, with some interesting differences reflecting topographic variations (Fig. 19, left). For all locations in CM, the strongest connections involved the caudal areas of auditory cortex and surround, including A1, ML, CL, CPB, Ri, and other portions of CM. Connections with rostral areas of auditory cortex were topographic,
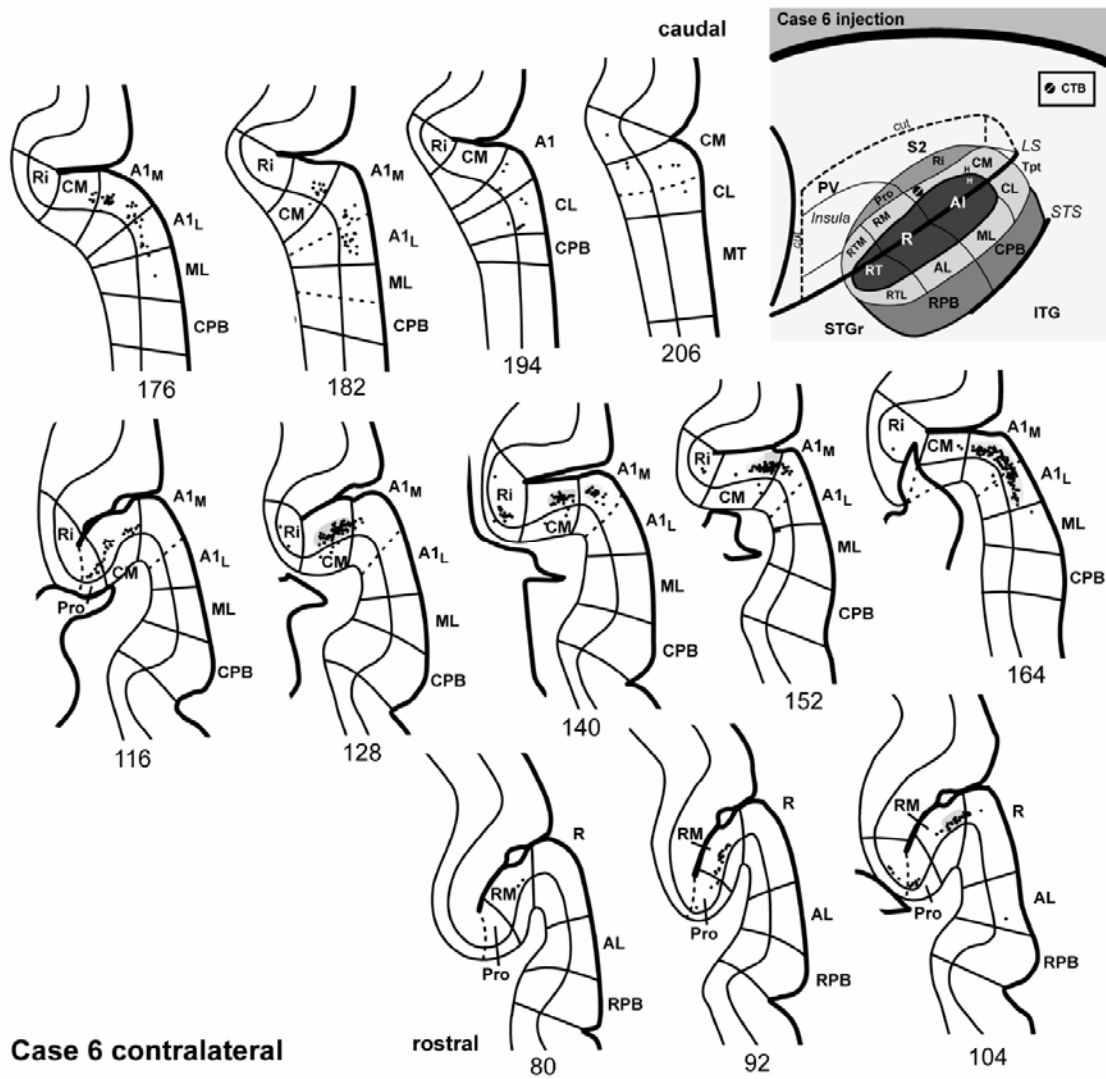
Figure 17. Interhemispheric cortical connections of rostral area CM, case 6. Series of serial sections are arranged from caudal (upper right) to rostral (lower left). Labeled cells (filled circles) and terminals (shading) are drawn onto each section, showing borders between areas identified by architectonic criteria. *Inset*, schematic of marmoset auditory cortex showing location of CTB injection in rostral CM in the contralateral hemisphere.
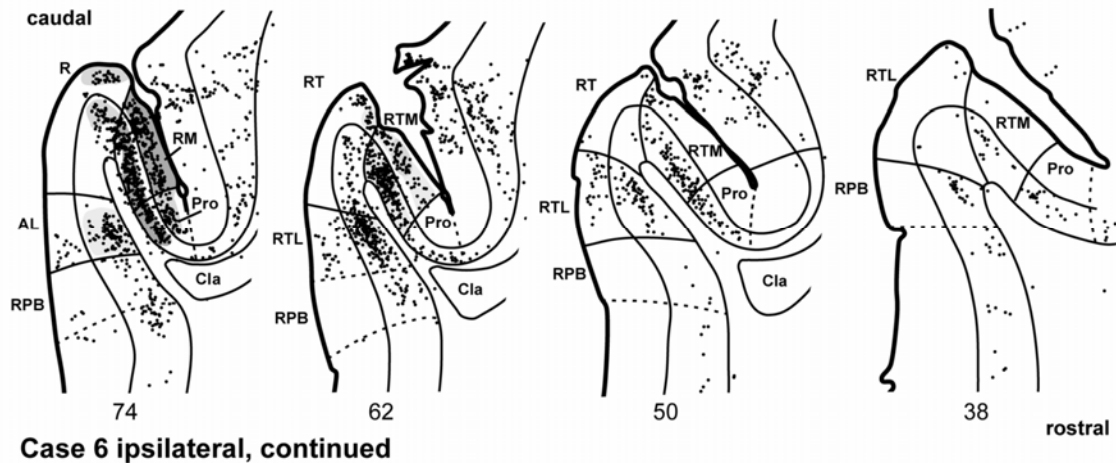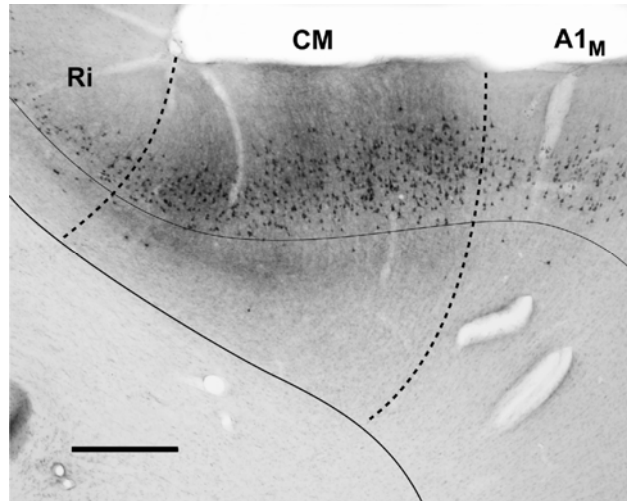
Figure 18. CTB-labeled cells and terminals in Ri, CM, and A1M contralateral to the injection of CM (case 7). Labeled cells are concentrated in layer III of all areas. In CM, terminals formed bands in layers III and V, and also radial columns that spanned layers I - III. Scale bar, 500 µm.

depending on the location of the CM injection, and favored projections to CM from cells in the infragranular layers. Caudal CM had relatively weak connections with RM and Pro, mostly infragranular projections from RPB, and almost no connections with the most rostral areas at the level of RT, including RT, RTM, and RTL. Rostral CM had strong reciprocal connections with RM, Pro, R, and AL. Connections with RT were minimal, and connections with RTM, RTL, and RPB tended to become infragranular-dominant with distance from the injection site. Both rostral and caudal sites in CM exhibited continuous reciprocal connections within CM that extended into RM, although injections of rostral CM resulted in a greater extension of labeling into RM and RTM. This was consistent with weak connections with caudal CM observed after injections of RM (see below). All locations in CM had strong reciprocal connections with parts of A1, but an interesting topographic pattern was revealed involving the core. Caudal CM had broad connections with $A1_L$ and $A1_M$ caudally, weak connections with rostral $A1_M$, and no
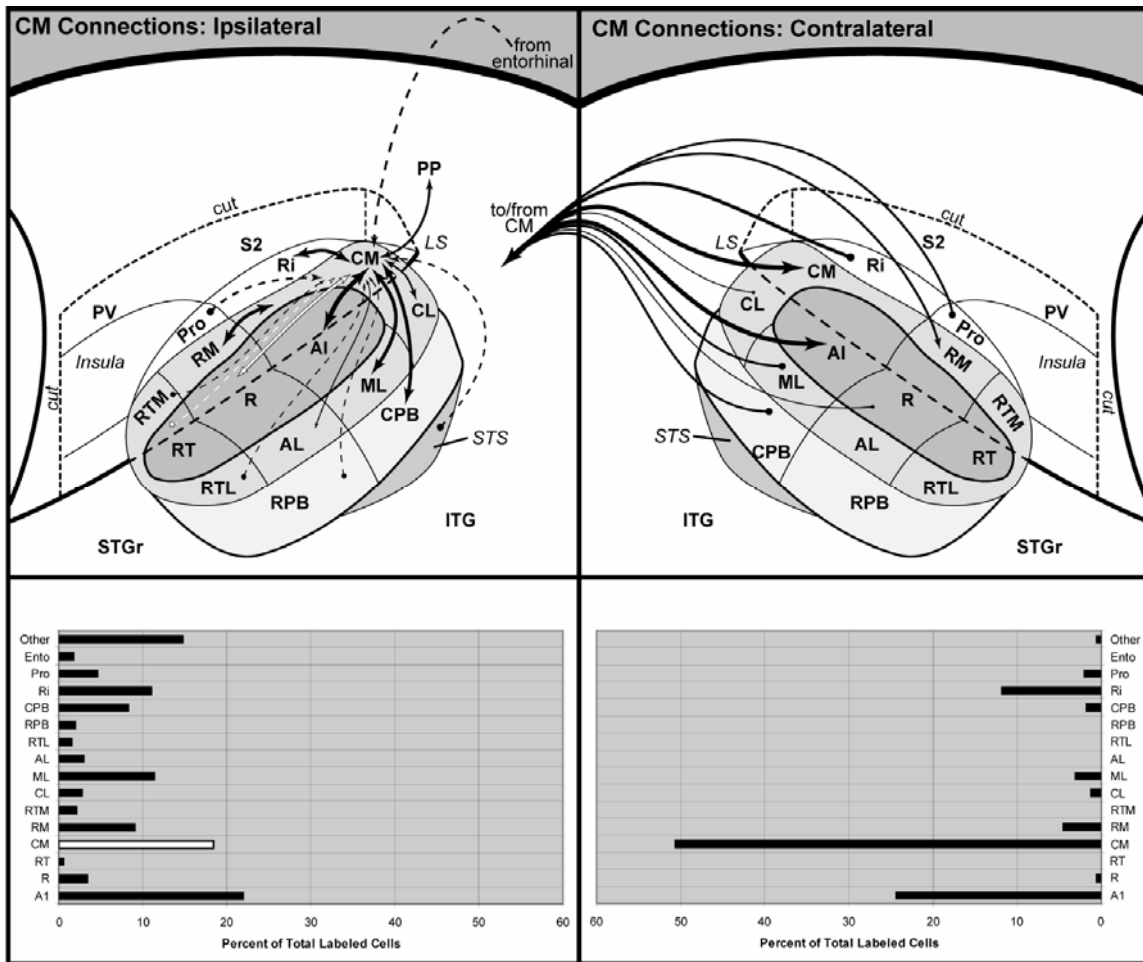
Figure 19. Summary of ipsilateral (left) and interhemispheric (right) connections of CM. Top panels illustrate connections (arrows) of CM on schematic diagram of marmoset auditory cortex. Arrow size is proportional to connection strength, as indicated in the histograms below each panel. Double arrows indicate reciprocal connection. Single arrows indicate unidirectional projections. Dashed lines indicate infragranular projection. White arrows (R, RT) indicate connections with CM confined to medial half of each area. Summary does not reflect absent infragranular projections observed in rostral fields after caudal CM injection (case 3, see text). *Bottom left*, white bar indicates that cell counts for ipsilateral CM may be inaccurate (deflated) due to masking by the tracer injection.

connections with R or RT. Rostral CM had strong connections only with the medial

halves of A1, R, and RT near the injection and rostrally, but dense broad connections

with $A1_M$ and $A1_L$ caudally. Thus, the contrast between continuous label in the lateral

and medial belt coupled with the absence of label in parts of the core formed elongated

gaps between the lateral and medial belt regions along the rostrocaudal axis of auditory cortex. A comparable pattern was also observed after injections of RM (see below).

Beyond auditory cortex, connections were consistently found with cortex in the lower layers of STS and the entorhinal cortex. There was no clear evidence of an anterograde projection from CM to either of these regions. Connections with somatosensory cortex were clearly established with Ri, but connections with S2 and other somatosensory areas remain uncertain. Finally, moderate numbers of labeled cells were consistently observed in posterior parietal cortex after CM injections, indicating a reliable connection with areas in that region.

The interhemispheric connections of CM (Fig. 19, right) favored contralateral CM, and additional strong connections with A1 and Ri. The connections with CM and A1 were largely reciprocal. Other connections included inputs from RM, Pro, and a weak projection from ML. Connections with all areas were concentrated in layer III.

Ipsilateral connections of RM

In case 1 tracer injections were made into RM, R, and AL after multiunit recordings were used to identify the reversal in the tonotopic gradient between areas A1 and R (Fig. 20a). The BDA injection was made into RM by a vertical penetration that passed through the overlying parietal cortex 0.5 mm medial to the edge of the lateral fissure at AP +10 mm. This was accompanied by cell and terminal labeling of somatosensory cortex not observed in case 2 in which the injection was made directly into RM after sulcus retraction. The injection site was poorly responsive to pure tones, but responded well to 1/3-octave bandpass noise, with a best center frequency of 6.9 kHz.

Figure 20. Ipsilateral cortical connections of areas RM and R, case 1. Series of serial sections are arranged from caudal (upper left) to rostral (lower right), and continue onto the next page. BDA-labeled cells (filled squares) and terminals (shading) are drawn onto each section, showing borders between areas identified by architectonic criteria. Cells labeled by FR (open triangles), FE (open circles), and double-labeled cells (asterisk). FE and FR injections indicated by dashed outlines in sections 144, 159. FB*, location of FB injection extending into white matter below area ML (not plotted). *Inset*, schematic of marmoset auditory cortex showing location of BDA injection in RM, FR in medial R and FE in lateral R.
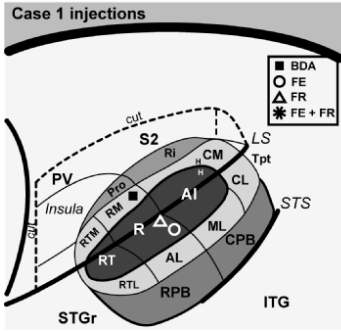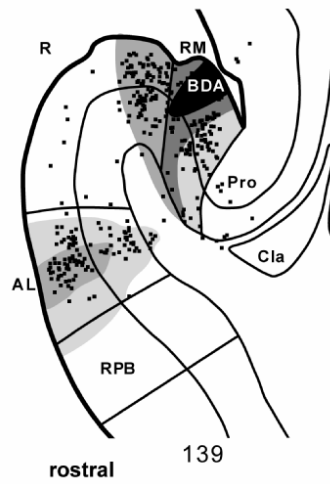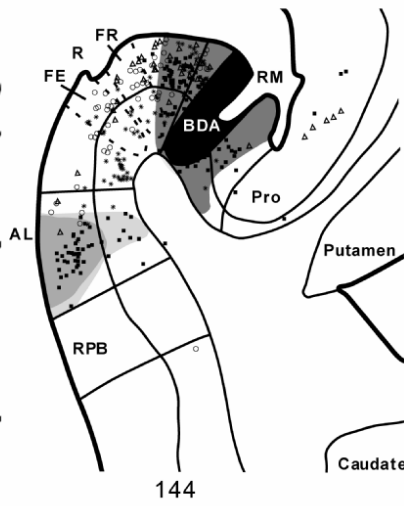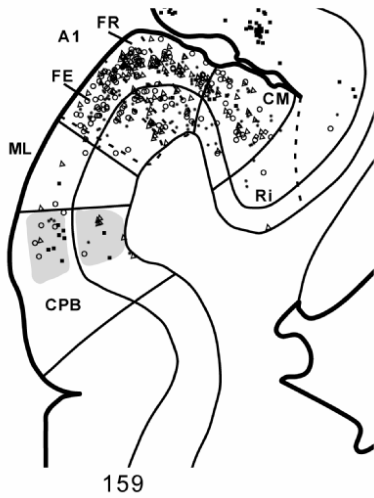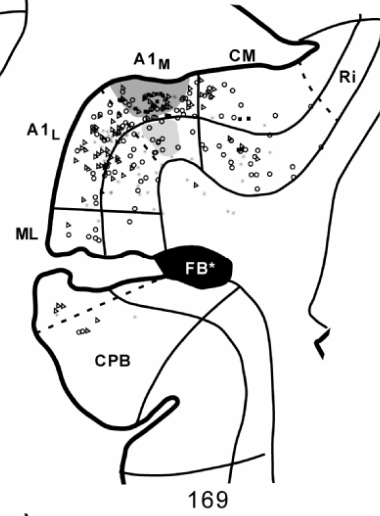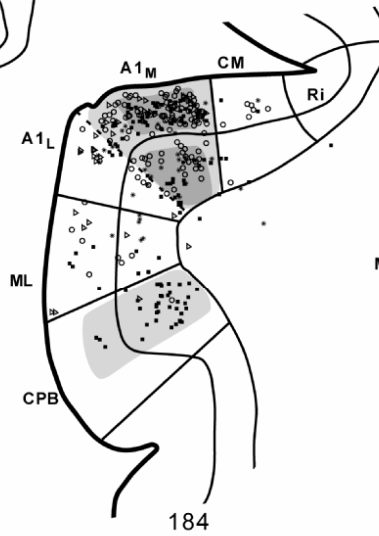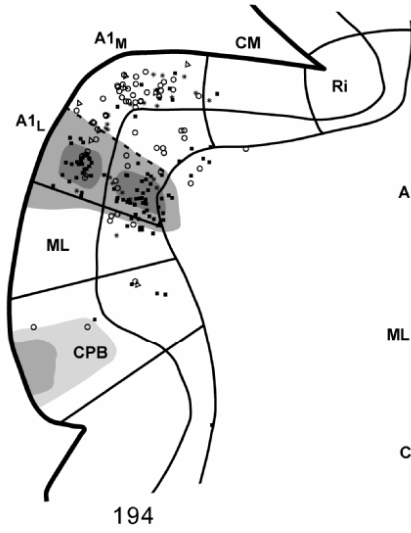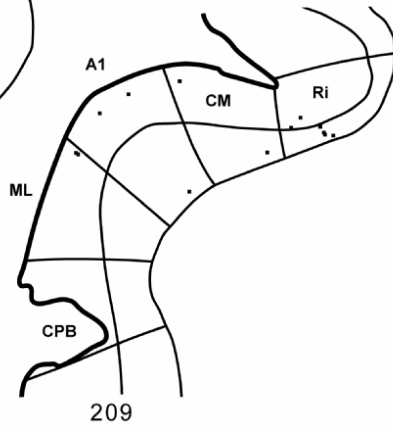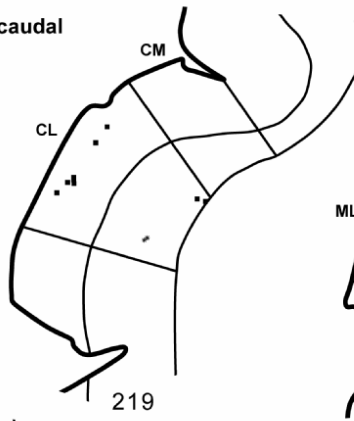
Case 1 ipsilateral
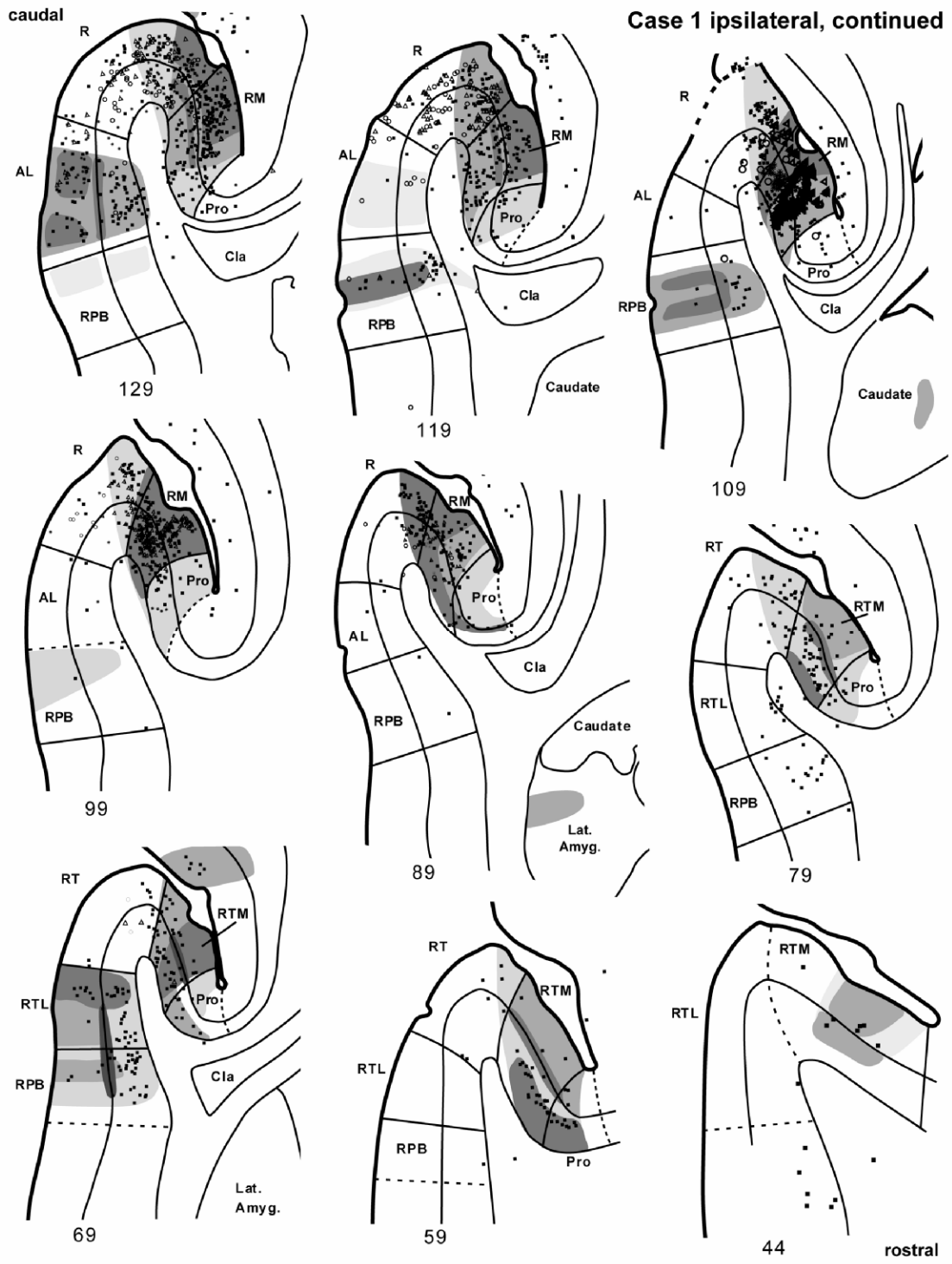
Figure 20 (continued)

In the most caudal sections near the caudal edge of A1 (#219 – 209), labeled cells were scattered in A1, ML, CL, CM, and Ri. Rostrally, as A1 emerged (#194), a dense focus of labeled cells and terminals labeled the lateral division of A1 ($A1_L$) in the infragranular and supragranular layers, while the medial part of A1 ($A1_M$) contained a few supragranular cells. This patch was separated from a secondary patch of label in supragranular CPB by ML, which was mostly devoid of label (Fig. 8). In a series of sections rostral to this zone (#184 – 159), the concentration of labeled cells and terminals in CPB was slightly greater in the infragranular layers. In $A1_M$ at this level, labeled terminals were both infragranular and supragranular, while labeled cells were more numerous in layer III. CM also contained a few labeled cells. In section #144 the RM injection spanned all cortical layers, stopping just short of the white matter in lateral RM. The diffusion zone appeared to include the medial edge of R, although labeling in R did not extend significantly beyond this point. The appearance of labeled cells in the ventral medial geniculate (MGv) of this case suggested that there was some involvement of medial R (de la Mothe et al, 2006b). Dense labeling continued in RM for about 2 mm to its rostral terminus near section #89, where lighter connections continued in RTM. By contrast, R and parts of AL were nearly devoid of label across this range, forming an elongated gap between the medial and lateral belt regions (Fig. 13). The heaviest connections within RM included the supragranular and infragranular layers with a lighter band of anterograde projections in layer IV. Labeled cells were consistently found medial to RM and RTM in Pro, between the medial belt and insula, where labeled cells were usually infragranular. Along part of this range (#144 – 119) a dense patch of labeled cells and terminals was located in supragranular and infragranular AL. Anterograde terminal

71

labeling in AL was densest in a cell-free band corresponding to layer IV. As this patch

diminished (#119), a different patch of labeled cells and terminals began to emerge in

RPB, which became quite dense over several sections (#119 – 99). Anterograde

projections to RPB favored the supragranular layers, although the terminal band in layer

IV remained prominent. A focal projection to the ventral caudate nucleus (Fig. 21c-d)
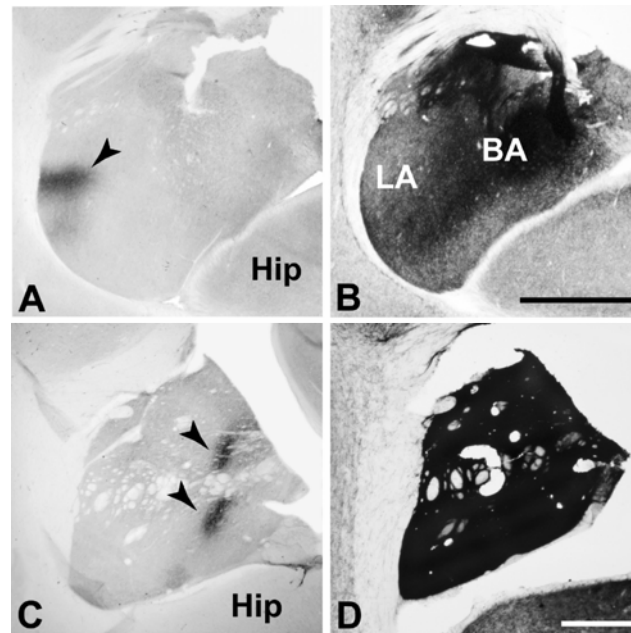
Figure 21. Anterograde BDA projections (arrows) to subcortical structures from RM
injection (case 1). (A) Patch of BDA-labeled terminals in lateral nucleus of the amygdala.
(B) Acetylcholinesterase (AChE) stain of section corresponding to panel A. (C)
Elongated strip of BDA-labeled terminals in the ventral caudate nucleus. (D) AChE stain
of section corresponding to panel C. BA, basal nucleus of the amygdala; Hip,
hippocampus. Scale bars, 1 mm (A & B); 2 mm (C & D).

was also present in several of these sections (#129 –109). In the most rostral sections

(#69 – 44), the strongest labeling was within RTM. While terminals and cells were in

both supragranular and infragranular layers, layer IV received the densest terminal

projection. Labeled cells were more numerous below layer IV. RT had almost no

labeling, maintaining the gap between the medial and lateral belts observed caudally. In presumptive RTL, a dense focus of label was contained across cortical layers, with a dense terminal band in layer IV. A separate patch of label with similar connections was located in RPB. A focalized projection to the lateral nucleus of the amygdala (Fig. 21a-b) was present in a few rostral sections (#89 – 79).

In case 2 BDA was injected directly into RM after retraction of the lateral fissure (Fig. 22). The injection extended across all cortical layers and labeled cells in the core, belt, and parabelt regions. In this same case, other areas were injected with different tracers (R, CL/A1), as reflected in the reconstructions. In the most caudal section (#131), a patch of labeled cells and terminals overlapped in $A1_L$ at its border with ML, similar to case 1. Rostrally, (#143 – 155), a patch of label was found in $A1_M$, with weaker extension into CM. Labeling in CM increased rostrally (#161) as the border with RM neared. Just caudal to the border of A1 and R (#173), labeled cells and terminals were concentrated in CM. Layer III contained most of the labeled cells, but anterograde labeling was heavy in both supragranular and infragranular layers. Weaker cell and terminal labeling extended into $A1_M$. Lighter labeling was contained within CPB at this level, as in case 1. Further rostrally (#185 – 197), labeling was strong in RM, the medial portion of R, and RPB. These two zones were separated by sparse labeling in the intervening cortex, corresponding to AL and the lateral portion of R, where a different tracer injection was located. The patch of intense label in RPB extended across the cortical layers for about 1.5 mm along the rostral-caudal axis of the sulcus. The RM injection was located rostral to this zone (#215 – 227). The heaviest label remained in RM, but also included the medial portion of R and Pro, located between RM and the insula. The injection may have

73

Figure 22. Ipsilateral cortical connections of areas RM and R, case 2. Series of serial sections are arranged from caudal (upper left) to rostral (lower right), and continue onto the next page. BDA-labeled cells (filled squares) and terminals (shading) are drawn onto each section, showing borders between areas identified by architectonic criteria. FR-labeled cells are indicated by open triangles. Hatching, diffusion and local tissue damage from FB injection involving CL and A1 (cells not plotted). *Inset*, schematic of marmoset auditory cortex showing location of BDA injection in RM and FR injection in lateral R.

Case 2 injections

BDA
FR

S2
PV
cut
Ri CM
CM
Tpt
Pro CL
RTM RM AI
Insula R ML
RT CPB
AL STS
RTL RPB ITG
STGr

caudal

A1
FB
CM
Ri
ML
CPB
131

A1
CM
Ri
ML
CPB
143

A1M CM
A1L Ri
ML
CPB
155

A1M CM
A1L Ri
ML
Cla
CPB
161

A1 CM
ML
Cla
CPB
173

R RM
FR
AL Cla
RPB
185

R RM
FR
AL Pro
Cla
RPB Caud
197

rostral

Case 2 ipsilateral

75
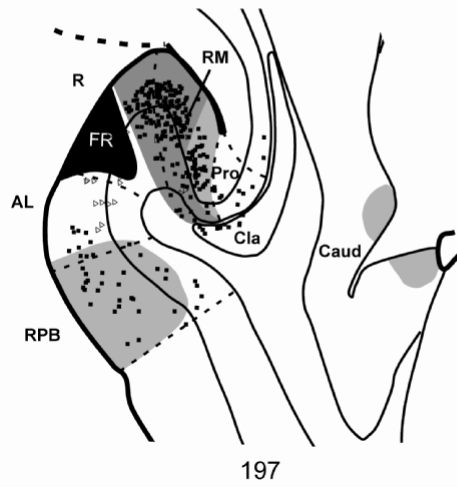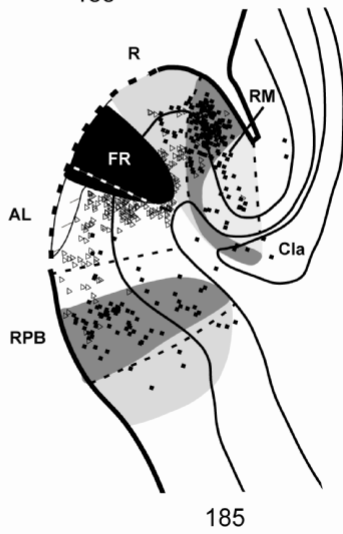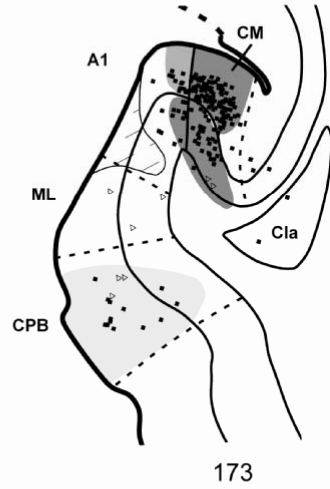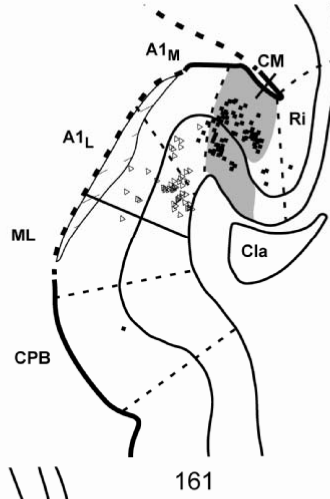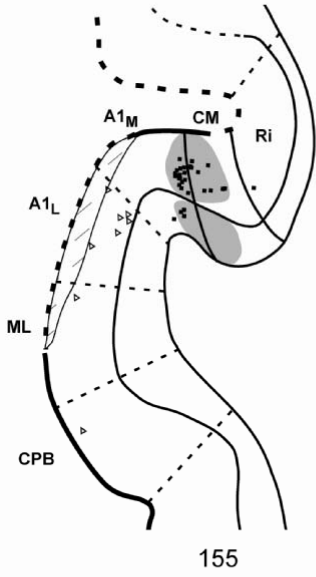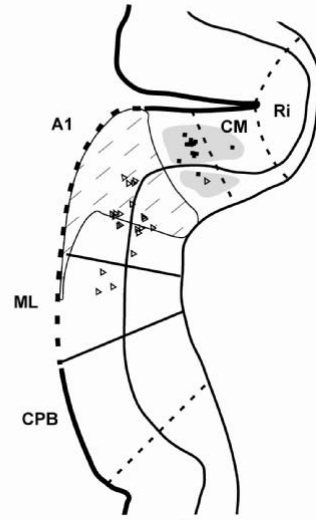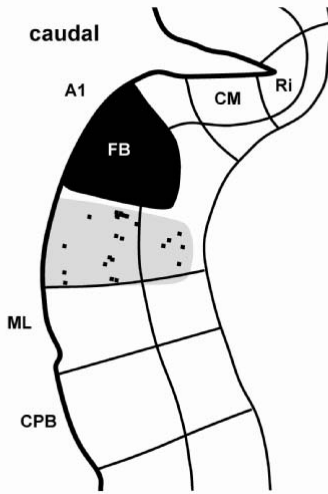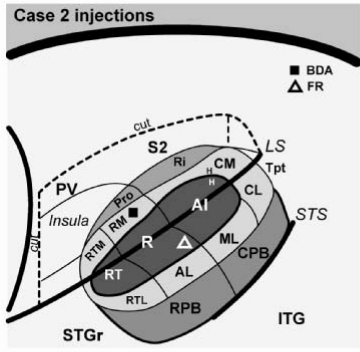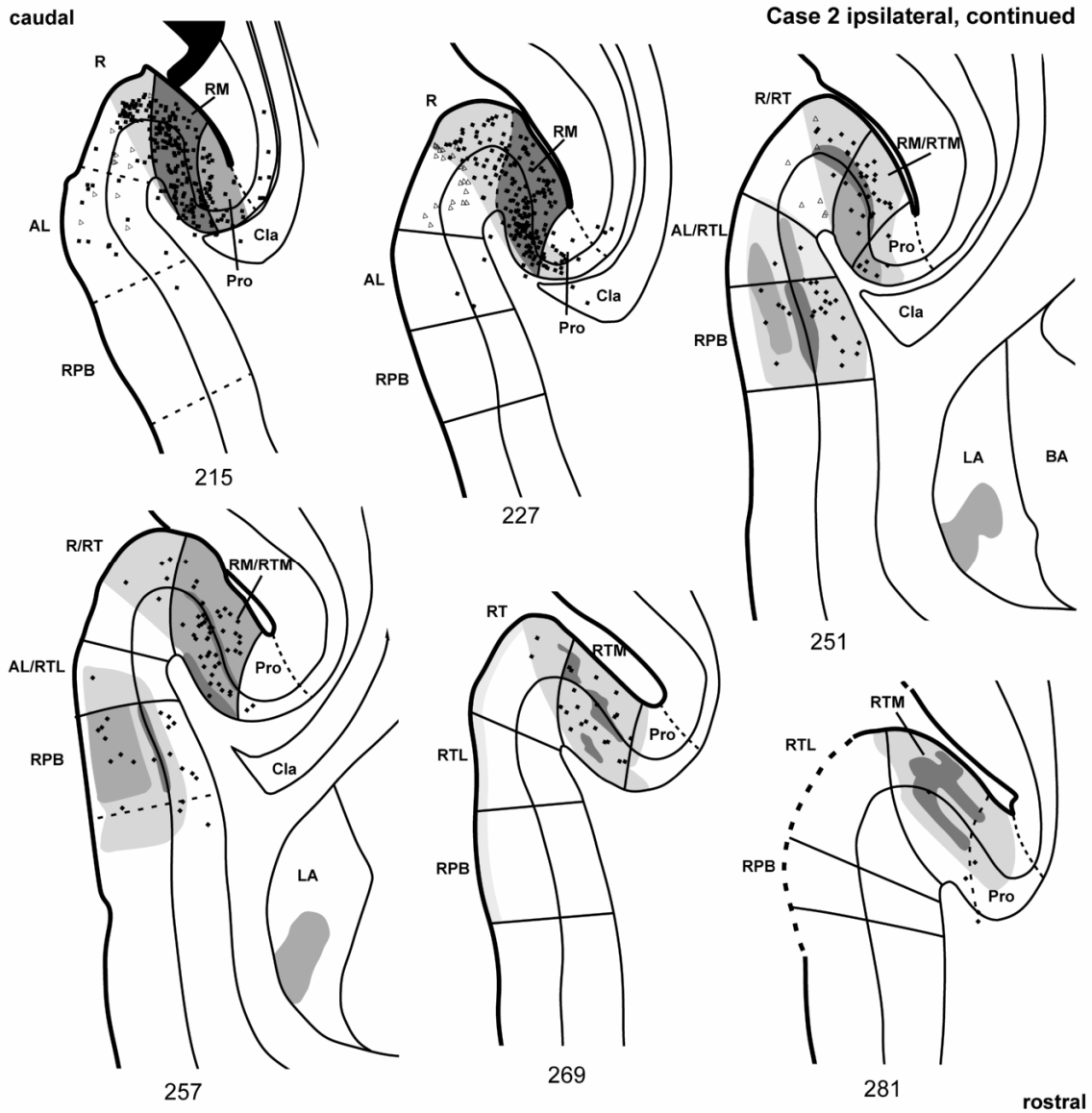
Figure 22 (continued)

involved the medial edge of R, as some labeled cells were found in the MGv near the

MGpd border (de la Mothe et al., 2006b). A patch of anterograde label extended across a

few sections in the ventral caudate nucleus at this level (# 197 – 215), as in case 1 (Fig.

21). Nearing the estimated border of R and RT (#257 – 251), labeling in RM and medial

R continued to be strong. However, in contrast to sections caudal to the injection site,

anterograde labeling in rostral RM was concentrated in layer IV, whereas it was sparse in layer IV of R, reflecting a strong feedforward projection to this area. Another patch of labeled cells and mostly terminals appeared in RPB and AL/RTL at this level, although less dense than in more caudal sections. At this same level, anterograde labeled terminals were also found in the lateral division of the amygdala (Fig. 21). In the most rostral sections (#269 – 281) containing the core area, RT, labeled terminals continued to fill the medial belt (RTM), with concentrations in layer IV and lower V/VI. Weaker anterograde projections could be seen under high magnification in the lateral belt and parabelt as RT was displaced by the merging of RTL and RTM.

Interhemispheric connections of RM

In case 1, cells labeled by the RM injection were concentrated in layer III of the contralateral medial belt and core regions, as in case 2, but additional numbers of cells were found in the core due to encroachment of the injection upon R at its medial border with RM (Fig. 23). In the most caudal sections containing A1 (#184 – 154), labeled cells were located in A1 and rostral CM. Cells were infragranular (#184) or distributed among infragranular and supragranular layers. In more rostral sections containing A1 (#144 – 109), cells were nearly all supragranular. Rostrally, in sections containing R (#99 – 54), labeled cells occupied layer III of R and RM.

In case 2, BDA-labeled cells from the RM injection were concentrated in layer III of the contralateral medial belt and core regions (Fig. 24). In caudal sections containing A1 (#107 – 167), labeled cells were confined to rostral CM and A1m. Rostral to A1, the

77

Figure 23. Interhemispheric cortical connections of areas RM and R, case 1. Series of serial sections are arranged from caudal (upper right) to rostral (lower left). BDA-Labeled cells (filled squares) and terminals (shading) are drawn onto each section, showing borders between areas identified by architectonic criteria. Cells labeled by FR (open triangles), FE (open circles), and double-labeled cells (asterisk). *Inset*, schematic of marmoset auditory cortex showing location of BDA injection in RM, FR in medial R and FE in lateral R in the contralateral hemisphere.
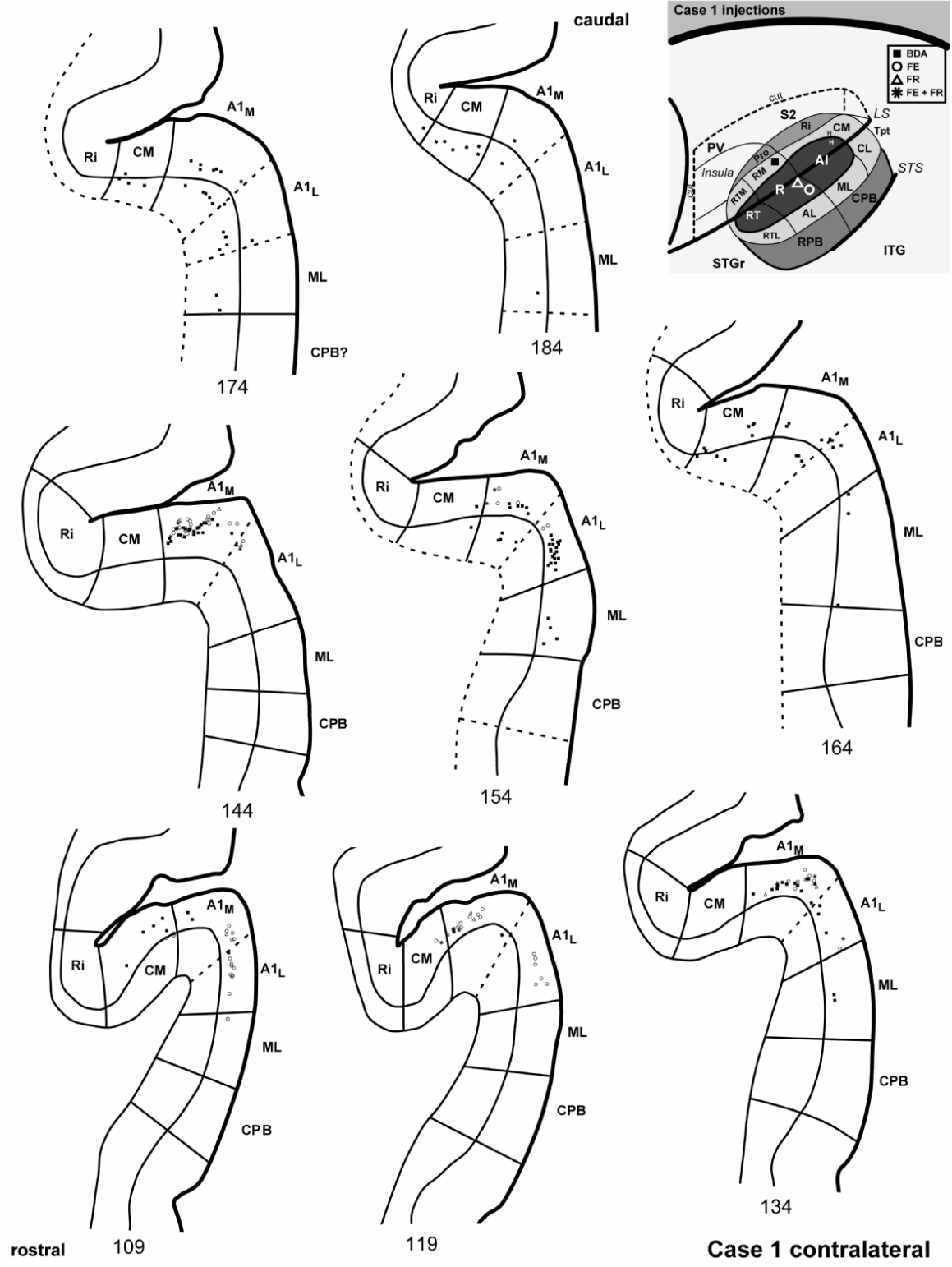
Case 1 contralateral, continued
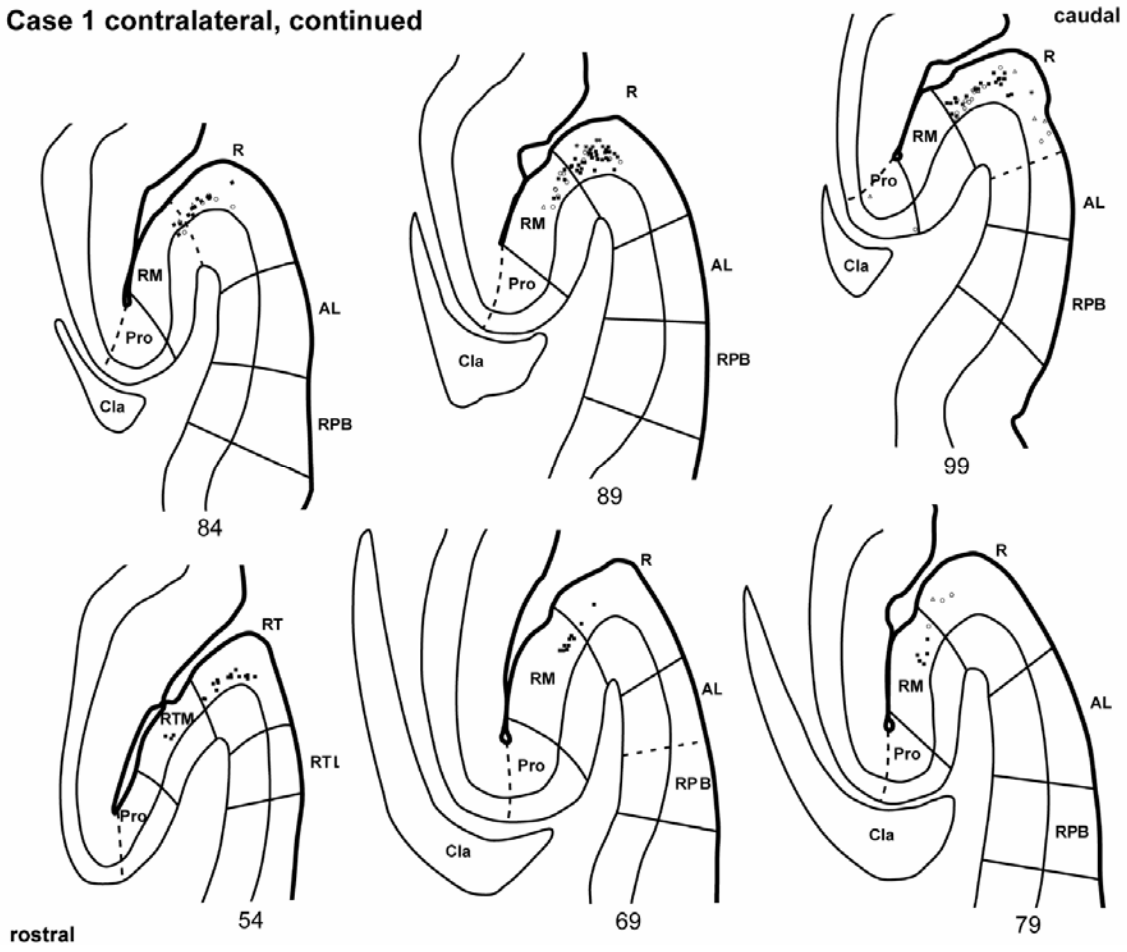
Figure 23 (continued)

Figure 24. Interhemispheric cortical connections of areas RM and R, case 2. Series of serial sections are arranged from caudal (upper right) to rostral (lower left). BDA-Labeled cells (filled squares) and terminals (shading) are drawn onto each section, showing borders between areas identified by architectonic criteria. Cells labeled by FR (open triangles). *Inset*, schematic of marmoset auditory cortex showing location of BDA injection in RM and FR in lateral R in the contralateral hemisphere.
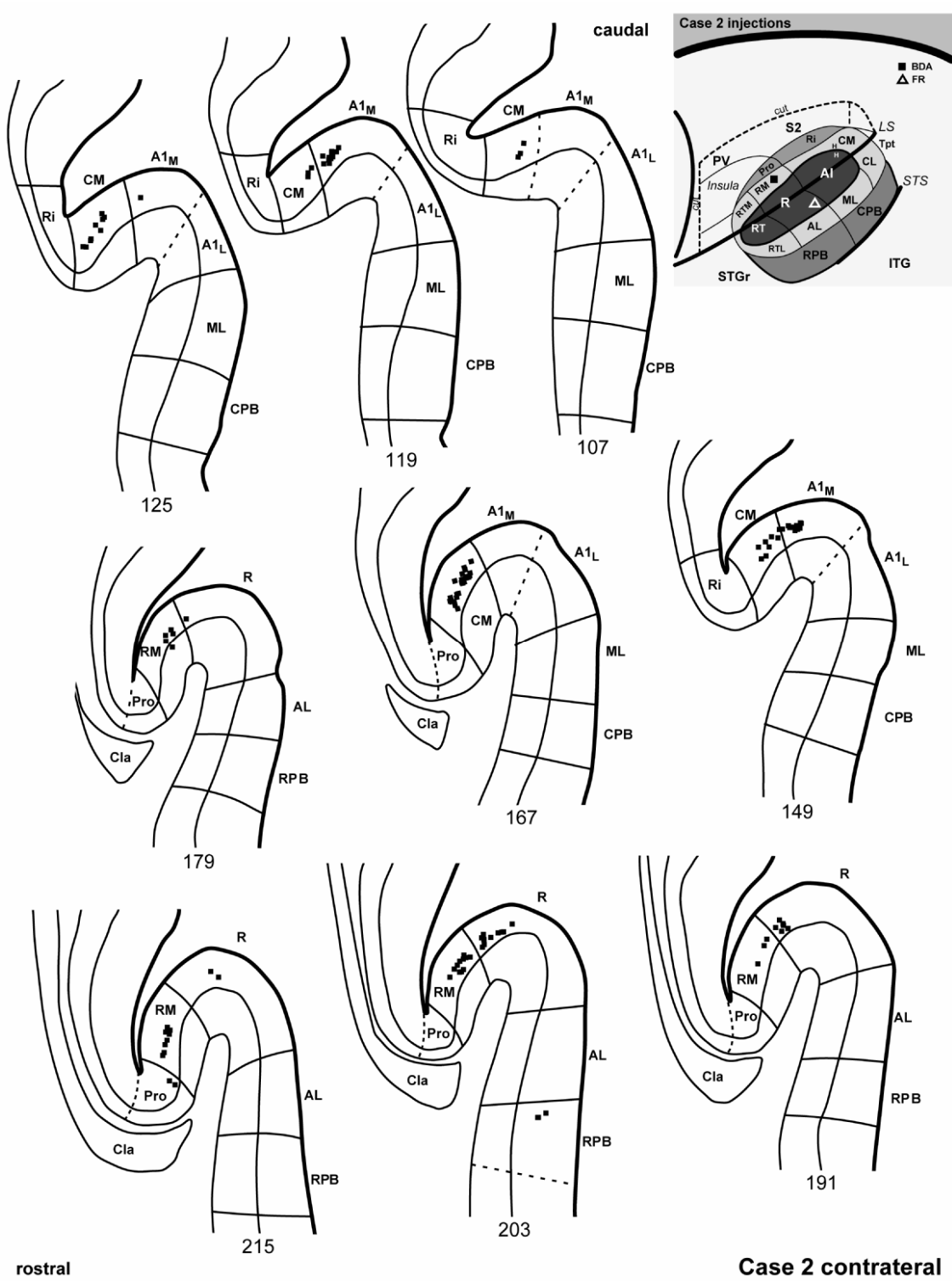
same pattern continued with cells limited to layer III of RM and R. Two cells were found in RPB of one section (#203).

In both cases, there was no evidence of anterograde terminal labeling in the contralateral hemisphere, despite dense projections to the thalamus (de la Mothe et al., 2006b), and throughout the ipsilateral hemisphere. It cannot be determined whether this was due to poor interhemispheric transport of BDA, or whether this reflected a unique property of RM.

Summary of RM connections

While there were some minor variations between the two cases in which injections were made into RM, the overall patterns were the same (Fig. 25, left). Dense reciprocal interconnections extended continuously along the medial belt from CM through RTM, although the connection with CM became weaker with distance from the RM/CM border. Connections with the lateral belt and parabelt were reciprocal and dense, but focalized, reflecting patchy rather than continuous connections. Parabelt connections included patches in both CPB and RPB. Connections with the rostral lateral belt (AL, RTL) were dense, but very sparse with the caudal belt (ML, CL) indicating topographic specificity favoring the rostral belt areas. The projections from RM to the belt and parabelt areas rostral to the injection site typically included strong terminal labeling of layer IV, while projections to caudal areas were usually weak in layer IV. Connections with the core were characterized by a continuous gap in which RT and the lateral portions of both A1 and R were nearly devoid of labeled cells and terminals. Only the medial parts of these areas were labeled, possibly reflecting slight encroachment of the RM injections into medial R. On the other hand, significant involvement of R should have produced
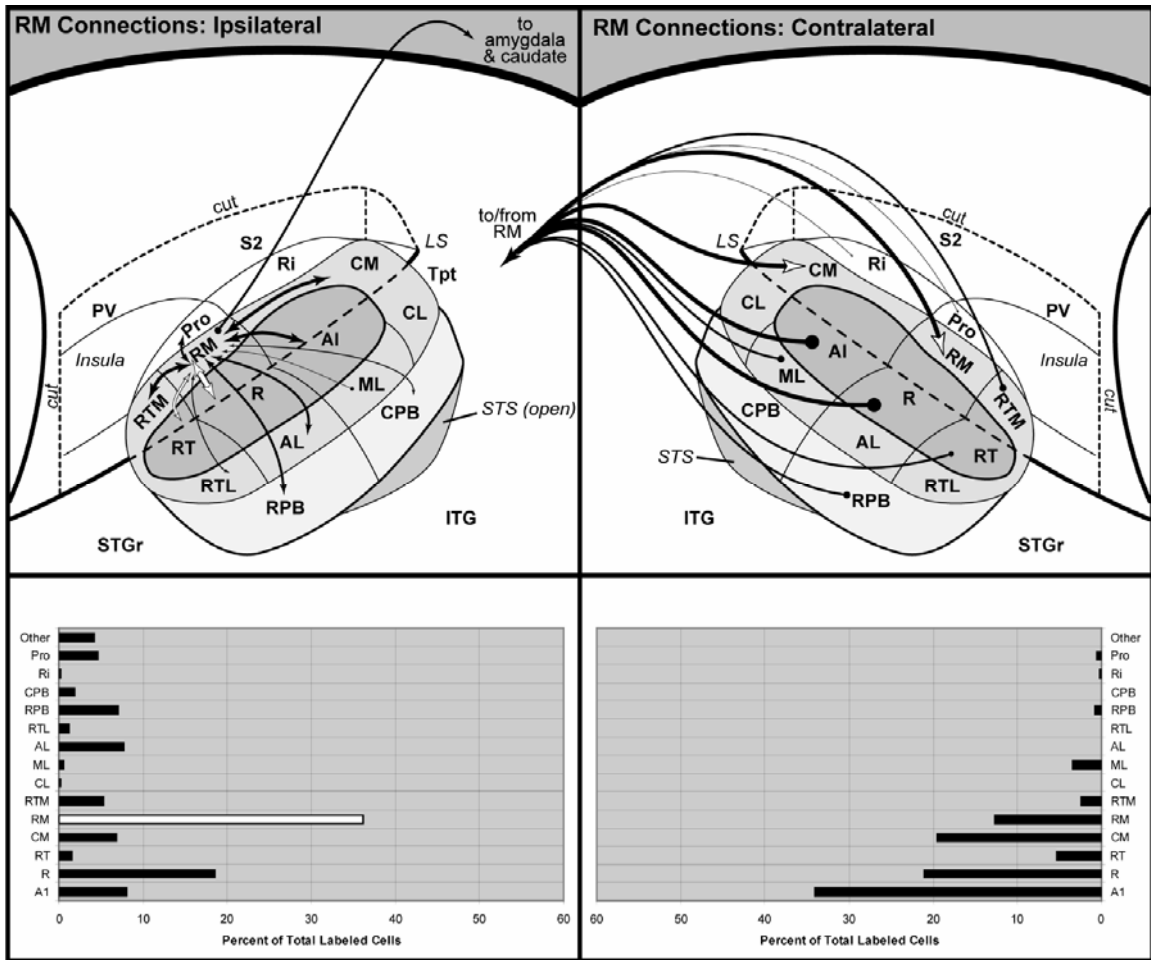
Figure 25. Summary of ipsilateral (left) and interhemispheric (right) connections of RM. Top panels illustrate connections (arrows) of RM on schematic diagram of marmoset auditory cortex. Arrow size is proportional to connection strength, as indicated in the histograms below each panel. Double arrows indicate reciprocal connection. Single arrows indicate unidirectional projections. Open arrowheads indicate probable reciprocal connections based on other injections in this study. White arrows (RM - R, RM - RT) indicate connections between areas confined to medial half of R and RT. There was no clear interhemispheric BDA transport after either RM injection. *Bottom left*, white bar indicates that cell counts for ipsilateral RM may be inaccurate (deflated) due to masking by the tracer injection.

more widespread labeling within the core. In any event, there was a continuous gap in the

connections between the medial and lateral belts extending from one end of the core to

the other, suggesting that RM has restricted connections with the core. Compared to CM,

RM had fewer connections beyond auditory cortex. In both cases focal projections targeted the lateral amygdala and ventral caudate nuclei. In contrast with CM, RM does not appear to have significant connections with somatosensory cortex or the STS.

Interhemispheric connections of RM (Fig. 25, right) strongly favored contralateral RM, with secondary inputs from R, $A1_M$, and CM. Labeled cells in all areas were concentrated in layer III. As noted above, there was no evidence of anterograde projections to contralateral RM in either case, as predicted from the connections of CM. This observation requires further investigation.

Ipsilateral connections of A1

In case 4, injections were made into the core areas A1 and R (Fig. 26). The CTB injection of A1 extended across all layers of cortex (#260), and mainly labeled cells and terminals in the core and belt areas ipsilaterally. A small number of cells were labeled in layer V of presumptive parabelt areas, reflecting a weak feedback projection from that region. Caudal to A1 and CM, labeled cells were located in the infragranular layers of temporoparietal areas that were architectonically distinct from CM and Ri (#196). The lateral area may correspond to the gyral portion of Tpt observed in the macaque monkey (Galaburda and Pandya, 1983). Just rostral to these fields, labeled cells and terminals were concentrated in the infragranular and supragranular layers of CM (#220 – 244), reflecting a strong reciprocal connection between A1 and CM. By inspecting consecutive sections (#228 – 276), it can be seen that the density of connections between A1 and CM was patchy, reflecting topographic variation. This feature is illustrated in figure 27. Within A1, labeled cells and terminals were continuously distributed along its entire

Figure 26. Ipsilateral cortical connections of area A1 and R, case 4. Series of serial sections are arranged from caudal (upper left) to rostral (lower right). CTB-labeled cells (filled circles) and terminals (shading) are drawn onto each section, showing borders between areas identified by architectonic criteria. Cells labeled by FR (open triangles). *Inset*, schematic of marmoset auditory cortex showing location of CTB injection in A1 and FR in R.

Case 4 injections

CTB
FR

caudal

rostral

Case 4 ipsilateral

87
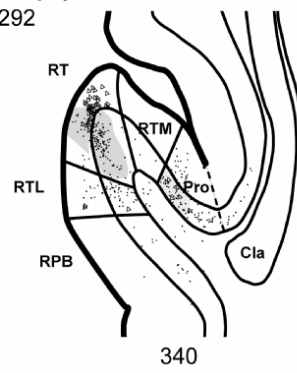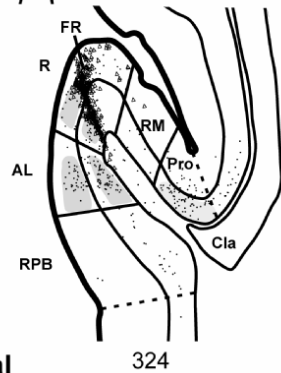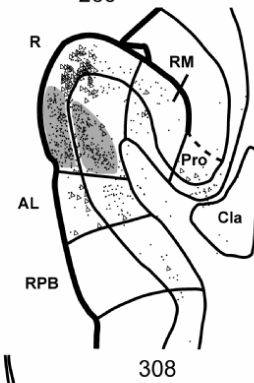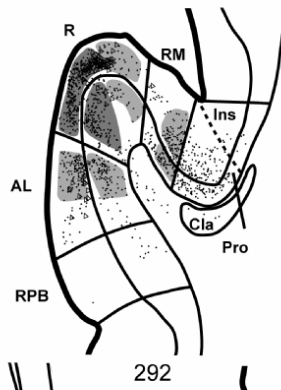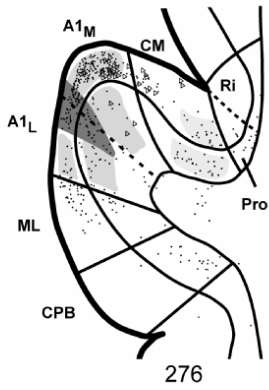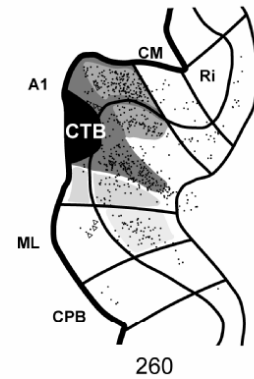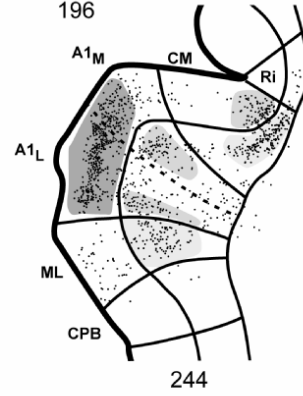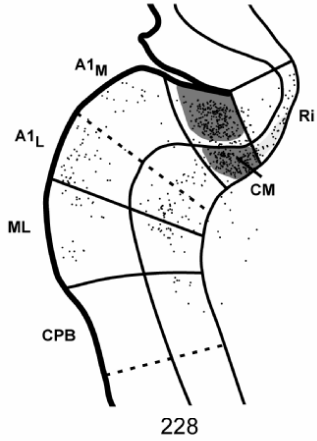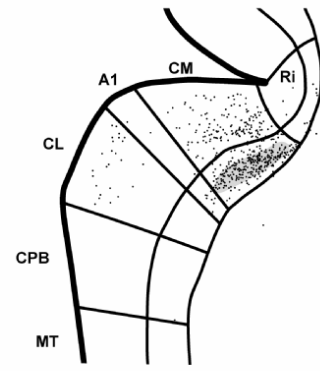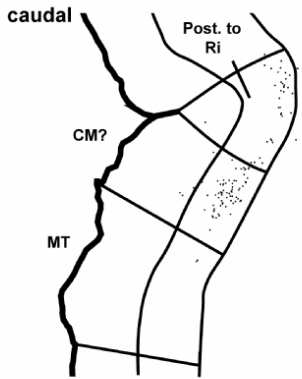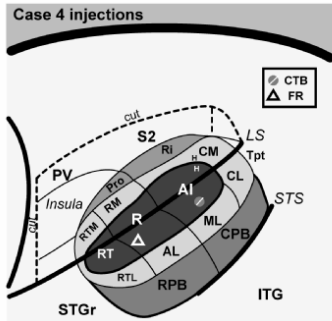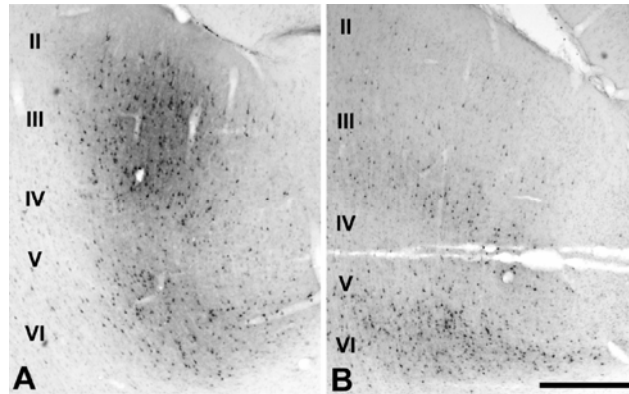
Figure 27. Patchy distribution of labeled cells and terminals in adjacent sections of area CM after injection of CTB into A1. (A) Density of label is highest in layer II/III. A secondary zone of labeled cells and terminals overlap in layers V/VI. (B) Adjacent section showing weaker anterograde projections to layer II/III. Scale bar, 500 μm.

rostrocaudal axis (#228 – 276), extending rostrally into R and RT of the core (#284 –

340). Rostral and caudal to the injection site (#260), reciprocal connections were revealed

with supragranular and infragranular layers of the lateral belt areas. Density decreased

with distance from the injection site, but connections were maintained along the entire

rostrocaudal axis of the belt. Connections with the rostral and caudal divisions of the

parabelt were characterized by the labeling of infragranular cells, but not terminals,

indicating a feedback projection from the parabelt to A1. In the rostral medial belt region,

A1 had dense reciprocal connections with RM (#284 – 292) that extended across cortical

layers. In contrast to the continuous band of connections observed for most other areas,

the connection with RM spanned a relatively small rostrocaudal distance, indicative of

focal topography. Labeled cells and terminals were continuous in Pro over a broad range

(#284 – 340), and tended to dominate in the infragranular layers, whereas RM had few

labeled cells in its most rostral sections. In the areas medial to the medial belt region,

including Ri, and the insula, labeled cells, but not terminals, were consistently found and
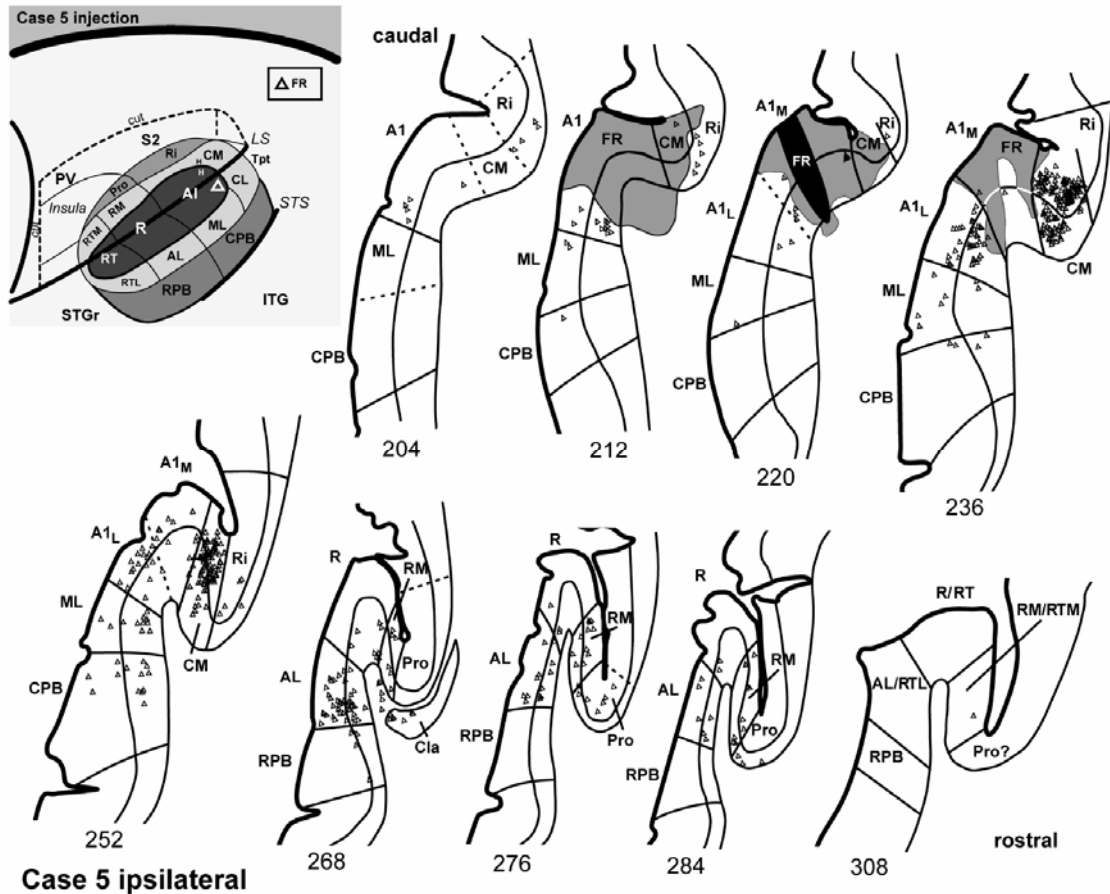
Figure 28. Ipsilateral cortical connections of area A1, case 5. Series of serial sections are arranged from caudal (upper left) to rostral (lower right). FR-labeled cells (open triangles) are drawn onto each section, showing borders between areas identified by architectonic criteria. FR, fluororuby tracer. Black shading, core of FR injection. Gray shading, heavy labeling and diffusion of FR injection. *Inset*, schematic of marmoset auditory cortex showing location of FR injection into lateral A1.

these were generally concentrated in the infragranular layers. Like the projections to A1

from the parabelt region, this pattern reflects feedback to A1 from, but not to, these areas.

Given the sensitivity of CTB and dense parallel projections to core and belt areas, it is

unlikely that any significant connection of A1 was not represented in this case.

In case 5 the FR injection was placed into A1 (Fig. 28). The most caudal sections (#188 –

220) included the FR injection into lateral A1. Labeled cells at this level were mostly

contained within A1, with scattered cells in ML and CM. Moving rostrally from the injection (#228 – 252), labeled cells were most dense in layers III and V of CM. Labeling in lateral A1 was less dense, and favored layer III. In ML, labeled cells were more numerous in the infragranular layers. In CPB, labeled cells were sparse and mostly infragranular. Rostrally, at the level of R (#260 – 308), labeled cells in R were almost exclusively infragranular, while sparse labeling in AL slightly favored infragranular. Labeled cells in RM were in infragranular and supragranular layers.

Ipsilateral connections of R

In case 1, two injections were placed within R, just rostral to the A1/R border (Fig. 20). The FR injection was made about 0.5 mm from the edge of the lateral sulcus. The FE injection was about 1.5 mm from the sulcus near AL, but also included some of the white matter below the site. In the most caudal sections containing labeled cells (#194 – 184), the greatest number of cells was found in $A1_M$. Cells from both injections and double labeled cells overlapped in this zone, especially in the supragranular layers. Labeled cells in $A1_L$ were fewer in number. A few cells were found in ML and CM. Rostrally, up to the border with R (#169 – 159), the concentration of cells continued to favor A1 over other areas, but was more balanced between $A1_M$ and $A1_L$. CM contained a moderate number of labeled cells from both injections and double-labeled cells, as well. A small number of cells were located in ML and scattered in CPB. The strongest connections were observed rostral to A1 (#144 – 119), where most of the labeled cells were found within R, followed by RM, then AL. Both single- and double-labeled cells were found in these areas. Further rostral (#109 – 59), few cells were found in R. Instead,

90

labeled cells were most numerous in RM, and these were mostly FR, rather than FE. This is consistent with the stronger connections between RM and medial part of R observed after injections of RM (see above). Finally, in the most rostral sections containing RT, only scattered cells were found in either RT or RM.

In case 2 the FR injection was made into R laterally, at its border with AL (Fig. 22). The diffusion zone appeared to encroach slightly upon AL, although labeled cells in the thalamus were restricted to a narrow band in the MGv, reflecting a clean core injection. In the most caudal sections (#143 – 161), labeled cells were concentrated in $A1_L$ and just a few cells in ML. Rostral to the border of A1 and R (#173 - 215) labeled cells were concentrated in both R and AL, especially around the injection site. A few cells were found in supragranular RPB, possibly reflecting slight involvement of AL by the injection. Further rostral (#227 – 251) cells were found only in R and RT. From rostral to caudal, only scattered cells were found in either CM or RM, consistent with weak connection between lateral R and RM.

In case 4, injections were made into the core areas A1 and the lateral half of R (Fig. 26). In caudal sections containing A1 (#244 – 284), FR cells were located in supragranular A1, and became concentrated medially near the border with R. Additional cells were in CM and ML. Rostrally, most of the labeled cells were clustered in supragranular R (CTB #292 – 332). Some cells were also found in caudal AL, and scattered in RM and Pro. In the most rostral section (#CTB 340), most of the cells were in supragranular RT, with additional cells in RTL and Pro. Scattered cells were found in infragranular RPB.

Interhemispheric connections of A1 and R

In case 4, the injections of CTB and FR into A1 and R labeled cells primarily in the core and medial belt regions of the opposite hemisphere (Fig. 29). In the most caudal sections of the contralateral hemisphere (#172 – 148), cells and terminals labeled by the CTB injection of A1 were largely confined to the lower half of layer III in area CM (#148 – 172), reflecting a strong reciprocal connection between A1 and contralateral CM. A few cells, but no terminals, were found in the deep middle layer of Ri, medial to CM (#156), indicating a one-way projection to A1. Rostral to these sections, the greatest concentration of labeled cells and terminals was found in layer III of A1 laterally, matching the position of the injection in the opposite hemisphere (#108 – 132). The patch of homotopic label in A1 extended rostrally into R/RT for about 2 mm (#36 – 92). In one section there were labeled cells in caudal AL and RM, but not in sections further rostral, suggesting that the interhemispheric connection with A1 was focal, rather than continuous as in the core. For the FR injection into R, transport was relatively weak, covering a narrower range (CTB# 116 – 76). The cells in these sections were mostly distributed along the core in supragranular R and A1.

In case 5, most of the labeled cells from the FR injection of A1 labeled cells in contralateral $A1_M$, with much weaker extension rostrally into A1 (Fig. 30). The second greatest concentration of cells was found in CM, followed by Ri. Scattered cells were located in ML or CL of the lateral belt. Cells were exclusively located in layer III.

In case 1, the two injections of R resulted in a similar pattern of label, although greater numbers of cells were labeled by the more lateral FE injection (Fig. 23). Overall, most of the labeled cells were contained within A1 and R, with fewer cells in the lateral
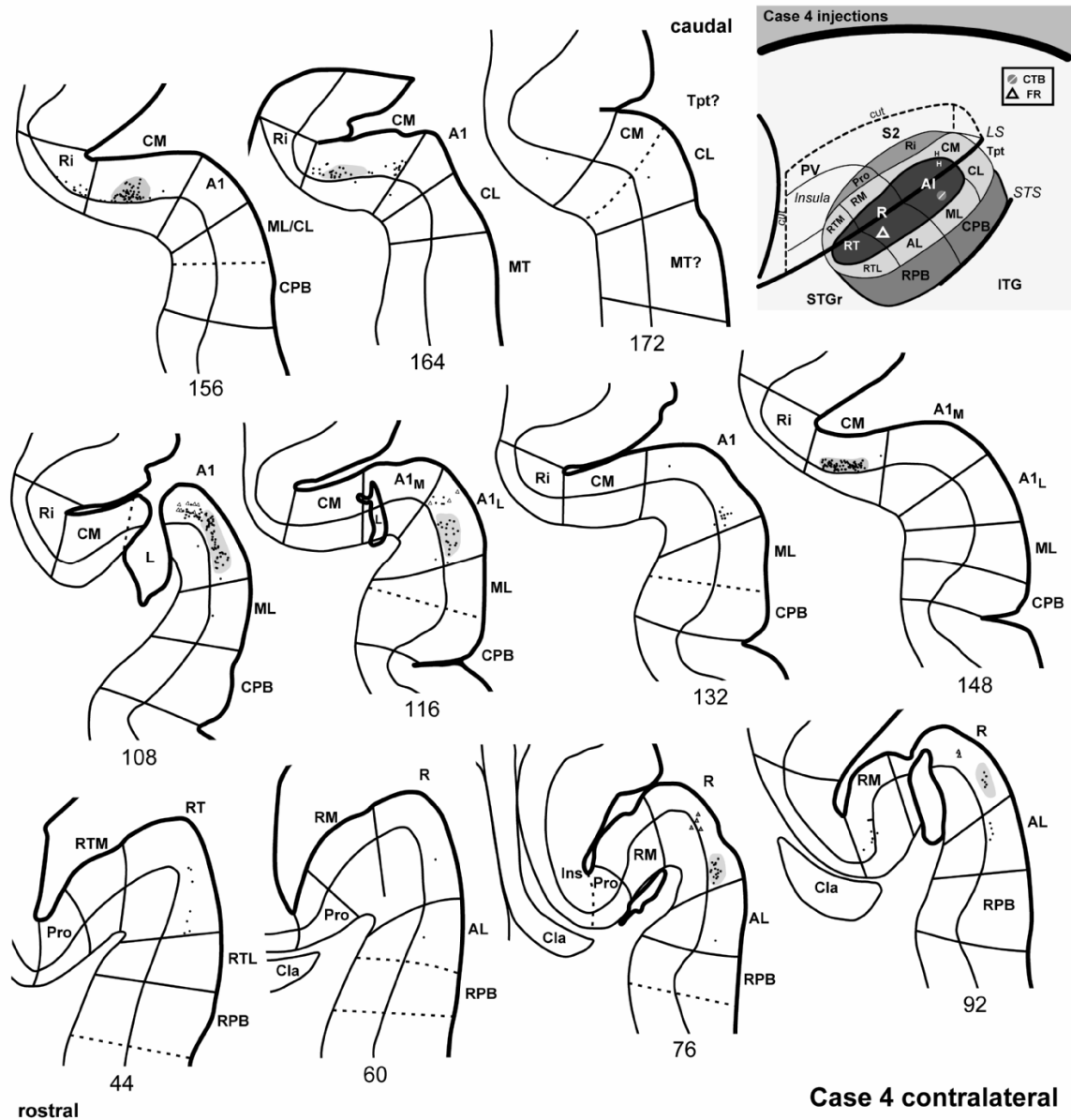
Figure 29. Interhemispheric cortical connections of area A1 and R, case 4. Series of serial sections are arranged from caudal (upper right) to rostral (lower left). CTB-labeled cells (filled circles) and terminals (shading) are drawn onto each section, showing borders between areas identified by architectonic criteria. FR-labeled cells (open triangles). L, lesion. *Inset*, schematic of marmoset auditory cortex showing locations of CTB injection in A1 and FR in R in the contralateral hemisphere.

and medial belts. Caudally, in sections containing A1 (BDA #154 - 99), labeled cells

were concentrated in layer III of A1. A few cells in A1 were double-labeled by both
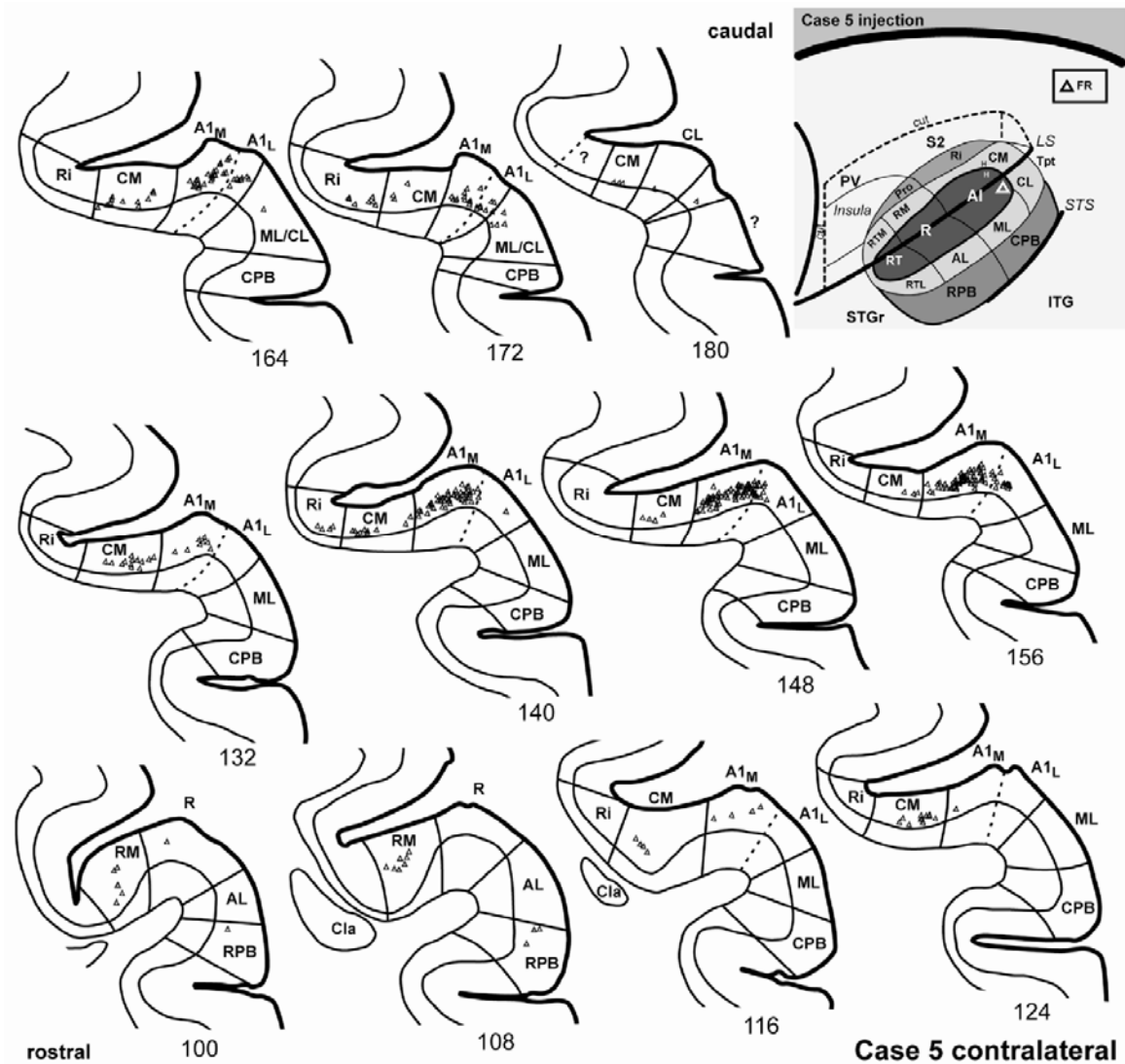
Figure 30. Interhemispheric cortical connections of area A1, case 5. Series of serial sections are arranged from caudal (upper right) to rostral (lower left). FR-labeled cells (open triangles) are drawn onto each section, showing borders between areas identified by architectonic criteria. *Inset*, schematic of marmoset auditory cortex showing locations of FR injection into A1 in the contralateral hemisphere.

injections. There were no cells in CM across this range until near the border between

A1and R (BDA #119 – 99), where cells were found in layer III. Rostrally, in sections

containing R (BDA #79 – 99), labeled cells were located in layer III of R and RM. A few

double-labeled cells were in R. A small number of cells were scattered in layer III of ML. There were no labeled cells in Ri of any sections.

In case 2, no labeled cells were found in the opposite hemisphere after FR injection of R, even though labeled cells were numerous ipsilaterally and in the thalamus (de la Mothe et al., 2006b).

Summary of A1 and R connections

After injections of A1 in two cases, the densest connections were within the core, where labeled cells and terminals were continuously distributed along its entire rostrocaudal extent, including R and RT (Fig. 31, left). Connections with the lateral belt were reciprocal and also continuous from rostral to caudal, but less dense overall. Focal, but strong reciprocal projections were revealed with portions of the medial belt areas RM and CM, which were otherwise lightly labeled. There were no injections of medial A1, so it was not possible to confirm whether it had denser connections with most of the medial belt, as suggested by injections of RM and CM. Connections with the parabelt region and areas medial to the medial belt (i.e., Ri, Pro) were mostly characterized by feedback projections from cells in the infragranular layers, but there was some evidence of a forward projection to Pro from A1. There were no connections between A1 and cortex ventral to the parabelt in the STS.

Injections of R primarily labeled cells in the core in a continuous band that extended away from the injection sites into A1 caudally and RT rostrally (Fig. 32, left). The relative medial-lateral position of the injection was generally reflected by the positions of the labeled cells in the core of both hemispheres. Connections with the lateral

belt favored AL, with fewer cells in either ML or RTL. Labeling in the medial belt was dependent on injection location. Injections of lateral R produced scattered labeling in RM, CM, or RTM. In contrast, one injection of medial R produced strong labeling in RM, with additional labeling in CM. This pattern is consistent with the gap in connections with the lateral core areas after injections in RM (see above). Very few cells were found in RPB after R injections.

Interhemispheric homotopic and heterotopic connections were generally reciprocal, and limited to the deep part of layer III after injections of A1 or R (Figs. 31 – 32, right). The densest connections of both areas were homotopic, but both divisions of the core were strongly interconnected between hemispheres. The densest heterotopic connections of A1 were with CM, while R was similarly linked to CM and RM. A1 also received inputs from Ri, but no connections were found after injections of R in the opposite hemisphere. Connections with the lateral belt were very sparse for A1 and especially R. There were no connections with the parabelt or insula.

Laminar specificity of connections

Since BDA and CTB transport is both anterograde and retrograde, it was possible to visualize the laminar distribution of labeled cells and terminals in areas connected to the injection site. In the present study, several distinct types of connection patterns were observed. Ipsilaterally, most of the connections between and within areas were characterized by groups of labeled pyramidal cells in supragranular (layer II/III) and infragranular (layer V/VI) layers, overlapped by a haze of anterograde label (Fig. 27).
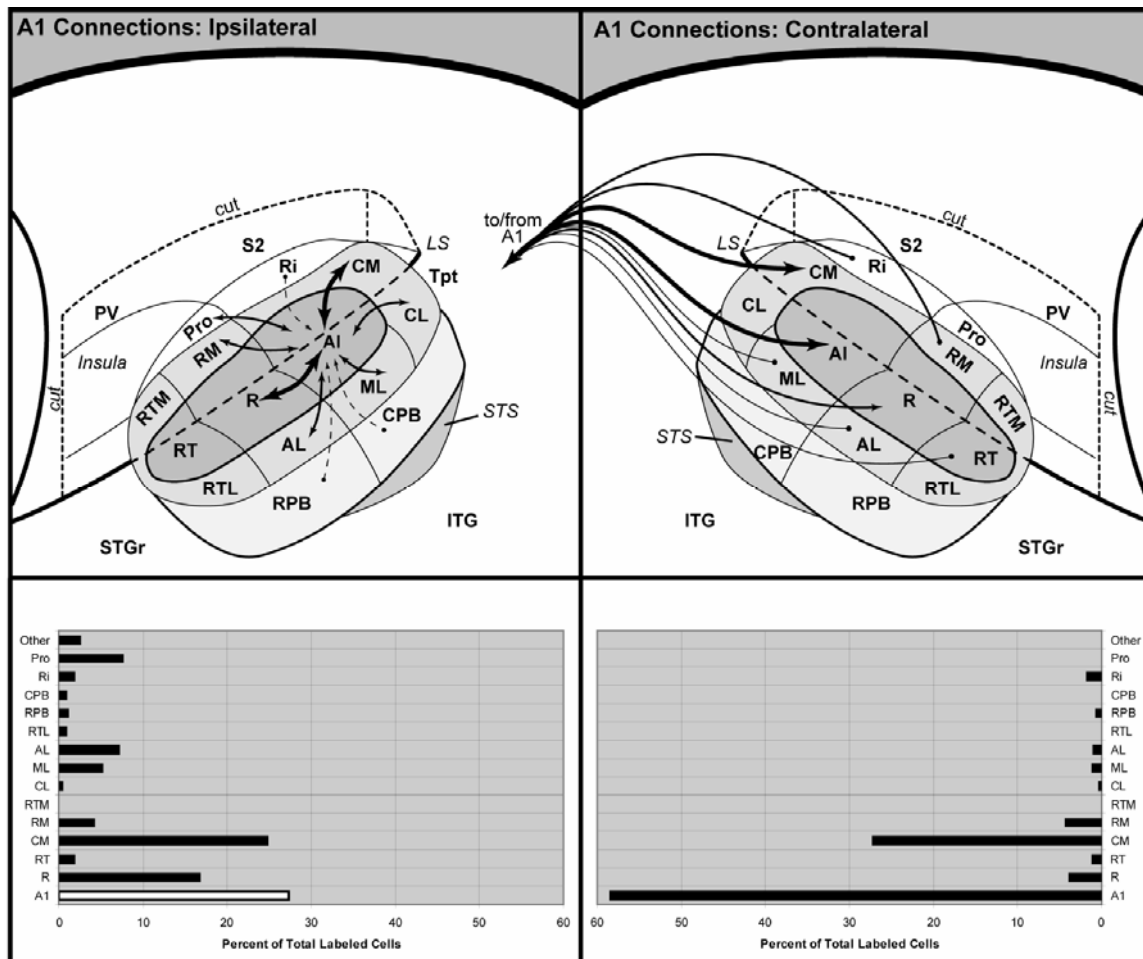
Figure 31. Summary of ipsilateral (left) and interhemispheric (right) connections of A1. Top panels illustrate connections (arrows) of A1 on schematic diagram of marmoset auditory cortex. Arrow size is proportional to connection strength, as indicated in the histograms below each panel. Double arrows indicate reciprocal connection. Single arrows indicate unidirectional projections. Dashed lines indicate infragranular projection. *Bottom left*, white bar representing ipsilateral A1 indicates that cell counts may be inaccurate (deflated) in the area injected by the tracer.
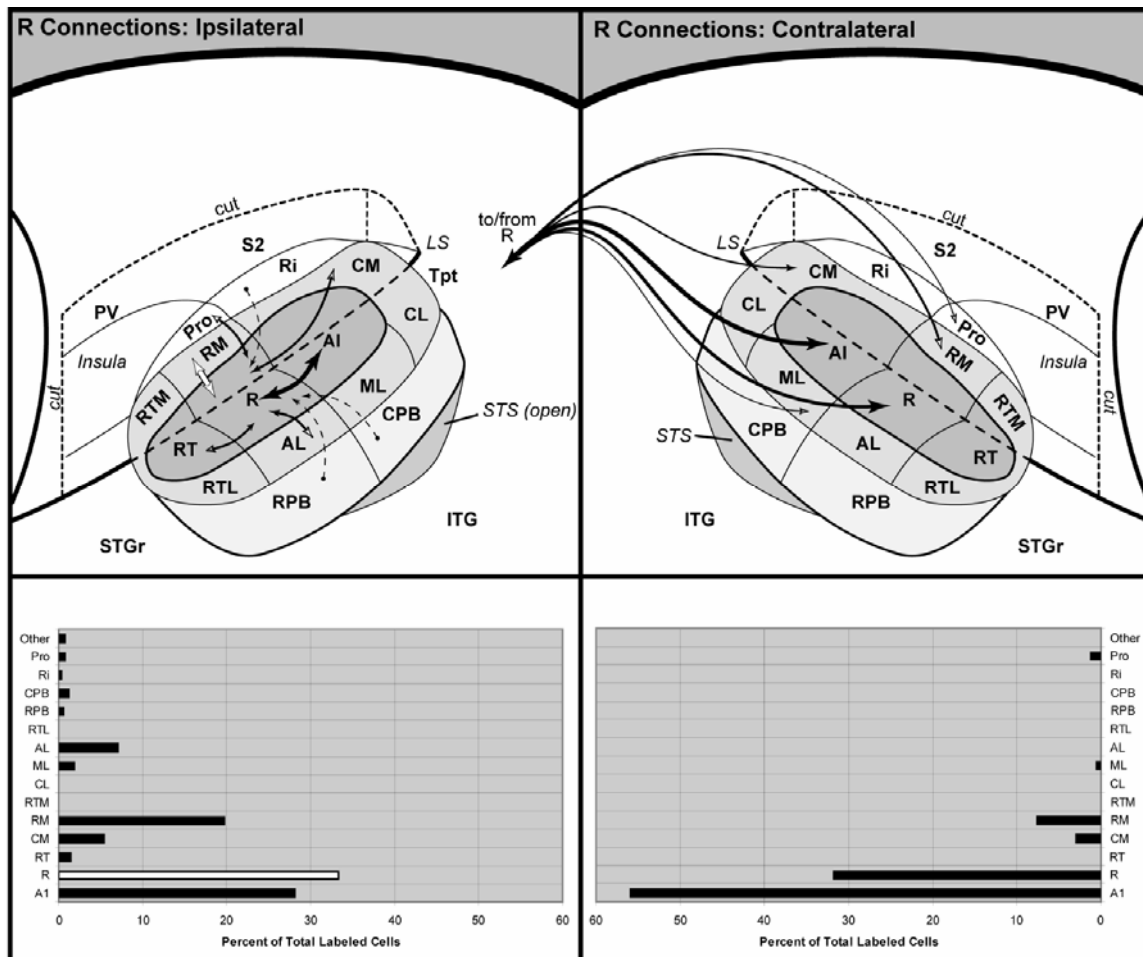
Figure 32. Summary of ipsilateral (left) and interhemispheric (right) connections of R. Top panels illustrate connections (arrows) of R on schematic diagram of marmoset auditory cortex. Arrow size is proportional to connection strength, as indicated in the histograms below each panel. Double arrows indicate reciprocal connections verified by other injections in these areas, as results were based on retrograde tracers. Open arrowheads indicate that the projection is assumed to be reciprocal based on laminar distribution of cells, but could not be verified using retrograde tracers. Single arrowheads indicate unidirectional projections. Dashed lines indicate infragranular projection. White arrow (RM - R) indicates connection with RM favored the medial half of R. *Bottom left*, white bar indicates that cell counts for ipsilateral R may be inaccurate (deflated) due to masking by the tracer injection.

98

The density of the anterograde terminal labeling was commensurate with the density of labeled cells in the area.

A second pattern was commonly observed near injection sites and sometimes in dense projections to distant areas. Here, patches of anterograde label formed a continuous column that spanned all layers. These columns were sometimes adjacent to columns exhibiting a different projection pattern, but within the same architectonic field (Fig. 13b).

A third pattern was restricted to interhemispheric connections. These were generally characterized by overlapping labeled cells and terminals confined to layer III. In some instances, the anterograde label formed a continuous column that spanned layers I – III (Fig. 17). A secondary band of anterograde label was sometimes observed in layer V, associated with very dense cell labeling above in layer III. Often, there were labeled cells without clear evidence of anterograde labeling (e.g., projection from Ri to A1).

In a fourth pattern, observed ipsilaterally, connections between certain areas were characterized by projections from labeled cells, but not terminals, located in the infragranular layers of one or more areas. This pattern typified projections from the parabelt to the core, from rostral auditory areas to caudal CM (Fig. 13), and from entorhinal cortex to CM (Fig. 14a). A similar pattern was noted previously after injections of caudal lateral belt/parabelt region in macaques (Galaburda and Pandya, 1983). This type of projection probably reflects strictly feedback to one or more layers of the target areas. Because our injections spanned all cortical areas in most cases, we could not determine the laminar targets of those projections.

In some areas, a fifth pattern was sometimes found. After RM injections, dense projections to layer IV were found in sections containing RM, RTM, AL, and RPB rostral to the injection site (Fig. 13a, b). The heavy layer IV projection was in addition to normal (type 1) labeling in the other layers. This pattern indicates that an exceptionally strong feedforward projection overlaps with the thalamocortical projections in layer IV in those areas. In contrast, caudally directed projections from injections in RM produced the typical dense labeling above and below layer IV, but weak terminal labeling within. This fifth pattern was also observed after CM injections in projections to ML, and to a lesser extent, CPB, but not within CM (Fig. 13c,d). Galaburda and Pandya (1983) also described a strong layer IV projection to rostral fields from those located caudally. In the caudal direction, they reported that the lower laminae of rostral areas projected to layer I of caudal areas. They also found a layer I projection from the medial belt to the core and lateral belt. We did not observe a prominent projection to layer I in this study from any of our injections in the core or medial belt, suggesting that methodological differences may account for the discrepancy between studies.

Discussion

In the present study, the anatomical organization of auditory cortex in primates was studied in marmoset monkeys by concurrent analysis of architectonic features and connections of areas in the core (A1, R) and medial belt (CM, RM) regions. Overall, these findings indicate that the organization of the marmoset auditory cortex is comparable to other New and Old World primates. In addition to confirming regional distinctions between the core and medial belt, the data revealed clear differences between

RM and CM. These findings are discussed below along with their functional implications.

RM and CM are functionally-distinct auditory areas

The main finding of the present study was that RM and CM represent anatomically-distinct areas of auditory cortex. Placed within the context of several other observations, we conclude that RM and CM are functionally-distinct areas, as well. First, RM and CM are architectonically dissimilar. CM is much more primary-like, as revealed by dense myelination across layers III to VI, and elevated expression of parvalbumin and cytochrome oxidase in the thalamo-recipient layers. The attenuation of these features in RM was more similar to that of the lateral belt areas. The architectonic profiles of RM and CM are consistent with descriptions of corresponding areas in other primates (Galaburda and Pandya, 1983; Hackett et al., 1998a; Imig et al., 1977; Jones and Burton, 1976; Jones et al., 1995; Kosaki et al., 1997; Morel et al., 1993; Morel and Kaas, 1992; Pandya and Sanides, 1973).

Second, thalamic inputs to RM and CM arise from different divisions of the MGC (de la Mothe et al., 2006b). CM was dominated by projections from the MGad and multisensory nuclei, whereas RM received inputs mainly from the MGpd. The architecture and inputs to MGad and MGpd in macaque monkeys suggest that they may relay information to cortex from distinct subcortical auditory pathways (Hashikawa et al., 1995; Jones, 1997; Jones, 2003; Molinari et al., 1995).

Third, the connections of RM and CM within auditory cortex of both hemispheres were topographically distinguishable. CM was more strongly interconnected with A1 and

caudal areas outside the core (ML, CL, CPB), while the connections of RM favored areas rostral to these. The most caudal portion of CM had especially weak connections with the rostral fields. Overlap in the connections of RM and CM occurred mainly in the middle third of auditory cortex, then became increasingly divergent toward its rostral and caudal poles. Similar trends have been noted after injections of core, lateral belt, and parabelt in other primates, suggesting that there is limited direct communication between the most rostral and caudal domains of auditory cortex (Galaburda and Pandya, 1983; Hackett et al., 1998a; Luethke et al., 1989; Morel et al., 1993; Morel and Kaas, 1992). Compared to CM or RTM, however, RM appears to have more widespread connections with caudal and rostral fields, consistent with its more central location along the rostrocaudal axis (Hackett et al., 1998a; Jones et al., 1995).

Fourth, RM and CM have unique connections with areas beyond auditory cortex. RM projected to the lateral amygdala and ventral caudate nuclei. CM did not project to these nuclei, but received strong inputs from entorhinal cortex, and dense reciprocal connections with Ri and posterior parietal cortex. RM had no significant connections with any posterior parietal or somatosensory field. These results provide indirect anatomical support for observations of bimodal auditory and somatosensory activity in CM of macaque monkeys (Fu et al., 2003; Schroeder et al., 2001). The results are also consistent with studies in macaques which demonstrated topographic segregation of connections between the rostral and caudal belt and parabelt with functionally-distinct regions of prefrontal and posterior parietal cortex (Hackett et al., 1999; Lewis and Van Essen, 2000; Raczkowski et al., 1976; Romanski et al., 1999a; Romanski et al., 1999b). As noted for connections within auditory cortex, the segregation of connections with

auditory-related fields becomes more strict with rostral or caudal distance from the "pivotal center" of auditory cortex, which we loosely define as the border of A1 and R.

Comparisons of anatomical and physiological profiles across studies indicate that area RM of marmosets corresponds to the following areas identified in other primates: "proA" (Galaburda and Pandya, 1983; Pandya and Sanides, 1973); "a" (Merzenich and Brugge, 1973); "A-m" or "M" (Jones et al., 1995; Kosaki et al., 1997); "Pi" (Burton and Jones, 1976; Cheung et al., 2001); and "RM" (Hackett et al., 1998a; Imig et al., 1977; Morel et al., 1993; Morel and Kaas, 1992; Romanski et al., 1999a). Accordingly, area CM of marmosets corresponds to the following areas, at least in part: "paAc" (Galaburda and Pandya, 1983; Pandya and Sanides, 1973); "P-m" (Jones et al., 1995; Kosaki et al., 1997); "PA" (Jones and Burton, 1976; Robinson and Burton, 1980a); and "CM" or "C" (Brugge, 1982; Imig et al., 1977; Merzenich and Brugge, 1973; Morel et al., 1993; Morel and Kaas, 1992; Pfingst and O'Connor, 1981; Rauschecker et al., 1997; Romanski et al., 1999a). With respect to differences in the size and extent of CM between studies, these are most likely due to differences in interpretation, rather than differences between species or individual animals of the same species. We noted gradients in the both the architecture and connections of CM that could be used to justify its division into areas medial and caudal to A1 (e.g., MM, middle medial; CM, caudomedial). This distinction has been proposed and illustrated in summary diagrams of the macaque monkey, but so far not verified (Kaas and Hackett, 1998; Kaas and Hackett, 2000). Further studies will be required to resolve this issue.

Serial and parallel processing in the core and medial belt

Injections of the core and medial belt areas in this study revealed that RM and CM have strong reciprocal connections with infragranular and supragranular layers of the core. Rostrocaudal topography was evident in these connections, such that RM was more densely connected with R and RT, while CM had stronger connections with A1. In addition, RM and rostral CM had connections with all three core areas, whereas caudal CM had only sparse infragranular inputs from the rostral core. In addition to inputs from the core, RM and CM had topographic connections with the belt and parabelt. These connections involved cells in supragranular and/or infragranular layers, and were generally reciprocal. Remarkably, the strongest connections of RM and CM were from within the medial belt, accounting for 40% of all labeled cells, versus 27% in the core. The remainder was mostly distributed among the lateral belt and parabelt. In contrast, injections of the core revealed reciprocal supragranular and infragranular connections with the medial and lateral belt areas, but only sparse connections with infragranular cells in the parabelt. Thus, it appears that the core region of marmosets is instructing the medial and lateral belt areas via strong reciprocal connections at all rostrocaudal levels, while the belt and parabelt regions are also strongly interconnected. This is consistent with findings in other primates (Aitkin et al., 1988; Hackett et al., 1998a; Morel et al., 1993; Morel and Kaas, 1992), from which it has been concluded that the parabelt region receives auditory cortical inputs through an intermediate stage of processing in the belt region (Kaas and Hackett, 1998; Rauschecker et al., 1997).

To these results it should be added that both RM and CM receive dense inputs from the MGpd and MGad, respectively, while the primary inputs to R and A1 arise from

the MGv (de la Mothe et al., 2006b). These connections reflect inputs from at least two separate subcortical auditory pathways. At present, it is not clear from either the anatomy or physiology whether neurons in the core or thalamus represent the primary drive to neurons in the medial belt. Most physiological studies indicate that either a reversal or disruption in the tonotopic gradient occurs at the A1/CM border, and that neurons in CM are more broadly-tuned than those in A1 (Imig et al., 1977; Kajikawa et al., 2005; Kosaki et al., 1997; Merzenich and Brugge, 1973; Rauschecker et al., 1997; Recanzone et al., 2000a). Recanzone and colleagues added that neurons in CM had longer response latencies and were relatively more selective for spatial location than neurons in A1 (Recanzone, 2001; Recanzone et al., 2000b), as previously noted (Rauschecker et al., 1997), similar to the caudolateral belt area (Tian et al., 2001). These response properties support the conclusions of Rauschecker et al (1997) that auditory information is processed in series between A1 and CM. In that key study, responses to tones were abolished in CM after A1 ablation, but remained responsive to complex sounds, whereas responses in R were unaffected by the A1 lesion. Responses to complex sounds in CM were thought to be preserved because they were mediated by intact inputs from the MGd. This conclusion may be consistent with the results of a recent study in macaques, in which latencies for tones were longer in CM than A1, while latencies for noise bursts were shorter (Lakatos et al., 2005). In contrast, Kajikawa et al (2005) reported that average minimum response latencies for tones and noise were shorter in CM of marmosets. Short latency responses in CM have been reported by others, as well (Bieser and Muller-Preuss, 1996; Scott et al., 2000).

Thus, while the precise nature of the relationship between the medial belt and core remains to be determined, it can be concluded that responses in CM are at least partly dependent on intact feedforward inputs from A1, consistent with its position in the auditory cortical hierarchy (Rauschecker et al., 1997). Simultaneous recordings from the core, medial belt, and perhaps thalamus would be especially useful in this resolving some of these issues, particularly if laminar array electrodes could be employed to examine timing across laminae in cortex (Lakatos et al., 2005; Schroeder and Foxe, 2002).

Sources of somatosensory input to auditory cortex

Perhaps the clearest difference between RM and CM revealed by the results of the present study was the strong reciprocal connection between CM and Ri. This somatosensory area occupies the fundus of the lateral sulcus caudal to the insula, separating S2 on the upper bank from CM on the lower bank, and appears to correspond to the ventral somatosensory area (VS). The somatosensory features of Ri have been fairly well-studied in both New and Old World primates (Burton et al., 1995; Cusick et al., 1989; Disbrow et al., 2003; Friedman and Murray, 1986; Friedman et al., 1986; Krubitzer et al., 1995; Leinonen, 1980; Qi et al., 2002). There is also evidence that parts of Ri may have vestibular function, as well (Akbarian et al., 1992; Akbarian et al., 1994; Grusser et al., 1990a; Grusser et al., 1990b; Guldin et al., 1992).

The significance of the connections between Ri and CM is that it represents the most likely source of somatosensory input to CM, and perhaps other areas of auditory cortex, as observed in macaque monkeys. In studies of caudal somatosensory areas, Robinson and Burton reported finding unimodal and bimodal auditory and somatosensory

responses in Ri and Pa, which corresponds to CM (Robinson and Burton, 1980a; Robinson and Burton, 1980b; Robinson and Burton, 1980c). In Ri, 74% of 199 units were responsive to somatosensory stimulation. In Pa, 57% of 75 units were responsive to cutaneous stimulation. Most of these responses were confined to the upper body and nearly half of the receptive fields were bilateral. About 16% of the neurons in Pa and the extension of Ri onto the lower bank of the lateral sulcus were responsive to auditory or convergent auditory-somatosensory stimulation, although Pa was not completely mapped. Neurons responsive only to somatic stimulation were intermingled with those responsive only to sound. In addition, three neurons responded to auditory, visual, and somatic stimulation in the caudal part of Pa, while additional auditory or visual responses were located further caudal. These neurons may have been located in the portion of Tpt the wraps onto the lower bank of the lateral sulcus from the STG (Leinonen et al., 1980). These results were recently confirmed by additional studies of CM in macaques (Fu et al., 2003; Schroeder and Foxe, 2002; Schroeder et al., 2001) and a corresponding field in humans (Foxe et al., 2002; Caetano, 2005). In these studies, a majority of neurons in CM were responsive to both auditory and somatic stimulation in the form of electrical stimulation of the median nerve in the hand or mechanical stimulation of the upper body. Both cutaneous and proprioceptive responses were observed at short latencies, matching those evoked by auditory stimulation. In contrast, control recordings in the adjacent core area, A1, revealed no significant response modulation by somatosensory stimulation, suggesting that the inputs responsible for bimodal activity in CM are not likely to characterize all auditory areas equally.

Given the proximity of Ri to CM, it is not surprising that Ri could be a source of somatosensory input to CM, as well as other nearby areas, including CL and Tpt. In cats, auditory-somatosensory interactions were found in a comparable zone located between the suprasylvian and anterior ectosylvian sulci (Berman, 1961a; Berman, 1961b; Carreras and Andersson, 1963; Dehner et al., 2004), and also within the AES (Clemo and Stein, 1983). In primates, it has often been overlooked that Ri has connections with cortex in the vicinity of the caudal belt region. Following injections of WGA-HRP into physiologically defined locations along the lateral sulcus of marmoset monkeys, labeled cells were found in the caudal fundus, corresponding to Ri (Aitkin et al., 1988). One injection, placed into presumptive A1 (BF = 8 kHz), labeled a narrow band that spanned layers in Ri. A more caudal injection in either A1 or CM (BF = 16 kHz) also labeled cells and terminals in Ri and extended slightly onto the upper bank. In macaque monkeys, degeneration was observed in Ri and posterior insula after lesions of cortex corresponding to the lateral belt and parabelt (Pandya et al., 1969; Pandya and Rosene, 1993; Pandya and Sanides, 1973). Tracer transport studies have also revealed sporadic evidence of such connections in several primate species (Friedman et al., 1986; Galaburda and Pandya, 1983; Hackett et al., 1998a; Morel et al., 1993; Morel and Kaas, 1992). In contrast, there is little evidence for significant connections between S2 and auditory cortex (Burton et al., 1995; Disbrow et al., 2003; Friedman et al., 1986; Jones and Powell, 1969; Krubitzer and Kaas, 1990; Lewis and Van Essen, 2000; Qi et al., 2002). In the present study labeled cells were consistently found after two of four injections involving CM. When labeled cells were found in S2, it appeared to be the result of spread of the tracer into a lesion or track in the upper bank, though we could not

rule out a legitimate projection with certainty. However, the absence of connections with S2 from the other two CM injections suggests that significant connections are unlikely. In one case, the heavy labeling of Ri stopped cleanly at the border with S2 on the upper bank.

The discovery of multisensory convergence in CM is even less surprising, given recent evidence of visual interactions involving auditory cortex. Neurons in layer VI of core, belt, and parabelt areas have been found to project to layer I of areas 17 and 18 of visual cortex (Falchier et al., 2002; Rockland and Ojima, 2003). There is also limited evidence that the connections may be reciprocal. These findings echo reports that eye position modulates the responses of neurons in the inferior colliculus, core, and caudal belt (Fu et al., 2004; Groh et al., 2001; Werner-Reiss et al., 2003).

Considered together, all of these findings suggest that multisensory influences of one variety or another may be discovered in other areas of auditory cortex. The findings of the present study indicate that Ri is the most likely source of somatosensory input to CM and perhaps other caudal fields. Given the absence of significant projections to RM, however, any multisensory interactions that may be identified in this field are likely to arise from another source.

Significance of connections with areas outside auditory cortex

After injections of RM in this study, strictly anterograde projections were discovered in the lateral nucleus of the amygdala and the ventral caudate. Although these projections were not observed after CM or core injections, only CM received inputs from

the entorhinal cortex, further distinguishing the functional segregation of the rostral and caudal auditory areas.

The projections from RM to the amygdala have not been observed in previous studies, although some projections have been found in the insula and medial temporal pole (Aggleton et al., 1980; Herzog and Van Hoesen, 1976). The projection from RM is in line with previous findings in primates in that connections with the amygdala tend to be stronger among rostral fields of auditory cortex, reaching a maximum in the temporal pole, but are weak or absent with caudal areas corresponding to the lateral belt or parabelt (Aggleton et al., 1980; Herzog and Van Hoesen, 1976; Kosmal et al., 1997; Turner et al., 1980; Yukie, 2002). In that regard, the absence of CM projections to the amygdala in the present study is consistent with the topographic gradients observed laterally. Similarly, the lack of inputs from the core is also consistent with previous studies in primates. The inputs from the rostral areas of auditory cortex to the amygdala may influence other cortical areas that receive projections from this structure (Romanski et al., 1993).

The RM projection to the tail of the caudate nucleus has also not been previously reported, though the existence of this input is not surprising since most of the lateral belt and parabelt areas of primate auditory cortex are known to project to some part of the caudate or putamen (Borgmann and Jurgens, 1999; Yeterian and Pandya, 1998), similar to what has been observed in other mammals (Reale and Imig, 1983; Romanski and LeDoux, 1993). The striatal projections of the core are less clear. Borgmann et al (1999) found no evidence of projections to the striatum after injections of the core despite strong projections from areas corresponding to the lateral belt and parabelt. In apparent contrast, Yeterian and Pandya (1998) reported a "modest" projection after injection of a large part

110

of the core that appeared to involve A1 and R. However, this injection also extended into area RM (area ProA), and labeled parts of the putamen, and head and tail of the caudate. Therefore, it is not clear whether the label resulted from projections from the core, RM, or both. The absence of striatal connections after injection of CM in the present study was somewhat surprising, since Yeterian and Pandya (1998) found projections to the putamen and head and tail of the caudate after an injection that included this area. However, that injection also involved Tpt, which has strong projections to the striatum.

Area CM was the only area in this study to exhibit connections with the entorhinal cortex. After CTB injections in rostral and caudal CM, labeled cells were distributed along most of the rostrocaudal extent of the inferior temporal lobe, but restricted to the lower layers of this cortex. There was no evidence of an anterograde projection to this region, despite dense anterograde projections to auditory areas of the temporal lobe in the same tissue sections. Injections of RM produced neither anterograde nor retrograde labeling in the entorhinal cortex. These findings are only partly consistent with other studies in primates. After injections in various divisions of the entorhinal cortex in macaque monkeys, labeled cells in the vicinity of auditory cortex are typically located in the insula, temporal pole and rostral parts of the STG corresponding to rostral areas of the medial belt, lateral belt, and parabelt (Insausti et al., 1987; Van Hoesen and Pandya, 1975). Caudally, at the level of A1 or caudal CM, labeled cells are not found in auditory cortex, but tend to be limited to the upper bank of STS. These results indicate that the rostral auditory cortex projects to entorhinal cortex, though our BDA injections into RM revealed no projections in marmosets. The strong entorhinal projection to CM in the present study may not have been observed in previous studies involving retrograde tracer

injections in entorhinal cortex, or superior temporal lesions. At present, the known connections suggest that rostral auditory areas project to entorhinal cortex, but only some caudal auditory fields (i.e., CM) receive inputs from this region.

Additional connections were found between CM and the posterior parietal cortex after injections of both regions. Labeled cells after CM injections were plotted, but not analyzed or reconstructed because of concern that some of the labeling was due to unintended uptake by cortex in the upper bank of the lateral sulcus. However, a BDA injection just behind the caudal terminus of the lateral sulcus in one case revealed the presence of retrogradely labeled cells in CM, CL, and Ri, as well as light anterograde projections to these same areas (Fig. 14). These findings may be consistent with previous observations of connections between the caudal belt region (i.e., CM, CL, Tpt) and the intraparietal sulcus in macaques (Lewis and Van Essen, 2000). The rostral auditory areas do not appear to have posterior parietal connections.

Finally, we are uncertain about prefrontal connections of the medial belt region in marmosets. Blocks of tissue containing parts of the prefrontal cortex were removed from the main block prior to sectioning and generally not processed. Interested readers are referred to related studies in macaques (Romanski et al., 1999a; Romanski et al., 1999b).

Correspondence with auditory cortex of other mammals

In our analysis of the results of this study and those related to it (de la Mothe et al., 2006b; Kajikawa et al., 2005), we were impressed by similarities in the organization of the monkey and cat auditory cortex noted earlier by Jones and Burton (Jones and Burton, 1976). They suggested that the primate parainsular field (RM) may represent the

homologue of area AII in the cat, and the postauditory field (CM) the homologue of the anterior ectosylvian region situated between AII and SII in the cat, known as the anterior auditory field, AAF. A number of findings in the present and previous studies support this hypothesis. First, AAF and CM occupy similar positions in auditory cortex, relative to AI. In the cat, ferret and several other species AAF and A1 share a high characteristic frequency border (Imig and Reale, 1980; Knight, 1977; Lee et al., 2004; Phillips and Irvine, 1982; Rouiller et al., 1991; Wallace et al., 1991). In primates, the tonotopic gradient in A1 has been found to reverse or be disrupted at its caudal border with CM (Cheung et al., 2001; Imig et al., 1977; Kajikawa et al., 2005; Kosaki et al., 1997; Merzenich and Brugge, 1973; Rauschecker et al., 1997; Recanzone et al., 2000a). Second, the response properties of neurons in AAF and CM are very similar to those in A1, except for significantly broader tuning bandwidth (Eggermont, 1998; Kajikawa et al., 2005; Knight, 1977; Kowalski et al., 1995; Tian and Rauschecker, 1994). Third, though primary-like in the ways described above, CM and AAF are not primary fields. In primates, the MGv is the major input to the core areas (A1, R, RT), and in cats, the MGv projects strongly to A1, PAF, and VPAF. In contrast, CM and AAF have strong inputs from AI and thalamic inputs that include the posterior nuclei and the rostral pole of the MGC (i.e., MGad, Pol) (de la Mothe et al., 2006b; Lee et al., 2004). Fourth, AAF and CM adjoin somatosensory cortex, including a poorly defined region of cortex in which auditory and somatosensory representations appear to converge (see above discussion).

On the basis of these comparisons, it is quite clear that CM resembles AAF more than any other area of auditory cortex. While these common features are not sufficient to establish *homology* between these areas (i.e., inherited from a common ancestor), the

areas could aptly be described as *corresponding*. To the extent that AAF and CM are corresponding areas, like A1, comparisons of auditory cortex organization across taxa become more meaningful and findings in one species can be more broadly applied. With time evidence may accumulate supporting the correspondence of other areas, as well (e.g., PAF-R; VPAF-RT; AII-RM). In any event, it is not anticipated that corresponding areas will be identical. Rather, they are simply more likely to have retained common features than other areas. In that sense, the identification of corresponding areas is meaningful and instructive.

Correspondence of CM with posteromedial fields in other primates

While the correspondence between areas identified as CM is fairly well-established for monkeys, it is less certain for other primates, including humans. In a recent study, the core region in monkeys was identified in chimpanzees and humans on the basis of common architectonic features (Hackett et al., 2001). In that same study, correspondence was also proposed between CM in monkeys and a distinct field in chimpanzees and humans located at the medial terminus of Heschl's gyrus, known as TD (von Economo & Koskinas, 1925). Additional areas extend posterior and laterally to fill out the planum temporale region, which is larger in chimpanzees and humans. Thus, on architectonic grounds, parts of the planum temporale appear to correspond to CM, CL, ML, AL, and Tpt in monkeys (Hackett, 2002; Sweet et al., 2005). In functional imaging studies, the planum temporale, and subregions within, are activated during a variety of tasks, including perception of speech and environmental sounds, speech production, and spatial perception (Griffiths and Warren, 2002). Of special interest is fMRI evidence of

114

auditory-somatosensory convergence in this area in humans (Foxe et al., 2002). Although further elaboration of these ideas is beyond the scope of this paper, it is important to continue to identify links between taxonomic groups in future studies of auditory cortex to broaden the applicability of research findings regardless of species and thereby improve our understanding of the auditory system.

Consistency with working model of primate auditory cortex

A general conclusion reached in the present study was that the organization of the marmoset auditory cortex conformed well to the working model based on studies of New World and Old World primates. While the core-belt-parabelt schema is the most well-developed for the macaque monkey, it is important to note that findings in New World primates (e.g., owl monkey, squirrel monkey) were equally influential in the development of this model (Imig et al., 1977; Morel and Kaas, 1992). In marmosets, however, anatomical studies have largely focused on the organization of the core region, especially AI (Aitkin et al., 1988; Luethke et al., 1989). Thus, one motivation for conducting the current study in marmosets was to determine whether the core-belt-parabelt model might also characterize this species. This appears to be especially important since the marmoset has become a popular model for neurophysiological study of the auditory cortex (Aitkin et al., 1986; Bendor and Wang, 2005; deCharms et al., 1999; deCharms and Merzenich, 1996; Eliades and Wang, 2005; Kajikawa et al., 2005; Kajikawa and Hackett, 2005; Liang et al., 2002; Lu et al., 2001a; Lu et al., 2001b; Lu and Wang, 2004; Luczak et al., 2004; Luethke et al., 1989; Nagarajan et al., 2002; Philibert et al., 2005; Wang and Kadia, 2001; Wang et al., 1995).

With some exceptions, the present study revealed that the architectonic characteristics of the marmoset superior temporal region were comparable to those described for the macaque monkey (Galaburda and Pandya, 1983; Hackett et al., 2001; Hackett et al., 1998a; Jones and Burton, 1976; Jones et al., 1995; Morel et al., 1993; Pandya and Sanides, 1973) and other New World primates (Imig et al., 1977; Jones and Burton, 1976; Luethke et al., 1989; Morel and Kaas, 1992). The size of auditory cortex was smaller, about one-third the size of macaques, but major architectonic features were qualitatively similar, reflecting the typical medial-lateral and rostral-caudal architectonic gradients observed in other primates. On the other hand, a comparative quantification of architectonic details (e.g., cell types, cell size, cell or fiber density) may ultimately reveal significant species differences that were not addressed by this study. To date, however, detailed architectonic analyses of these features have not been conducted for auditory cortex of primates other than humans. One surprising difference between marmosets and other primates was that acetylcholinesterase (AChE) expression was relatively uniform across major regions of auditory cortex. Typically, elevated AChE density in the layer III/IV band is a reliable and robust marker of the core region, where it is coextensive with dense expression of cytochrome oxidase and parvalbumin. In this study, however, its expression was greatly reduced compared to tissue from other primates processed in our laboratory using the same histochemical protocol (Hackett et al., 2001). In contrast, adjacent sections processed for cytochrome oxidase and parvalbumin revealed the expected pattern of expression in the core (see Figs. 5, 6, 8). It is not known whether species differences or methodological factors account for this finding.

Additional support for a core-belt-parabelt system of organization was found in the patterns of connections between regions. Injections of the medial belt revealed topographic connections with the medial belt, lateral belt, core, and parabelt regions, as expected. Likewise, injections of the core labeled cells and terminals within the core and belt regions, consistent with previous results in marmosets and tamarins (Aitkin et al., 1988; Luethke et al., 1989). The discovery of labeled cells, but not terminals, in the infragranular layers of the parabelt after injections of A1 or R was unexpected, given previous findings in macaques and owl monkeys (Hackett et al., 1998a; Morel et al., 1993; Morel and Kaas, 1992). However, an infragranular projection from the parabelt to the core would not have been observed after injection of retrograde tracers into the parabelt. In addition, the absence of anterograde label in the parabelt after core injections, and the absence of retrogradely labeled cells in supragranular layers of the parabelt in this study indicate that the projection from the parabelt is strictly feedback in nature. Thus, the overall pattern of connections in the marmoset is consistent with the working model in that information flow proceeds outward from the core to the parabelt via an intermediate stage of processing in the belt (Kaas & Hackett, 1998). But, the model may need to be amended to include the present observation that feedback projections from the parabelt directly targeted the core in marmosets (Figs. 31-32).

Finally, physiological studies of the marmoset corroborate some of the subdivisions identified anatomically in the present study. On the basis of tonotopic reversals, Bendor and Wang (2005) identified A1, R, and RT on the surface of the STG near the lateral sulcus, extending previous findings in this species concerning the location and tonotopic organization of A1 (Aitkin et al., 1988; Aitkin et al., 1986; Kajikawa et al.,

2005; Luethke et al., 1989; Philibert et al., 2005). Both the size and extent of the core

areas identified match the present findings. We would add, however, that up to about

one-third of the core extends medially into the lateral sulcus, and has not been mapped in

some studies. The significance of this may relate to the present observations concerning

differences between the medial and lateral halves of the core. In brief, the lateral halves

of the core areas had sparse connections with RM or rostral CM, while relatively dense

connections were concentrated medially in the core. The pattern was different in caudal

CM, which had somewhat strong connections with $A1_M$ and $A1_L$ caudally, and $A1_L$

rostrally. Some evidence for such patterns can be found in a previous study of marmosets

(Aitkin et al., 1988). Although these patterns may simply reflect strict topographic

constraints, the patterns could also reflect functional specificity within the medial and

lateral halves of the core that is preserved in its output to other areas. As noted above

(Fig. 6), the medial half of the core, at least in A1, was more densely myelinated than the

lateral half, consistent with previous distinctions made in other primates, including

humans (Galaburda and Pandya, 1983; Hackett et al., 2001; Pandya and Sanides, 1973).

The division of $A1_M$ and $A1_L$ near the edge of the lateral sulcus cuts across the

rostrocaudal gradient of isofrequency contours, thus, there may be functional differences

between these divisions of A1. For example, recordings in A1 of owl monkeys and cats

indicate that the representation of response parameters other than characteristic frequency

may be spatially represented in maps that do not coincide with isofrequency contours

(Read et al., 2002; Recanzone et al., 1999; Schreiner, 1998). Further study will be needed

to clarify the functional significance of these details.

Conclusions

The results of this study indicate that the organization of the marmoset monkey auditory cortex closely matches that of other primates, in line with our working model of primate auditory cortex. The medial belt areas RM and CM represent functionally-distinct areas of auditory cortex and of the medial belt region. Both areas receive dense projections from the core and are broadly connected with medial belt, lateral belt, and parabelt regions. Individually, RM and CM have distinctive architectonic features and patterns of connections. In particular, CM receives somatosensory inputs from the retroinsular somatosensory area (Ri), and has additional connections with STS, posterior parietal, and entorhinal cortex. RM does not appear to have connections with somatosensory fields, but does project to the lateral nucleus of the amygdala and tail of the caudate nucleus. In addition, the collective findings suggest that primate CM may correspond to areas TD in humans and AAF in other mammals. Architectonic features and connections distinguish the core areas A1 and R from the belt and parabelt regions of auditory cortex. Projections to the core from the parabelt originated from infragranular cells, but there was no evidence that the core projects directly to the parabelt. These findings suggest minor revisions to the model.

CHAPTER III

THALAMIC CONNECTIONS OF AUDITORY CORTEX IN MARMOSET
MONKEYS: CORE AND MEDIAL BELT REGIONS

Introduction

Our working model of primate auditory cortex organization (Kaas & Hackett, 1998; Kaas et al., 1999; 2000; Hackett, 2002) defines *auditory cortex* as those cortical areas that are the principal targets of neurons in either the ventral (MGv) or dorsal (MGd) divisions of the medial geniculate complex (MGC). By this definition, three regions of the superior temporal cortex are known to comprise auditory cortex in primates: core, belt, and parabelt (Fig. 33). Each of these regions is further subdivided into two or more distinct areas. In addition, there are a number of *auditory-related* fields in temporal, prefrontal, and posterior parietal cortex that do not receive inputs from the principal divisions of the MGC, but depend on corticocortical inputs from one or more areas of auditory cortex. The dorsal superior temporal sulcus (STS) and rostral temporal lobe have connections with nuclei in the posterior thalamus, but sparse inputs from MGC. With respect to thalamocortical inputs to auditory cortex, the primary (lemniscal) auditory pathway projects mainly upon the core region via the MGv. Projections to the belt and parabelt regions arise largely from the MGd, while all areas in all three regions receive a substantial diffuse input from the magnocellular (MGm) division of the MGC (Jones, 1997; Jones, 2003).

As described in the companion to this article (de la Mothe et al., 2006a), the belt areas bordering the core region occupy an intermediate position in the auditory cortical

120

Figure 33. Schematic models of macaque (A) and marmoset (B - D) monkey auditory cortex. In panels A - C the lateral sulcus (LS) of the left hemisphere was graphically opened (cut) to reveal the locations of auditory cortical areas on its lower bank. The circular sulcus (CiS) has been flattened to show the position of the rostromedial (RM) and rostrotemporal medial (RTM) areas that occupy its lateral wall. The upper bank of the LS is partly opened (cut) to show the locations of the retroinsular area (Ri) in the fundus, second (S2) and parietoventral (PV) somatosensory areas on the upper bank, and insula (Ins). The three areas that comprise the core region of auditory cortex (dark shading) are located on the lower bank (A1, auditory area 1; R, rostral; RT, rostrotemporal). The core is surrounded by seven or eight areas that belong to the belt region (light shading) (CM, caudomedial; CL, caudolateral; ML, middle lateral; RM, rostromedial; AL, anterolateral; RTM, rostrotemporal medial; RTL, rostrotemporal lateral). The proisocortex area (Pro) is a putative addition to the medial belt. The core and lateral belt regions are mostly contained within the lateral sulcus in macaques, but extend onto the superior temporal gyrus (STG) in the marmoset. On the surface of the STG are two areas that make up the parabelt region (medium shading) (RPB and CPB, rostral and caudal parabelt). The rostral part of the STG (STGr) extends to the temporal pole. The temporal parietotemporal area (Tpt) occupies the caudal end of the STG and extends onto the supratemporal plane within the LS. Tonotopic gradients within areas are indicated by H (high frequency) and L (low frequency). Other sulci shown include the arcuate sulcus (AS), central sulcus (CS), intraparietal sulcus (IPS), and superior temporal sulcus (STS). (B, inset) Photographic image of the marmoset right hemisphere. (D) Schematic of the marmoset right hemisphere, medial view, showing the plane of section (diagonal lines) used in the present study for histological processing of the thalamus.
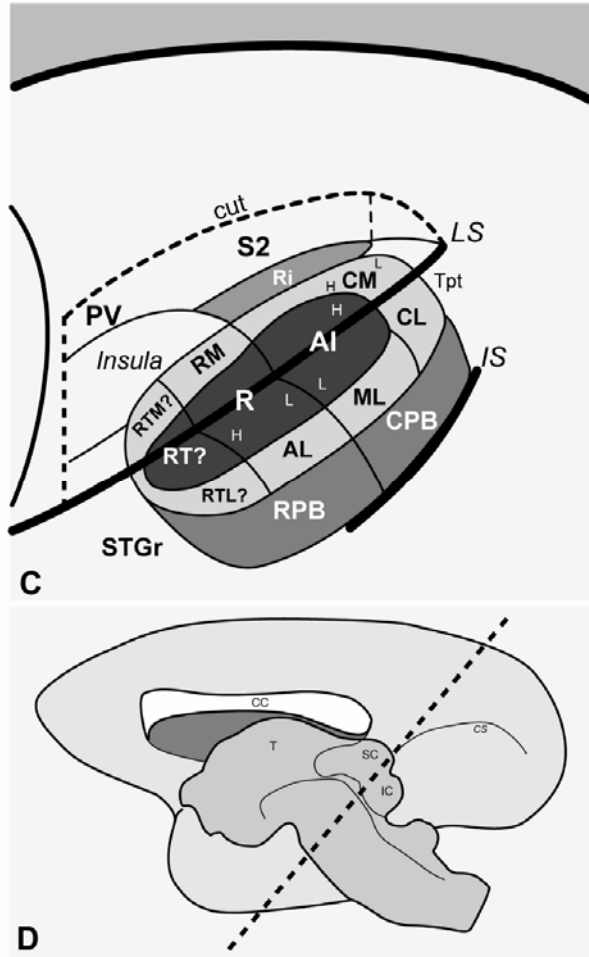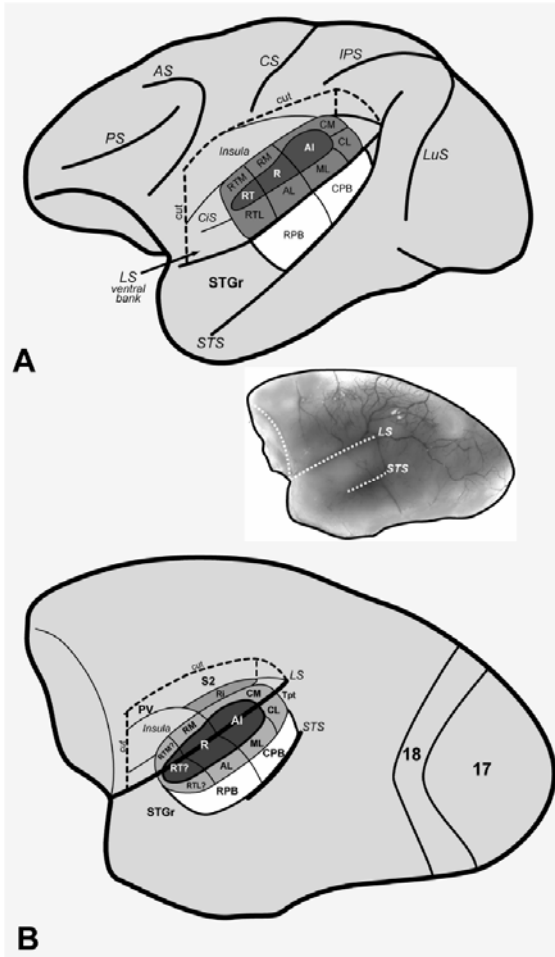
processing hierarchy (Fig. 33). Outputs from the core mainly target the belt areas, which project to the parabelt region and auditory-related fields (Hackett et al., 1998a; Kaas and Hackett, 2000). Because many of the belt areas remain poorly-defined, we have tended to view the region as homogeneous. However, anatomical and physiological evidence is beginning to reveal that each of the belt areas is likely to represent a discrete functional module, characterized by a unique anatomical and neurophysiological profile.

One part of that profile concerns the cortical and thalamic connections of each field. To date the lateral belt areas (i.e., CL, ML, AL, RTL) have been the most well-studied, whereas the medial belt areas (CM, RM, RTM) have received little attention. One of the clearest differences among the lateral belt areas is that the caudal and rostral fields target functionally-distinct regions of auditory and auditory-related cortex (Galaburda and Pandya, 1983; Jones et al., 1995; Lewis and Van Essen, 2000; Morel et al., 1993; Morel and Kaas, 1992; Romanski et al., 1999a; Romanski et al., 1999b), suggesting that segregated pathways arise from different parts of auditory cortex (Kaas and Hackett, 2000; Rauschecker, 1998; Romanski et al., 1999b). This topography is consistent with evidence of functional segregation within the lateral belt (Rauschecker and Tian, 2000; Rauschecker and Tian, 2004; Rauschecker et al., 1995; Tian et al., 2001). Compared to the lateral belt, much less is known about the medial belt areas. After injections of different regions of prefrontal cortex in macaques, labeled cells were relatively sparse in the medial belt compared to the lateral belt, limiting conclusions about frontally-directed projections (Romanski et al., 1999a). Injections of the rostral (RPB) and caudal (CPB) divisions of the parabelt region of macaques revealed a topographic gradient in their connections with the medial belt areas (Hackett et al.,

1998a). Area RM was broadly connected with RPB and CPB, while CM and RTM had stronger connections with CPB and RPB, respectively. The results of the companion study also revealed clear topographic differences in the cortical connections of RM and CM of marmoset monkeys (de la Mothe et al., 2006a). In addition to stronger connections with caudal areas of auditory cortex, CM also has substantial connections with the retroinsular (Ri) area of somatosensory cortex, posterior parietal cortex, and entorhinal cortex. Injections of RM did not label these areas, but did reveal projections to the lateral nucleus of the amygdala and tail of the caudate nucleus. Thus, on the basis of architecture and cortical connections, RM and CM appear to be functionally-distinct areas of the belt region in marmosets.

With respect to thalamocortical connections of the belt region, the principal inputs to the belt areas arise from the MGd, along with additional inputs from MGm, posterior nucleus (Po), suprageniculate (Sg), limitans (Lim), and medial pulvinar (PM) (Burton and Jones, 1976; Jones, 2003; Jones and Burton, 1976; Molinari et al., 1995; Morel et al., 1993; Morel and Kaas, 1992; Pandya et al., 1994; Rauschecker et al., 1997). Architectonic studies of the macaque monkey indicate that the MGd has at least two subdivisions, but it is not known how the belt areas may differ with respect to these inputs (posterior, MGpd; anterior, MGad), (Burton and Jones, 1976; Hackett et al., 1998b; Jones, 2003; Molinari et al., 1995). Generally, the rostral and caudal areas of auditory cortex tend to receive inputs from caudal and rostral portions of the MGC, respectively. Moreover, given the observation that cutaneous somatosensory stimulation drives neuronal responses in CM of macaques, it is possible that the belt areas may also differ with respect to non-auditory or multisensory inputs (Fu et al., 2003; Schroeder et

al., 2001). Thus, while little is known about the response properties of neurons in any division of the primate MGC, including the MGd, regional variations in function may be reflected in disparate projections to auditory cortex.

The general goal of the present study and its companion (de la Mothe et al., 2006a) was to expand our understanding of auditory cortex organization by comparing the cortical and thalamic connections of the medial belt areas, RM and CM, with adjacent core areas, R and A1. The results were also used to test the following specific predictions of the model with respect to thalamocortical connections: (1) RM and CM receive thalamic inputs from different subdivisions of the MGC; (2) The thalamocortical connections of the medial belt areas are distinct from those of the core (Aitkin et al., 1988; Luethke et al., 1989); and (3) The organization of the marmoset auditory thalamus approximates that of the macaque monkey and other primates.

Materials and Methods

Animal subjects

The experiments described in this report were conducted in the auditory research laboratories at Vanderbilt University in Nashville, TN. Six adult marmosets (*Callithrix jacchus jacchus*) served as animal subjects in the present study. The experimental history of each animal is included in Table 2. All procedures involving animals followed NIH Guidelines for the Use of Laboratory Animals, and were approved by the Vanderbilt University Institutional Animal Care and Use Committee.

Table 2. Experimental history of animal subjects. Areas of tracer injections (A1, auditory core area 1; R, rostral core; RM, rostromedial belt; CM, caudomedial belt; CPB, caudal parabelt; CL, caudolateral belt; AL, anterolateral belt). Neuroanatomical tracers (CTB, cholera toxin subunit B; BDA, biotinylated dextran amine; FB, fast blue; FE, fluoroemerald; FR, fluororuby). Asterisk (*) indicates tracer injections in the lateral belt or parabelt that were not analyzed for inclusion in the present study, but are illustrated in some reconstructions.

Case	Sex	Areas Injected	Tracer	%	Volume (ul)
1 (01-37)	M	RM R R *AL/ML	BDA FR FE FB	10 10 10 10	0.4 0.3 .4 0.25
2 (01-118)	M	RM R *CL	BDA FR FB	10 10 10	0.4 0.3 0.2
3 (02-17)	M	CM	CTB	1	0.4
4 (02-51)	M	A1 R	CTB FR	1 10	0.4 0.3
5 (02-60)	M	A1 *CPB	FR FB	10 10	0.3 0.2
6 (04-51)	M	CM *AL	CTB FR	1 10	0.4 0.3

General surgical procedures

Aseptic techniques were employed during all surgical procedures. Animals were premedicated with cefazolin (25 mg/kg), dexamethasone (2 mg/kg), cimetidine HCl (5 mg/kg), and robinul (0.015 mg/kg). Anesthesia was induced by intramuscular injection of ketamine hydrochloride (10 mg/kg) then maintained by intravenous administration of ketamine hydrochloride (10 mg/kg) supplemented by intramuscular injections of xylazine (0.4 mg/kg) or by isoflurane inhalation (2 – 3%). Body temperature was kept at 37°C with a water circulating heating pad. Heart rate, expiratory CO_2, and O_2 saturation were

continuously monitored throughout the surgery and used to adjust anesthetic depth. Oxygen was delivered passively through an endotracheal tube at a rate of 1 liter/minute.

The head was held by hollow ear bars affixed to a stereotaxic frame (David Kopf Instruments, Tujunga, CA). A midline incision was made exposing the skull, followed by retraction of the temporal muscle. A craniotomy was performed exposing the left dorsal superior temporal gyrus, lateral fissure, and overlying parietal cortex. After retraction of the dura, warm silicone was applied to the brain to prevent desiccation of the cortex. Photographs of the exposed cortical surface were taken for recording the locations of electrode penetrations in relation to blood vessels and the lateral sulcus.

Retraction of the parietal operculum and neuroantomical tracer injections

Tracer injections were made into target areas through a pulled glass pipette affixed to a 1 µl Hamilton syringe. The pipette was advanced into cortex under stereo microscopic observation to a depth of 1000 µm using a stereotaxic micromanipulator. After manual pressure injection of the tracer volume (Table 2), the syringe was held in place for 10 minutes under continuous observation to maximize uptake and minimize leakage. Injections of the core areas (A1, R) were made directly into the lateral surface of the superior temporal gyrus (STG) after removal of the dura (see Fig. 32b-c). Injections of medial belt targets within the lateral fissure were achieved in one of two ways. In cases 1 and 3, BDA or CTB were injected into RM or CM by passing the syringe through the overlying parietal cortex. Depth was controlled by stereotaxic measurements and verified by recordings made using a tungsten microelectrode affixed to the syringe. In all other cases, access to injection targets within the lateral fissure was achieved by retraction of

the banks of the lateral fissure, as recently described (Hackett et al., 2005). Briefly, after microdissection of the arachnoid membrane around blood vessels at the edge of the lateral sulcus, the upper bank was gently retracted using a stereotaxic arm and blunt dissection of arachnoid within the sulcus. Once the desired opening was achieved, tracer injections were made directly into target areas relative to gross anatomical landmarks and blood vessel patterns.

Auditory stimulation and recordings

For most of the cases included in this report, detailed recordings were obtained seven days after tracer injections during a terminal experiment that averaged 24 hours in duration. The recording sites were concentrated in A1 and CM using a battery of stimuli, including tones, broad band noise, frequency modulated tones, and marmoset vocalizations. The tonotopic maps derived from these recordings were marked by electrolytic lesions and aided the reconstructions of architecture and connections, primarily at the borders of A1 and CM. The physiological results of these experiments and methodological details are reported elsewhere (Kajikawa et al., 2005; Kajikawa and Hackett, 2005). In one case (case 1) the left hemisphere was mapped prior to tracer injections. Injections into RM and R were made just rostral to the border of A1 and R based on a reversal in the tonotopic gradient. Because neuronal responses could be abolished or otherwise altered within or near tracer injections, post-injection recordings were confined to the opposite hemisphere in all other cases.

Perfusion and histology

At the end of the terminal recording experiment a lethal dose of pentobarbital was administered intravenously. Just after cardiac arrest the animal was perfused through the heart with cold (4 degrees C) saline, followed by cold (4 degrees C) 4% paraformaldehyde dissolved in 0.1 M phosphate buffer (pH 7.4). Immediately following the perfusion the brains were removed and photographed. The cerebral hemispheres were separated from the thalamus and brainstem, blocked, and placed in 30% sucrose for 1 to 3 days. The thalamus was cut perpendicular to long axis of the brainstem in the caudal to rostral direction at 40 µm, as shown in Fig. 32d. In each series of sections every sixth section was processed for the following set of histochemical markers: (i) fluorescent microscopy; (ii) biotinylated dextran amine (BDA) or cholera toxin subunit B (CTB); (iii) myelinated fibers (MF) (Gallyas, 1979); (iv) acetylcholinesterase (AChE) (Geneser-Jensen and Blackstad, 1971); (v) stained for Nissl substance with thionin; (vi) cytochrome oxidase (CO) (Wong-Riley, 1979); or (vii) parvalbumin immunohistochemistry.

Analysis and reconstruction of connections

The X-Y locations of cell somata labeled by retrograde axonal transport of each tracer were plotted using a Neurolucida system (MicroBright Field, Inc., Williston VT). Auditory cortical areas were identified in sections stained for the histochemical markers listed above, as described in the companion paper (de la Mothe et al., 2006a). Subdivisions of the MGC and surrounding nuclei of the posterior thalamus were guided by previously established architectonic criteria in New World marmoset and owl

monkeys (Aitkin et al., 1988; FitzPatrick and Imig, 1978; Morel and Kaas, 1992), as well as Old World macaque monkeys (Burton and Jones, 1976; Hackett et al., 1998b; Jones, 2003; Molinari et al., 1995). The architectonic details are illustrated in figures 33 – 35 and described in the Results. For each histochemical marker, the borders of individual areas and patches of anterograde terminal labeling were drawn onto plots of labeled cells by alignment of blood vessels and common architectonic features using a drawing tube affixed to a Zeiss Axioscope. These drawings were used to create the schematic reconstructions. In most figures, every other section was chosen for illustration. For each tracer injection, the percent of total labeled cells was derived by dividing total cell counts for each thalamic nucleus by the total number of cells in the thalamus labeled by that injection. Digital images were acquired using a Nikon DXM1200F digital camera and Nikon E800S microscope. These images were cropped, adjusted for brightness and contrast using Adobe Photoshop 7.0 software, but were otherwise unaltered. Final figures containing images and line drawings were made using Canvas 8.0 software (Deneba Systems, Inc., Miami, FL) and Adobe Illustrator 10.0 (Adobe Systems, Inc.).

Results

Thalamic architecture and subdivisions

Delineation of thalamic nuclei and their subdivisions was accomplished in adjacent series of sections stained for Nissl, cytochrome oxidase (CO), acetylcholinesterase (AChE), myelinated fibers (F), and in some cases, parvalbumin (Figs. 34 - 36). Cytoarchitecture, as revealed in sections stained for Nissl, was the principal means of nuclear identification. Density shifts in the other preparations,
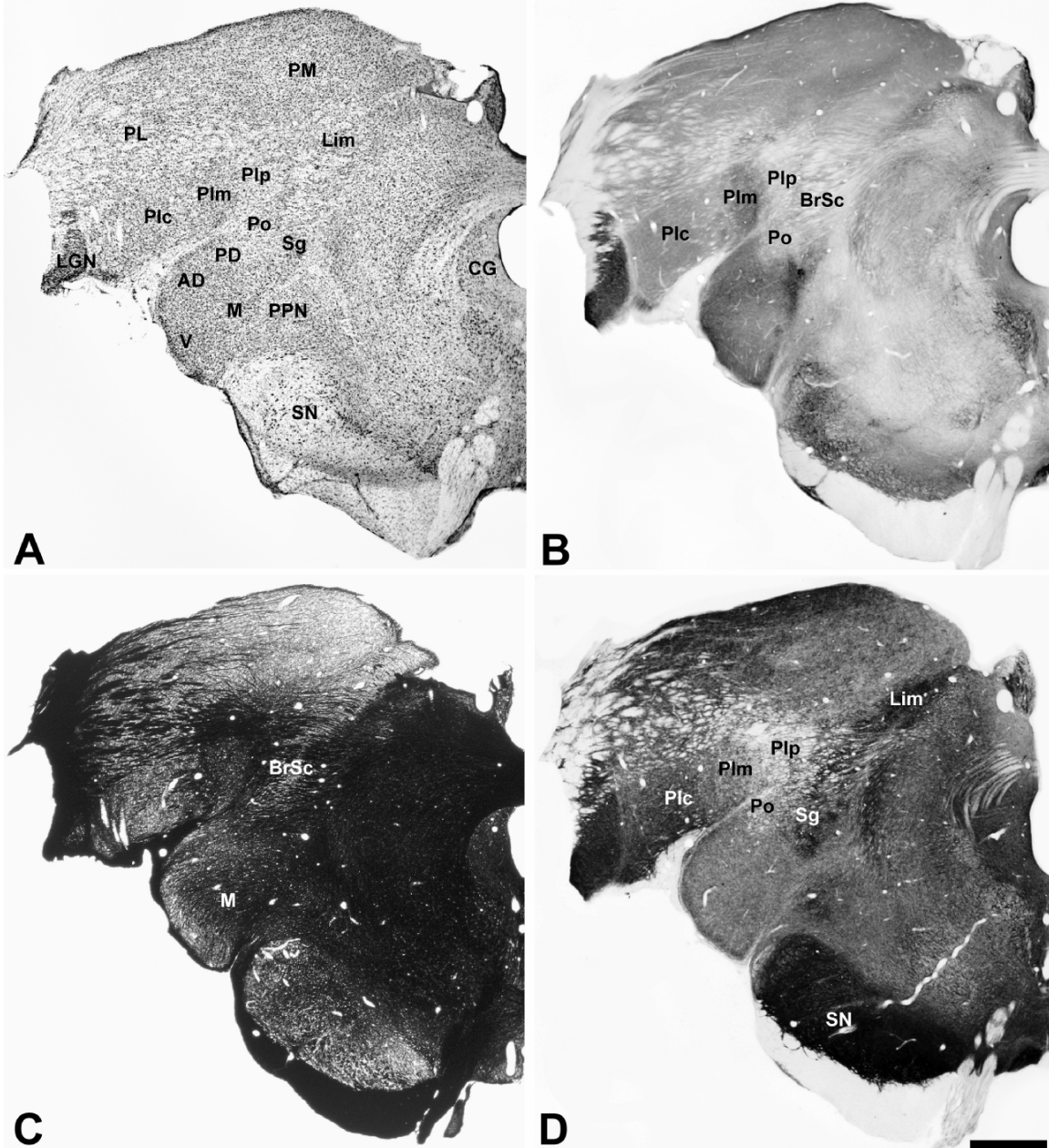
Figure 34. Architecture of the marmoset posterior thalamus. (A) Thionin stain; (B) cytochrome oxidase stain; (C) Myelin stain; (D) acetylcholinesterase stain. Abbreviations for nuclei and fiber tracts in panels A and C given in the Table of abbreviation. Scale bar, 1 mm.

especially CO, reinforced border identification as transitions in expression density often matched the cytoarchitectonic border. Patterns of labeled cells were related to these architectonic divisions to derive final reconstructions. For all cases described in this

Figure 35. Architectonic features of the marmoset medial geniculate complex. Series of adjacent sections are arranged from caudal (A – C) to rostral (V – X). In each row, adjacent tissue sections were stained for Nissl substance (left column), cytochrome oxidase (center column), and acetylcholinesterase (right column). Nuclear subdivisions are outlined in the Nissl-stained sections (dashed lines). Asterisks indicate zone of dense acetylcholinesterase staining. Arrows denote blood vessel profiles common to sections in a given row. See list of abbreviations for additional details. Scale bar, 500 µm.
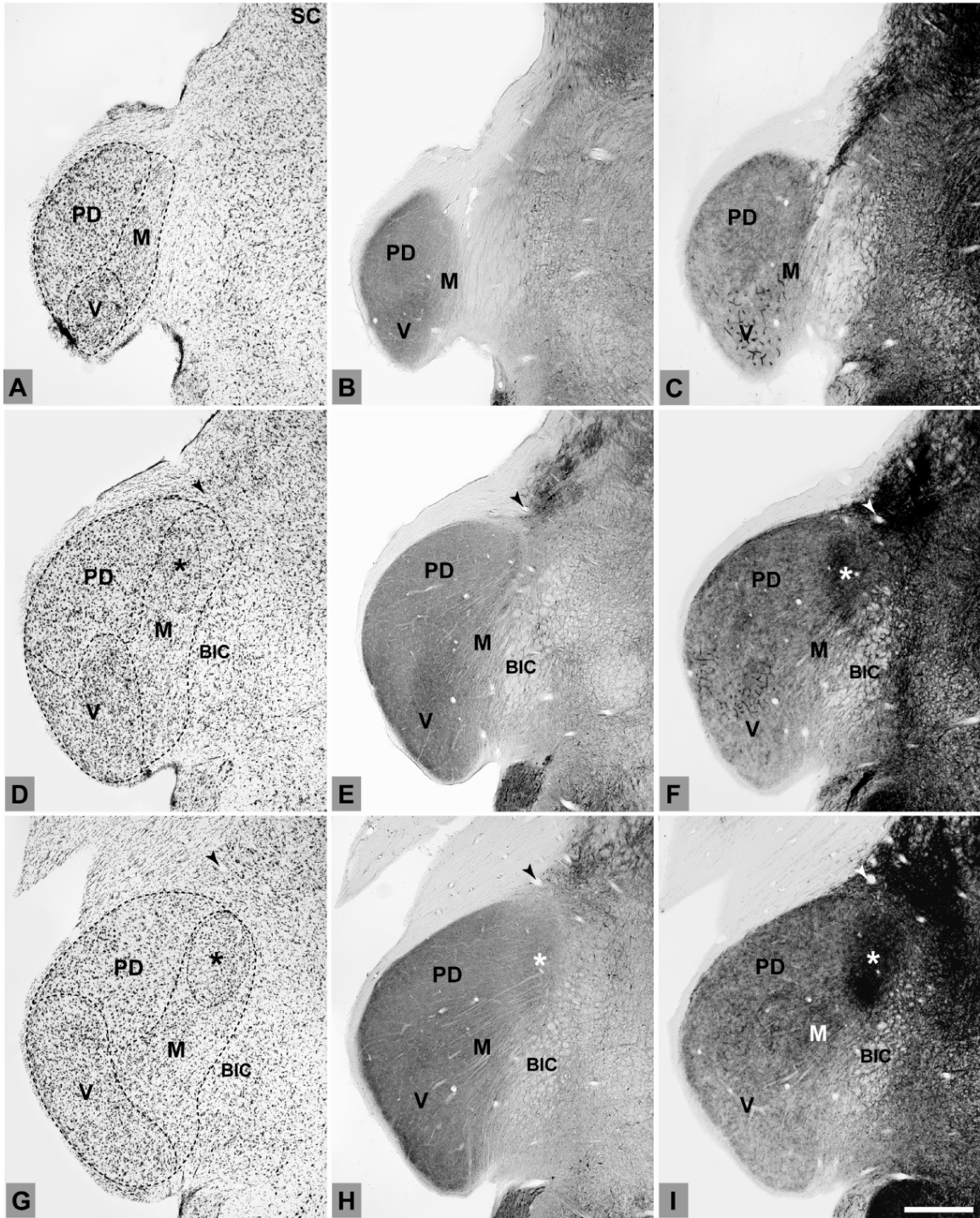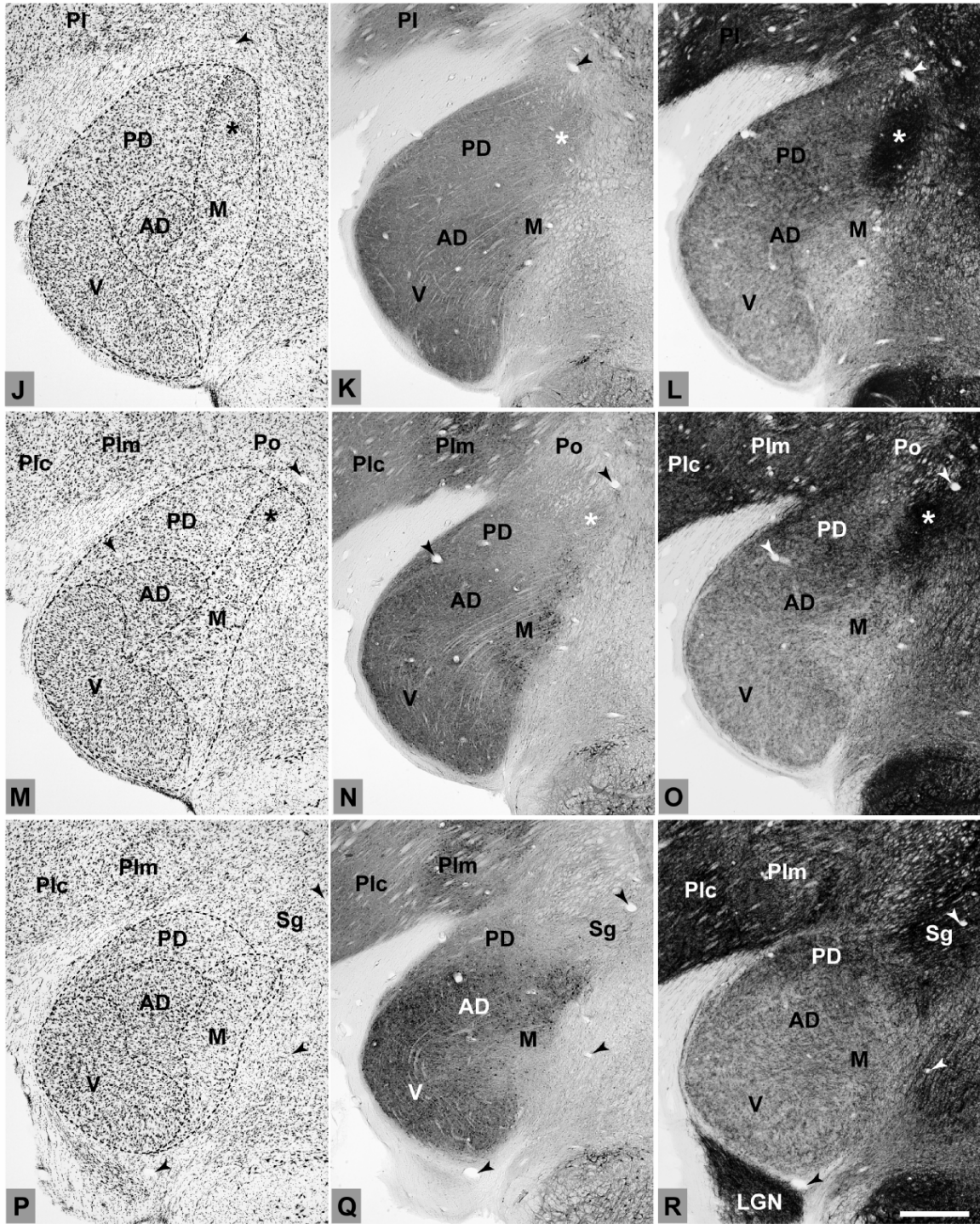
Figure 35 (continued)
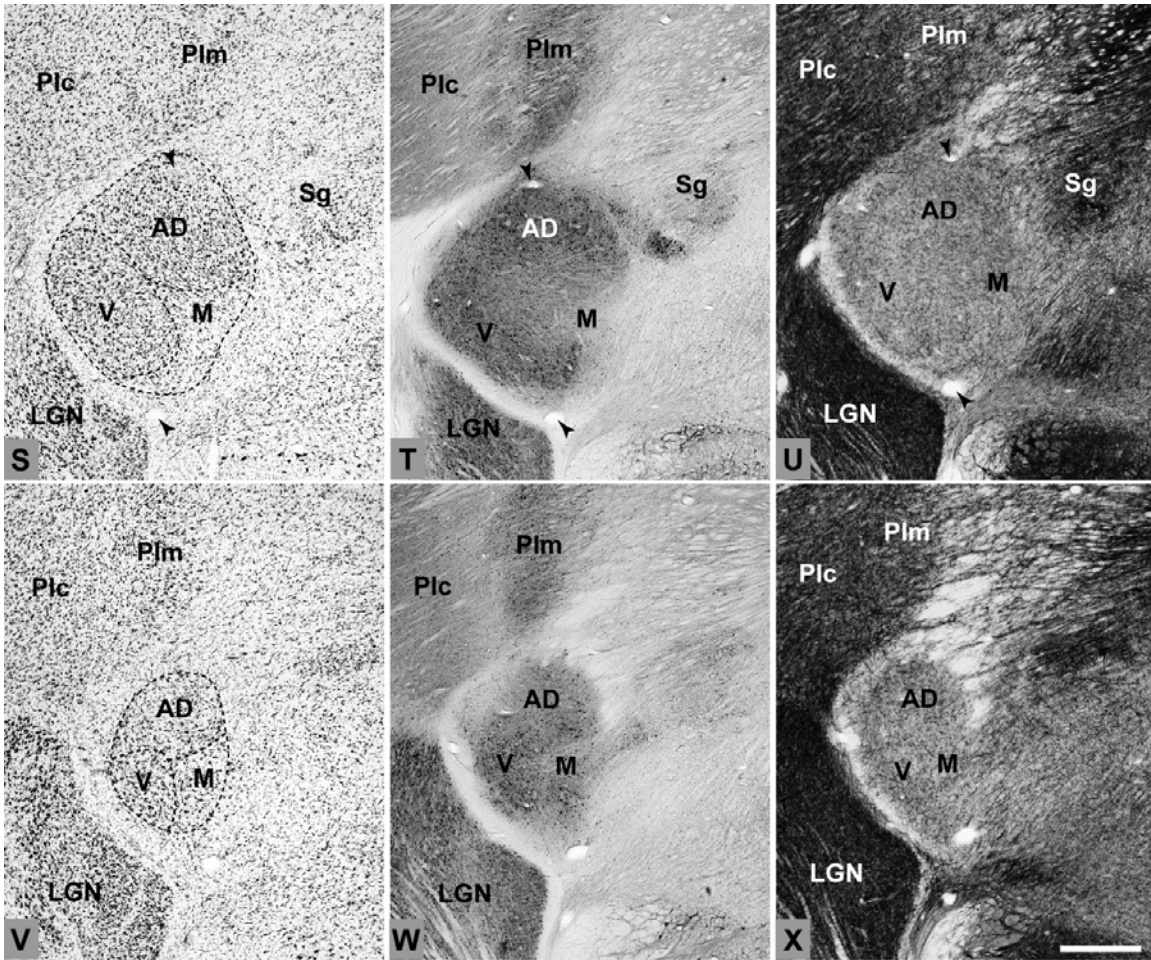
Figure 35 (continued)

report, the plane of section was perpendicular to the long axis of the brainstem and spinal

cord, and therefore slightly horizontal to a standard coronal plane (Fig. 33d).

The dorsal division of the MGC consisted of two main divisions, MGpd and

MGad. The MGpd occupied most of the caudal pole of the MGC where it was populated

mostly by medium-sized cells of uniform spacing that was notably less dense than the

MGv and MGad (Fig. 35a – c). As the MGC expanded in size rostrally, the MGpd was

gradually displaced on its ventral and ventromedial borders by the emergence of the MGv

and expansion of the MGm (Fig. 35d – i). In CO preparations, MGpd staining was
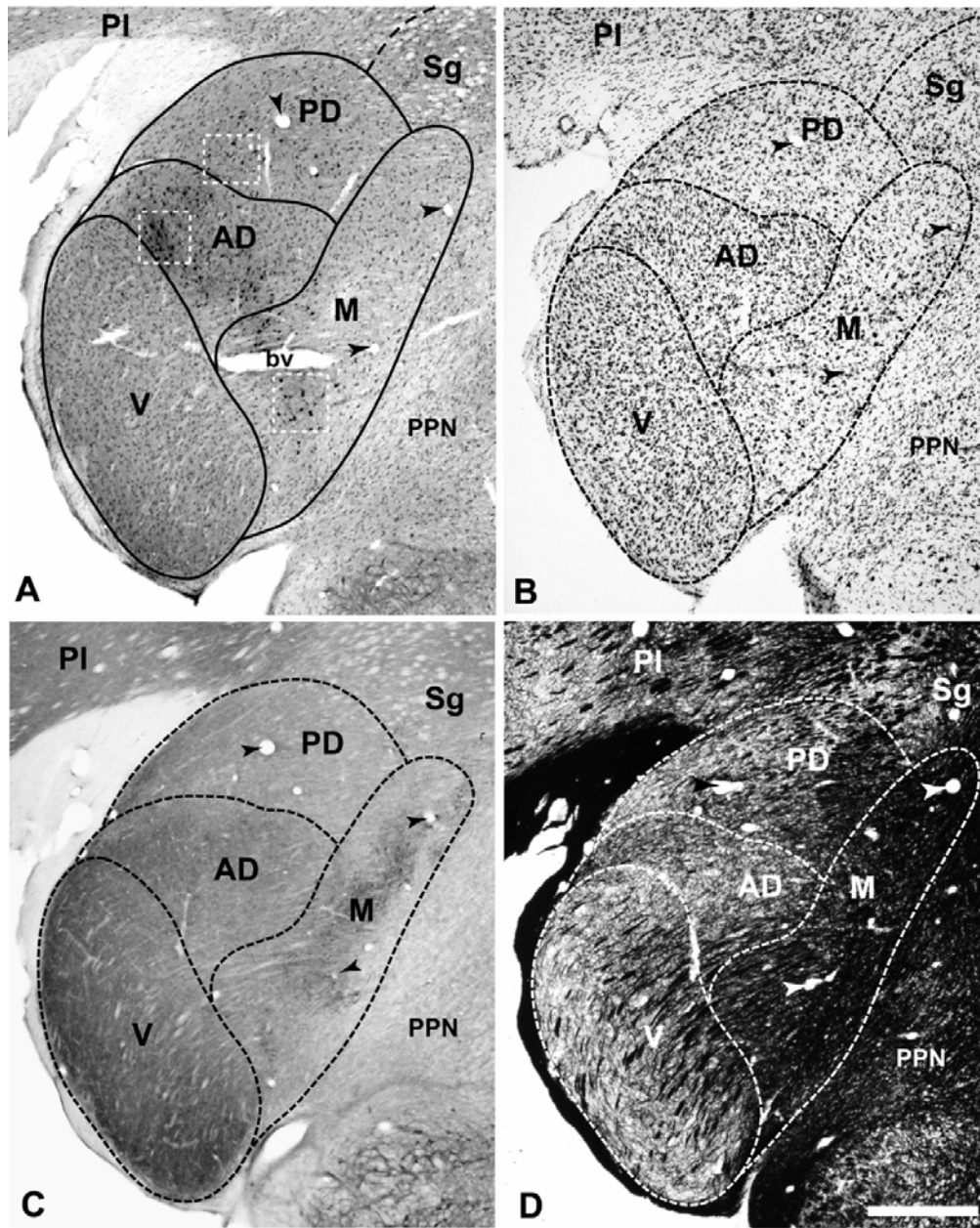
Figure 36. Architectonic features and labeled cells of marmoset monkey thalamus, case 4. (A) CTB-labeled cells and terminals in MGad, MGpd, and MGm after CM cortex injection. Insets (white dashed boxes) correspond to panels in Fig. 5. (B) Nissl stain; (C) Cytochrome oxidase stain; (D) Myelin stain. Arrowheads in all panels mark common blood vessels. bv, blood vessel profile. Scale bar, 500 µm.
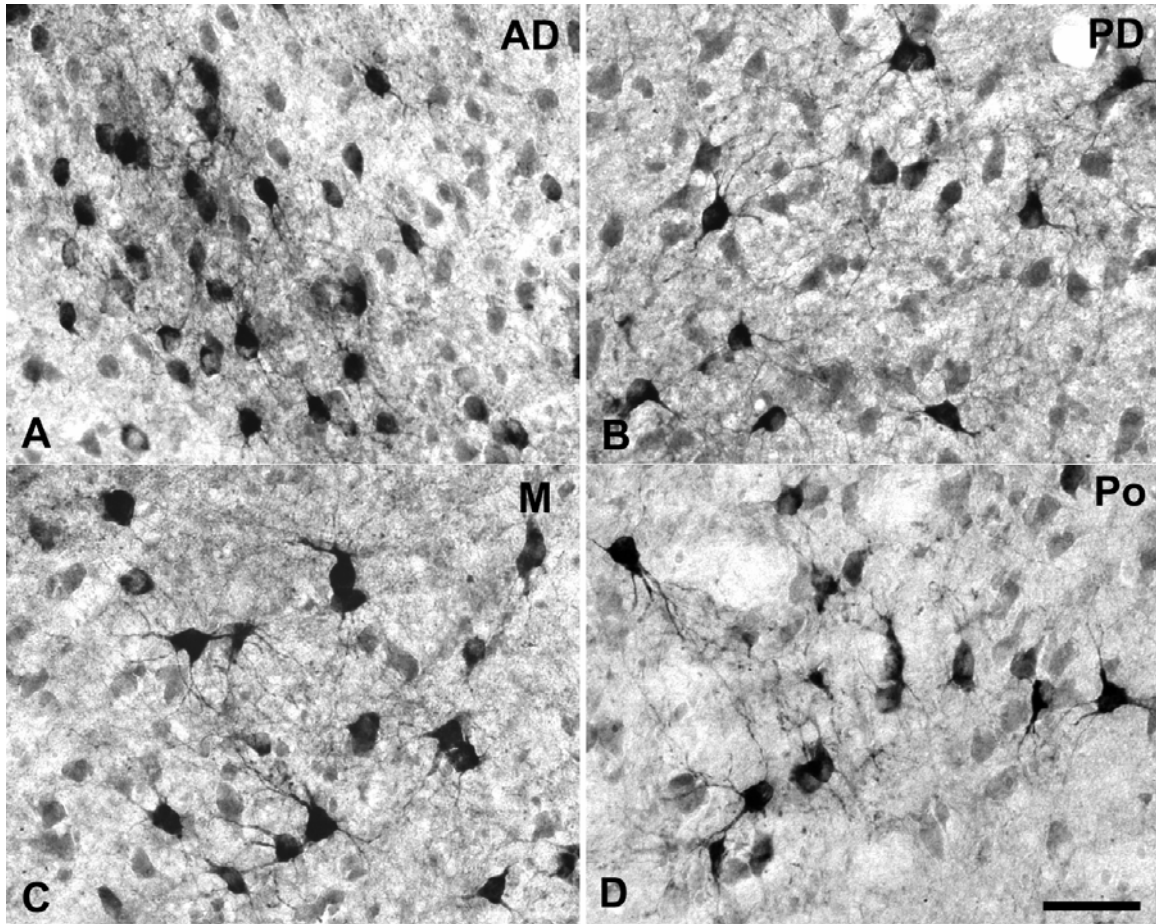
Figure 37. CTB-labeled cells and terminals in different divisions of the MGC from Fig. 4, case 4. (A) MGad; (B) MGpd; (C) ventral MGm; (D) Posterior nucleus (Po), not shown in Fig. 4. In all panels lateral is to the left, dorsal is up. Scale bar, 50 µm.

moderate in intensity, and less intense than MGv (Fig. 35b, e, h). Cells labeled by tracer

injections of the medial belt were frequently multipolar, and often larger than unlabeled

cells in this division (Figs. 36a, 37b, 38a-b). Further rostral, the MGpd decreased in size

as the MGad emerged and became larger toward the rostral pole (Fig. 35j – r). Like the

MGv, the MGad stained more darkly for CO than MGpd. In contrast, the MGpd stained

more darkly for AChE.
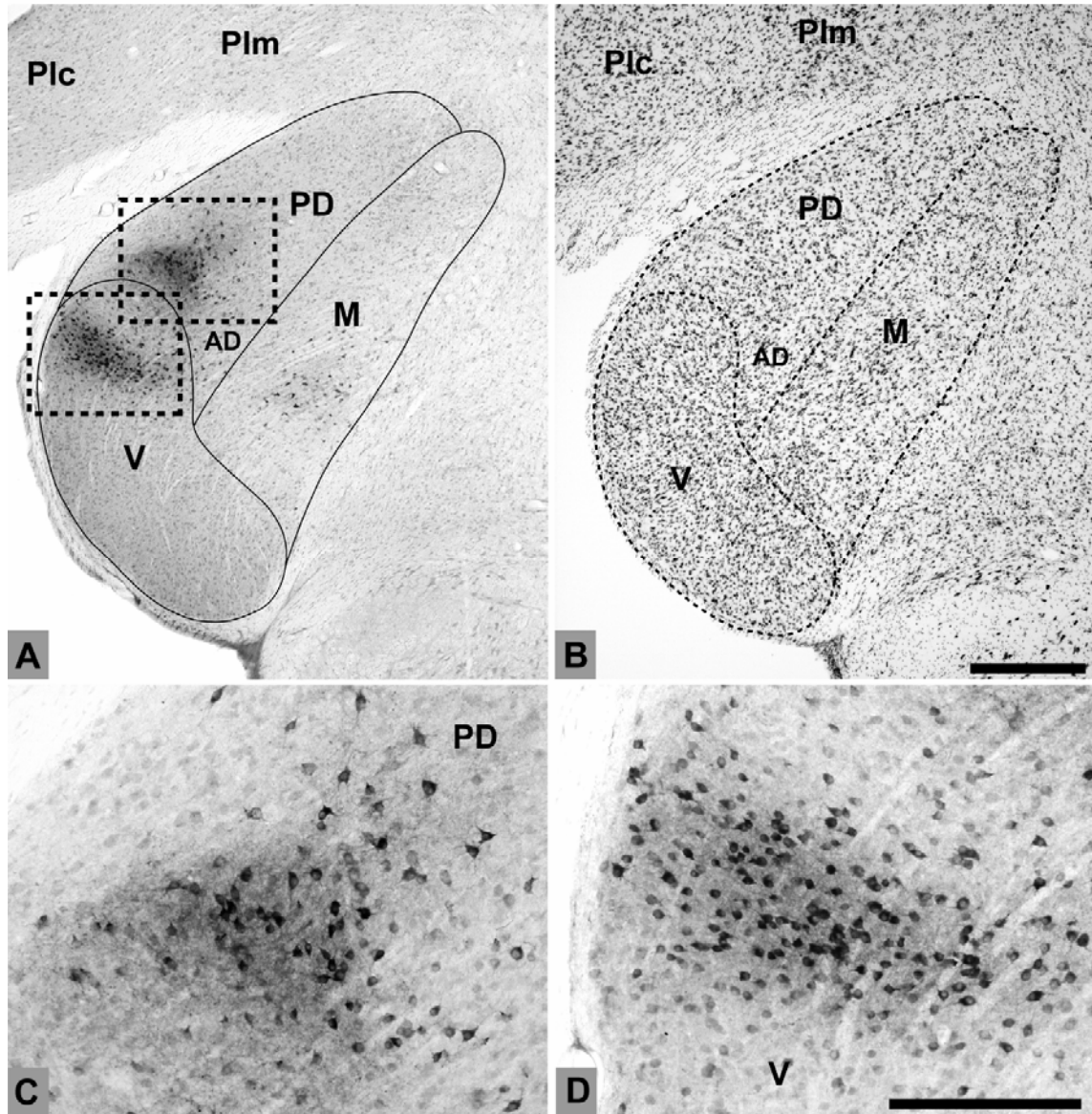
Figure 38. BDA-labeled cells and terminals, case 2. (A) Dual foci of label MGpd and MGv after an injection that encroached upon RM and R, respectively. Dashed lines correspond to panels C and D; (B) Thionin stain for Nissl; (C) Labeled cells and terminals in MGpd; (D) Elongated string of label in dorsal MGv. Scale bars, (A-B) 500 µm; (C-D) 100 µm.

In the plane of section used in these experiments, the MGad emerged from a

location between the MGpd, MGv, and MGm where it gradually enlarged to occupy most

of the rostral pole of the MGC (Fig. 35j – r). This pattern was consistent across cases. In some sections, where the architecture were ambiguous, this region was marked as the transitional zone (Z), as adopted in macaque monkey (Hackett et al., 1998b; Molinari et al., 1995). MGad was distinguished from the MGpd by greater cell density, darker staining for CO, and weaker AChE expression. Compared to the MGv, cell spacing in MGad was similar, but cells were slightly larger, sometimes multipolar, and their arrangement less orderly (Fig. 35, left column). Examples of labeled MGad cells are illustrated in Fig. 36a. In myelin-stained sections, the MGad had a matrix-like arrangement of fibers that contrasted with the lamellar patterns in the MGv (Fig. 36d).

The MGv emerged near the caudal pole of the MGC (Fig. 35a – c), expanding in more rostral sections to occupy most of the ventrolateral quadrant of the MGC, then diminishing near the rostral pole (Fig. 35v – x). The principal neurons of the MGv were small, compared to those of other subdivisions. In this plane of section, cells in the middle third of the MGv were arranged in parallel laminae that tended to radiate laterally in arcs from the medial boundary of the MGv (Fig. 35j, m, p). These rows appeared to coincide with fibrodendritic laminae visible in CO and fiber sections. Near its border with the MGpd or MGad, the laminae flattened and became more laterally oriented (Figs. 35j, m, p; 36b - d; see also 38 a, c). CO density reached a maximum in the MGv, and was fairly uniform throughout, although CO density in the MGad was comparable to MGv in many sections. Examples of labeled MGv cells after a BDA injection involving R are shown in Fig. 38a, d.

The MGm was the most heterogeneous in the MGC. The largest cells were CO-dense and located in a magnocellular region that occupied the ventral two-thirds of the

division (Figs. 35g – p; 36a - b; 37c). In its dorsal third, cells were smaller and the border with the MGpd or Sg was ambiguous in some sections. A unique feature of the dorsal MGm was that these cells were coextensive with a region of very dense AChE expression (Fig. 35d – l, asterisks). The outlined region in the Nissl sections correspond to the location of the AChE-dense patch. At lower magnification (Fig. 34d), it can be seen that this patch in dorsal MGm appears to be related to an elongated band of dense AChE staining that involves the limitans (Lim) and suprageniculate (Sg) nuclei and extends into the dorsomedial MGC. Rostrally, the dense AChE region receded from the MGC to involve only the Lim and Sg (Fig. 35p – u). CO staining was patchy and very dark for the largest cells, but not especially useful in the delineation of MGm borders other than with the MGv. Fiber density was the highest in the MGm as the fibers of the brachium of the inferior colliculus emerged here enroute to the lateral divisions of the MGC (Fig. 36d).

The posterior nucleus, Po, was defined as the region dorsal to MGpd/MGad, ventral to PM, medial to PI, and lateral to Sg/Lim (Fig. 34). Clear borders were usually not present. The architectonic features of Po are blurred by banded fibers of the brachium of the superior colliculus (Fig. 34b, c: BrSC), around which islands of moderately-large cells were stranded (Fig. 36d). The Sg and Lim nuclei tended to blend with Po medially, but could usually be segregated, as Sg and Lim were located within the AChE-dense region that extended from the ventromedial boundary of PM to the dorsal border of MGm (Fig. 34d; 35m - o). Laterally, Po bordered the medial divisions of the inferior pulvinar (PIm, PIp). Since this region was traversed by the BrSC, borders were sometimes difficult to distinguish in Nissl sections, but the subdivisions of PI could be delineated in CO and AChE (Figs. 34, 35) according to criteria established in recent studies (Gray et

140

al., 1999; Stepniewska and Kaas, 1997; Stepniewska et al., 2000). PM was easily

identified in the dorsomedial cap of the thalamus as a large region with evenly-spaced

cells of moderate size (Fig. 34a).

Description of thalamocortical connections

Tracer injections targeted CM in 2 cases, RM in 2 cases, A1 in 2 cases, and R in 3

cases (Table 2). The thalamocortical connection patterns of each injection site are

described for each of these areas below, beginning with CM. The number of labeled cells

associated with injection of the dextran, FR, was consistently lower than cases in which

BDA or CTB were injected, reflecting their greater sensitivity. Although fewer cells were

labeled in the thalamus with FR, the proportion of labeled cells across nuclei appeared to

be maintained.

Thalamic connections of CM

In case 6, the CTB injection was made across all cortical layers into rostral CM

medial to A1 (Fig. 39). In the most caudal sections (#332 – 338), retrogradely-labeled

cell soma were distributed throughout most of MGm, with a few cells in MGpd, and none

in MGv. Anterograde labeling of axon terminals was sparse. As MGad began to emerge

(#344 – 356), dense foci of overlapping cells and terminals were concentrated there. This

projection tended to involve cells along the ventral edge of MGad, near its border with

MGv (Figs. 36a, 37a). A few labeled cells were located in the ventral half of MGpd in

these sections (see Fig. 37b). The ventral MGm contained the most labeled cells (Fig.

37c), although some were found dorsally, in the smaller-celled portion of MGm. Labeled

Figure 39. Thalamic connections of CM, case 6. Series of reconstructed serial sections are arranged from rostral (upper left) to caudal (lower right). CTB-labeled cells (filled circles) and terminals (shading) are drawn onto each section, showing borders between areas identified by architectonic criteria. *Inset*, schematic of marmoset auditory cortex showing location of CTB injection in rostral CM.

Case 6 injections

rostral

386

380

374

368

362

356

350

Case 6   344

338

332   caudal

143
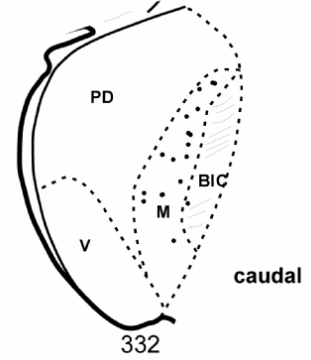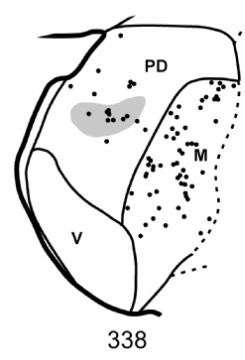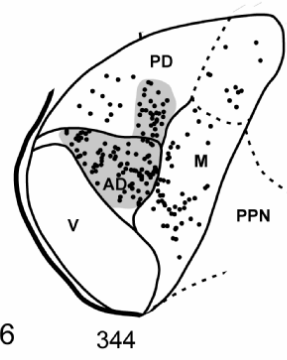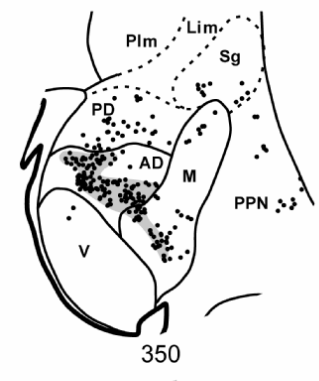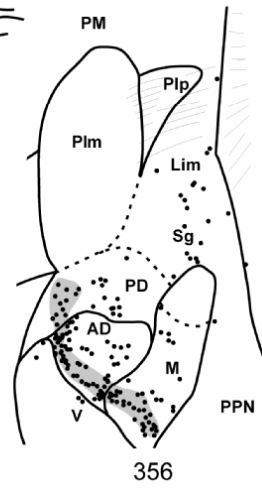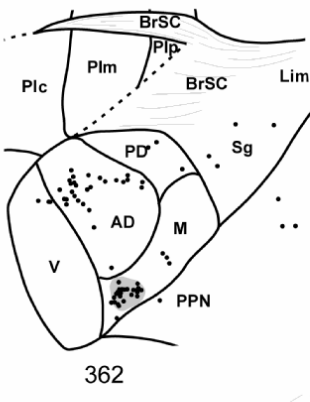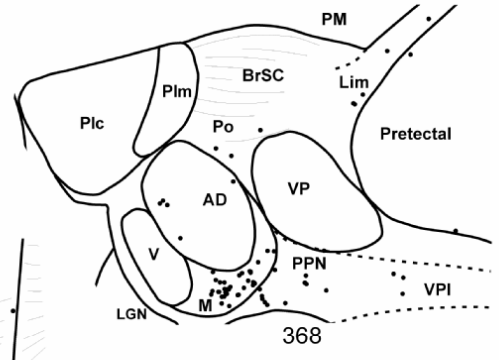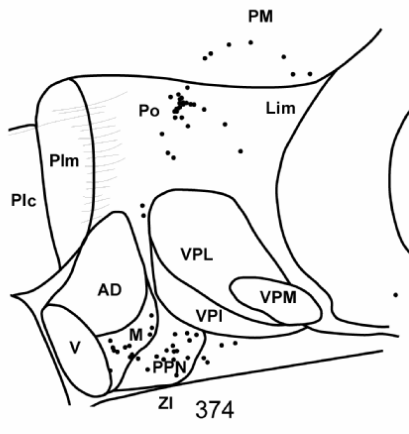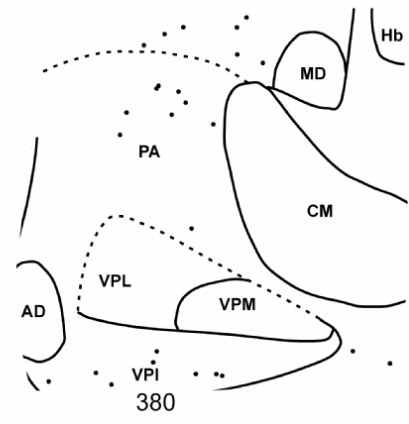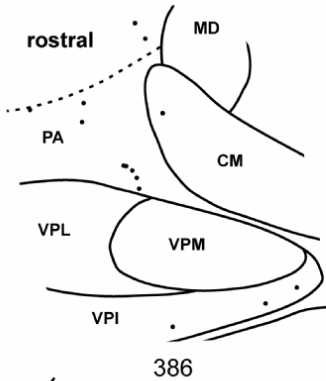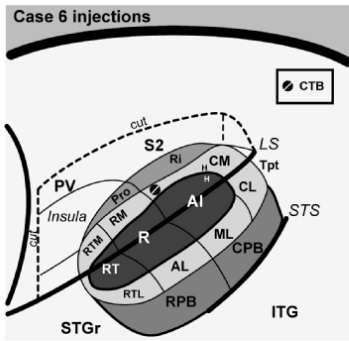
cells were also located in the Sg and Lim in these sections, along with a few cells

between the MGm and pretectal area (e.g., #350). Note that the pattern of anterograde

labeling in section 356 formed a continuous line that extended along the MGv border

within MGad and MGm. As the MGC began to diminish in size rostrally (#362 – 368),

labeled cells persisted in discrete groups of cells in MGad and MGm. Additional cells

were found in groups in Po (Fig. 37d), and scattered in Sg, Lim, and PM. Labeled cells

were also found medial to MGM in PPN and the inferior division of the ventroposterior

nucleus (VPI) in these sections, and those further rostral.

In case 3 (Fig. 40), the pattern of labeled cells involved the same nuclei as case 6,

but the concentration of labeled cells in the MGC favored the rostral part of the MGad

and there were many more cells among the posterior group of nuclei (Po, Sg, Lim) and

PM. This pattern was attributed to a more caudal placement of the CM injection

compared with case 6. In the more caudal sections (#147 – 159) a group of labeled cells

occupied the dorsal cap of the MGm in an AChE-dense region that was displaced by the

Sg rostrally (#165). The mixture of small and larger cells made precise delineation of the

dorsal MGm and Sg rather difficult in the caudal sections, owing to much more

horizontal plane of section. Otherwise, labeled cells in the MGm were mostly located

ventrally, as in case 6, above (#153 – 171). Labeled cells in the dorsal divisions of the

MGC were concentrated in the rostral MGad, extending to its rostral pole where it

borders the lateral division (VPL) of VP (#177 – 189). There were no labeled cells in

MGv, and few in MGpd. Over this same range, numerous cells were found outside of the

MGC in Sg, Lim, and especially Po. Further rostral (#195 – 201) numerous cells were

144

Figure 40. Thalamic connections of CM, case 3. Series of reconstructed serial sections are arranged from rostral (upper left) to caudal (lower right). CTB-labeled cells (filled circles) and terminals (shading) are drawn onto each section, showing borders between areas identified by architectonic criteria. *Inset*, schematic of marmoset auditory cortex showing location of CTB injection in caudal CM.

145

concentrated in the ventromedial portion of PM, extending from a line of cells in rostral Po.

Summary of CM connections

  The principal auditory thalamic connections of CM arose from the MGad and MGm (Fig. 41). Connections with MGpd were much weaker, and there was no significant input from MGv. Topographic differences were noted between injections of rostral (case 6) and caudal (case 3) parts of CM. The connections of caudal CM with the MGC were largely restricted to MGad and MGm, whereas the rostral CM injection in case 6 produced additional labeling in MGpd. In addition, caudal CM had greater connections with multisensory nuclei outside of the MGC including Sg, Lim, Po, and PM. These findings are consistent with the topographic differences evident in the cortical connections of these cases (de la Mothe et al., 2006a). Rostral CM had more widespread connections with rostral and caudal auditory cortex, whereas the connections of case 6 were more limited to the caudal fields. In addition to the thalamic connections, corticotectal projections after CM injections were clustered in the dorsomedial (dm) region of the inferior colliculus (IC) rostrally. Caudally, the projection extended to the pericentral shell forming the ventromedial boundary of the IC (Fig. 42). In some sections, weaker projections were observed in the lateral nucleus (ln) such that a nearly continuous ring of pericentral terminal labeling encircled the central nucleus except for the lateral dorsal cortex (dc).
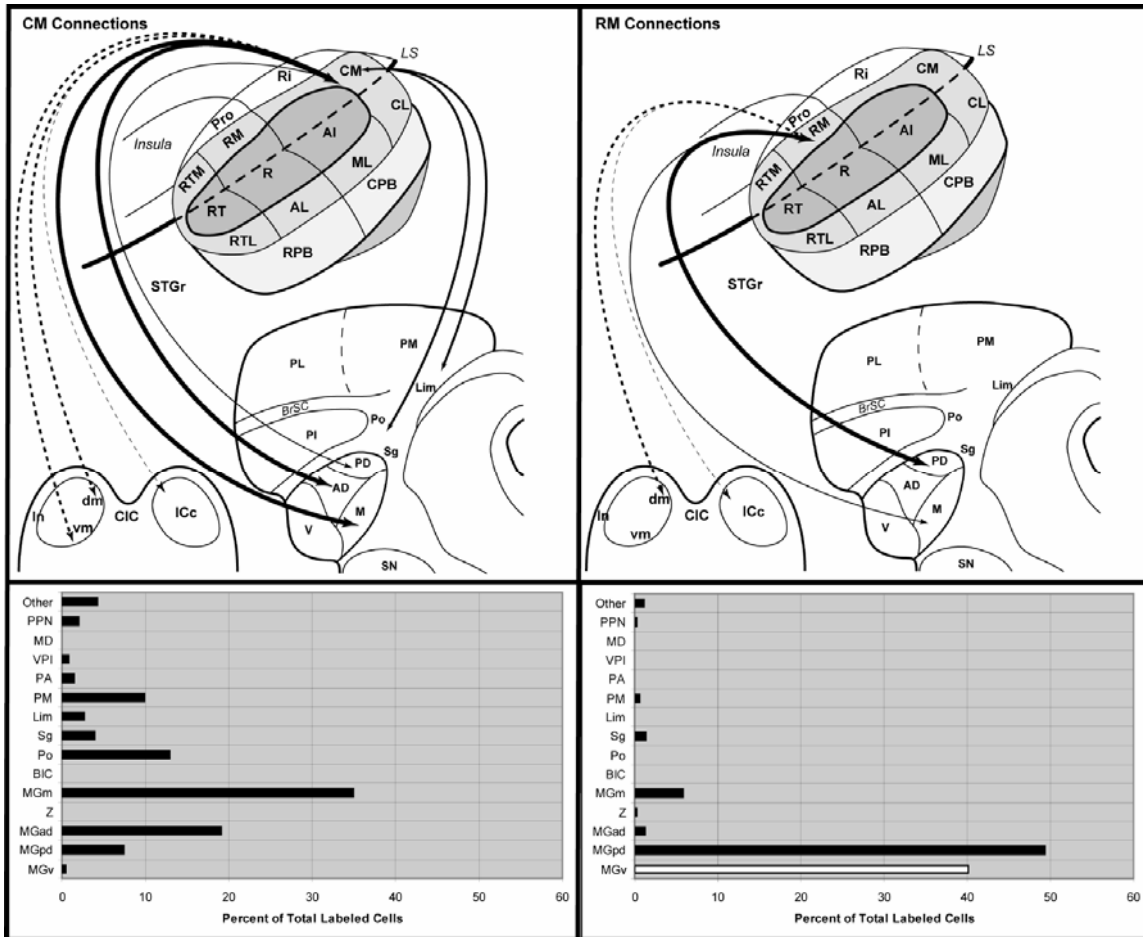
Figure 41. Summary of thalamic and midbrain connections of CM and RM. Top panels illustrate subcortical connections (arrows) of CM and RM on schematic diagrams of marmoset auditory cortex, thalamus, and inferior colliculus. Arrow and line size is proportional to connection strength, as indicated in the histograms below each panel. Lines were not drawn for connections representing less than 5% of total. Double arrows indicate reciprocal connection. Dashed arrows indicate corticotectal projections. *Bottom right*, white bar indicates that cell counts for MGv are likely to be inflated due to involvement of the medial edge of the core area R by the RM injections.

Thalamic connections of RM

In case 1 (Fig. 43), the BDA injection was placed in RM. Labeled cells and terminals were concentrated heavily throughout nearly the entire extent of MGpd (# 144 – 116). There was some involvement of the adjacent core area, R, by the injection, as there were labeled cells extending across the border between MGpd and MGv (#132,

147
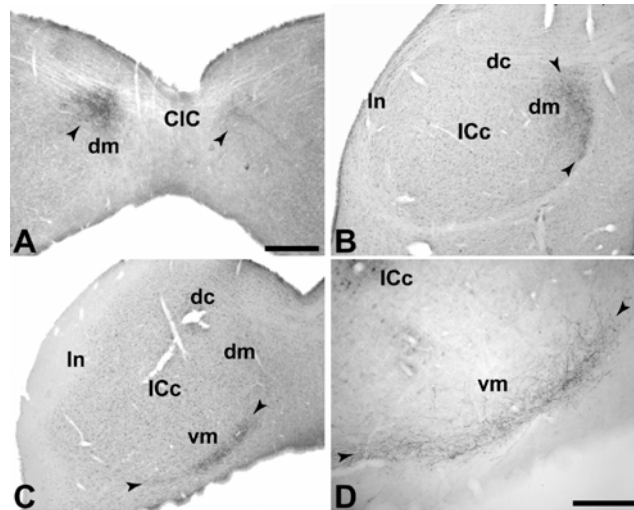
Figure 42. Anterograde terminal labeling in the inferior colliculus. (A) Cluster of labeled terminals bilaterally in the dorsomedial (dm) portion of the inferior colliculus (IC) after BDA injection of RM. Terminal labeling is denser ipsilateral to the injection. (B) Terminal labeling in dm after CTB injection of CM. (C) Terminal labeling in the ventromedial (vm) portion of the IC after same CTB injection as panel B, but further caudal. (D) BDA labeling in the vm region after CM injection. Arrowheads mark zones of terminal labeling. CIC, commissure of the IC; dc; dorsal cortex of the IC; ln, lateral nucleus of the IC; ICc, central nucleus of the IC Scale bars, 500   m (A-C); 250   m (D).

128). Labeled cells in MGad were relatively few, and confined mainly to its caudal

extension where it emerged between MGv and MGpd. In MGm, two foci of label were

noted. The ventral grouping occupied a similar location to that associated with CM

injections (#128 – 124). The dorsal projection involved the AChE-dense region that

merged into Sg, as noted for the CM cases above (#132 – 120). There were only a few

labeled cells in Sg and PM (#100), and no cells in Po or Lim in this case.

In case 2 (Fig. 44), the BDA injection was placed in RM. As in case 1 (Fig. 43),

the additional involvement of the medial edge of R was suggested by the appearance of

labeled cells in dorsal MGv at its border with MGpd and MGad (Fig. 38). The

distribution of labeled cells in MGv contrasts with the injection of R in this same case

(open triangles). Consistent with case 1, the labeled cells were concentrated in MGpd
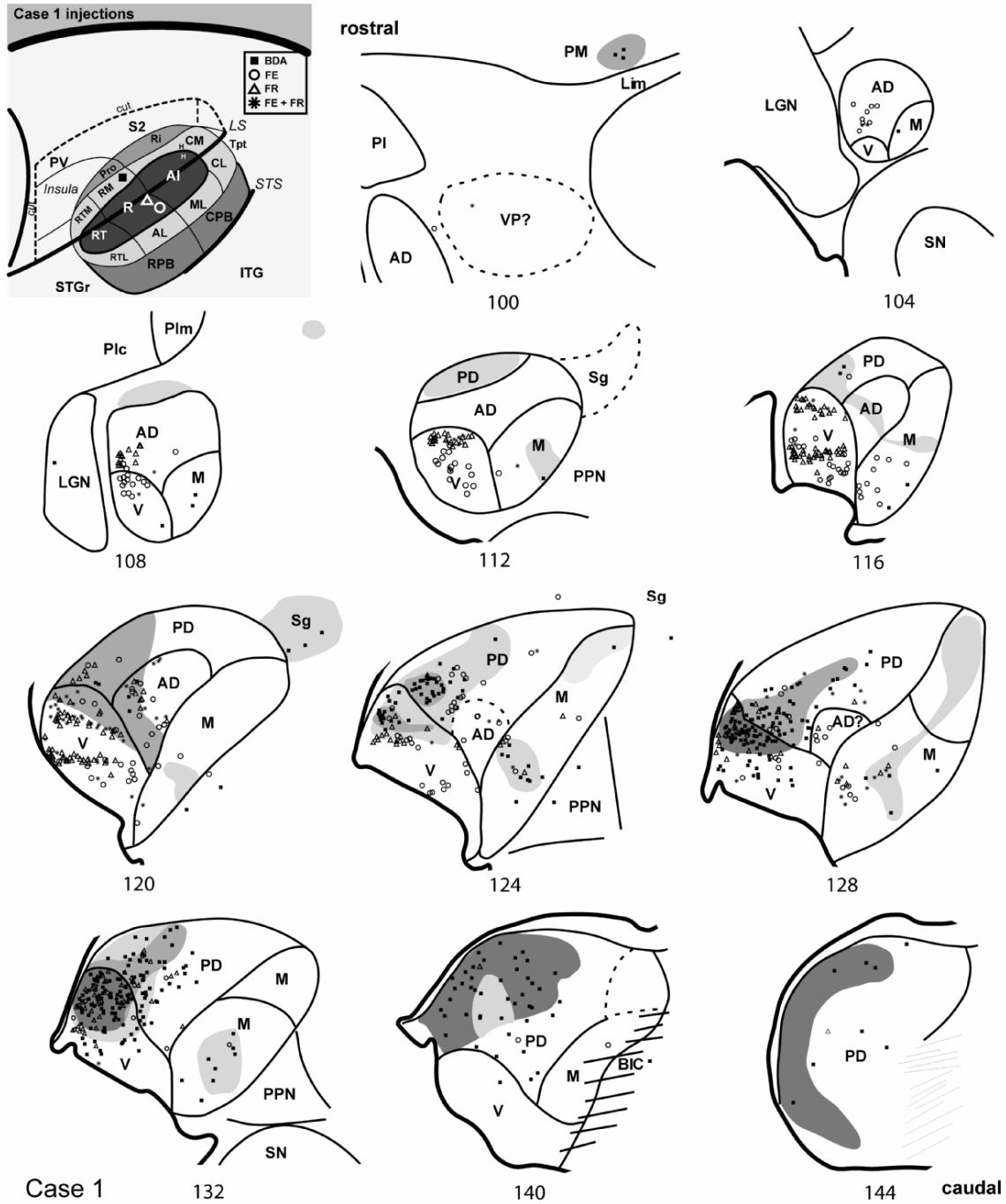
Figure 43. Thalamic connections of RM and R, case 1. Series of reconstructed serial sections are arranged from rostral (upper left) to caudal (lower right). BDA-labeled cells (filled squares) and terminals (shading) are drawn onto each section, showing borders between areas identified by architectonic criteria. Cells labeled by fluororuby (FR) are indicated by open triangles, and cells labeled by fluoroemerald (FE) indicated by open circles. Asterisks indicate double-labeled cells (FR + FE). *Inset*, schematic of marmoset auditory cortex showing locations of BDA injection in caudal RM, and FR/FE injections in caudal R.
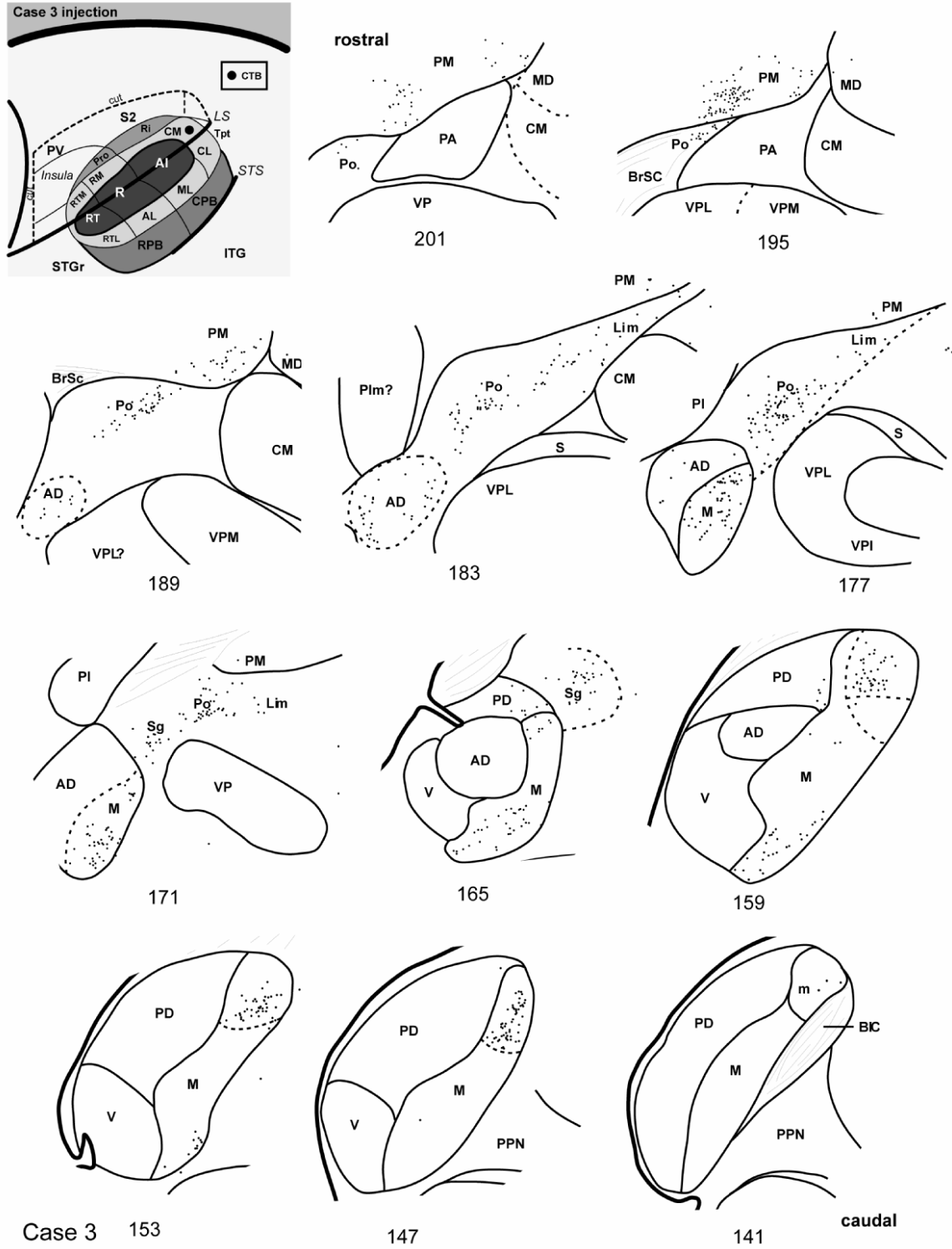
149

Figure 44. Thalamic connections of RM and R, case 2. Series of reconstructed serial sections are arranged from rostral (upper left) to caudal (lower right). BDA-labeled cells (filled squares) and terminals (shading) are drawn onto each section, showing borders between areas identified by architectonic criteria. Cells labeled by fluororuby (FR) are indicated by open triangles. *Inset*, schematic of marmoset auditory cortex showing location of BDA injection in RM and FR in caudal R.

Case 2 injections

BDA
FR

S2
PV
Insula
Ri CM Tpt LS
Pro AI CL
RTM RM ML STS
R
RT AL CPB
RTL RPB
STGr ITG

rostral

PM
MD
PA
65

PM
Lim
Po/PA
71

PM
PL
PI
Po
VP
77

PM
PI
Po
LGN
AD
83

PI
AD
LGN
89

AD M
V
LGN
95

Sg
PD
AD
M
V
LGN
101

PD Sg
AD
M
V
107

PD
M
Z
V
PPN
Case 2   113

PD
M
BIC
V
119
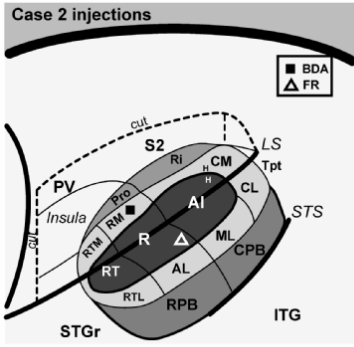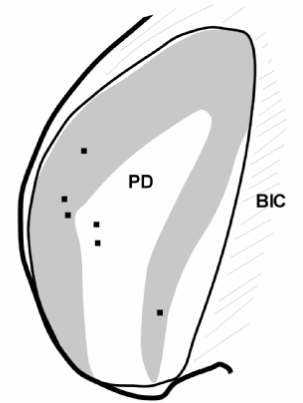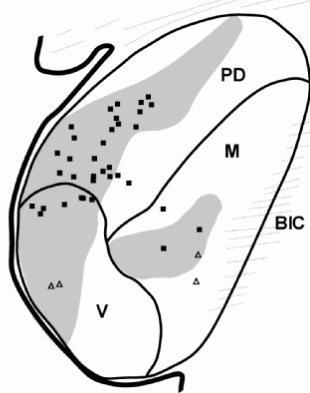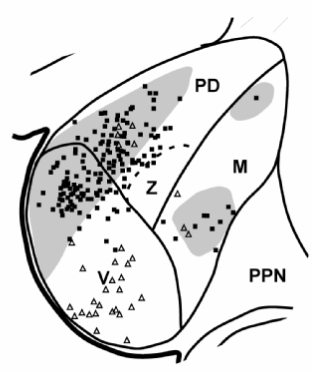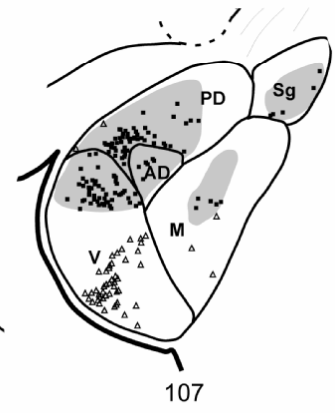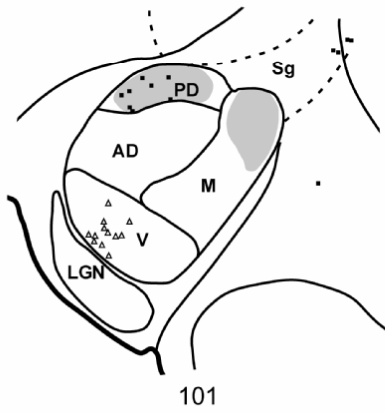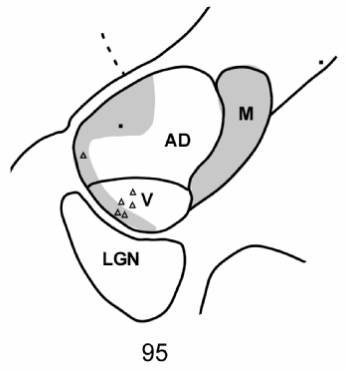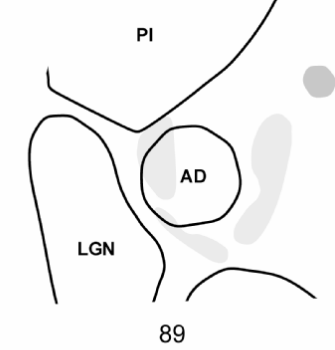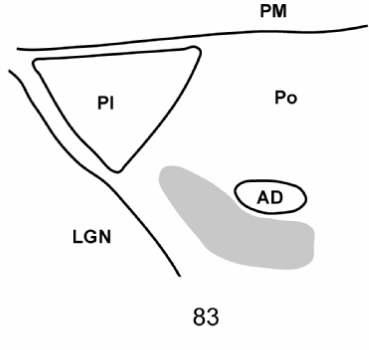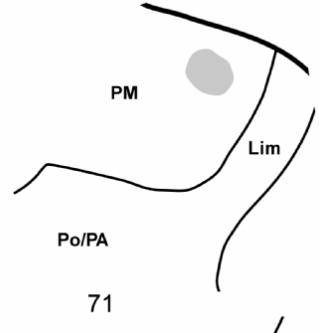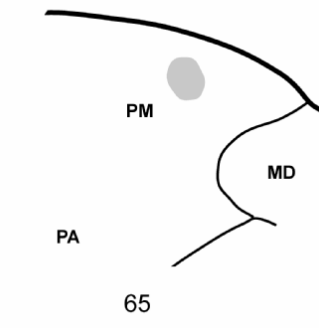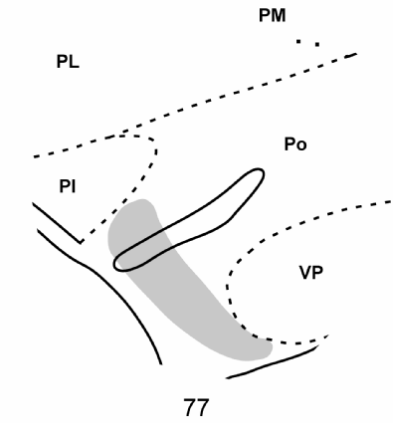
PD
BIC
125   caudal

rather than MGad (#125 – 95). Dense overlapping anterograde and retrograde labeling

was present in MGpd from sections near the caudal pole (#125) to its rostral termination

(#101). In MGm, the label was similar to the cases above, being concentrated ventrally in

one group, and then rostrally in an AChE-dense zone that merged into Sg. Overall, there

were few labeled cells in Po, Sg, Lim, or PM, consistent with the other RM injection.

There were, however, patches of anterograde label near the rostral pole near MGad (#89

– 77), and also dorsomedial PM.

Summary of RM connections

Compared to CM, the thalamic connections of RM were almost completely

restricted to the MGC (Fig. 41). The principal connections arose from the MGpd, with

secondary projections from MGm. There were only sparse connections with MGad, and

connections with MGv appeared to be related to involvement of R by the injection.

Connections with multisensory nuclei outside of the MGC were also sparse. These

patterns reflected clear topographic differences between the connections of RM and CM.

Corticotectal projections were clustered in the dorsomedial region of the IC, with

minimal spread to the central nucleus. There was no clear projection to the ventromedial

shell or external nucleus, as observed after CM injections (Fig. 42).

Thalamic connections of A1

The core area, A1, was targeted in cases 4 and 5. In case 4 (Fig. 45), labeled cells

were located in MGm in the most caudal sections (#190 – 202) where MGm and MGpd
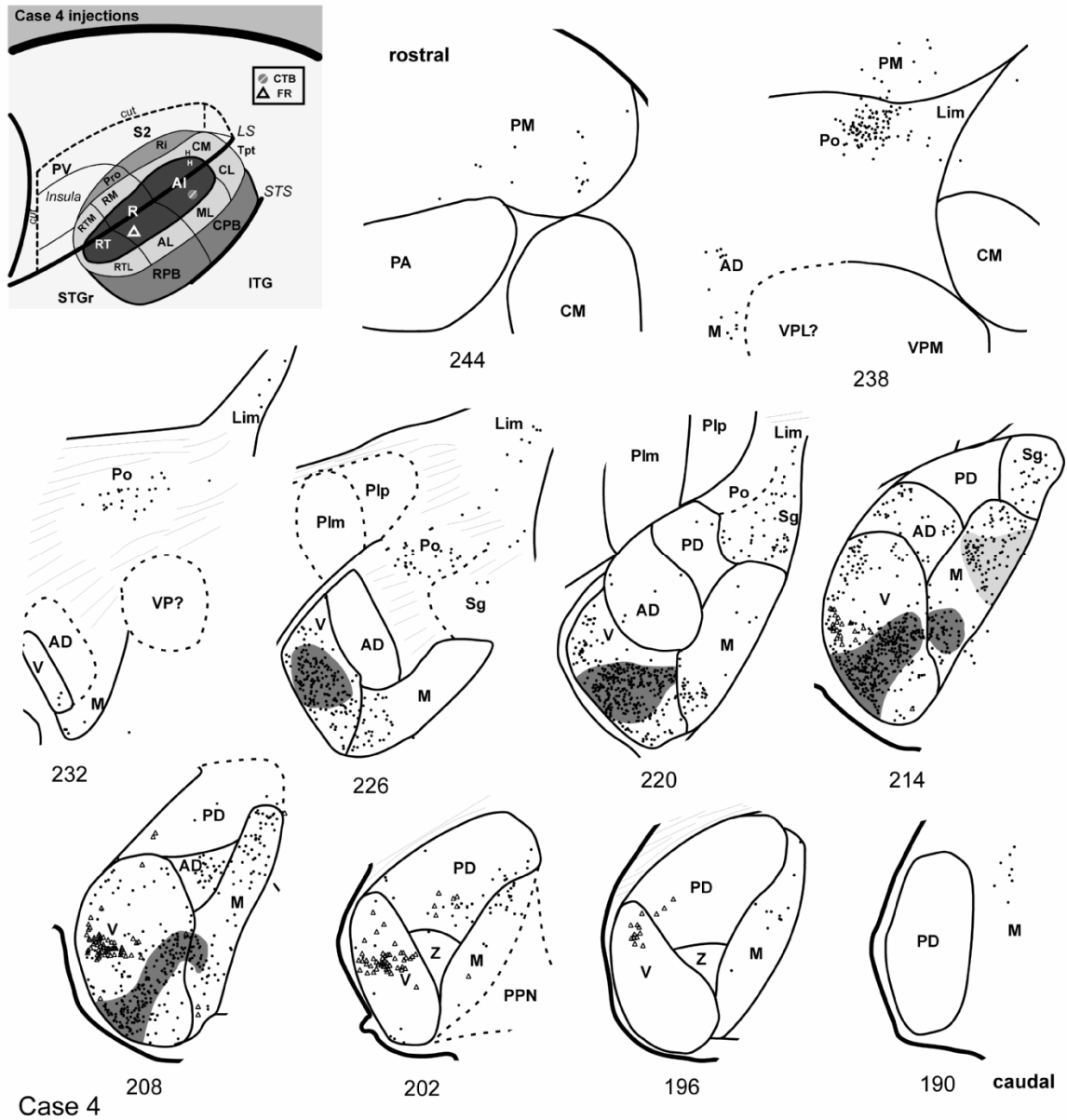
Figure 45. Thalamic connections of A1 and R, case 4. Series of reconstructed serial sections are arranged from rostral (upper left) to caudal (lower right). CTB-labeled cells (filled circles) and terminals (shading) are drawn onto each section, showing borders between areas identified by architectonic criteria. Cells labeled by fluororuby (FR) injection in rostral R are indicated by open triangles. *Inset*, schematic of marmoset auditory cortex showing location of CTB injection in A1 and FR in rostral R.

153

comprised the caudal pole of the MGC. As MGv emerged in more rostral sections (#208 – 226), a dense strip of labeled cells and terminals appeared in MGv that was oriented ventrolaterally, consistent with the orientation of its principal cells and fibers (Fig. 36). Labeled cells with more variable dendritic orientation were scattered elsewhere in MGv, especially dorsolaterally near the border with MGad, which also contained a moderate number of labeled cells. The MGv cells labeled by this injection were located ventromedial to the strip of cells labeled by the injection of R in this same case (#202 – 214), as described below. Few labeled cells were found in MGpd in this case. In MGm, two foci of label were evident over several sections (#202 – 226). The ventral grouping was at times continuous with the strip of labeled cells in MGv, and was overlapped by dense anterograde label (#208 – 214). The dorsal group of cells in MGm was overlapped by weaker anterograde projections, which extended into Sg and Lim as these nuclei became prominent rostrally (#214 – 226). As the MGC began to diminish in size (#226 – 238), labeled cells in Po were grouped between the inferior pulvinar (PI) and the dorsal MGC (#226). Rostrally, the grouping in Po shifted to occupy a position near the ventral border with PM. A few cells were labeled in ventrolateral PM, near those in Po (#238 – 244).

In case 5 the FR injection of A1 was located near the caudal border with CM (Fig. 46). The most caudal sections (#173 – 179) had a strong projection from MGm, with a slight dorsal emphasis. As in case 4, the main projection from this injection arose from the MGv, but the focus of labeled cells was in its dorsomedial quadrant, with scattered cells dorsolaterally (#179 – 191). Cells were also labeled in MGad over this same range. Labeled cells were not found in MGpd. Rostrally, a few labeled cells were located in Sg,
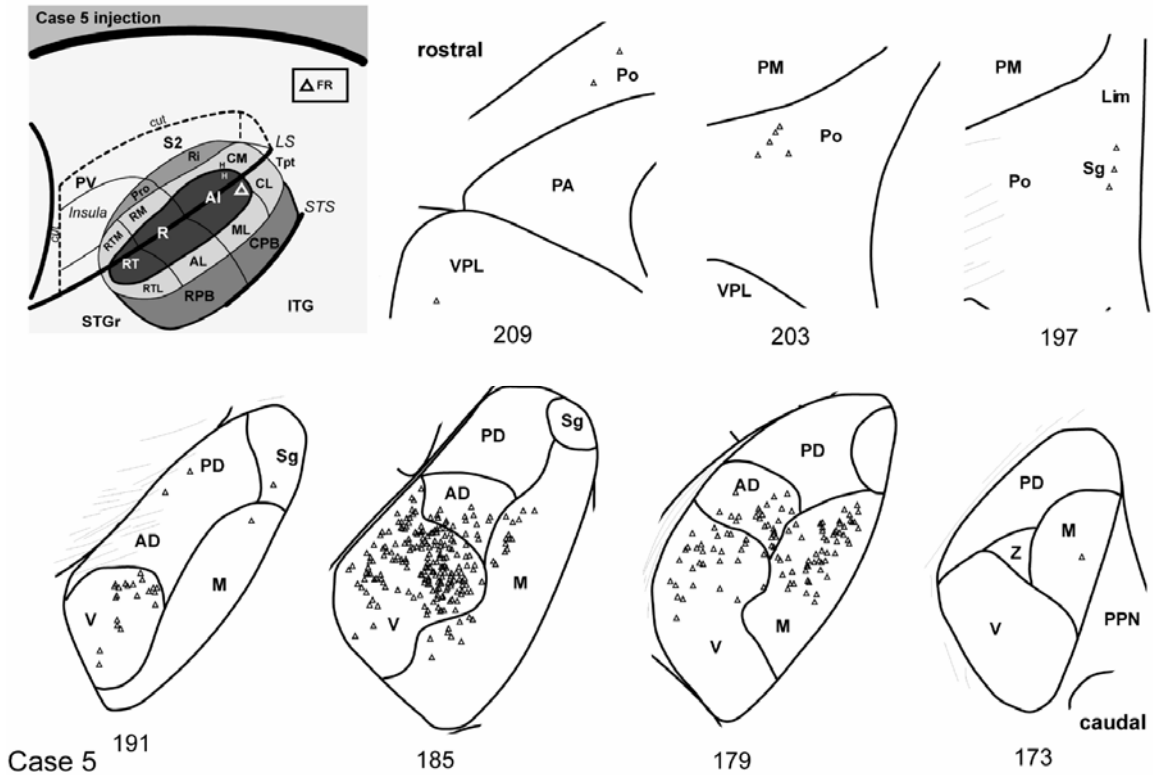
Figure 46. Thalamic connections of A1, case 5. Series of reconstructed serial sections are arranged from rostral (upper left) to caudal (lower right). FR-labeled cells (open triangles) are drawn onto each section, showing borders between areas identified by architectonic criteria. *Inset*, schematic of marmoset auditory cortex showing location of FR injection in caudomedial A1.

Lim, and Po (#197 – 209). The location of labeled cells in Po, was consistent with the A1 injection in case 02-51.

Summary of A1 connections

In both cases, the greatest concentration of labeled cells after injection of A1 was located in the MGv (Fig. 47). In case 4 the locus was ventrolateral, whereas in case 5 cells were concentrated dorsomedially. The topographic difference reflects the tonotopic organization of A1 and the MGv, as higher frequencies are represented in caudal A1.
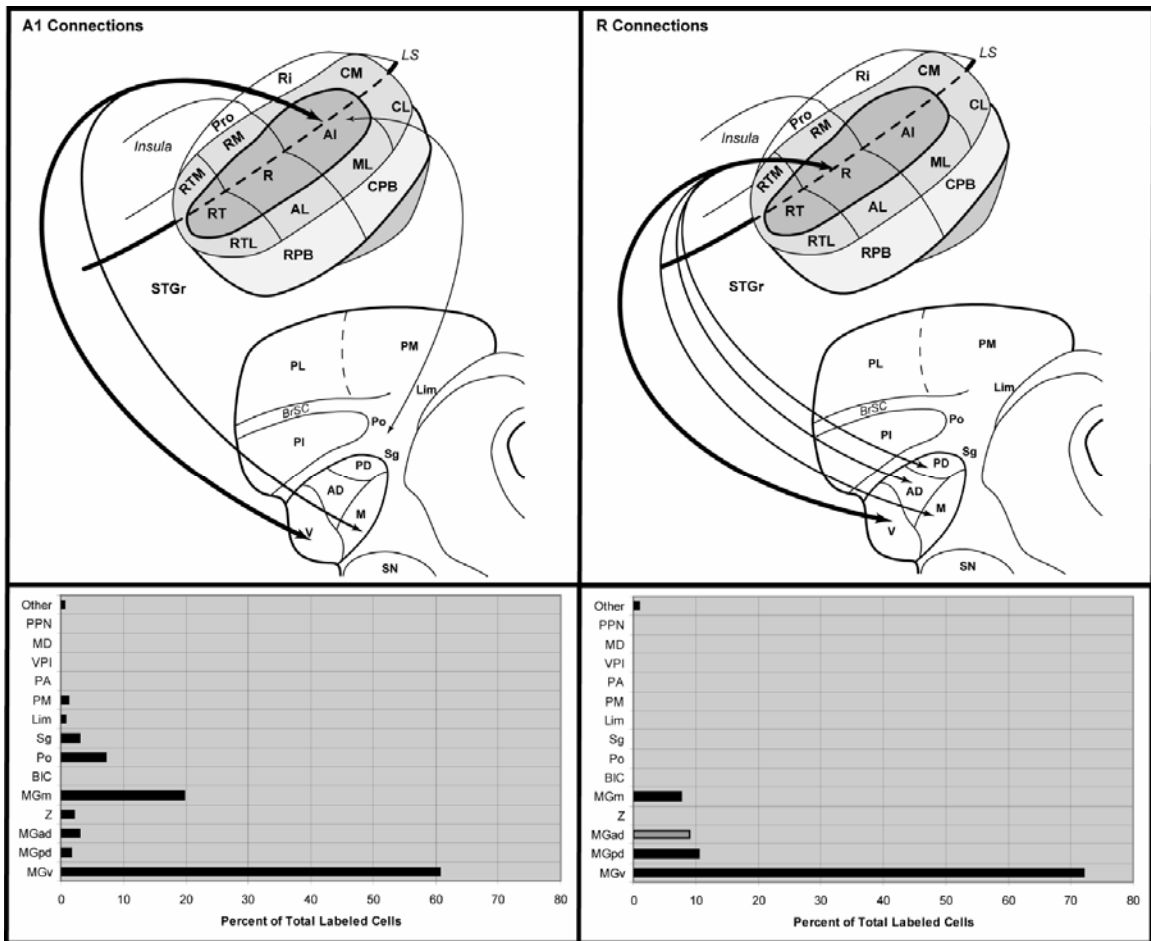
Figure 47. Summary of thalamic connections of A1 and R. Top panels illustrate connections (arrows) of A1 and R on schematic diagrams of marmoset auditory cortex and thalamus. Arrow size is proportional to connection strength, as indicated in the histograms below each panel. Lines were not drawn for connections representing less than 5% of total. Double arrows indicate reciprocal connection. *Bottom right*, grey bar indicates that cell counts for MGad due to connections in case 1, not observed in cases 2 and 4.

Labeled cells were also found in MGad in both cases, but not MGpd, consistent with the

rostrocaudal topography between auditory cortex and the MGC. The connections with

MGm are consistent with architectonic and topographic differences between its dorsal

and ventral domains, as observed after injections of CM and RM. Finally, labeled cells

were located in Po and Sg. Although fewer cells were labeled from the FR injection, this

likely reflects differences in the sensitivity of CTB and FR, as the proportion of labeled cells distributed between nuclei was comparable.

Thalamic connections of R

The core area, R, was injected in with retrograde fluorescent tracers in cases 1, 2, and 4. In case 2 (Fig. 44), the FR injection was placed in caudal R, near the border with A1, and lateral to a BDA injection in RM. The main projection to R arose from an elongated cluster of cells in ventrolateral MGv that spanned several sections (#119 – 95). Note the segregation of this cluster from the dorsolateral grouping of labeled cells from the BDA injection of RM that appeared to involve the medial edge of R. This pattern was repeated in case 1 (see below). Labeled cells in MGm were located ventrally in near proximity to BDA-labeled cells (#119 – 107). A few cells were found in ventrolateral MGpd (#113 – 107).

In case 4 (Fig. 44), the FR injection was placed in rostral R, near its border with RT. A CTB injection was placed in A1. The FR injection labeled a band of cells in the middle of MGv oriented lateral to medial (#202 – 208). Otherwise, FR cells were scattered dorsally in MGv (#196 – 202). The main strip of cells was dorsal to labeling from the A1 injection, described above. A few cells were labeled in ventral MGpd and MGm (#196 – 208).

In case 1 closely-spaced injections of FR and FE were placed in the caudal portion of R in line with the BDA injection of RM (Fig. 43). The FR injection was placed into the crown of the STG, and FE was injected about 1 mm lateral to FR. Overlapping bands of labeled cells from both injections were located in the middle and dorsal half of

the MGv, oriented from lateral to medial, as in case 4 (#128 – 116). Double-labeled cells were also located in these bands. In more rostral sections (#112 – 108), labeled cells persisted in the MGv, but those labeled by the more lateral FE injection tended to be located further ventral. Damage to the MGv in sections 140 – 116 prevented evaluation of the ventrolateral corner of the nucleus. In MGm, single and double-labeled cells from both injections overlapped in the ventral half of the nucleus in most sections (#132 – 112). Labeled cells were found in MGpd and MGad near the border with MGv, and cells from the FE injection appeared in MGad to the rostral pole. Thus, compared to more rostrally-placed injections of R, labeled cells in caudal R extended further caudally in the MGC, and appeared to have more cells in MGad. There were no labeled cells in Sg, Po, or PM from either R injection.

Summary of R connections

Injections of R in all cases revealed a preferential connection with MGv, and secondary projections from MGm (Fig. 47). Connections with MGpd or MGad were sparse, by comparison, and there were almost no connections with the multisensory nuclei. In all cases, the main projection to R derived from a radially-oriented cluster of cells in MGv aligned with the trajectory of axons within MGv (Fig. 36d, 38a). The clusters of labeled cells varied in relative location, reflecting topographic differences in the connections with R. In case 2, the injection of caudal R labeled a strip of cells ventral to those labeled by the injection of rostral R in case 4. The ventral location and orientation in MGv was almost identical to that produced by injection of rostrolateral A1 in case 4. These topographic patterns are consistent with the tonotopic organization of

158

both fields, and suggest that topographically-discrete sectors in MGv may project to matching tonotopic domains in different areas of the core. It was not possible to determine from our data, however, whether single cells in the MGv project to both A1 and R. In addition, the injections of RM that appeared to encroach on the medial edge of R labeled cells in a group in the extreme dorsolateral corner of MGv that extended into the ventral MGad. In case 1, the injections of FR into the medial and caudal part of R also labeled cells in this zone, in addition to a more ventral band. These patterns suggest possible topographic differences in the connections of lateral and medial domains of R.

Discussion

In the present study, neuroanatomical tracers were injected into four different areas of auditory cortex to reveal the sources of their thalamic inputs. In the medial belt region, areas RM and CM were targeted. In the core region, injections were made into R and A1, which are adjacent to RM and CM, respectively. The results indicated that these areas are distinct with respect to their thalamocortical connections, consistent with hypotheses derived from our working model of the primate auditory cortex. The significance of these results are discussed in more detail below with respect to the functional roles of these areas and the corticocortical connections described in the companion paper (de la Mothe et al., 2006a).

Connections of RM and CM with the MGC

One of the main findings of the present study was that the thalamocortical inputs to RM and CM derived from different subdivisions of the auditory thalamus. The primary

input to RM was MGpd, while the main input to CM was MGad (Figs. 41, 48). The

rostrocaudal topography exhibited by these projections was generally consistent with that
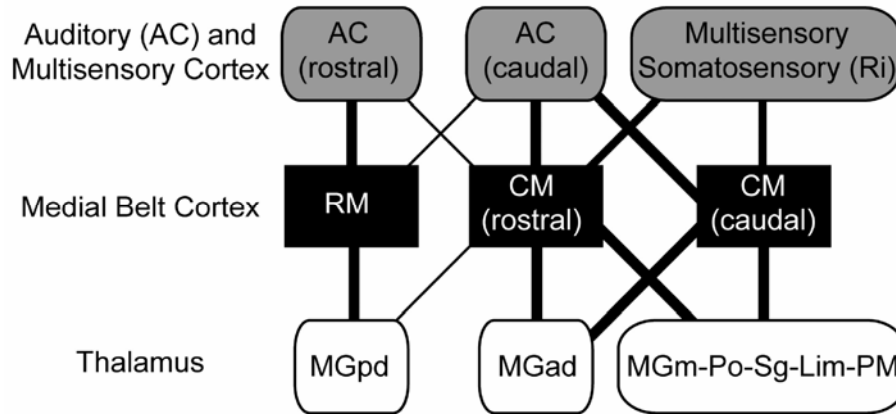
Figure 48. Summary of main cortical and thalamic connections of the medial belt areas, RM and CM (black shading). Relative connection strength is represented by line width. RM has dense cortical connections with other rostral areas of auditory cortex (AC, light shading), weaker connections with caudal AC fields, and minimal connections with somatosensory or multisensory areas of cortex. The arbitrary division between rostral and caudal AC is centered at the border of A1 and R, extending laterally and medially through the belt and parabelt areas (see Fig. 1). Thalamic connections (no shading) strongly favor MGpd. Rostral and caudal portions of CM have dense connections with caudal AC and multisensory areas, especially the somatosensory area, Ri. Rostral CM has moderate connections with rostral AC, whereas caudal CM has few. The thalamic connections of CM favor MGad and the multisensory nuclei.

noted for other areas of auditory cortex, in that the rostral MGC tends to project more

densely to caudal areas of auditory cortex, and vice versa (Burton and Jones, 1976;

Hackett et al., 1998b; Jones and Burton, 1976; Molinari et al., 1995; Morel et al., 1993;

Morel and Kaas, 1992; Pandya et al., 1994; Rauschecker et al., 1997). Rauschecker et al

(1997) found that injections of CM labeled MGd and Po, especially at more rostral levels

of the MGC. But this topography can vary by thalamic subdivision and cortical area. In

previous studies, for example, MGpd was more broadly connected with both rostral and

160

caudal areas of the lateral belt and parabelt, compared to MGad (Hackett et al., 1998b; Molinari et al., 1995). This contrasts with the rather distinct projections of MGpd and MGad to RM and CM described in this report.

The segregation of these two pathways is intriguing given certain the subset of primary-like response properties observed in CM and a hypothesis about the primate MGad. In cats, the lateral division of the posterior nuclear group (Pol) appears to correspond, at least in part, to the rostral pole (RP) of the MGC. This division receives its principal inputs from the central nucleus of the inferior colliculus (ICc), and has dense connections with both A1 and AAF (Andersen et al., 1980; Lee et al., 2004). Pol is also tonotopically organized, and populated by neurons with narrow tuning and short latencies comparable to MGv (Imig and Morel, 1984; Imig and Morel, 1985a; Imig and Morel, 1985b) Thus, these data imply that both MGv and Pol may belong to the primary (lemniscal) pathway. On anatomical grounds, Jones (Jones, 1997) has suggested that Pol (RP) may correspond to the MGad in monkeys, which expands to occupy the rostral pole of the MGC. Both nuclei contain small densely-packed cells and contain the highest density of parvalbumin-immunoreactive (PV-IR) cells in the MGC (Molinari et al., 1995). In monkeys, as in cats, MGv and MGad (Pol, RP) appear to receive inputs from the central nucleus of the inferior colliculus through a PV-IR pathway ascending in the brachium of the inferior colliculus (Molinari et al., 1995), linking both to the lemniscal pathway. Further, limited data from primates suggests that at least part of MGd is tonotopically organized (Gross et al., 1974), with latencies ranging from long to short, matching those of MGv (Allon et al., 1981). Thus, if MGad does, in fact, belong to the lemniscal auditory pathway, then the preferential connection between MGad and CM

may account for certain functional similarities observed between neurons in A1 and CM, such as tonotopic organization and short-latency responses to pure tones and noise bursts (Bieser and Muller-Preuss, 1996; Cheung et al., 2001; Kajikawa et al., 2005; Lakatos et al., 2005). In addition, the subcortical inputs to CM would be in line with the inputs to AAF of the cat and other mammals, since no other auditory cortical areas receive such a dense projection from MGad or Pol (RP)(Lee and Winer, 2005; Lee et al., 2004).

Inputs from the other divisions of the MGC to RM and CM were similar. First, neither area received substantial inputs from the MGv, in keeping with their designation as belt areas. In that respect, CM differs from AAF in the cat, since AAF receives significant inputs from MGv and RP (Pol) in that species (Lee et al., 2004). Second, both areas received significant dense inputs from segregated clusters of cells located in the ventral and dorsal parts of MGm. While it could not be determined whether any of these cells project to both RM and CM, it seems likely that overlapping MGm projections reflect some degree of functional congruence between the two areas. On the other hand, it is important to recognize that MGm is structurally diverse (Winer and Morest, 1983), and projects broadly to auditory cortex through at least two types of projections. One group, comprised mainly of calbindin-IR neurons, projects to layers I and II of cortex, while projections to the middle layers represent a mix of calbindin- and parvalbumin- IR neurons which tend to be organized in segregated clusters (Hashikawa et al., 1995; Jones, 2003; Molinari et al., 1995). While there has been some evidence of topography in the projections from MGm, it is not clear how this may reflect regional variations in function (Hackett et al., 1998b; Jones, 2003; Kosmal et al., 1997). For example, most MGm neurons respond reliably to auditory stimulation and there is some evidence of tonotopic

162

organization rostrally (Rouiller et al., 1989), but response properties vary widely. This profile is complicated by a wide range of nonauditory inputs which are known to drive responses to somatic, vestibular, visual, and nociceptive stimuli in mammals other than primates (Blum et al., 1979; Blum and Gilman, 1979; Bordi and LeDoux, 1994; Curry, 1972; Lippe and Weinberger, 1973; Love and Scott, 1969; Phillips and Irvine, 1979; Poggio and Mountcastle, 1960; Wepsic, 1966). If these properties have been retained in primates, they may contribute in some way to nonauditory responses observed in CM, and perhaps other auditory cortical areas. This subject is explored in more detail below.

Connections of RM and CM with other posterior thalamic nuclei

A secondary difference between RM and CM noted in the present study concerned their connections with nuclei outside of the MGC. CM had more inputs from Po, Sg, Lim, and PM (Figs. 9, 16). Although not intensively studied in primates, the potential significance of such projections to CM may relate to convergent auditory, somatosensory, and visual projections among these nuclei, which are generally regarded as multisensory (Linke and Schwegler, 2000). So far, multisensory (auditory, somatosensory) activity in auditory cortex has been explored in CM and A1, but only in CM have nonauditory responses been found (Fu et al., 2003; Robinson and Burton, 1980; Schroeder and Foxe, 2002; Schroeder et al., 2001). With respect to thalamic connections, CM and A1 both receive inputs from Po, Sg, and Lim, as well as MGm, yet only neurons in CM respond to both auditory and somatic stimulation. This dichotomy can be interpreted in several ways. First, it may be that inputs from these nuclei do not drive activity in cortex. In that case, the projections to CM from the retroinsular somatosensory

area, Ri, may be mostly responsible for somatosensory activity in CM, as suggested in the companion to this paper (de la Mothe et al., 2006a), since A1 lacks strong input from multisensory areas in cortex. Second, projections to A1 and CM may arise from functionally disparate subpopulations of neurons within each of the multisensory nuclei. The projections to CM from these nuclei are certainly much stronger than to A1, and may affect cortical activity differently in A1 and CM. Third, somatosensory activity in CM may depend on coincident inputs from thalamus and cortex. In that case, neuronal activity in A1 may be weakly modulated by inputs from multisensory nuclei in thalamus, but not driven, since A1 lacks strong inputs from a somatosensory area (e.g., Ri,). Currently, it is known from multichannel laminar recordings that convergent auditory and somatosensory activity in CM begins in layer IV at about 11 ms, then spreads rapidly to the supragranular and infragranular layers, characteristic of a feedforward pattern of projections (Schroeder and Foxe, 2002; Schroeder et al., 2001). This response profile is consistent with projections to layer IV and the deep part of layer III from parvalbumin-IR cells in MGad and MGm (Hashikawa et al., 1995; Hashikawa et al., 1991). In addition, multisensory nuclei other than MGm also appear to project to the middle cortical layers of cortex in this region. Burton and Jones (Burton and Jones, 1976; Jones and Burton, 1976) found that the projections of Po to CM (Pa) and Ri were concentrated in the lower half of layer III, with minor inputs to the upper half of layer IV. They also found that terminations of Sg and Lim in the granular insula (Ig) were concentrated in lower III and upper lamina IV, coextensive with the pyramidal cells in IIIb, suggesting a similar profile may hold for CM and perhaps Ri. These patterns seem consistent with the laminar profile of connections of A1 and CM observed in the companion study (de la Mothe et al.,

164

2006a). Injections in CM revealed dense inputs from infragranular and supragranular layers in A1 and Ri. In addition, a CTB injection of A1 revealed overlapping anterograde and retrograde connections centered on the middle cortical layers of CM, as well as layer V. Thus, multisensory inputs from both the cortex and thalamus appear to converge in layer III of CM. The functional significance of this connection pattern could be addressed by coupling simultaneous laminar recordings from A1 and CM with recordings and systematic deactivation of thalamic nuclei and Ri.

Corticotectal projections of RM and CM

Injections of both RM and CM revealed projections to the dorsomedial region of the inferior colliculus bilaterally, but stronger ipsilaterally. In addition, CM projections extended ventromedially, within a narrow pericentral shell that wrapped around the ventral boundary of the central nucleus and continued dorsolaterally into the lateral nucleus. The projection to the dorsomedial region has been observed after auditory cortical injections involving the core and belt regions of primates and other species (FitzPatrick and Imig, 1978; Luethke et al., 1989; Morel and Kaas, 1992; Winer et al., 2002). The pattern of projections appears to differ between tonotopic and non-tonotopic areas of auditory cortex (Winer et al., 2002). In the present study, the more extensive labeling of ventral and lateral pericentral shell observed after CM injections may reflect functional distinctions between RM and CM. Of particular interest are the observations of auditory and somatosensory interactions in the lateral (external) nucleus of cats (Aitkin et al., 1978; Aitkin et al., 1981). If this organization has been conserved in primates, it would be consistent with the multisensory features of CM. We did not find corticofugal

165

projections to the superior colliculus (SC) or any other subcortical structure. In cats, injections of the anterior ectosylvian sulcus resulted in projections to the SC, but no projections were found after injections involving any of the other auditory fields (e.g., A1, AAF, AII)(Meredith and Clemo, 1989). The absence of a projection to SC suggests that CM probably does not correspond to AES in cats. The absence of projections to other subcortical nuclei is intriguing, given evidence of widespread corticofugal inputs from auditory cortex throughout the brainstem of other species (Winer, 2005). Additional studies may be needed to examine these connections in primates.

Thalamocortical connections of A1 and R

The main projection to the core areas A1 and R derived from cells grouped in discrete topographic domains within the MGv (Fig. 47). The locations of these clusters varied with location within A1 and R in patterns that reflected the tonotopic organization of both areas. High frequency parts of A1 and R were connected with relatively dorsal and dorsomedial portions of MGv, while low frequency domains in A1 and R were linked to the ventral part of MGv. Similar results were previously obtained after A1 injections in marmosets and other primates (Aitkin et al., 1988; FitzPatrick and Imig, 1978; Luethke et al., 1989; Morel et al., 1993; Morel and Kaas, 1992; Rauschecker et al., 1997), although the extent of label in MGv was often larger, depending on the tracer used and the injection size.

Additional connections of A1 and R in the present study in some ways echoed those of RM and CM. Like CM, A1 had more connections outside of MGC than did R, especially with Po and Sg. A similar pattern can be found in owl monkey auditory cortex,

where injections of A1 labeled more cells in Sg, Lim and Po than injections of either R or RT (Morel and Kaas, 1992). As discussed above, this pattern appears to reflect greater involvement of the caudal auditory fields (i.e., A1, CM) with multisensory activity in the cortex and thalamus, and may represent a functional distinction between A1 and the rostral core areas, R and RT. Otherwise, the connections of A1 and R were consistent with our working model of primate auditory cortex, in which the core areas receive primary (lemniscal) inputs from the MGv, whereas the main input to the belt areas arise from the MGad and MGpd.

Conclusions

The results of the current study indicate that the medial belt areas RM and CM of the marmoset monkey have distinctive and identifiable patterns of thalamocortical connections (Fig. 48). When these results are considered alongside those of the companion paper (de la Mothe et al., 2006a), it is quite clear that RM and CM represent anatomically-distinct areas of auditory belt cortex. RM receives inputs from the MGpd, and is broadly connected with both rostral and caudal areas of auditory cortex. Thalamic inputs to CM arise mainly from the MGad, and CM has stronger connections with caudal areas of auditory cortex. In addition, CM has a greater proportion of inputs from multisensory nuclei in the posterior thalamus. Parallel inputs to the core areas A1 and R arise from the MGv. These connections are topographically organized in the MGv in a manner that reflects the tonotopic organization of A1 and R. The architectonic features of the marmoset MGC indicated that the subdivisions identified in the macaque monkey can

also be identified in marmosets using the same criteria, suggesting that the organization

of the MGC is highly conserved among primates.

CHAPTER IV

CORTICAL CONNECTIONS OF AUDITORY CORTEX IN MARMOSET
MONKEYS: LATERAL BELT AND PARABELT REGIONS

Introduction

Throughout the last number of years a working model of primate auditory cortex

has developed based on studies from both old world and new world monkeys (for

reviews, see Kaas and Hackett, 1998; Kaas et al., 1999; 2000; Hackett, 2002; Jones,

2003; Pandya, 1995; Rauschecker, 1998) (Fig. 49). In this model, auditory cortex is

defined as the regions of cortex that receive preferential input from the ventral (MGv)

and/or dorsal (MGd) divisions of the medial geniculate complex. While some other areas

of cortex are responsive to auditory stimuli (rostral superior temporal gyrus (STGr),

temporal pole, superior temporal sulcus (STS), posterior parietal, and prefrontal cortex),

these areas do not receive significant input from the MGC and are reliant on auditory

cortex for auditory input. These areas are referred to as auditory-related or auditory

association cortex.

Based on this definition, three regions of auditory cortex are identified; core, belt

and parabelt. The core is made up of 3 areas (A1, R, RT) and is surrounded by a belt

region both medially and laterally. The medial belt is divided into 3-4 areas (CM/MM,

RM, RTM) and the lateral belt is divided into 4 areas (CL, ML, AL and RTL). Located

laterally adjacent is the parabelt which is divided into rostral (RPB) and caudal (CPB)

areas.
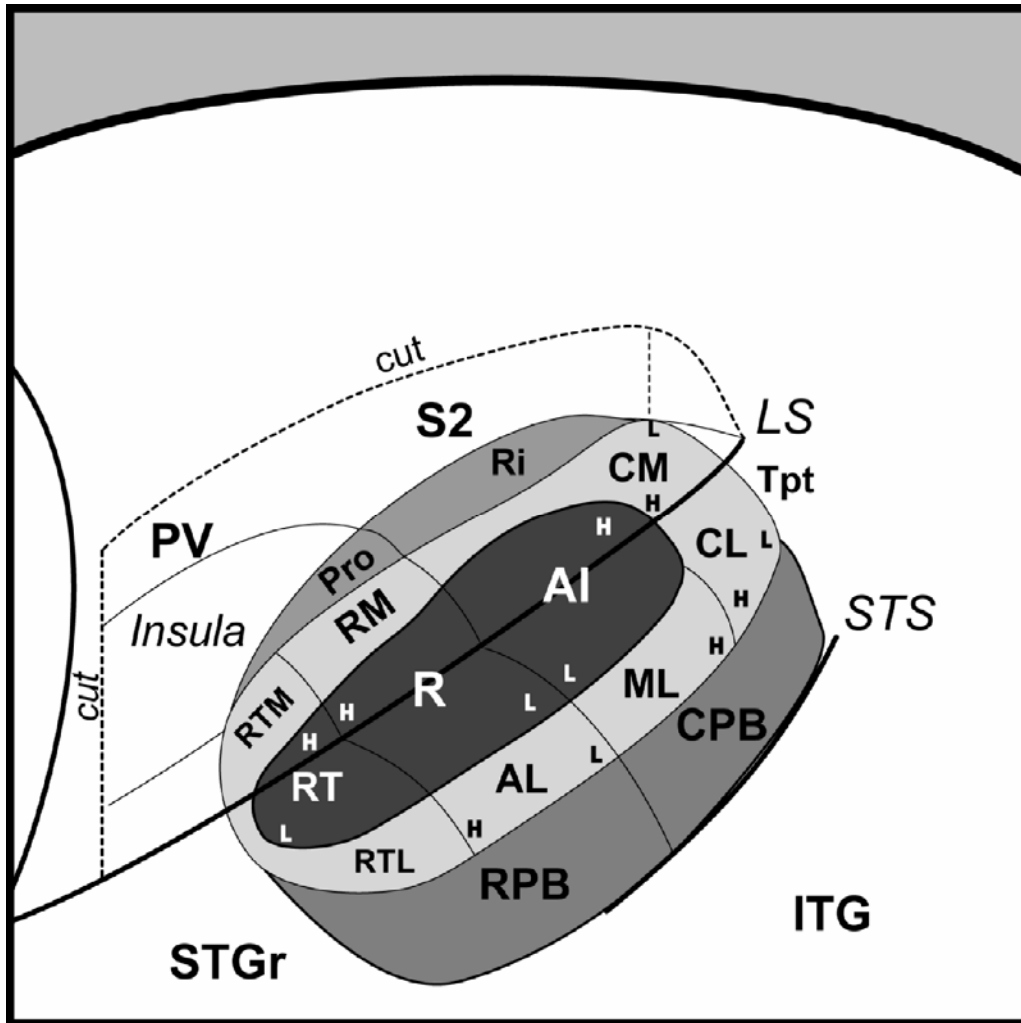
Figure 49. Schematic of the primate auditory cortex based illustrated on a marmoset brain The lateral sulcus (LS) of the left hemisphere was graphically opened (cut) to reveal the locations of auditory cortical areas otherwise hidden. The three regions of auditory cortex are identified with varying degrees of shading: core (dark shading), belt (light shading), parabelt (medium shading).

An important aspect of the model is that information is thought to be processed both serially and in parallel (Hackett and Kaas, 2004; Hackett et al. 1998a,b; Kaas and Hackett, 1998; Kaas et al. 1999; Rauschecker, 1998; Rauschecker et al. 1997) Evidence for a processing hierarchy comes from both anatomical and physiological methods. Connectional data shows that the core projects to the belt region, but does not project to

the parabelt (Hackett et al., 1998a; Morel et al., 1993; Morel and Kaas, 1992). It does, however, receive feedback projections from the parabelt (de la Mothe et al., 2006a). Additionally it has been demonstrated physiologically that neuron responses in CM appears to be at least partially reliant on A1 (Rauschecker et al., 1997). Thus information is thought to flow from the core to the belt, and then from the belt to the parabelt in a serial manner. The core, belt and parabelt are all made up of multiple areas and information is also thought to be processed in parallel within the various subdivisions of a region. This occurs via thalamocortical projections in which one division of the MGC projects to multiple areas in a region (MGv projects to core areas A1, R, RT), as well as via corticocortical projections in which a cortical area projects to multiple areas within a region (e.g., A1 projects to multiple caudal belt fields: CM, CL, ML).

While the absence of projections from the core to the parabelt has been established in the macaque, it has yet to be determined if the marmoset follows a similar pattern. Based on previous studies of the medial belt and core areas in the marmoset in which the findings were comparable to those reported in other species and the primate model in general (de la Mothe et al., 2006a, b), it is reasonable to hypothesize that a similar connectional pattern will be revealed.

Multiple areas have been identified in the lateral belt and the parabelt of the marmoset, yet the connectional profile of the areas in these regions remains limited. The companion studies of the medial belt established differences between rostral and caudal areas in the marmoset and provides a basis for the prediction of distinct connection patterns of rostral and caudal areas of lateral belt as well as the parabelt. It has already been established that there are architectonic differences between rostral and caudal areas

171

of the lateral belt and parabelt in the marmoset. De la Mothe et al., 2006a, reported that while there were some features of architecture that were common to the lateral belt as well as the parabelt, both regions revealed a gradient pattern whereas more caudal areas had more dense expression of CO, AChE, and myelination and this expression decreased rostrally.

Additionally, anatomical and physiological evidence has been reported to reveal differences between rostral and caudal areas of both the belt and parabelt. Three areas (CL, ML, and AL) have been identified physiologically in the lateral belt based on reversals of tonotopic organization (Rauschecker et al., 1995; Rauschecker and Tian, 2004), which has been confirmed in fMRI (Petkov et al., 2006). Additionally there have been functional differences reported between the caudal and rostral areas of the lateral belt (Tian et al., 2001; Tian and Rauschecker, 2004). In Tian et al., 2001, the caudal lateral belt area, CL, was found to be more responsive to spatial stimuli and the rostral lateral belt area, AL, was more responsive to variations in monkey calls. This was followed up with a study of FM sweeps in the lateral belt areas AL, ML, and CL, which revealed significant differences in the neurons' preferences to the sweeps between the areas: slower in the rostral lateral belt and faster in the caudal portion (Tian et al., 2004).

Connectional studies have also identified differences between the rostral and caudal lateral belt areas (Morel and Kaas, 1992; Romanski et al., 1999) as well as differences between the rostral and caudal parabelt areas (Hackett et al., 1998; Romanski et al., 1999). Injections into the lateral belt closer to the A1/R border label cells throughout the core and in neighboring belt areas, while injections in the rostral portion had stronger connections with more rostral areas and was not connected with the more

172

caudal belt areas (Morel and Kaas, 1992). This pattern of rostrocaudal topography was echoed in the parabelt where caudal injections had stronger connections with caudal areas and rostral injections with rostral areas, with less distinct patterns with proximity to the A1/R border (Hackett et al., 1998). Differences between both the rostral and caudal lateral belt and parabelt were also illustrated from connections with prefrontal cortex in which injections into rostral PFC (anterior and orbital PFC) labeled cells in the rostral belt and parabelt areas while the caudal belt and parabelt areas were connected with the arcuate region, caudal principalis, and ventrolateral PFC.

The purpose of the present study was to refine and extend the working model of primate auditory cortex by examining the cortical connections of the lateral belt and adjacent parabelt in the marmoset monkey. This species has become an important neurophysiological model for auditory cortex, and while a general organization has been proposed for the primate model, the organization of these regions in the marmoset is unknown. Tracer injections were made in rostral and caudal lateral belt as well as rostral and caudal parabelt to facilitate a comparison of areas within regions (caudal vs. rostral), as well as between regions (belt vs. parabelt). Specifically, the following predictions of the model were tested: (1) The marmoset auditory cortex includes a lateral belt and parabelt region that have distinctive architecture and connections; (2) The lateral belt and parabelt regions contain subdivisions that have topographically distinct patterns of connections.

Method

The experiments proposed in this report were conducted in accordance with the

Vanderbilt University Animal Care and Use Committee Guidelines and the Animal

Welfare Act under a protocol approved by the Vanderbilt University Institutional Animal

Care and Use Committee. Seven adult marmosets (*Callithrix jacchus jacchus*) served as

animal subjects in the present study. The experimental history of each animal is included

in Table 3.

Table 3. Experimental history of animal subjects and relevant injections. Areas of tracer
injections (CL, caudolateral belt; ML, mediolateral belt; AL, anterolateral belt; CPB,
caudal parabelt; RPB, rostral parabelt). Neuroanatomical tracers (CTB-red, cholera toxin
subunit B 594; FR, fluororuby; DY; diamidino yellow), aqueous concentration and
volume injected are listed for each tracer.

Case #	Case	Sex	Areas Injected	Tracer	%	Volume (µl)
1	(01-89)	M	CL/CM	FR	10	0.3
			CPB	DY	10	0.3
2	(03-59)	M	CPB	CTB-red	1	0.35
3	(04-40)	M	RPB	CTB-red	1	0.35
4	(04-51)	M	AL	FR	10	0.3

General Surgical Procedures

Microinjections of anatomical tracers were made into subdivisions of auditory

cortex in marmoset monkeys under aseptic conditions. Marmosets were premedicated

with cefazolin (25mg/kg), dexamethozone (2mg/kg), cimetidine HCl (5mg/kg), and

robinul (0.015mg/kg). Anesthesia was induced by inhalation of 5% isoflurane or by

intramuscular injection of ketamine hydrochloride (10 mg/kg), and the animals were

intubated, then maintained by intravenous administration of ketamine hydrochloride (10 mg/kg) supplemented by intramuscular injections of xylazine (0.4 mg/kg) or maintained with (2-3%) isoflurane and Nitrous Oxide with Oxygen (50/50) 1 liter/minute. Body temperature was maintained at 37°C with a water circulating heating pad. Vital signs (heart rate, expiratory CO_2, and O_2 saturation) were continuously monitored throughout the surgery and were used to adjust the levels of anesthesia.

A stereotaxic instrument (David Kopf Instruments, Tujunga, CA) was used to stabilize the head of the monkey. A midline incision was made exposing the skull, followed by the retraction of the left temporal muscle. A craniotomy was performed exposing the superior temporal gyrus and the lateral sulcus, followed by the cutting and retraction of the dura. Warm silicone was applied periodically to the brain to prevent dessication of the cortex during photography and injections of tracers. Photographs were then taken to facilitate later reconstruction of the injection sites based on blood vessels and sulci. Following the injections, the exposed area of the brain was covered with softened gelfilm, the craniotomy was closed with dental acrylic, and the overlying temporal muscle and skin sutured back into place. Antibiotic gel was applied along the suture line. After the surgery, the endotracheal tube was removed and vital signs were monitored during the recovery period until vitals became stable and the animal was returned to its cage where it was monitored until recovery was complete. Daily injections of penicillin G (10 000 units i.m.) were given for 5 to 7 days after surgery, along with Banamine (1 mg/kg) as needed for analgesia.

Tracer Injections

Injections of tracers were made into target areas using 1-2 µL syringes, with a pulled glass pipette tip, attached to a hydraulic microdrive. Injections were made into the lateral belt and parabelt regions by using landmarks and blood vessels, on the lateral surface of the superior temporal gyrus (STG), to locate auditory cortex. The injections were made directly into the auditory areas (Fig. 2). In all cases the injections made were manual pressure injections of various amounts (Table 3) after which the syringe remained for approximately 10 minutes under continuous observation to maximize uptake and minimize leakage. The tracers used were cholera toxin-B 594 (CTB-red); fluororuby (FR); and diamidino yellow (DY). Due to the various levels of sensitivity of the tracers the amounts and solution concentrations were varied accordingly as shown in the table (typically, 0.01-0.05 µL and 3% fluorescents and 1% for CTB).

Perfusion

Upon completion of a recording session, results reported elsewhere (Kajikawa et al., 2005, 2008) a lethal dose of pentobarbital was administered. Just before cardiac arrest the animal was perfused through the heart with warm saline followed by cold 4% paraformaldehyde dissolved in 0.1 M phosphate buffer. Immediately following the perfusion the brain was removed and photographed, the two hemispheres and the brainstem were separated and placed in 30% sucrose for several days and then blocked.

Histology and Data Analysis

The hemispheres were cut perpendicular to the lateral sulcus in either caudal-to-

rostral or rostral-to-caudal direction at 40 µm (see Fig. 3, chapter 2). Depending on the case, series of sections were processed for: (i) fluorescent microscopy; (ii) BDA; (iii) CTB (iv) myelin (Gallyas, 1979); (v) acetylcholinesterase (Geneser-Jensen and Blackstad, 1971); (vi) stained for Nissl substance with thionin (vii) cytochrome oxidase (CO) (Wong-Riley, 1979); or (viii) parvalbumin immunohistochemistry (PV).

Cells labeled with fluorescent tracers were all plotted on an X-Y plotter (Neurolucida) coupled to a Leitz microscope under ultraviolet illumination. Photographs and drawings of each section were made, noting architectonic boundaries, the location of blood vessels, and the distribution of labeled cells. Reconstruction of the architecture was based on previously identified criteria in marmosets (see chapter 2; de la Mothe et al., 2006a) A composite drawing was made from adjacent sections processed for tracer label, acetylcholinesterase, myelin, CO, and Nissl by aligning common architectonic borders and blood vessels (Fig. 4). Reconstructions of the composite images were achieved using Canvas 7.0 software (Deneba software, Miami, FL, USA). The final composites were analyzed to reveal the individual connection patterns and the connection patterns of injections at similar or dissimilar locations. In most figures, every other section was selected for illustration. Cell counts were performed on all auditory areas and converted to percentages in order to better compare the general connection patterns between tracers due to variability in tracer sensitivity. While sensitivity of the tracers did vary, regardless of the actual number of cells labeled, the general patterns revealed by injections of specific areas were maintained regardless of the tracer used.

Photographs were made using a Spot-2 camera mounted on a Nikon E800 microscope and adjusted for brightness, contrast, text added, and cropped using Adobe

Photoshop v6.0 software (Mountain View, CA, USA). Other than the adjustments

mentioned, the images were not altered in any way.

<center>Results</center>

Ipsilateral connections of CM/CL

In case 1, the injection was made caudal to A1 that involved both CM and CL

(Fig. 50). Caudally there were some weak connections with Tpt (#52) with stronger

connections in supragranular and infragranular layers of CM, CL and Ri (#64-76). Just

caudal to A1, near the injection site, the connection pattern in CM and CL continued with

denser label in CM, but cells were absent from Ri (#88). As A1 emerged, there were

strong supragranular and infragranular connections in A1, CM, ML, and Ri (#100-148).

The overall strength of connections decreased rostrally with distance from the injection

site, but labeled cells were consistently denser in CM. From the caudal emergence and

throughout CPB there were labeled cells in both supragranular and infragranular layers,

with the strongest connections more caudal in the area, closer to the injection site.

Transitioning into rostral auditory cortex, connections were weak overall and mainly

involved AL and RPB (#160-184). Label was sparse or absent from RM and R.

Contralateral connections of CM/CL

In case 1, the injection of FR into CM and CL labeled cells primarily in layer III

of the medial belt and lateral belt, as well as the core region of caudal auditory cortex,

mirroring the injection site in the opposite hemisphere (Fig. 51). Caudally there was

<center>178</center>

Figure 50. Ipsilateral cortical connections of areas CM/CL and CPB, case 1. Series of serial sections are arranged from caudal (upper left) to rostral (lower right), and continue onto the next page. FR labeled cells (open triangles) and DY labeled cells (filled circles) are drawn onto each section, showing borders between areas identified by architectonic criteria. Black shading illustrates injection site. Dashed line in section 100 denotes where the label is artificially cut off dorsally due to interference from FR injection. *Inset*, schematic of marmoset auditory cortex showing location of FR injection into CM/CL, and DY into CPB.

Case 1 injections

Caudal

CM/CL

Tpt?

52

CM

CL

64

CM

Ri

CL

CPB

76

CM

CL

FR

DY

Ri

CPB

88

A1

ML

CPB

DY

Ri

CM

100

A1

CM

ML

DY

Ri

CPB

112

A1

CM

ML

Ri

CPB

124

A1

ML

CPB

CM

Ri

136

A1/R

ML

CPB

CM

Ri

148

R

AL

RPB

RM

Pro

Cla
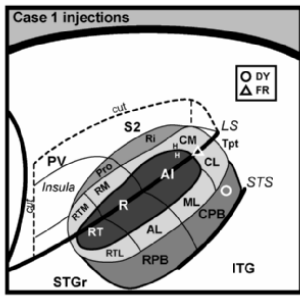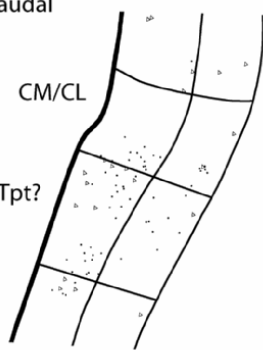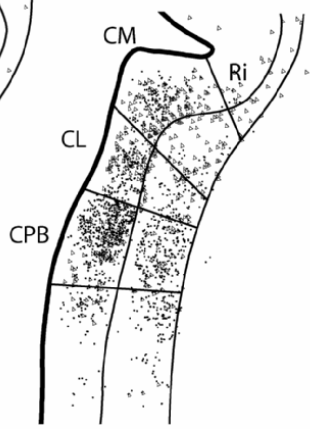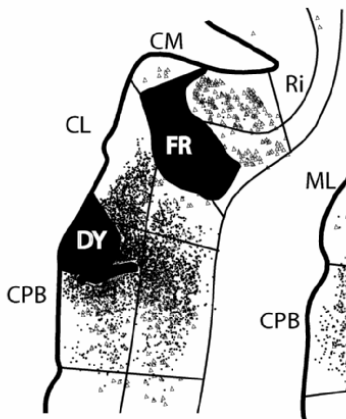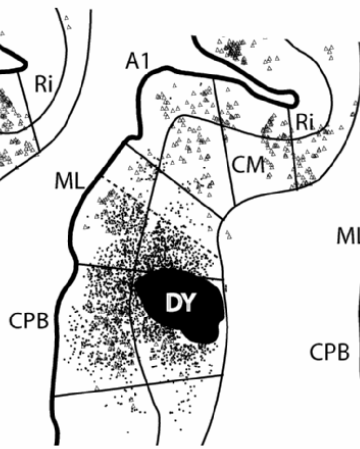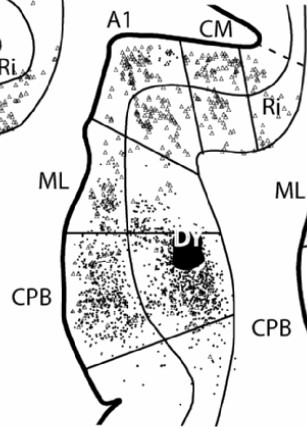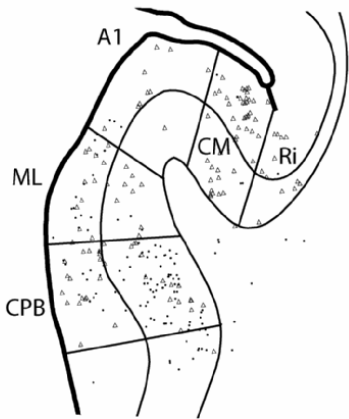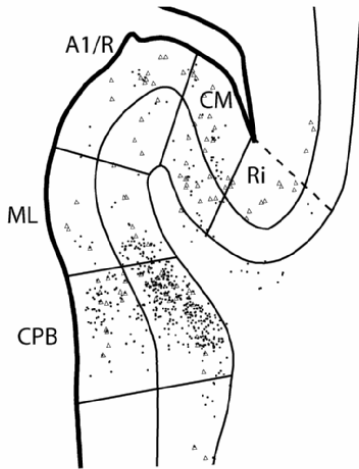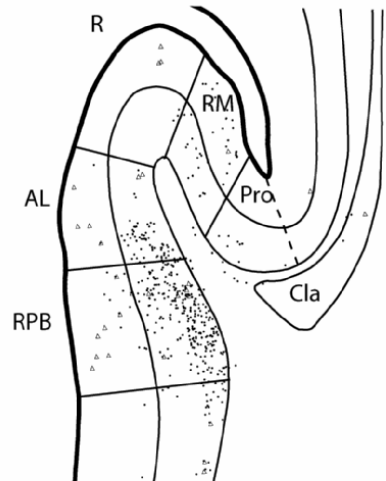
160

Case 1 ipsilateral

Rostral

180
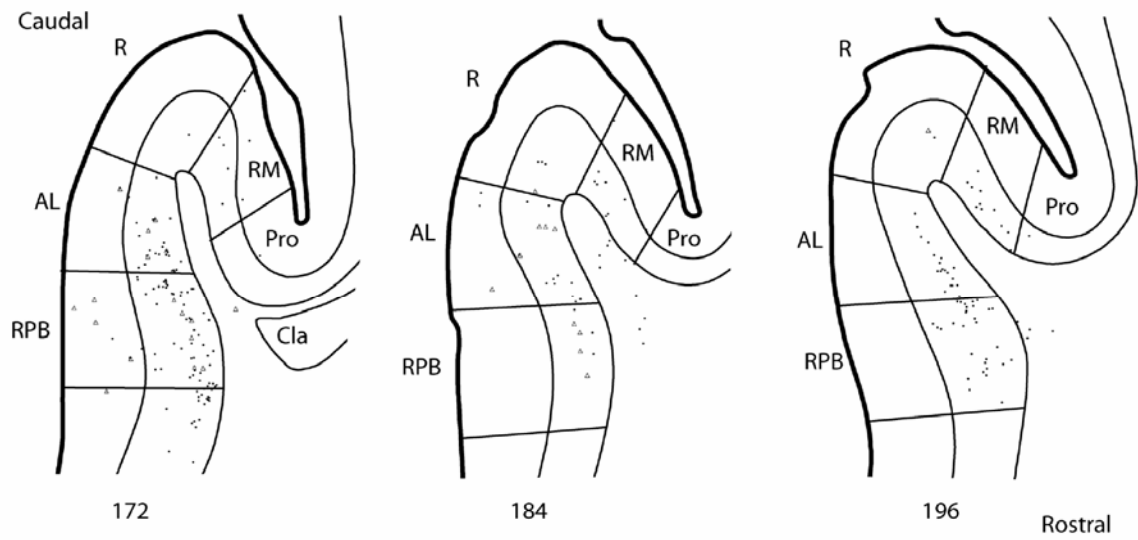
Case 1 ipsilateral, continued

Figure 50 (continued)

Figure 51. Interhemispheric cortical connections of CM/CL and CPB, case 1. Series of serial sections are arranged from caudal (upper right) to rostral (lower left). FR labeled cells (open triangles) and DY labeled cells (filled circles) are drawn onto each section, showing borders between areas identified by architectonic criteria. *Inset*, schematic of marmoset auditory cortex showing location of FR injection in CM/CL, DY in CPB in the contralateral hemisphere.

strong labeling in CM and CL with sparse labeling in CPB (#100-112). Label in CM

strengthened as A1 emerged and moderate label was present in A1, ML, and CPB (#124-

136). There was sparse label in CM, A1, and ML in the most rostral section (#148) and

overall the label was confined mainly to layer 3.

Summary of CM/CL connections

Outside the areas of injection, CM and CL, the strongest connections were with CPB

followed by A1, R and ML (Fig. 52). There were weaker connections with the more
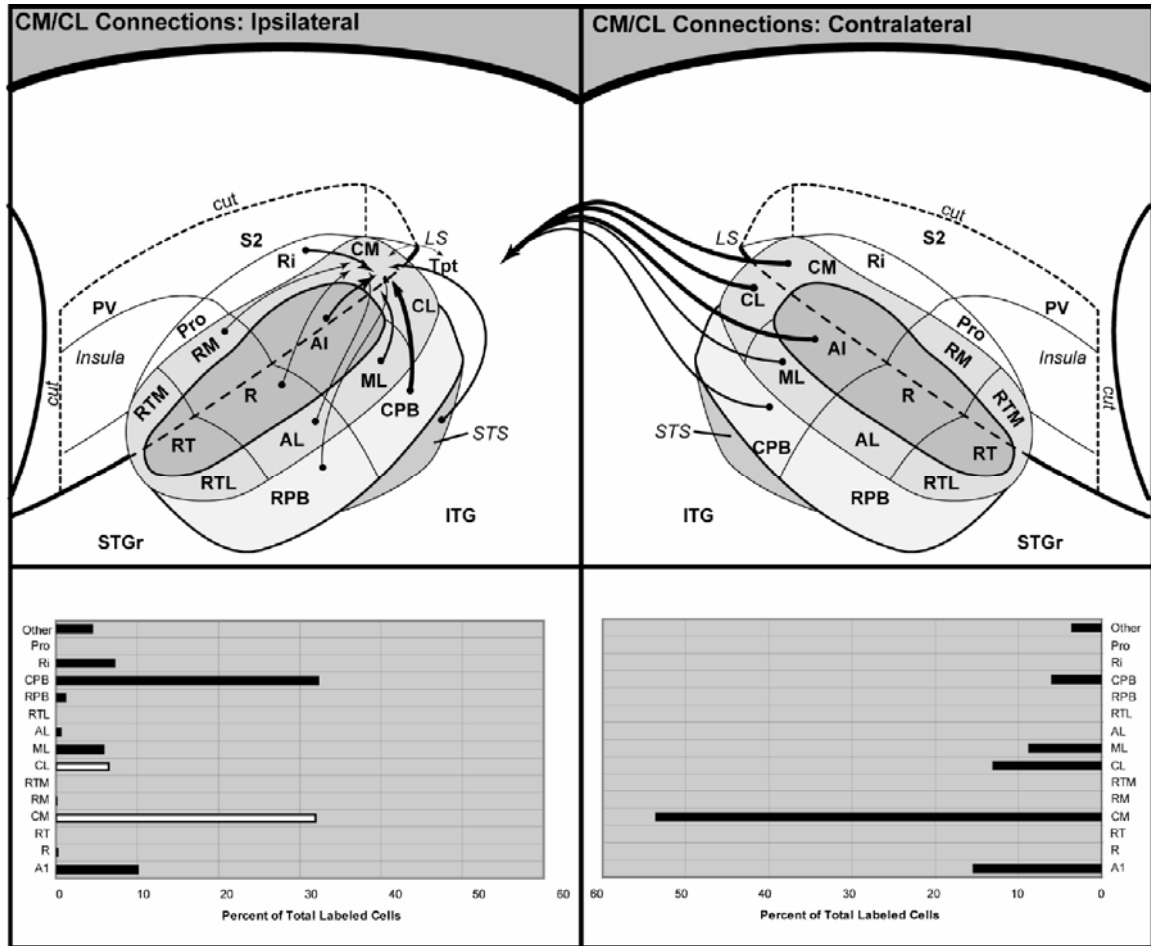
Figure 52. Summary of ipsilateral (left) and interhemispheric (right) connections of CM/CL. Top panels illustrate connections (arrows) of CM/CL on schematic diagram of marmoset auditory cortex. Arrow size is proportional to connection strength, as indicated in the histograms below each panel. Single arrows indicate unidirectional projections. Bottom left, white bar indicates that cell counts for ipsilateral CM/CL may be inaccurate (deflated) due to masking by the tracer injection.

rostral areas RM, R, AL, and RPB, but no connections with the most rostral extent of

auditory cortex. Label in the contralateral hemisphere was consistent with the area of

injection with label predominantly in CM as well as CL, A1, ML, and CPB. Judging

from the location of the injection site in the ipsilateral hemisphere as well as the

contralateral label, it appears that the injection, which borders CM and CL, may have

involved more of CM than CL.

Ipsilateral connections of RTL

In case 4, the injection was made into RTL rostral to the core area RT (Fig. 53). In the

most caudal sections there were weak connections in the supragranular layers of CM and

the lateral division of A1 and both the supragranular and infragranular layers of ML

(#130-118). Connections strengthened at the A1/R border (#106) with the transition into

rostral auditory cortex and with the pattern of predominantly supragranular connections

continuing in R and RM (#106-70). In AL connections were also present in both the

supragranular and infragranular layers in caudal R (#106-94), but shifted to

predominantly supragranular layers more rostral in the area (#82) and weakened

significantly right before the transition into RT (#70). Strength of connections increased

with the beginning of RT in areas RTL, RT and RTM, although connections were

strongest in RT (#58). Label was present in both the supragranular and infragranular

layers of RT and RTL, while confined predominantly to the supragranular layers in RTM.

At the rostral extent of auditory cortex where RT is no longer present, there were strong

connections in the supra and infragranular layers of RTL with weaker connections in

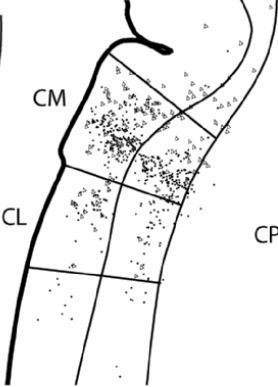RTM, RPB and Pro (#34). Until this point label was virtually absent from the parabelt,

184

Figure 53. Ipsilateral cortical connections of area RTL, case 4. Series of serial sections are arranged from caudal (upper left) to rostral (lower right), and continue onto the next page. FR labeled cells (open triangles) are drawn onto each section, showing borders between areas identified by architectonic criteria. Black shading illustrates injection site. *Inset*, schematic of marmoset auditory cortex showing location of FR injection into RTL

Caudal

Case 4 Injections

△ FR

S2
Ri
Tpt
PV
CM
LS
Pro
CL
Insula
AI
RM
STS
RTM
R
ML
RT
AL
CPB
RTL
RPB
STGr
ITG

A1m CM
Ri
A1L
ML
CPB

130

A1m
CM
A1L
Ri
ML
Cla
CPB

118

RM
A1/R
AL
Pro
Cla
RPB

106

RM
R
AL
Pro
Cla
RPB

94

R
RM
AL
Pro
Cla
RPB

82

R
RM
AL
Pro
Cla
RPB

70

RT
RTM
Pro
RTL
Cla
RPB

58

RTL
RTM
FR
Pro
RPB
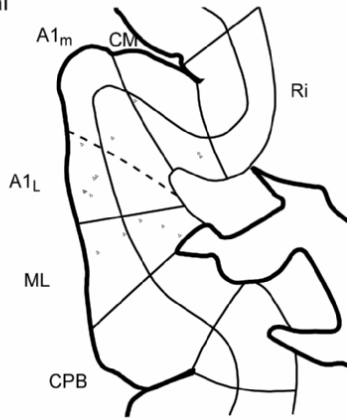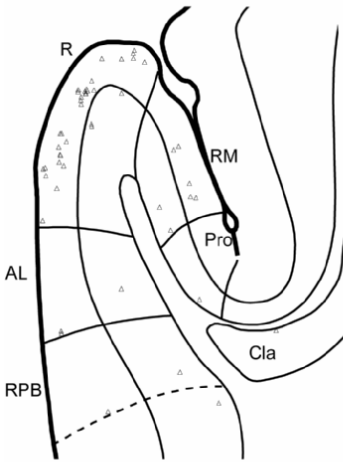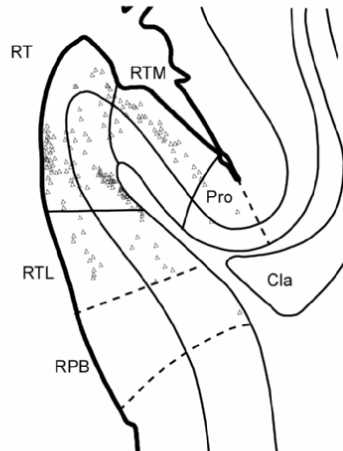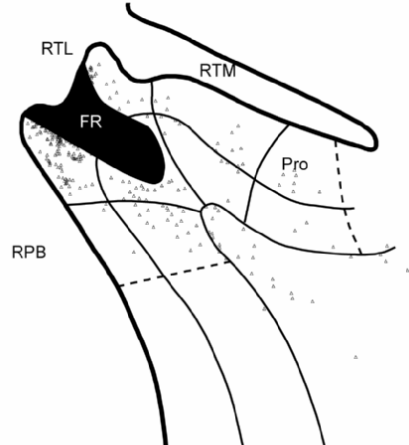
34   **Rostral**

Case 4 ipsilateral

186

with the exception of a few sparse cells in RPB (#106, 82-58). This pattern of weak

connections was also present in Pro throughout R and RT.

Contralateral connections of RTL

In case 4, cells labeled by the RTL injection were concentrated in layer III of the

rostral core and lateral belt regions with a few sparse cells in RPB (Fig. 54). Caudally

Figure 54. Interhemispheric cortical connections of area RTL, case 4. Series of serial sections are arranged from caudal (upper right) to rostral (lower left). FR labeled cells (open triangles) are drawn onto each section, showing borders between areas identified by architectonic criteria. *Inset*, schematic of marmoset auditory cortex showing location of FR injection in RTL in the contralateral hemisphere.

there was sparse label in R (#100) and moving rostrally, label was also present in AL

with the densest label at the R/RT border (#88-70). Label continued in RT and RTL

(#58-46) and was concentrated in RTL, rostral to RT (#28). Label was confined to the

supragranular layers throughout its rostrocaudal extent.

Summary of RTL connections

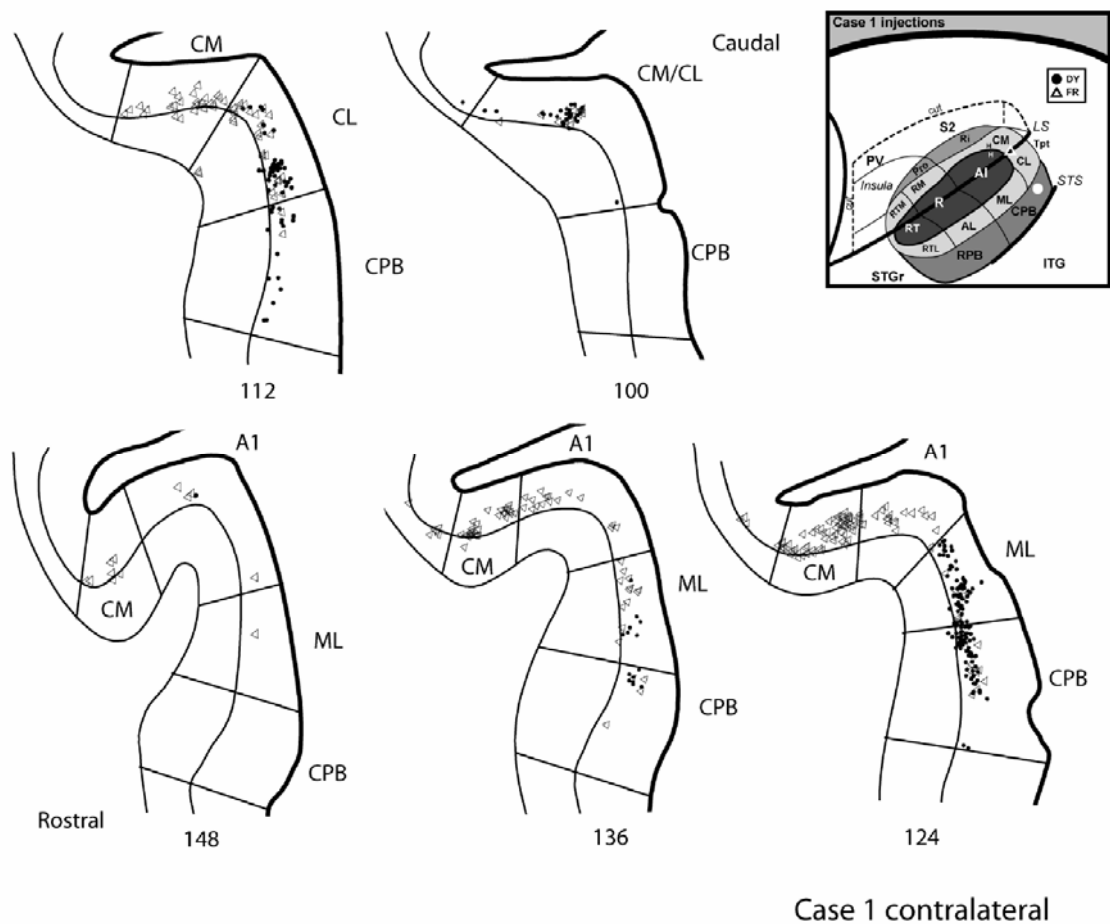   Other than the area of injection, RTL, label was found predominantly in the

rostral core areas R and RT as well as AL (Fig. 55). There were also moderate

connections with RTM and RPB, and weak connections with ML, RM and Pro, and the

rostral portions of A1 and CM. Label in A1 was almost exclusively in the lateral

division. Both the core areas A1 and R had label predominantly in the superficial layers.

The injection into RTL exhibited a pattern of rostrocaudal topography. Contralateral

label was present predominantly in RTL and the adjacent core area RT. There were also

connections from R and AL with weak label in RPB.

Ipsilateral Connections of CPB

      In case 1, the injection was made into the caudal portion of CPB just before the

caudal boundary of A1 (Fig. 50). Caudally there was weak labeling in both the

supragranular and infragranular layers of the combined areas CM and CL, with similar

labeling present in Tpt (#52). This pattern of label continued and connections

strengthened rostrally within the defined areas CM and CL (#64-88). This dense pattern

of label in both supragranular and infragranular layers continued in the lateral belt and

Figure 55. Summary of ipsilateral (left) and interhemispheric (right) connections of RTL. Top panels illustrate connections (arrows) of RTL on schematic diagram of marmoset auditory cortex. Arrow size is proportional to connection strength, as indicated in the histograms below each panel. Single arrows indicate unidirectional projections. Bottom left, white bar indicates that cell counts for ipsilateral RTL may be inaccurate (deflated) due to masking by the tracer injection.
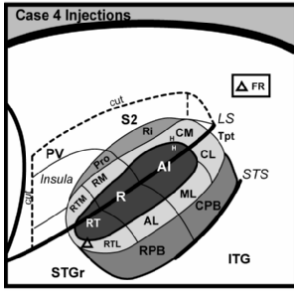
was present throughout area ML (#100-148), with the strongest connections in the most

caudal ML (#100-112), closer to the CPB injection. Beginning with the most caudal CPB

section and continuing throughout the CPB there was dense label in both the

supragranular and infragranular layers (#76-148). In addition, label was present ventral to

the CPB in the STS with the strongest connections in the caudal portion (#76-124).

Connections weakened rostrally and shifted to predominantly infragranular layers (#136-172). Area A1 had only sparse label throughout its rostrocaudal extent (#100-148) with even weaker connections in the more rostral core area, R (#160-196). While label was present in caudal CM, with the emergence of A1 in the adjacent rostral CM label was absent, or if present was very sparse (#100-136). As the transition occurs between caudal auditory cortex to rostral auditory cortex (A1/R border), there was an increase in labeled cells in both the supragranular and infragranular layers of the medial belt area RM (#148-172). This label was confined to the infragranular layers of RM in the most rostral sections (#184-196). This pattern of predominantly, or only infragranular connections was also present in the rostral lateral belt and parabelt areas AL and RPB (#160-196).

In case 2, the injection was made into the rostral portion of CPB close to the A1/R border (Fig. 56). In the most caudal section (#267), label was in both the supragranular and infragranular layers of Tpt, with some weak label in the most caudal portion of CL. Connections in the caudal belt areas (CM/CL) strengthened rostrally, and weak connections were present in the supragranular layers of the adjacent Tpt (#255). As CPB emerged, supragranular label was present and label in the caudal belt areas weakened (#243). At the level of A1, connections strengthened in the lateral belt, area ML, as well as the CPB, but label in CM medial to A1 was virtually absent. The strong connections in the supragranular and infragranular layers persisted until the A1/R border (#231-159), which coincided with the end of the area of diffusion from the injection.   As A1 was shifting into medial and lateral divisions, there appeared to be an area of transition both in the architecture and the connections along the ML/A1 border (#207). This shift from both supragranular and infragranular label to supragranular only appears to correspond
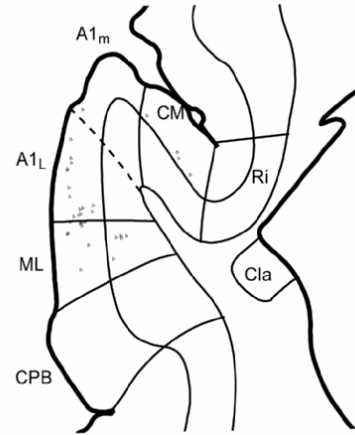
Figure 56. Ipsilateral cortical connections of area CPB, case 2. Series of serial sections are arranged from caudal (upper left) to rostral (lower right), and continue onto the next page. CTB-red labeled cells (open triangles) are drawn onto each section, showing borders between areas identified by architectonic criteria. Black shading illustrates injection site. *Inset*, schematic of marmoset auditory cortex showing location of FR injection into CM/CL, and DY into CPB.
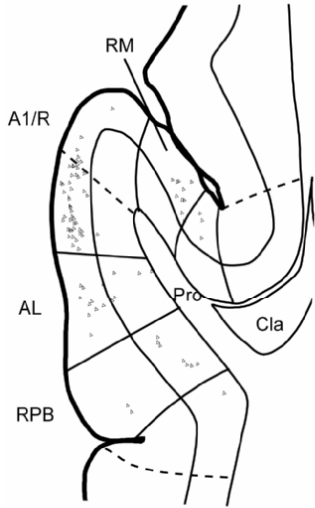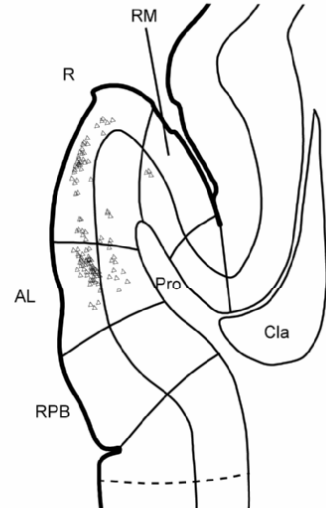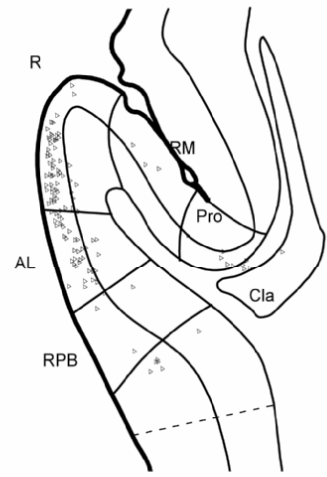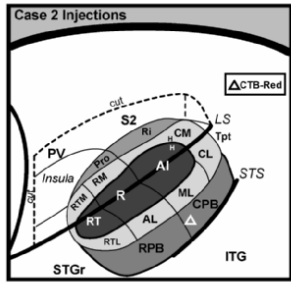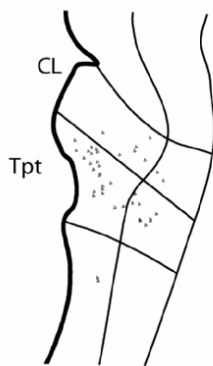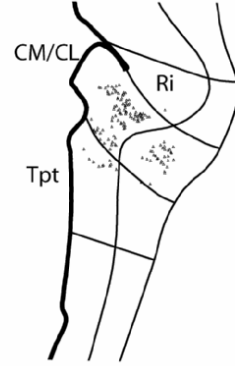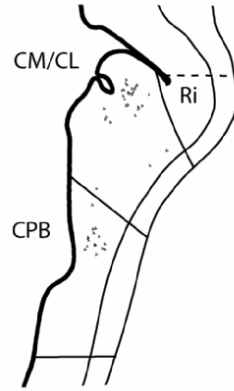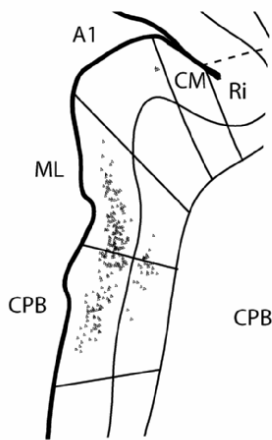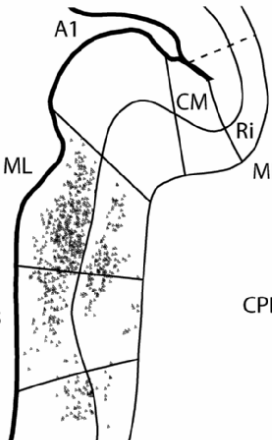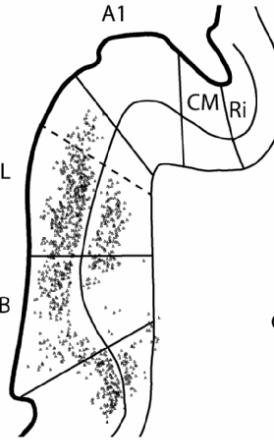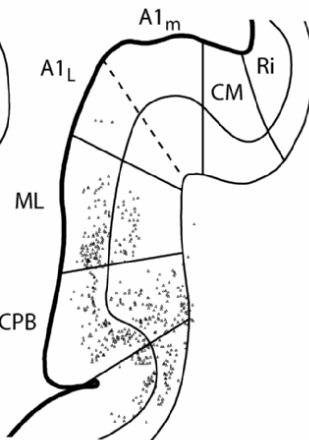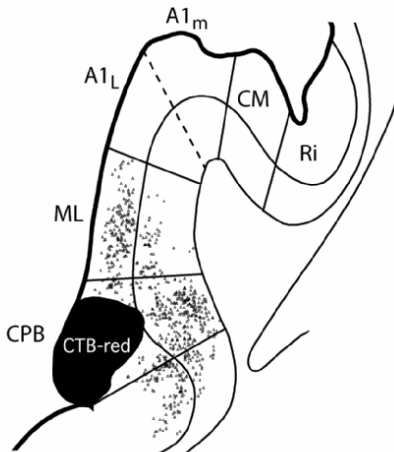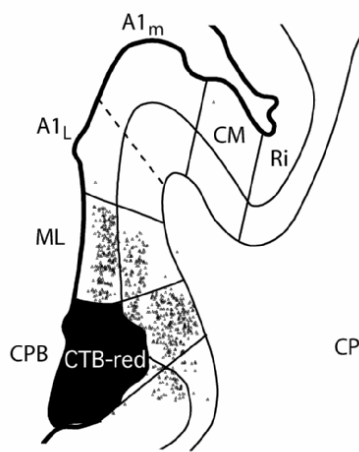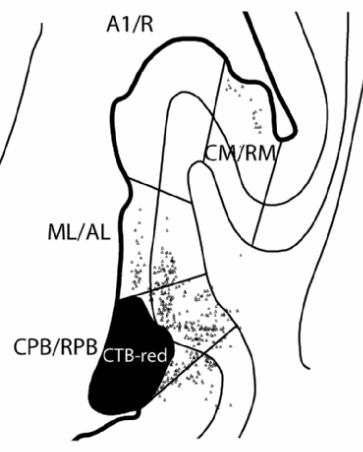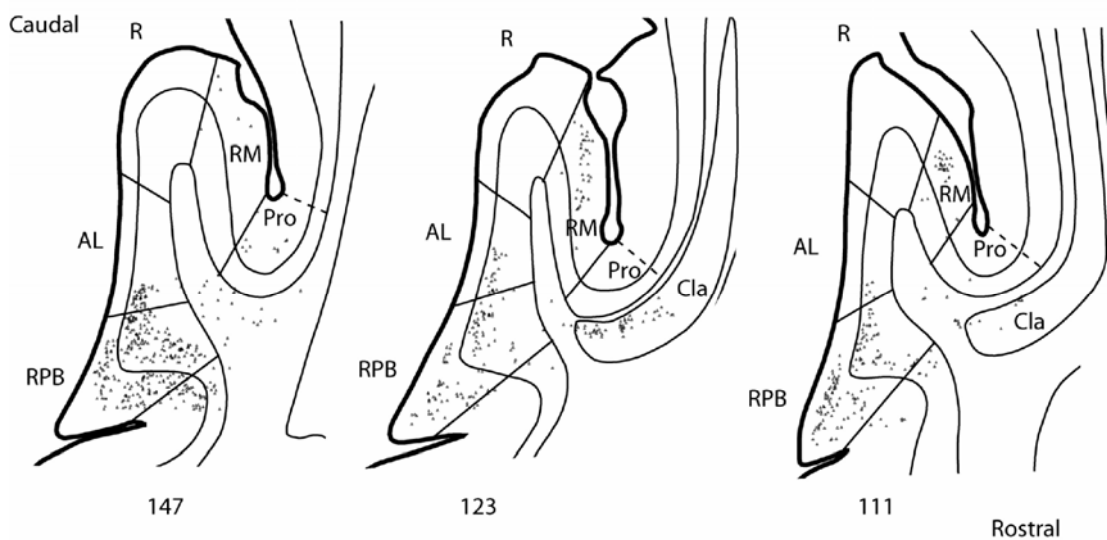
Case 2 ipsilateral

Case 2 ipsilateral, continued.

Figure 56 (continued)

193

with the emergence of the lateral division of A1. Due to lack of core-like architectonic features (i.e. lack of astriate myelination) we have defined the label as part of ML, but indicate that this is a zone of transition with the dashed line. While there was label in the most caudal medial belt section where CM and CL are combined (#255-#243), connections from the medial belt area CM, adjacent to A1, was absent. With the transition from caudal auditory cortex to rostral auditory cortex, label was present in RM, mainly in the supragranular layers (#159-111). Connections were present in the supragranular layers beginning with the most caudal section of CPB (#243), but throughout the remaining CPB as well as the RPB, label was present in both supragranular and infragranular layers (#231-111). This connection pattern was also present ventral to CPB in the STS, and weakened rostrally adjacent to RPB (#219-111).

Contralateral connections of CPB

In case 1, Label was concentrated in the supragranular layers of the caudal parabelt and lateral belt regions (Fig. 51). Most caudally, label was present in CM/CL (#100), but shifted to strictly area CL and CPB moving rostrally (#112). The densest label was present with the emergence of A1 and was confined to ML and CPB (#124). This pattern continued rostrally but connections weakened (#136). Sparse label was found in A1 in the most rostral section (#148).

In case 2, similar to case 1, label was concentrated in the lateral belt and parabelt regions of caudal auditory cortex (Fig. 57). In the most caudal section there was some sparse label in CL (#195) that strengthened rostrally in ML with the emergence of A1 (#189). Continuing rostral there was strong label in ML and CPB (#177-165) that shifts
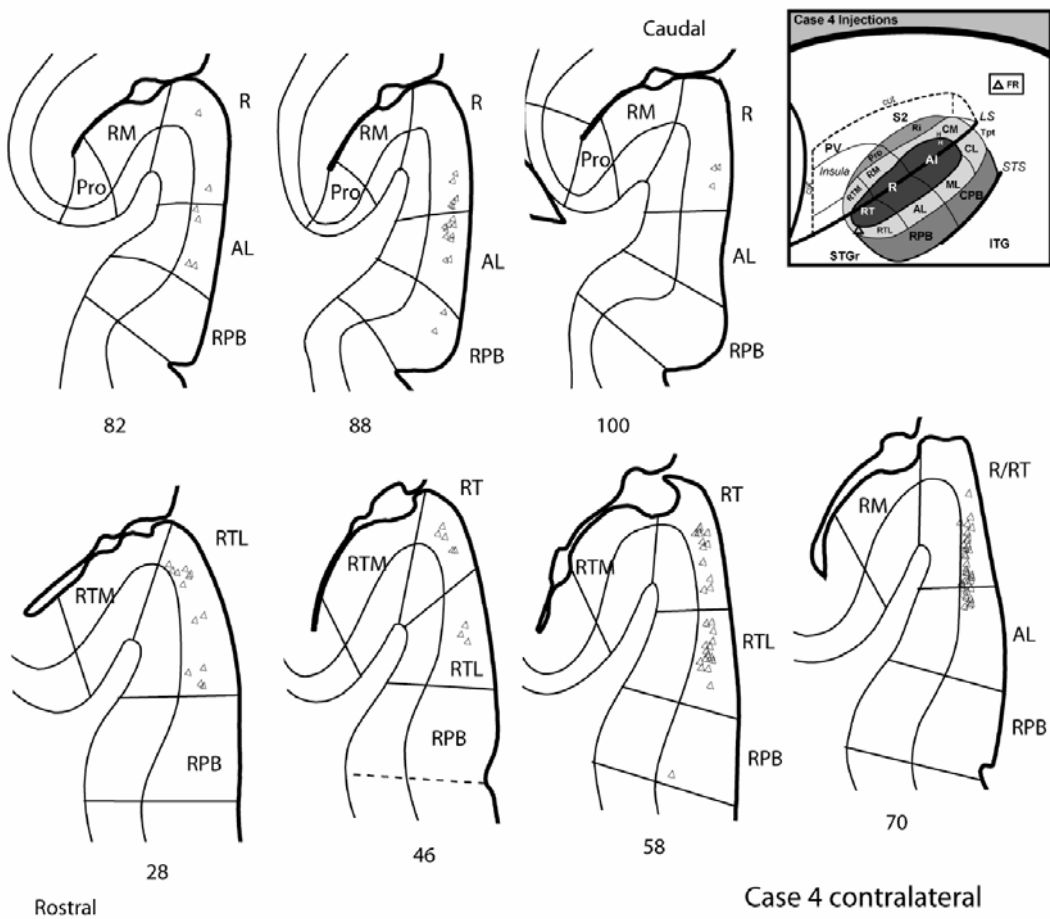
194
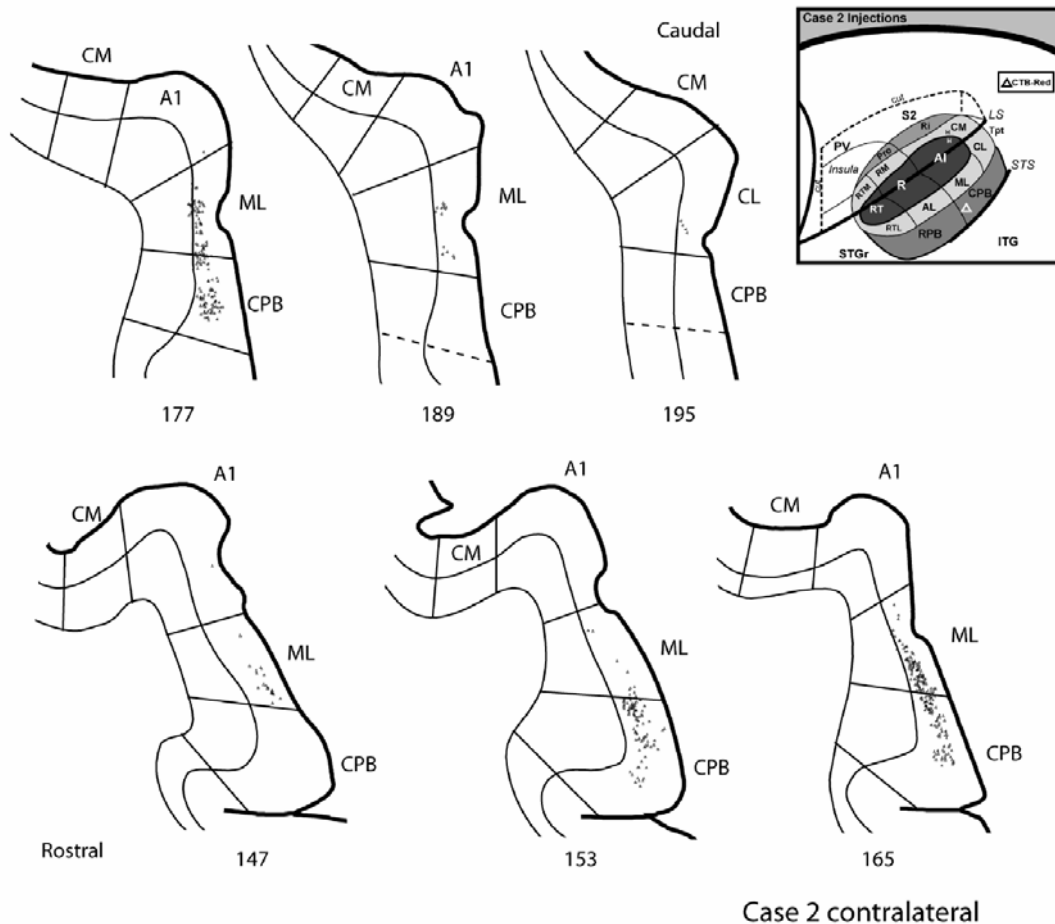
Figure 57. Interhemispheric cortical connections of area CPB, case 2. Series of serial sections are arranged from caudal (upper right) to rostral (lower left). CTB-red labeled cells (open triangles)) are drawn onto each section, showing borders between areas identified by architectonic criteria. *Inset*, schematic of marmoset auditory cortex showing location of CTB-red injection in CPB in the contralateral hemisphere.

to predominantly CPB (#153). At the rostral extent of the label, cells were concentrated

in ML (#147). Overall, the strongest label in this hemisphere mirrored that of the

injection site and was confined mainly to the superficial layers.

Summary of CPB connections

Other than the area of injection (CPB), the strongest connections were with the

195

adjacent lateral belt area, ML (Fig. 58). There were also connections with the
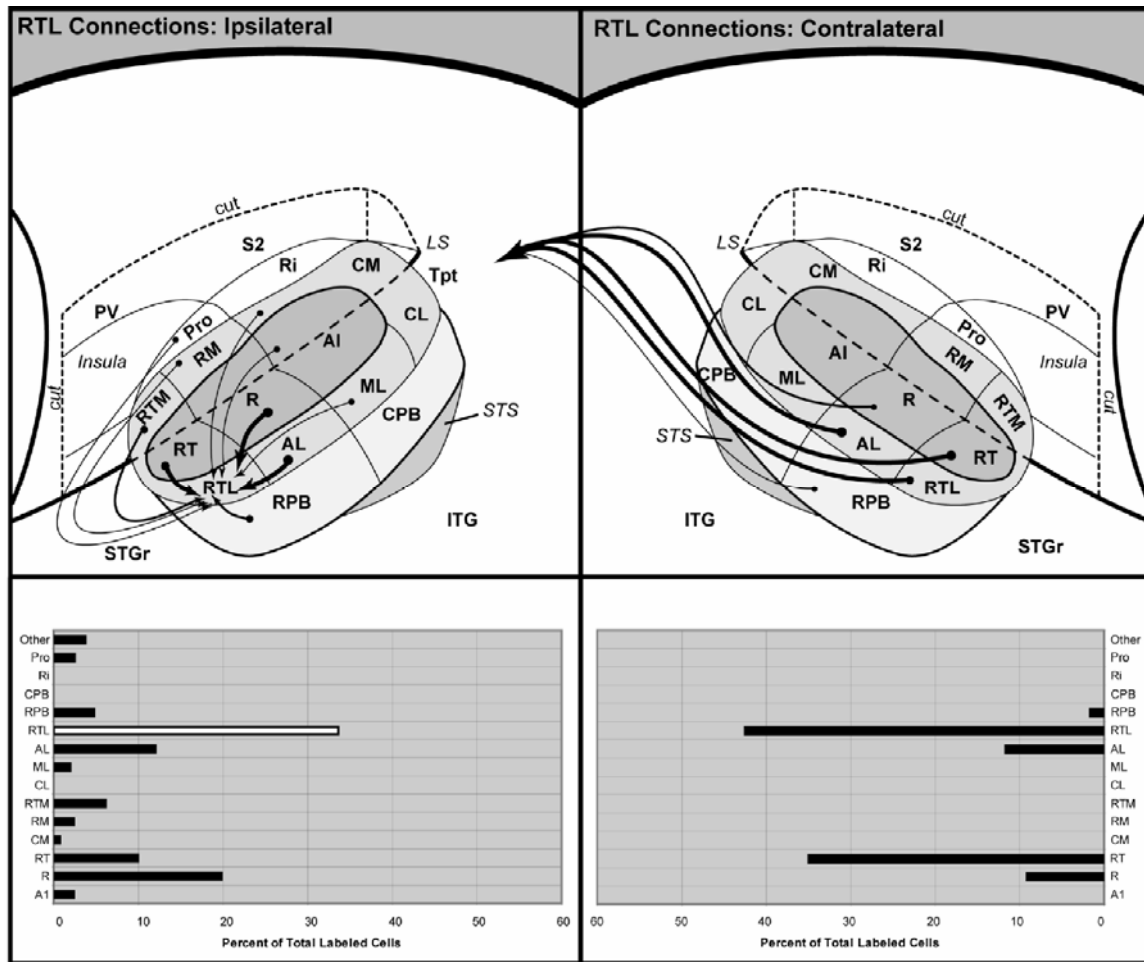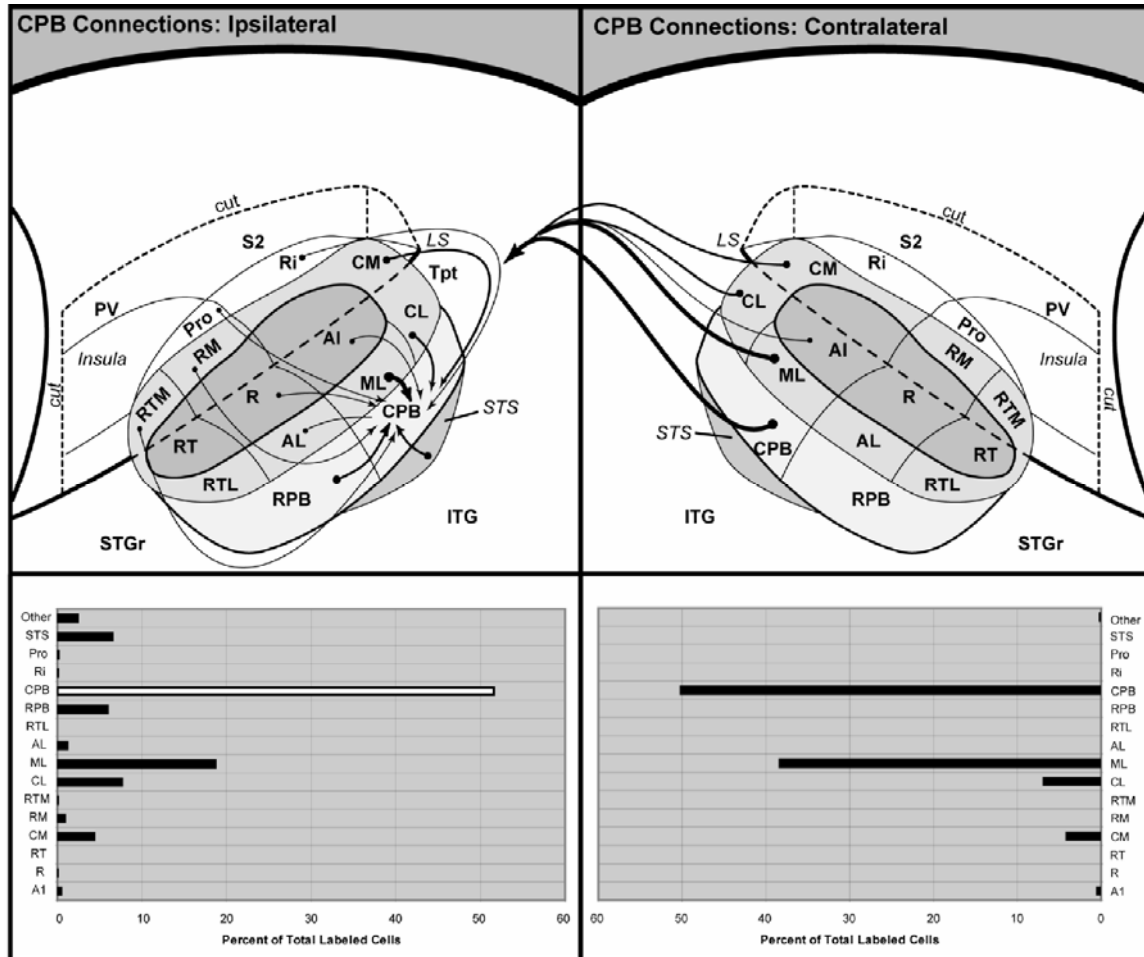

Figure 58. Summary of ipsilateral (left) and interhemispheric (right) connections of CPB. Top panels illustrate connections (arrows) of CPB on schematic diagram of marmoset auditory cortex. Arrow size is proportional to connection strength, as indicated in the histograms below each panel. Single arrows indicate unidirectional projections. Bottom left, white bar indicates that cell counts for ipsilateral CPB may be inaccurate (deflated) due to masking by the tracer injection.

neighboring areas RPB, CL and the STS, as well as CM. Label in CM was present

caudally but absent in the rostral portion medial to A1 in one case, and in the other case,

greatly reduced. RTL was also weakly connected with AL and RM, and very sparse label

was present in Ri, Pro, RTM, A1, and R. Contralateral label was strongest in the homotopic area of injection, CPB. There were also strong connections with the adjacent ML and weaker connections with the caudal belt areas CL and CM. Sparse label was present in A1.

Ipsilateral Connections of RPB

In case 3, the injection was made into the rostral portion of RPB at the level where RT is still present (Fig. 59). In the most caudal section connections were mainly in the infragranular layers of CL with weak infragranular connections in CM. With the emergence of A1, the majority of the label was present in supragranular and infragranular layers in the lateral belt, ML, and parabelt, CPB (#148-184). In the same sections there were only weak connections in A1, CM medial to A1, and Ri. There was a sudden surge of labeled cells in the medial belt at the transition from caudal auditory cortex to rostral auditory cortex. Labeled cells were present in both the supragranular and infragranular layers of RM, AL, and RPB with absent or weak connections in R (#196-232). This pattern is consistent throughout the auditory cortex until the R/RT border. At the transition into RT connections were mainly in the supragranular layers with some weak connections in the infragranular layers (#244-280). Label in RTM, RTL, and RPB was still present in the supragranular and infragranular layers but is more dense in the superficial layers in the medial and lateral belt areas (#244-280). In the most rostral section where the core area RT was no longer present and the medial and lateral belt areas have joined together, the majority of the labeled cells were present in RTL in both the supragranular and infragranular layers (#292). There was label also in the

Figure 59. Ipsilateral cortical connections of area RPB, case 3. Series of serial sections are arranged from caudal (upper left) to rostral (lower right), and continue onto the next page. CTB-red labeled cells (open triangles) are drawn onto each section, showing borders between areas identified by architectonic criteria. Black shading illustrates injection site. Dashed line indicates infragranular bias. *Inset*, schematic of marmoset auditory cortex showing location of CTB-red injection into RPB.
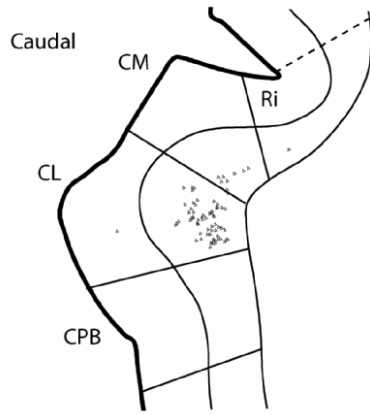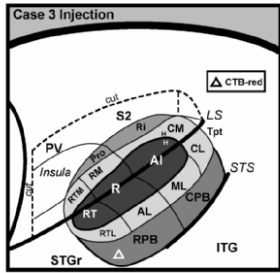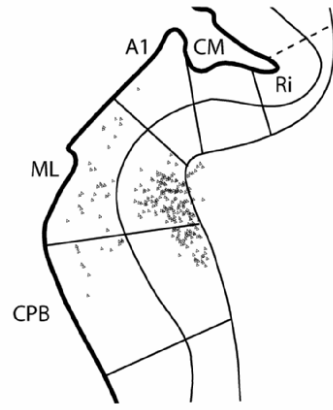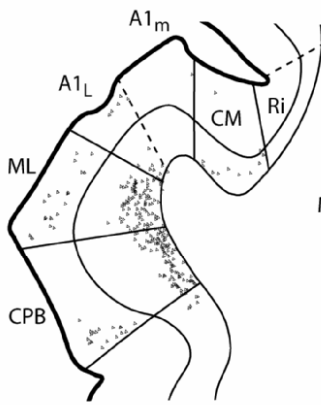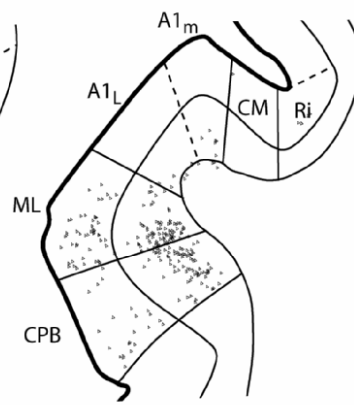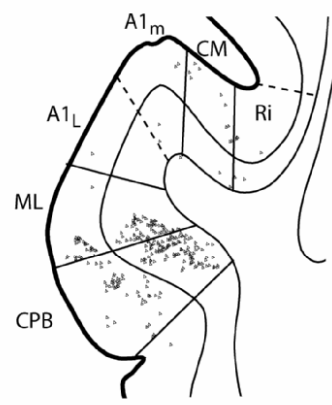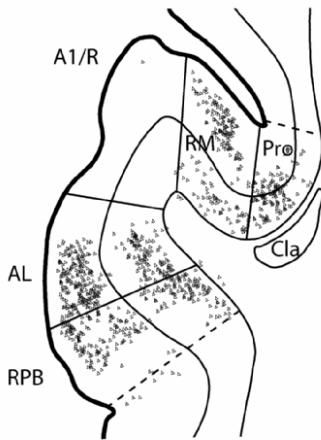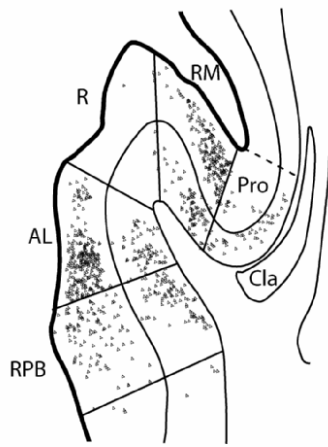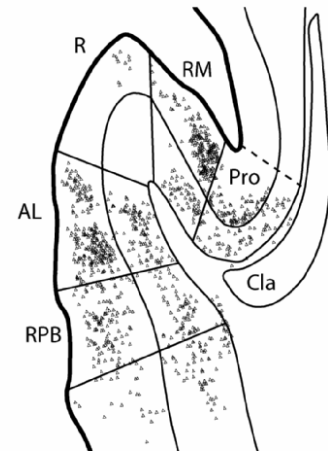
Case 3 ipsilateral
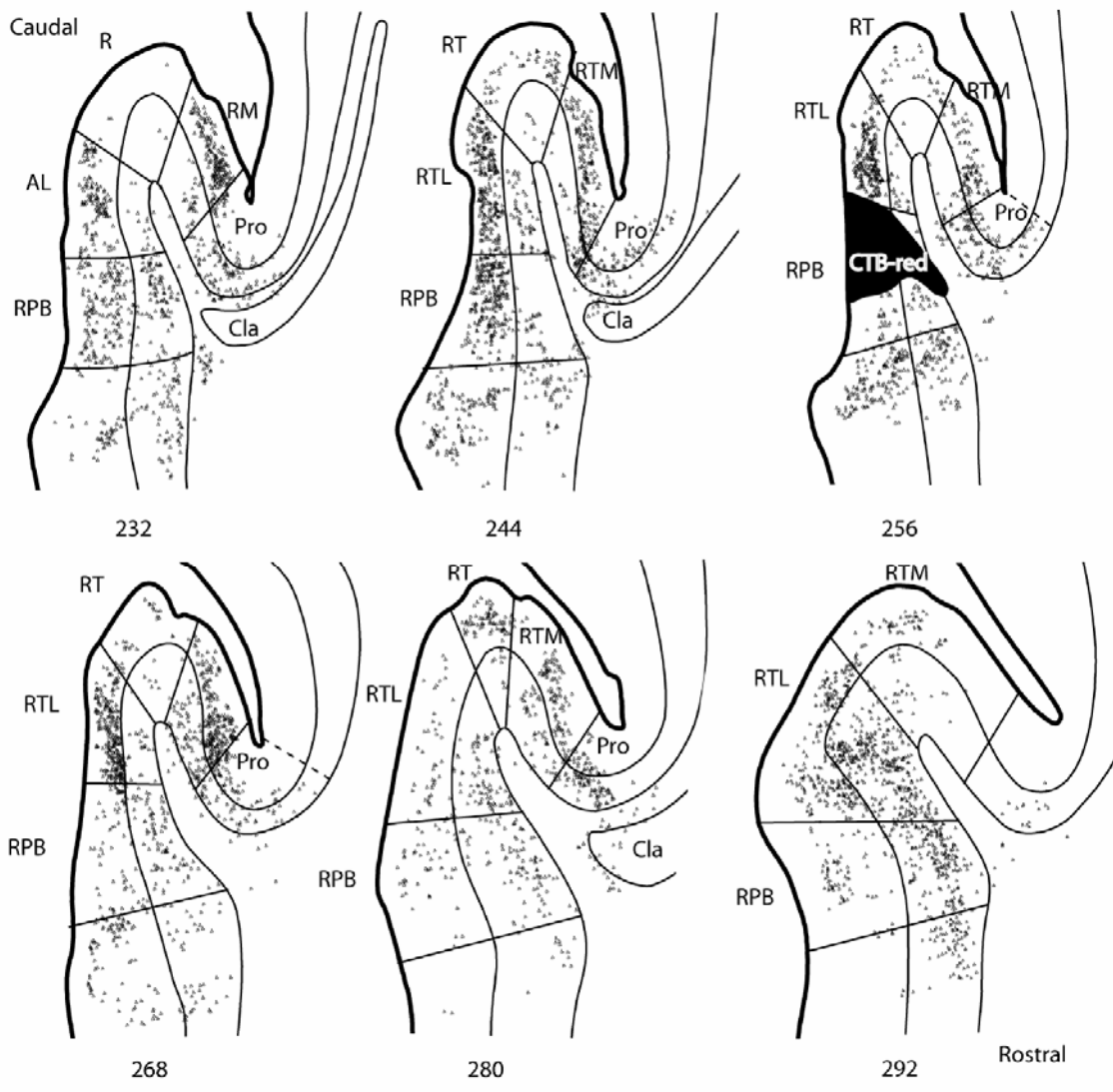
Case 3 ipsilateral, continued.

Figure 59 (continued)

supragranular and infragranular layers of RTM and RPB. Beginning at the transition of

the A1/R border where area Pro emerges medial to RM, label was present in the

supragranular and infragranular layers. This pattern persisted throughout the extent of

rostral auditory cortex, decreasing with the rostral border of the core, the end of area RT

(#196-292). Connections were present ventral to the parabelt in the STS, beginning with

the transition into rostral auditory cortex. Initially connections were weak (#196-208),

but strengthened rostrally in both the supragranular and infragranular layers (#220-268).

In the most rostral sections the connections were predominantly in the infragranular

layers (#280-292).

Contralateral connections of RPB

In case 3, label was present in layer III of each of the different rostral regions of

auditory cortex, but was concentrated in the parabelt and the lateral belt in the most

rostral sections (Fig. 60). Caudally label was present in RPB (#112) and some sparse

label was present in RM (#124). Closer to the R/RT border, label is stronger in RPB and

is also present in AL, RM, and Pro, with some weak label present in R (#136-148). Label

in RPB strengthens rostrally with the presence of RT, and label was also present in RTM

with sparse label in RTL and RT (#172). Moving rostrally this pattern continues with an

increase in labeled cells in RTL (#184-196). In the most rostral section the strongest

label was in RPB and RTL (#208). The densest concentration of label was rostrally in

RPB and RTL, which mirrored the injections site of the opposite hemisphere.
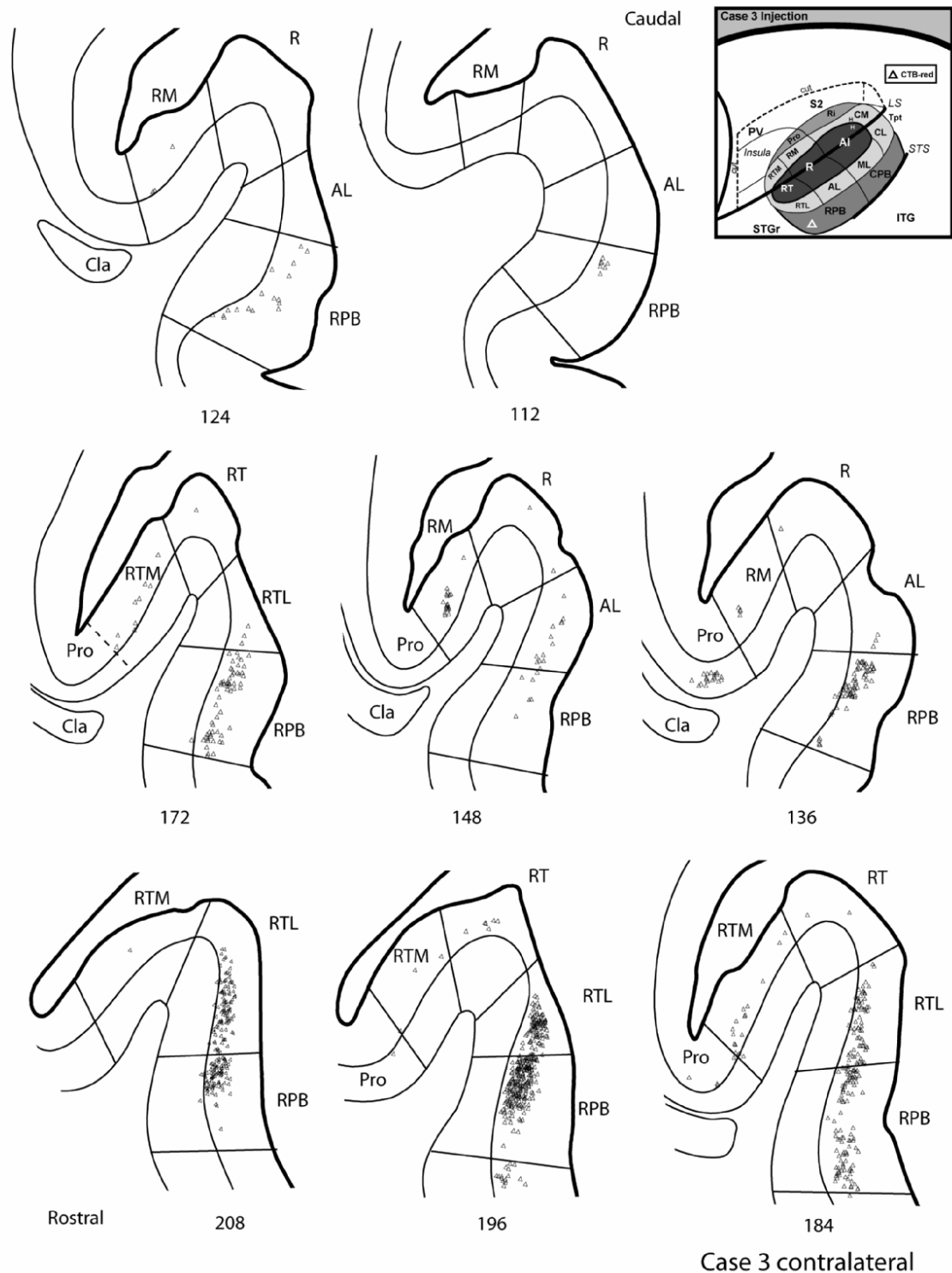
Figure 60. Interhemispheric cortical connections of area RPB, case 3. Series of serial sections are arranged from caudal (upper right) to rostral (lower left). CTB-red labeled cells (open triangles) are drawn onto each section, showing borders between areas identified by architectonic criteria. *Inset*, schematic of marmoset auditory cortex showing location of CTB-red injection in RPB in the contralateral hemisphere.

Summary of RPB connections

Outside the area of injection, the strongest connections were with the bordering

areas RTL, AL, and the STS (Fig. 61). There were additional connections with Pro, ML,
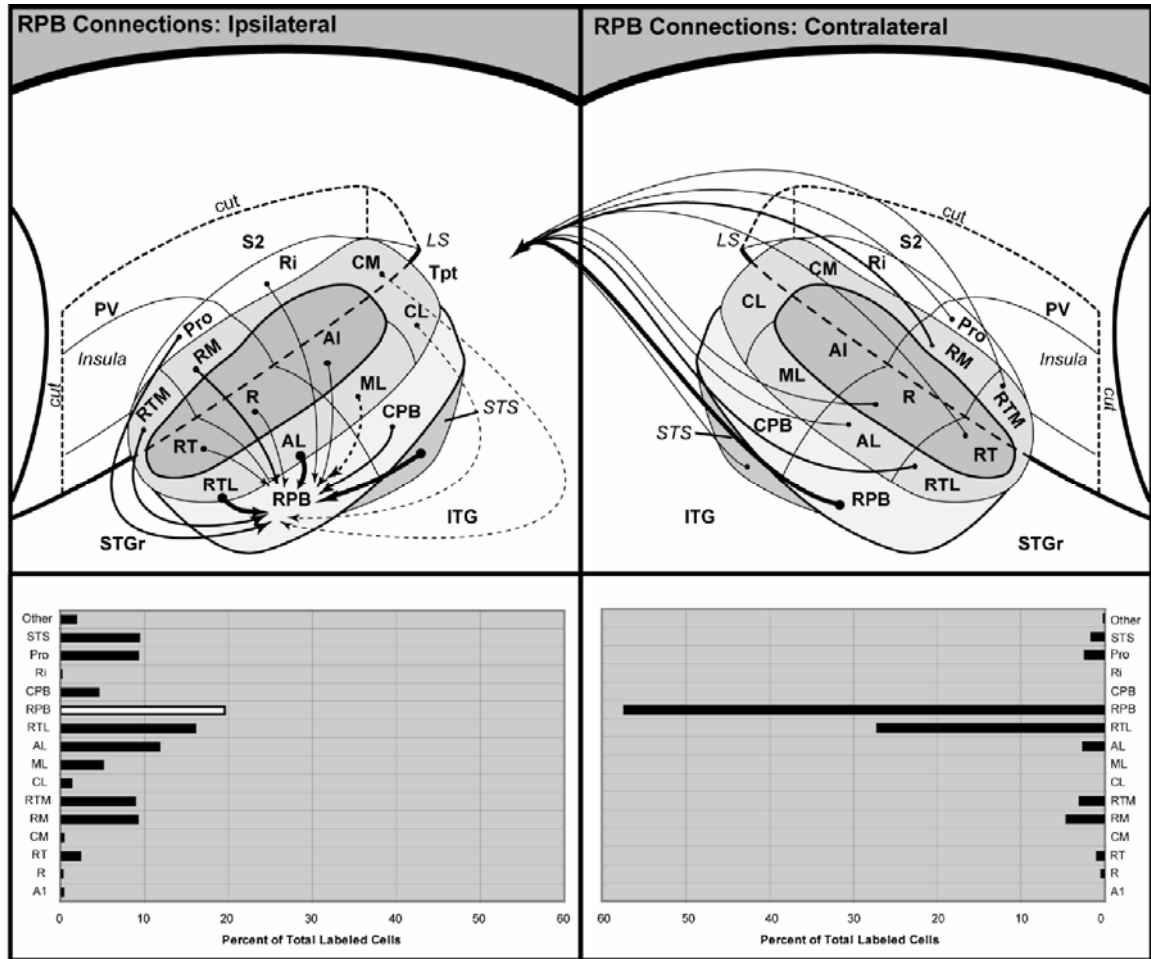
Figure 61.   Summary of ipsilateral (left) and interhemispheric (right) connections of
RPB. Top panels illustrate connections (arrows) of RPB on schematic diagram of
marmoset auditory cortex. Arrow size is proportional to connection strength, as indicated
in the histograms below each panel. Single arrows indicate unidirectional projections.
Bottom left, white bar indicates that cell counts for ipsilateral RPB may be inaccurate
(deflated) due to masking by the tracer injection.

RTM, RM and CPB as well as weak connection with the caudal areas Ri, CL, CM, and

the core areas A1 and R. Compared to the other core areas where label was sparse, there

was increased label in RT, predominantly in the supragranular layers. There was strong label in the medial belt once the transition was made into rostral auditory cortex, accompanied by strong label in the lateral belt and parabelt. The absence of label in R created a pronounced gap that was visible throughout R until the RT border. Percentage-wise the RPB had the most even distribution of label in the ipsilateral hemisphere of all of the lateral belt and parabelt injections. Label was strongest in RPB in the contralateral hemisphere, which is consistent with the area of injection. Strong connections were also present in RTL with moderate connections with RM. There were also weak connections with Pro, Al, RTM, and sparse label in RT and R.

Discussion

The current study examined the cortical connections of the lateral belt and parabelt regions and included injections into both rostral (RTL, RPB) and caudal areas (CM/CL, CPB). The results revealed rostrocaudal topography in both the lateral belt and the parabelt. Rostral areas were strongly connected with rostral areas and caudal injections revealed stronger connections with caudal areas. Overall the pattern of connections in marmosets was consistent with the working model and the flow of information in auditory cortex. Lateral belt connections were strongly connected with the core, belt, and parabelt regions, whereas the parabelt was strongly connected with the belt, but had only weak connections with the core. This is consistent with the idea of serial processing in which the core projects strongly to the belt but not the parabelt and the belt projects to the parabelt. The exception to this is the core area RT, which had significant connections with the RPB. These results are discussed in further detail below.

Regional distinctions between the lateral belt and the parabelt

There are two main differences in connection patterns that were identified between the lateral belt and parabelt regions. First, injections into the lateral belt revealed connections with the core, belt, and parabelt, while injections into the parabelt resulted in connections with the belt and parabelt regions, but only sparse label in the core areas A1 and R. The core area RT did have connections with RPB. Secondly, connections with the STS were mainly from the parabelt injections and were strongest with proximity to the rostrocaudal level of injection.

The lack of label throughout most of the core from the parabelt injections is consistent with the idea of serial processing in auditory cortex. The notion of serial processing comes in part from an influential study by Rauschecker et al., 1997, in which they recorded the responses of the core areas R and A1, as well as CM, before and after ablation to area A1. Following the ablation of A1 responses in R were unaffected; however the responses in CM to tonal stimuli were abolished, although there remained some responses to complex stimuli. These results suggest a dependence of CM on A1 for feedforward inputs and have supported the idea that the belt region surrounding the core is a second level of auditory cortex. The main anatomical support for serial processing comes from Hackett et al., 1998, where injections into the parabelt along the rostrocaudal extent revealed strong connections between the belt and parabelt but a lack of connections with the core. This is consistent with our findings in which injections into the parabelt revealed only sparse label in the core areas A1 and R from the CPB and RPB injections. It was only in the most rostral core area RT that this was not the case. In RT, there was significant labeling from the RPB injection but not from the CPB injections,

consistent with the rostrocaudal topography of the parabelt, but highlighting a unique feature of RT. Of the core areas, RT has been considered the least certain of this region. There is a clear tonotopic gradient present in RT with high frequencies sharing a border with R and low frequencies represented rostrally (Bendor and Wang, 2005, 2008; Petkov et al., 2006) and while it exhibits architectonic characteristics of the other two primary areas (koniocellular, dense expression of CO, Pv, and dense myelination), these features tend to be muted in comparison to the rest of the core. This is attributable perhaps to the overall rostrocaudal gradient of auditory cortex with more robust features caudally and decreasing in intensity rostrally (see chapter 2; de la Mothe et al 2006a; Galaburda and Pandya, 1983; Imig et al., 1977; Jones et al., 1995; Merzenich and Brugge, 1973; Morel and Kaas, 1992; Pandya and Sanides, 1973). This gradient was echoed physiologically in a study by Bendor and Wang (2008) in which neuron responses differed systematically between the core areas A1, R, and RT. For instance minimum response latencies were longer in the rostral core areas than A1, and the peak latency was longest in RT. It has been proposed in a previous chapter that CM may be a hybrid area that includes both belt like and core like features. Given that RT is the least certain area of the core region and that it exhibits the longest latencies as well as connections with the parabelt not present in other core areas, perhaps it is worth revisiting the possibility put forth by Morel and Kaas (1992) that RT is also an intermediate or hybrid area, one that combines core-like and belt-like features. Additional anatomical study of RT that includes tracer injections into the area, as well as a better understanding and comparison of response properties of surrounding belt areas, would help to clarify the position RT occupies in the primate model of auditory cortex.

Another main difference between the lateral belt and the parabelt regions were the connections with the STS. The parabelt had strong connections with the STS that included the dorsal bank and extended into the fundus, while the lateral belt had comparatively weaker connections with this region of cortex. The label was strongest in the STS around the rostrocaudal level of the injection and weakened with distance from the injection site; so that the CPB was strongly connected with caudal STS and rostral parabelt with the rostral STS. Additional studies have reported similar results in which injections into the parabelt revealed strong connections with the STS in macaques (Galaburda and Pandya, 1983; Hackett et al., 1998a; Morel et al., 1993). It appears that the core is strongly connected to the belt, the belt to the parabelt, and the parabelt to the STS, consistent with a serial flow of information that extends beyond auditory cortex.

Topographic connections of the rostral and caudal areas

The main connectional pattern revealed between caudal and rostral areas of the lateral belt and parabelt was rostrocaudal topography. The exception to this appeared to be area RM which was more strongly connected with CPB than the rostral portion of CM.

Label from the caudal belt injection was found in the core, medial and lateral belt, and parabelt areas predominantly in caudal auditory cortex.   While connections with RTL also followed this rostrocaudal topography, one difference was the lack of label in the parabelt in comparison to what was labeled from the caudal belt injection. RPB (5%) was connected to RTL, however, the strongest connections were with adjacent core (RT, R) and lateral belt areas (RTL, AL). In contrast the caudal belt injection had the strongest connections with CPB (32%) outside of the area of injection. It is unclear why there is such a discrepancy between the rostral and caudal belt areas with regards to the input

from the parabelt, however the injections were consistent with the rostrocaudal trend of auditory cortex (Cipolloni and Pandya, 1989; de la Mothe et al. 2006a; Fitzpatrick and Imig, 1980; Galaburda and Pandya, 1983; Hackett et al., 1998a; Jones et al. 1995; Leuthke et al. 1989; Morel and Kaas, 1992; Morel et al. 1993).

Injections into CPB labeled cells in the medial belt caudal to A1 and in RM, but label was sparse or absent in the portion of CM medial to A1 corresponding to a proposed area MM. Injections into caudal CM and rostral CM medial to A1 revealed distinct patterns of connections, as well as a shift in architecture from the more caudal portion of CM (see chapter 2; also de la Mothe et al., 2006a, b). Additionally there appears to be some evidence in imaging studies (Petkov et al., 2006) that identified a separate tonotopic map in the area that corresponds to MM. This needs to be followed up with physiological studies for verification and characterization of neuron responses.

The medial belt exhibited a different pattern of connections with RPB. At the transition into rostral from caudal auditory cortex there is a significant and sudden surge of label in the medial belt as well as the adjacent area Pro that continues throughout the rostral extent of auditory cortex. This increase in label medially along with the absence of label in R creates a clearly visible gap that continues rostrally until the border with RT. While the overall connections to the medial belt from the CPB injection were weaker in comparison to RPB, there were connections rostral to A1 with RM, consistent with what was reported by Hackett et al., 1998a. These RM connections with both rostral and caudal areas of the parabelt appear to be the exception to this trend of rostrocaudal topography. At the border between R and RT there was a shift in the pattern of label, from the previously described gap in R, to the presence of labeled cells in RT. While cells

are present in this most rostral core area, they are still weak compared to the dense label

of the surrounding belt areas. This is consistent with findings from Hackett et al., 1998a

where at least some of the rostral injections into the parabelt resulted in label rostral to R.

Consistency with the working model of primate auditory cortex

The overall organization of the marmoset auditory cortex revealed in this study is

consistent with the findings previously reported in this thesis (see chapter 2), as well as

the working model of primate auditory cortex. At least 2 areas, one caudal and one

rostral, were identified with unique patterns of connections in both the lateral belt and the

parabelt regions. Based on architectonic criteria established for the marmoset (see

chapter 2; de la Mothe et al., 2006a) these areas of injection were determined to be

CM/CL, RTL, CPB, and RPB. While previously the medial belt areas adjacent and

caudal to A1 have been combined as one area (CM), CPB injections revealed distinct

connection patterns between the two portions and support the notion that MM is a

separate area. This is consistent with distinct connection patterns revealed from medial

belt injections that accompany this study (see chapter 2; de la Mothe et al., 2006a, b).

A pattern of rostrocaudal topography was revealed from lateral belt and parabelt

regions that is consistent with what has been revealed in the medial belt and core regions

of the accompanying studies. The possible exception to this is RM, which is consistent

with the working model and it appears that in general, the topographic organization of the

marmoset auditory cortex is consistent with the working model.

Comparisons between regions provided additional support for the core, belt,

parabelt system in which the lateral belt was strongly connected with the belt, core, and

parabelt, but the parabelt had no significant connections with core areas A1 and R. Thus, information appears to flow from the core to the parabelt with the belt as an intermediate step. The core area RT appears to be the exception to this, as there are connections between RT and RPB. Since it is the least studied area of the core, additional studies of RT should be conducted in order to provide a better understanding of the position of this area in the working model.

<div align="center">Conclusions</div>

Overall, the results of the current study on the lateral belt and parabelt of marmoset auditory cortex are consistent with the working model of primate auditory cortex. Distinct patterns of connections were revealed between rostral and caudal areas of the lateral belt and parabelt regions. Both regions exhibited a rostrocaudal topography that is consistent with what has been reported in the medial belt and core regions of the marmoset (see chapter 2). Area RM appears to be the exception to this rostrocaudal trend in that it has connections with both the rostral and caudal portions of the parabelt. The core areas have strong connections with adjacent lateral belt areas; however, areas A1 and R did not have significant connections with the parabelt. RT appears to be the only area of the core with significant connections to the parabelt, specifically RPB. The model should be revised to reflect these findings.

CHAPTER V

THALAMIC CONNECTIONS OF AUDITORY CORTEX IN MARMOSET
MONKEYS: LATERAL BELT AND PARABELT REGIONS

Introduction

Our current working model of auditory cortex is constructed from a number of

studies of both New and Old World monkeys (Kaas & Hackett, 1998; Kaas et al., 1999;

2000; Hackett, 2002) (Fig. 62). A main component of this model is that auditory cortex

is defined as the region of cortex that receives preferential input from the MGC. Based

on this definition, three regions of the superior temporal cortex are identified as part of

auditory cortex in primates: core, belt, and parabelt. The core region, receives input

mainly from MGv and consists of three areas (A1, R, RT). It is surrounded both medially

and laterally by a belt region of 7-8 areas (CM, RM, RTM, CL, ML, AL, RTL) that

receives input preferentially from MGd (Fig. 62). The parabelt region, located lateral to

the belt, is divided into two areas (CPB, RPB) and also receives input from MGd (Fig.

62). Additional areas that are responsive to auditory stimuli (temporal, prefrontal, and

posterior parietal cortex), but that do not have principal inputs from the MGC are referred

to as auditory-related fields.

Information in auditory cortex is thought to be processed both serially and in

parallel (Hackett and Kaas, 2004; Hackett et al. 1998a,b; Kaas and Hackett, 1998; Kaas et

al. 1999; Rauschecker, 1998; Rauschecker et al. 1997). Serial organization is based in

part on connectional studies, where the core projects to the belt, but not the parabelt;
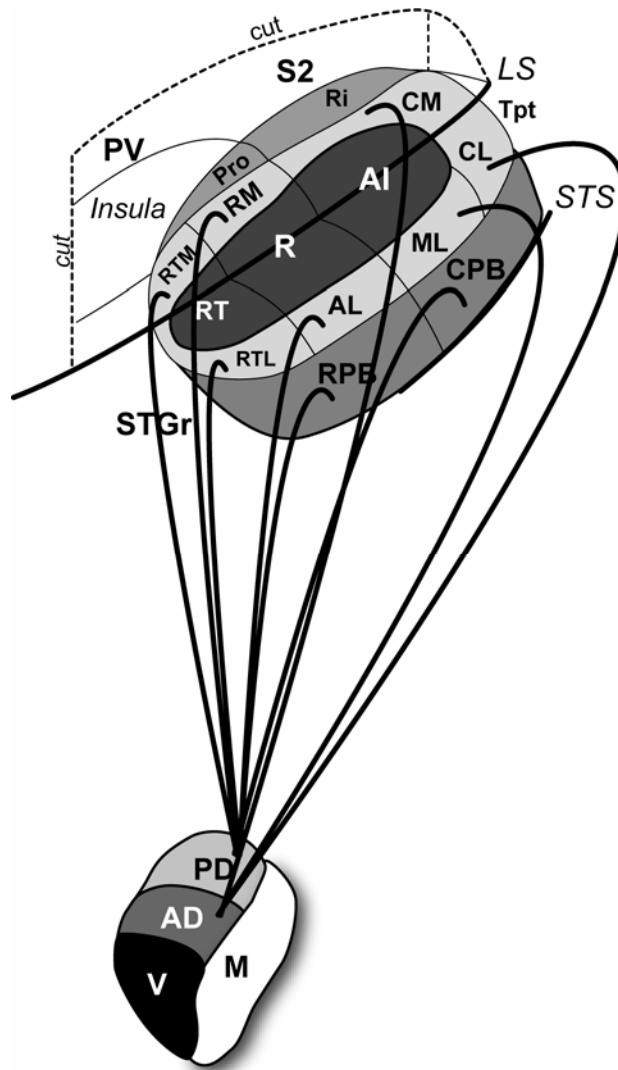
Figure 62. Schematic model of the primate auditory cortex illustrated on a marmoset brain with prinicpal inputs from the two divisions of MGd to belt and parabelt regions. The lateral sulcus (LS) of the left hemisphere was graphically opened (cut) to reveal the locations of auditory cortical areas otherwise hidden. The three regions of auditory cortex are identified with varying degrees of shading: core (dark shading), belt (light shading), parabelt (medium shading). The four divisions of the MGC are identified with varying degrees of shading: MGv (dark shading), Mgad (medium shading), MGpd (light shading), MGm (no shading). The principal inputs to the core region from MGv are not shown.

making the parabelt reliant on the belt for its cortical activation (Hackett et al., 1998a;

Morel et al., 1993; Morel and Kaas, 1992). Thus, the belt and parabelt regions exhibit

distinct cortical connection patterns in that the belt is strongly connected with both the core and the parabelt,while the parabelt is strongly connected with the belt. This hierarchy is also reflected in the thalamic conenctions to these various regions.

Primary areas receive their main thalamic input from MGv (Burton and Jones, 1976; Fitzpatrick and Imig, 1978; Luethke et al., 1989; Morel and Kaas, 1992; Morel et al., 1993; Pandya et al., 1994; Molinari et al., 1995), while both the belt and parabelt lack these strong MGv projections and receive their main inputs from MGd (Burton and Jones, 1976; Hackett et al., 1998b, Hackett et al., 2007; Molinari et al., 1995; Morel and Kass, 1992) (Fig. 62). Even though both regions receive principal input from MGd, one distinguishing characteristic between the thalamic inputs of the secondary belt region and the parabelt is the strong input the parabelt receives from the medial pulvinar (PM). PM differs from other multisensiry nuclei that project to auditory cortex (Sg, Lim, Po) in that it has connections with higher order areas such as prefrontal and limbic cortex (Romanski et al., 1997). This strong PM projection to the parabelt but not the belt is consistent with the notion that the parabelt is a later stage in hierarchichal processing in auditory cortex.

Injections into lateral belt and parabelt regions revealed topographic connection patterns with cortical areas (Hackett et al., 1998a, Morel and Kass, 1992; Romanski et al., 1999) as well as with MGd (Burton and Jones, 1976; Hackett et al., 1998b; Molinari et al., 1995; Morel and Kaas, 1992; Pandya et al., 1994). The dorsal division of the MGC has been subdivided into anterior and dorsal divisions (Burton and Jones, 1976, de la Mothe et al., 2006b; Hashikawa et al., 1995; Hackett et al., 2007a; Jones et al., 1995; Jones and Burton 1976; Molinari et al., 1995), and there is evidence of topography within MGd with projections from MGad to the caudal lateral belt and from MGpd to the rostral

lateral belt in macaque (Molinari et al., 1995). Hackett et al., 2007 also reported preferential connections of the caudal belt areas (CM and CL) with MGad. This is consistent with results from the accompanying medial belt studies where MGad was preferentially connected with CM and MGpd with RM (see chapter 2; also de la Mothe et al., 2006b). Based on these results it is reasonable to predict that rostral and caudal areas of the lateral belt and parabelt in the marmoset would reveal a similar pattern of input.

The goal of the present study was to refine our understanding of the working model of primate auditory cortex by examining the thalamocortical connections of the lateral belt (areas RTL and CM/CL) and comparing them with the laterally adjacent parabelt (areas RPB and CPB). By comparing both within regions rostral and caudally (RTL and CM/CL; RPB and CPB) as well as between auditory cortical regions (lateral belt and parabelt), a more comprehensive understanding of auditory cortical input may be established. Specifically, the following predictions of the model were tested: (1) the lateral belt and the parabelt regions have distinct patterns of thalamic input reflective of their hierarchichal order that include a lack of MGv projections and differnces in the projections from PM; and (2) the lateral belt and parabelt regions have topographically distinct patterns of thalamic input.

<div align="center">Materials and Methods</div>

The experiments proposed in this report were conducted in accordance with the Vanderbilt University Animal Care and Use Committee Guidelines and the Animal Welfare Act under a protocol approved by the Vanderbilt University Institutional Animal Care and Use Committee. Seven adult marmosets (*Callithrix jacchus jacchus*) served as

animal subjects in the present study. The experimental history of each animal is included

in Table 4.

Table 4. Experimental history of animal subjects and relevant injections. Areas of tracer injections (CL, caudolateral belt; ML, mediolateral belt; AL, anterolateral belt; CPB, caudal parabelt; RPB, rostral parabelt). Neuroanatomical tracers (CTB-red, cholera toxin subunit B 594; FR, fluororuby; DY; diamidino yellow), aqueous concentration and volume injected are listed for each tracer.

Case #	Case	Sex	Areas Injected	Tracer	%	Volume (µl)
1	(01-89)	M	CL/CM	FR	10	0.3
			CPB	DY	10	0.3
2	(03-59)	M	CPB	CTB-red	1	0.35
3	(04-40)	M	RPB	CTB-red	1	0.35
4	(04-51)	M	AL	FR	10	0.3

General surgical procedures

Microinjections of anatomical tracers were made into subdivisions of auditory

cortex in marmoset monkeys under aseptic conditions. Marmosets were premedicated

with cefazolin (25mg/kg), dexamethozone (2mg/kg), cimetidine HCl (5mg/kg), and

robinul (0.015mg/kg). Anesthesia was induced by inhalation of 5% isoflurane or by

intramuscular injection of ketamine hydrochloride (10 mg/kg), and the animals were

intubated, then maintained by intravenous administration of ketamine hydrochloride (10

mg/kg) supplemented by intramuscular injections of xylazine (0.4 mg/kg) or maintained

with (2-3%) isoflurane and Nitrous Oxide with Oxygen (50/50) 1 liter/minute. Body

temperature was maintained at 37°C with a water circulating heating pad. Vital signs

(heart rate, expiratory CO_2, and O_2 saturation) were continuously monitored throughout

the surgery and were used to adjust the levels of anesthesia.

A stereotaxic instrument (David Kopf Instruments, Tujunga, CA) was used to stabilize the head of the monkey. A midline incision was made exposing the skull, followed by the retraction of the left temporal muscle. A craniotomy was performed exposing the superior temporal gyrus and the lateral sulcus, followed by the cutting and retraction of the dura. Warm silicone was applied periodically to the brain to prevent dessication of the cortex during photography and injections of tracers. Photographs were then taken to facilitate later reconstruction of the injection sites based on blood vessels and sulci. Following the injections the exposed area of the brain was covered with softened gelfilm, the craniotomy was closed with dental acrylic, and the overlying temporal muscle and skin sutured back into place. Antibiotic gel was applied along the suture line. After the surgery, the endotracheal tube was removed and vital signs were monitored during the recovery period until vitals became stable and the animal was returned to its cage where it was monitored until recovery was complete. Daily injections of penicillin G (10 000 units i. m.) were given for 5 to 7 days after surgery, along with Banamine (1 mg/kg) as needed for analgesia.

Injections and perfusion

Injections of tracers were made into target areas using 1-2µL syringes, with a pulled glass pipette tip, attached to a hydraulic microdrive. Injections were made into the lateral belt and parabelt regions by using landmarks and blood vessels, on the lateral surface of the superior temporal gyrus (STG), to locate auditory cortex. The injections were made directly into the auditory areas. In all cases the injections made were manual pressure injections of various amounts (Table 4) after which the syringe remained for

216

approximately 10 minutes under continuous observation to maximize uptake and minimize leakage. The tracers used were cholera toxin-B 594 (CTB-red); fluororuby (FR); and diamidino yellow (DY). Due to the various levels of sensitivity of the tracers the amounts and solution concentrations were varied accordingly as shown in the table (typically, 0.01-0.05 µL and 3% fluorescents, 1% for CTB and 10% for BDA).

At the end of the survival period, a mapping session occurred in which electrophysiological data was recorded using non-sterile surgical procedures (see auditory stimulation). Upon completion of the recording session a lethal dose of pentobarbital was administered. Just before cardiac arrest the animal was perfused through the heart with warm saline followed by cold 4% paraformaldehyde dissolved in 0.1 M phosphate buffer. Immediately following the perfusion the brains were removed and photographed, the two hemispheres and the brainstem were separated and placed in 30% sucrose for several days and then blocked.

Histology and data analysis

The thalamus was cut perpendicular to long axis of the brainstem in the caudal to rostral direction at 40µm (see Fig. 32, chapter 3). Depending on the case, series of sections were processed for: (i) fluorescent microscopy; (ii) BDA; (iii) CTB (iv) myelin (Gallyas, 1979); (v) acetylcholinesterase (Geneser-Jensen & Blackstad, 1971); (vi) stained for Nissl substance with thionin (vii) cytochrome oxidase (CO) (Wong-Riley, 1979); or (viii) parvalbumin immunohistochemistry (PV).

Cells labeled with fluorescent tracers were all plotted on an X-Y plotter (Neurolucida) coupled to a Leitz microscope under ultraviolet illumination. Photographs

and drawings of each section were made, noting architectonic boundaries, the location of blood vessels and the distribution of labeled cells. Reconstruction of the architecture was based on previously identified criteria in marmosets (see chapter 3; de la Mothe et al., 2006b). A composite drawing was made from adjacent sections processed for label, acetylcholinesterase, myelin, CO and Nissl by aligning common architectonic borders and blood vessels (Fig. 4). Reconstructions of the composite images were achieved using Canvas 7.0 software (Deneba software, Miami, FL, USA). The final composites were analyzed to reveal the individual connection patterns and the connection patterns of injections at similar or dissimilar locations. Cell counts were performed on all auditory areas and converted to percentages in order to better compare the general connection patterns between tracers due to variability in tracer sensitivity. While sensitivity of the tracers did vary, regardless of the actual number of cells labeled, the general patterns revealed by injections of specific areas were maintained regardless of the tracer used.

Photographs were made using a Nikon DXM1200F digital camera mounted on a Nikon E800S microscope and adjusted for brightness, contrast, text added, and cropped using Adobe Photoshop v6.0 software (Mountain View, CA, USA). Other than the adjustments mentioned the images were not altered in any way.

<center>Results</center>

Thalamic connections of CM/CL

In case 1 (Fig. 63), an injection of FR was made into the caudal belt area just posterior to A1 that involved both CM and CL. In the most caudal sections there was sparse retrograde label in the posterodorsal, anterodorsal, and ventral divisions of the

<center>218</center>

Figure 63. Thalamic connections of CM/CL and CPB, case 1. Series of reconstructed serial sections are arranged from rostral (upper left) to caudal (lower right). FR labeled cells (open triangles) and DY labeled cells (filled circles) are drawn onto each section, showing borders between areas identified by architectonic criteria. *Inset*, schematic of marmoset auditory cortex showing location of FR injection in CM/CL and DY injections into caudal CPB.

219

MGC (#208-214). In general, the number of labeled cells increased rostrally with the strongest projections from MGad and MGm (#220-232). In the most rostral sections as the size of the MGC decreased the majority of label was focused in MGad (#238-244). Only sparse label was present throughout MGv. Connections were also present with MGpd, but were weaker relative to MGad. Overall the connections were focused more in the anterior portion of the MGC with the strongest connections from MGad and MGm. There were some sparse labeled cells in Sg as well as rostrally with VP and PI.

Thalamic connections of RTL

In case 4 (Fig. 64), a FR injection was made into the rostral belt area RTL. In the most caudal section there was strong label in MGpd, MGm, as well as connections with MGv (possibly due to encroachment of the RT border) (#340). These connections decreased rostrally, though remained present in these subdivisions (#346-364) and included sparse cells in Sg. Caudally there were weak connection with BIC and PPN (#340-352). In the most rostral sections sparse label was present in MGad, MGv, MGm, Po, Lim, PM, and CM (#370-384). The majority of the label from this injection was concentrated in the posterior portion of the MGC. Label in MGm was concentrated in the ventral third of the division.

Summary of thalamic connections of the lateral belt

Injections into both caudal and rostral portions of the lateral belt revealed connections that were confined mainly to the MGC of the thalamus (Fig. 65). Both areas had strong connections with MGm but differed in the relative location of these

Figure 64. Thalamic connections of RTL, case 4. Series of reconstructed serial sections are arranged from rostral (upper left) to caudal (lower right). FR labeled cells (open triangles) are drawn onto each section, showing borders between areas identified by architectonic criteria. *Inset*, schematic of marmoset auditory cortex showing location of FR injection in rostral RTL.

Rostral

Case 4 Injection

ΔFR

S2
PV
Insula
RTM
RT
RTL
Pro
RM
R
AL
RPB
Ri
CM
H
AI
ML
CPB
LS
Tpt
CL
STS
ITG
STGr

PM
MD
PA
CM
VPL

384

Po
Lim
Plm
AD
VPL
V
M
VPM
VPl
PPN
ZI

376

Plm
BrSC
Lim
Po
Pretectal
AD
VP
V
M
PPN
LGN
VPl

370

Plm
Lim
Sg
PD
AD
M
V

364

BrSC
Plm
Lim
Plc
Sg
PD
AD
M
V
PPN

358

PD
AD
M
V
PPN

352

PD
M
V

346

PD
M
V
BIC
Folded tissue

340

Caudal

222
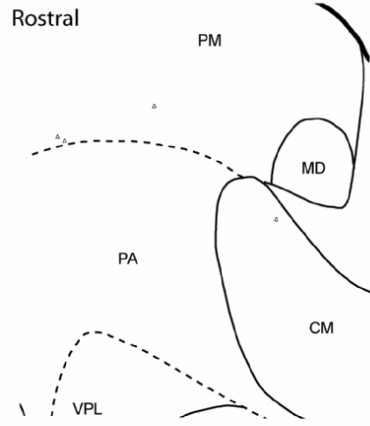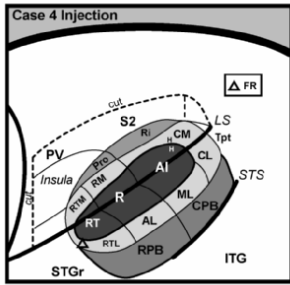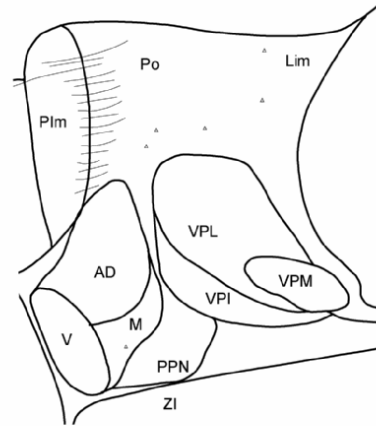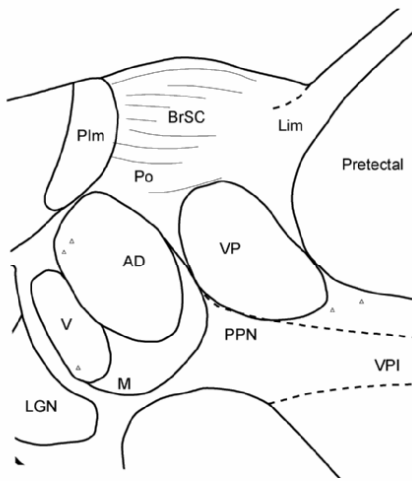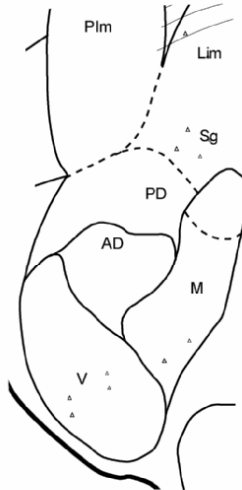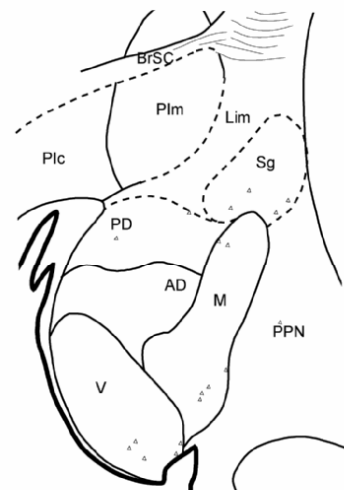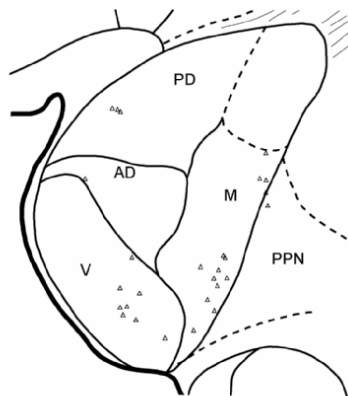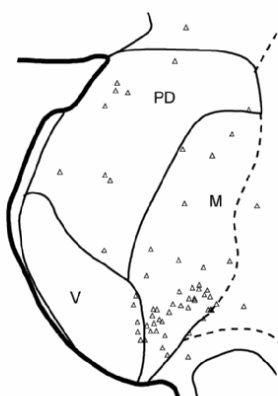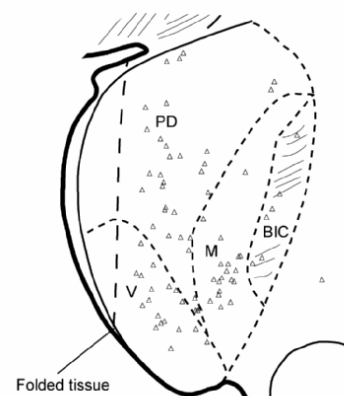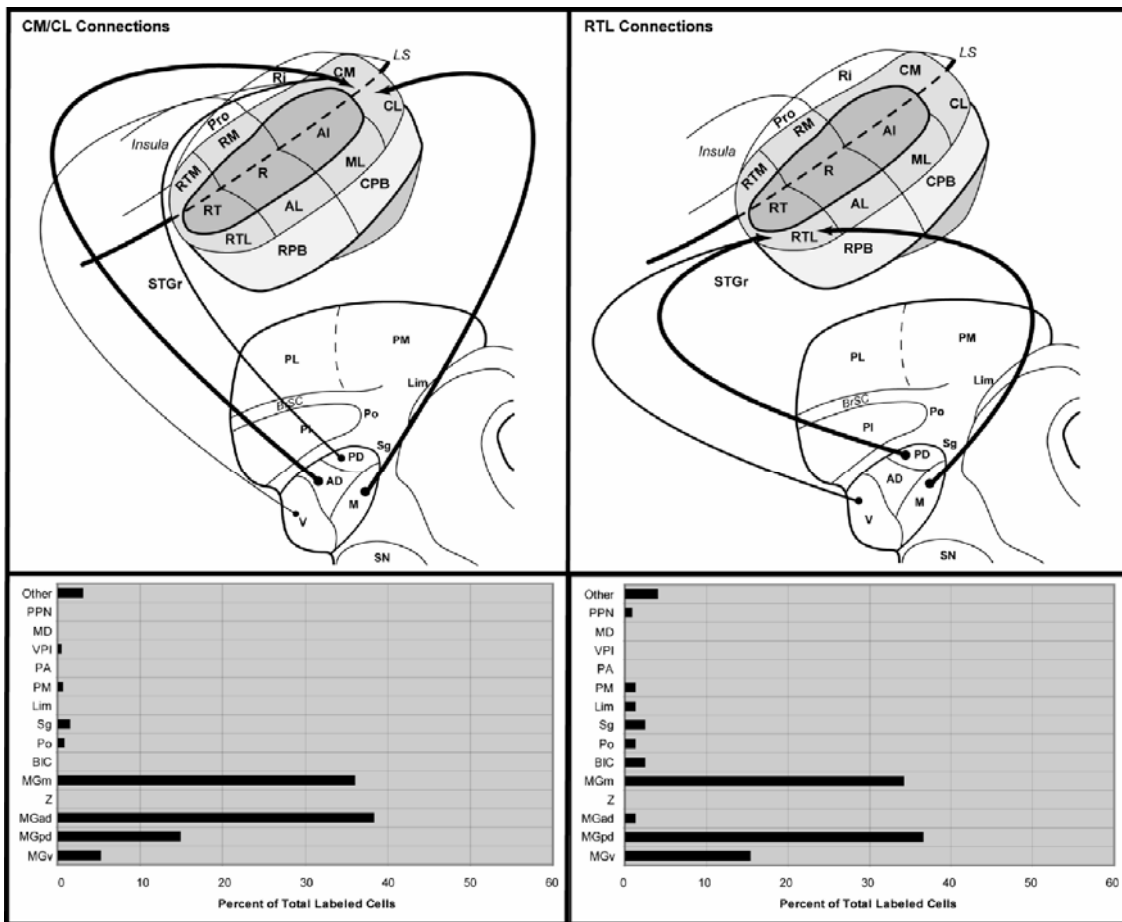
Figure 65. Summary of thalamic connections of CM/CL and RTL. Top panels illustrate subcortical connections (arrows) of CM/CL and RTL on schematic diagrams of marmoset auditory cortex and thalamus. Arrow and line size is proportional to connection strength, as indicated in the histograms below each panel. Lines were not drawn for connections representing less than 5% of total.

projections within the division. Label from the caudal belt injection was concentrated in

the dorsal half of MGm while labeled cells from the injection into RTL favored the

ventral portion. An additional difference between caudal and rostral lateral belt

injections was with regard to connections of MGad and MGpd. The CM/CL injection

revealed a preferential connection with MGad while RTL was preferentially connected

with MGpd.

Thalamic connections of CPB

In case 1 (Fig. 63), the DY injection was made into the caudal portion of CPB. In the most caudal sections, label was confined predominantly to the dorsal portion of MGm, which coincided with an AChE dense region, with sparse label also present in MGpd and Sg (#208-214). Moving rostrally, this AChE dense region of MGm was displaced by the Sg which coincides with label shifted to mainly Sg and sparse label remaining in MGm and MGpd (#220-226). Label continued to shift dorsally in the section to occupy Po, Lim, and PM (#232-228), and in the most rostral sections label was present exclusively in PM (#244).

In case 2 (Fig. 66), an injection of CTB-red was made into the rostral portion of CPB close to the A1/R border. There were strong connections caudally with MGpd and MGm as well as weak connections with PPN (#117-105). Labeled cells in MGm and MGpd were confined to the dorsal portions of those divisions, similar to the pattern of MGm in case 1, described above. More rostrally, labeled cells transitioned from MGC to mainly SG (#99-93) and this dorsal shift continued with labeled cells occupying Po and Lim in the more anterior sections (#87-75). In the most rostral section, strong connections were exclusively with PM and labeled cells were focused medially along the MD border and towards the dorsal edge of the section (#69-51). While the majority of the projections from MGC favored the more posterior portion, overall the strongest connections were anterior with the multisensory nuclei Sg, Po, Lim, and PM.

Thalamic connections of RPB

In case 3 (Fig. 67), an injection of FR was made into the rostral portion of RPB.

224
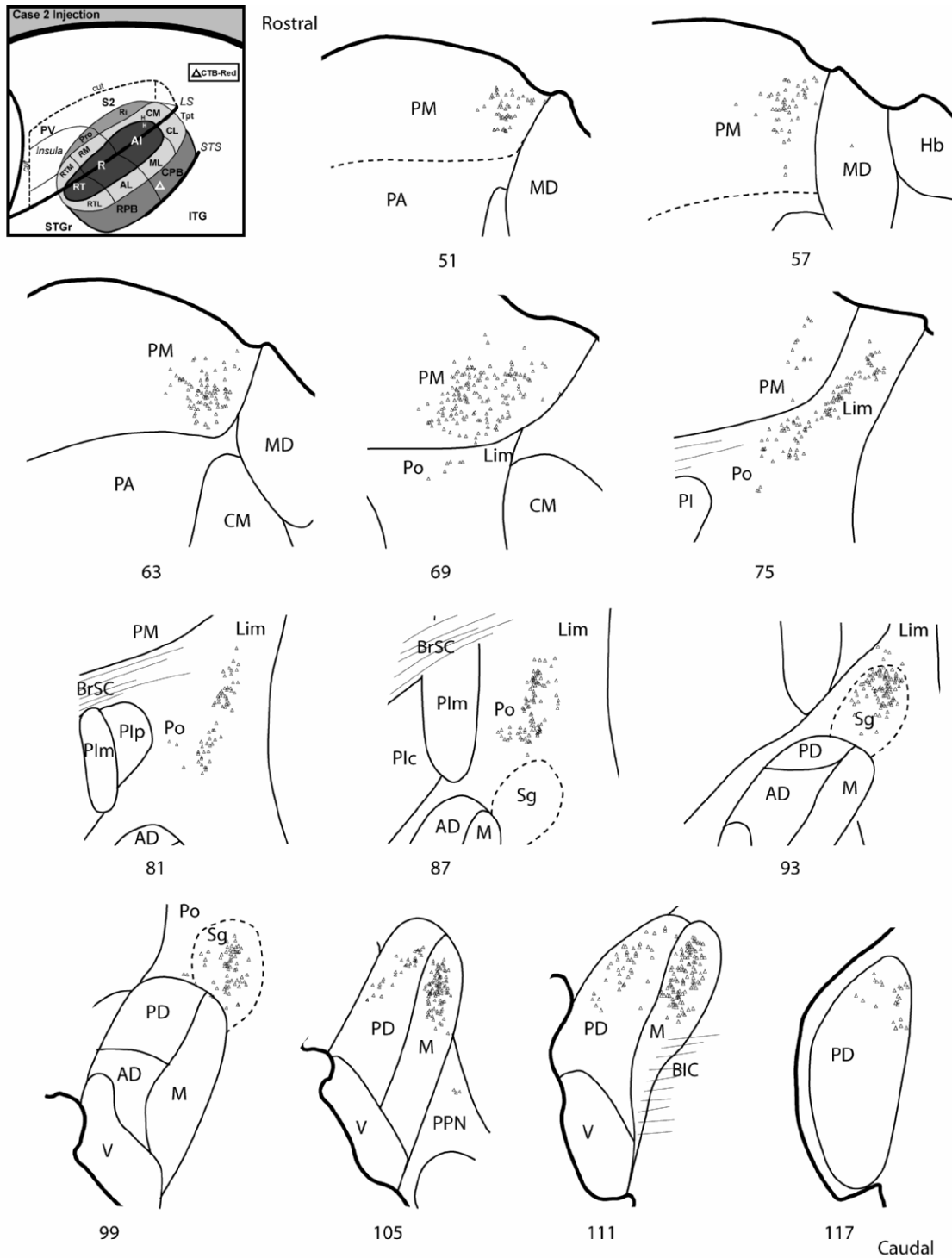
Figure 66. Thalamic connections of CPB, case 2. Series of reconstructed serial sections are arranged from rostral (upper left) to caudal (lower right). CTB-red labeled cells (open triangles) are drawn onto each section, showing borders between areas identified by architectonic criteria. *Inset*, schematic of marmoset auditory cortex showing location of CTB-red injection in rostral CPB.

225
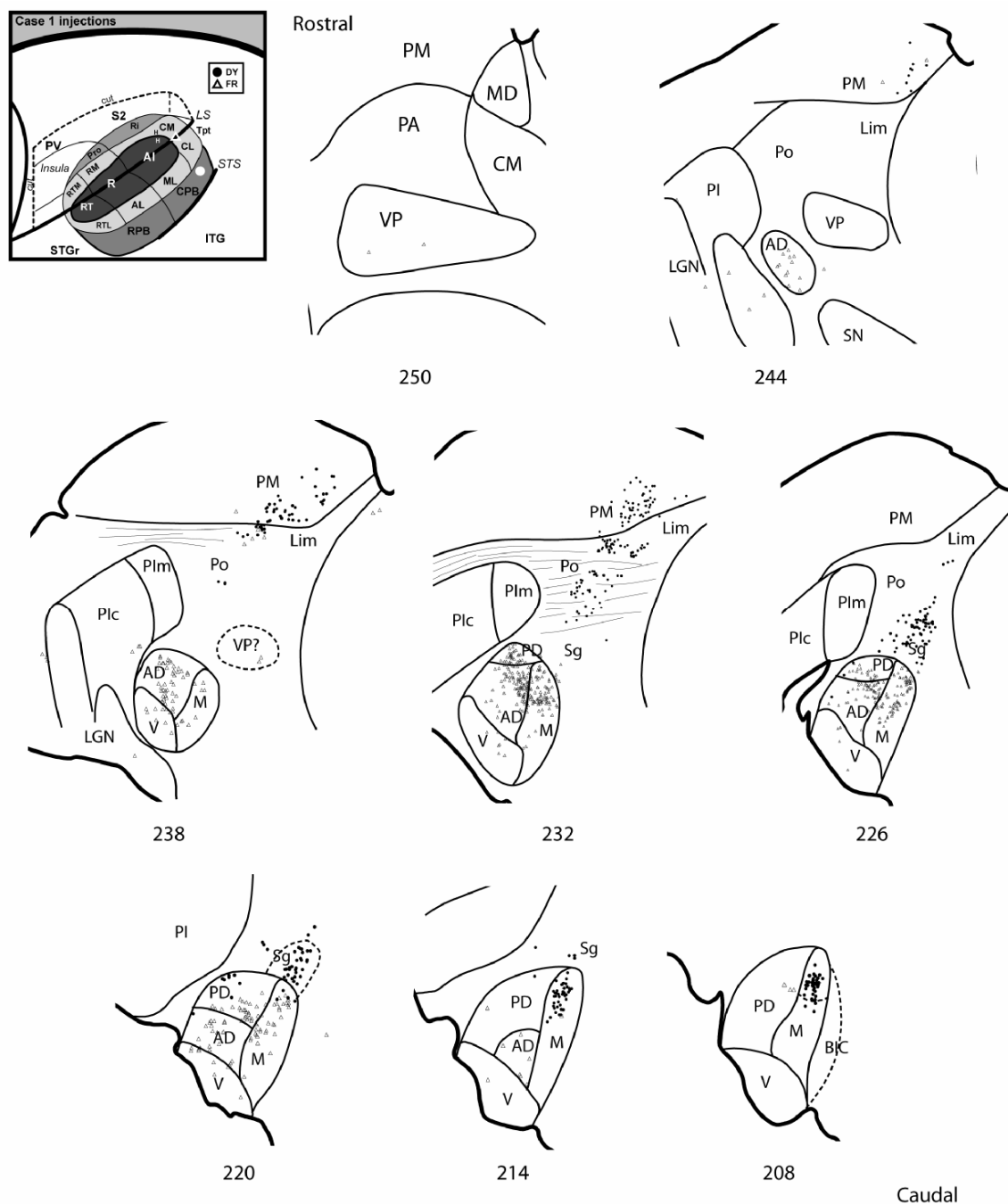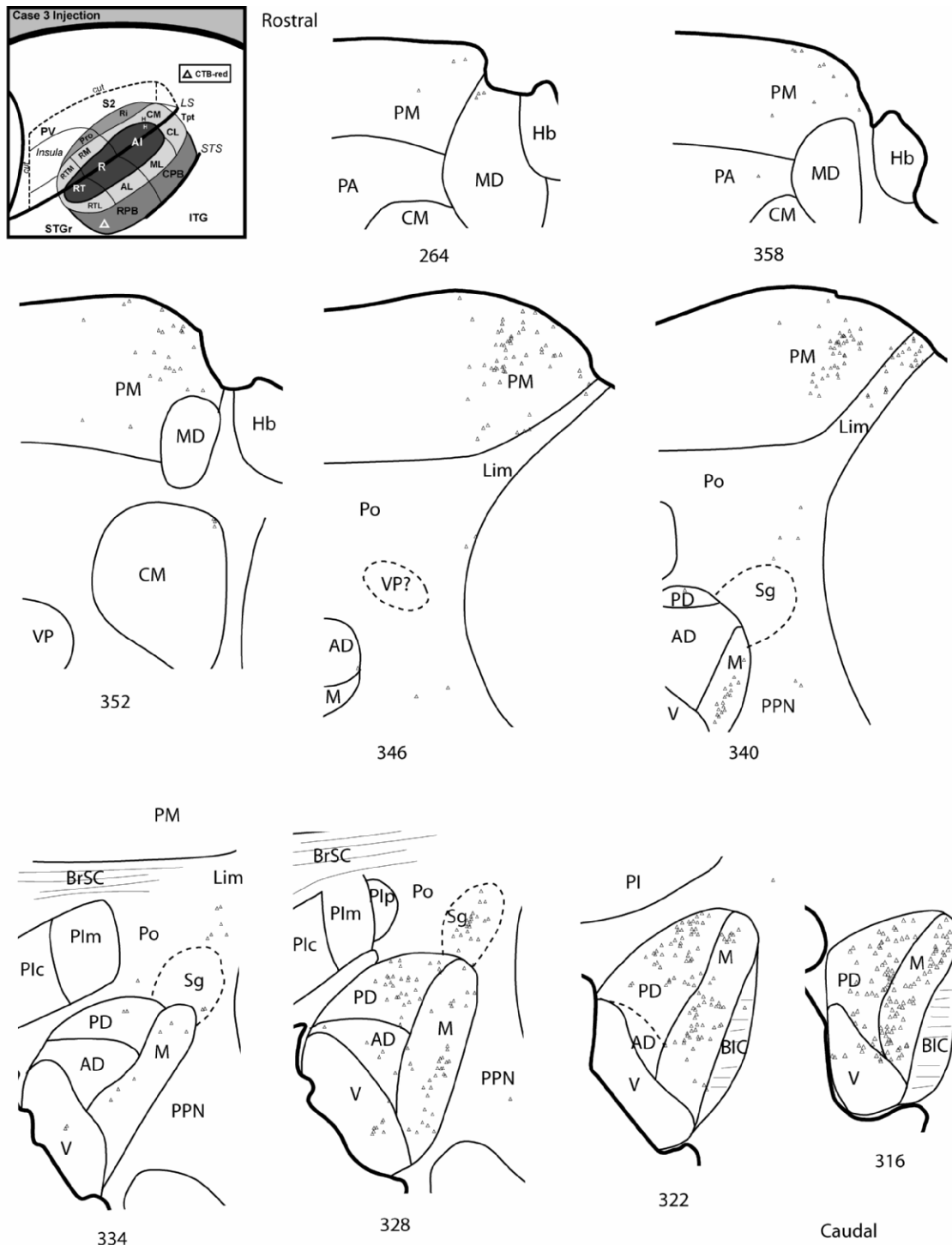
Figure 67. Thalamic connections of RPB, case 3. Series of reconstructed serial sections are arranged from rostral (upper left) to caudal (lower right). CTB-red labeled cells (open triangles) are drawn onto each section, showing borders between areas identified by architectonic criteria. *Inset*, schematic of marmoset auditory cortex showing location of CTB-red injection in RPB.

226

In the most caudal sections, label is distributed predominantly throughout the divisions of

MGm and MGpd (#316-322). Label remained in these divisions and expanded to include

Sg and some weaker connections with MGad and MGv (#328). There is a decrease in

overall labeling in the next rostral section which includes a few cells in Lim, Sg, MGpd,

MGm, and MGv (#334). Continuing rostrally, connections strengthened and were

present mainly in MGm, Lim, and PM with sparse label in Po and PPN (#340). In the

rostral sections, while there was sparse label in PPN, Lim, MD, and CM, the majority of

the label was confined to the medial portion of PM (#346-364).

Summary of thalamic connections of the parabelt

Injections into the parabelt revealed strong connections with MGm from both

rostral and caudal areas however caudal injections tended to have projections confined to

the dorsal portion of MGm (coinciding with a dense AChE region), while the rostral

injection revealed label distributed throughout MGm (Fig. 68). Differences were also

apparent from connections with MGpd which was strongly connected to RPB and

moderately connected to CPB. Connections between MGpd and the parabelt decreased

from rostral to caudal overall with weaker projections from caudal CPB relative to rostral

CPB. Additionally there were weak connections from MGv to RPB. Outside of the

MGC there were strong connections to CPB from Sg, Lim, Po, and PM with the inputs

from PM accounting for the largest percentage (35%). RPB also had strong connections

with PM and was moderately connected with Sg and Lim. It appears that rostral and

caudal injections into the parabelt involve mainly the same nuclei. The distribution of

labeled cells in these nuclei shift from a larger input from MGpd more rostrally to

227
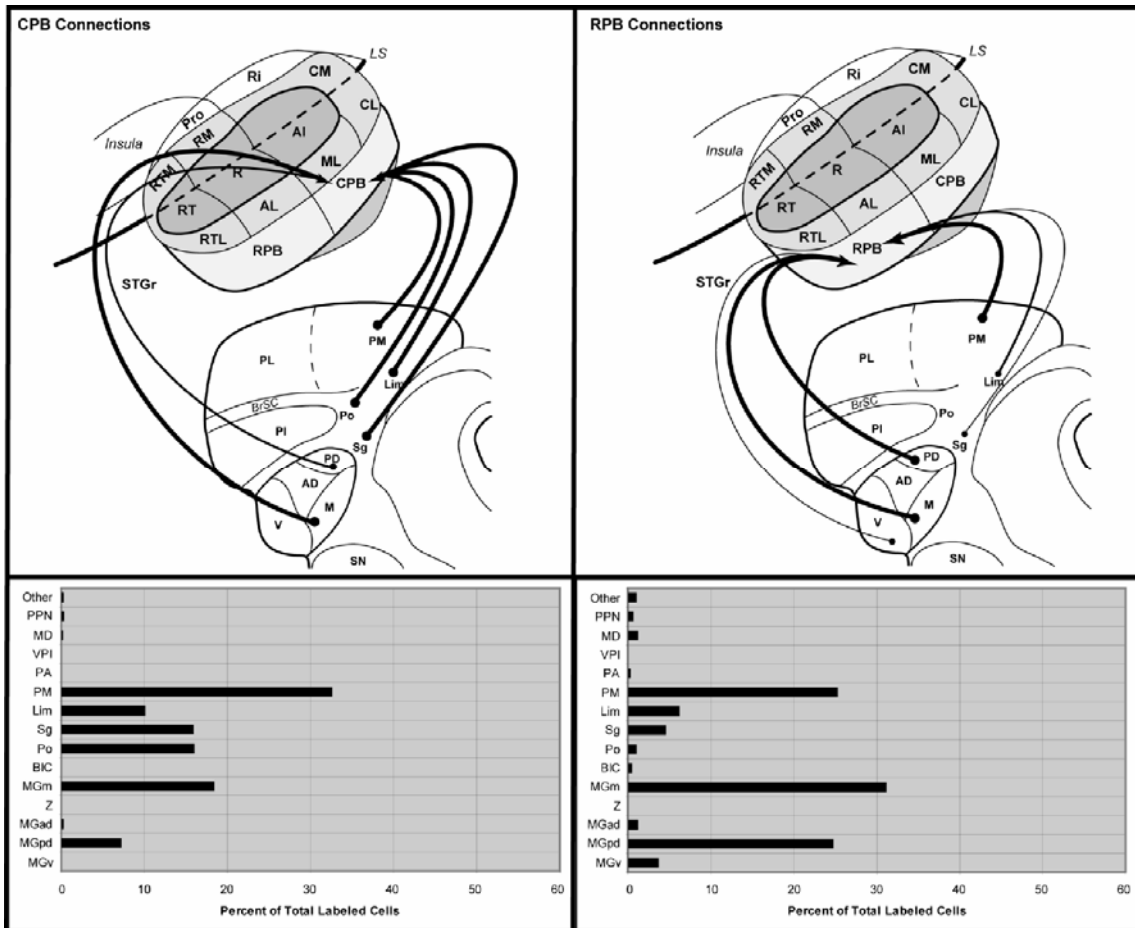
Figure 68. Summary of thalamic connections of CPB and RPB. Top panels illustrate subcortical connections (arrows) of CPB and RPB on schematic diagrams of marmoset auditory cortex and thalamus. Arrow and line size is proportional to connection strength, as indicated in the histograms below each panel. Lines were not drawn for connections representing less than 5% of total.

increased input of the multisensory nuclei with more caudal injections.

Discussion

In this study injections were made into rostral and caudal areas of the lateral belt (CM/CL, RTL) and the parabelt (CPB, RPB) regions. Results indicate that while each of the areas injected revealed distinct patterns of connections, similarities were revealed

between same regional areas (lateral belt, parabelt). The significance of these results is discussed below.

Regional comparison of the lateral belt and the parablet

Both the lateral belt and parabelt regions received strong input from MGm, consistent with results that MGm projects to all areas of auditory cortex (Burton and Jones, 1976; Hashikawa et al., 1995). Apart from this strong MGm input, the patterns of the two regions vary greatly. Input to the lateral belt appears to be confined mainly to the MGC whereas the parabelt region, in addition to the MGm input, also receives a strong projection from PM with additional inputs from MGpd, Sg, Lim, and Po. Concentration of cells in PM was mainly with the medial portion, which has been associated with auditory processing (Hackettet al., 1998; Romanski et al., 1997). This pattern of connections between the thalamus and the parabelt is consistent with findings from Hackett et al. (1998b) in which they reported topographic connections of the parabelt with the MGC as well as Sg/Lim and PM in macaque monkeys.

Comparison between rostral and caudal areas of the lateral belt and the parabelt

In the current study, differences were revealed in the projections from the MGC to the lateral belt where MGad projected to the caudal belt areas (CM, CL) and MGpd projected to RTL. Several studies have reported topography of auditory cortex with the MGC where rostral areas receive input from the posterior portion of the MGC and caudal areas receive input from anterior MGC (Burton and Jones, 1976; Hackett et al., 1998b; Leuthke et al., 1989; Molinari et al., 1995; Morel and Kaas, 1992; Pandya et al., 1994).

Morel and Kaas (1992), reported topographic connections with the lateral belt from MGd but did not distinguish between the anterior and posterior divisions. Studies that have made a distinction between the two divisions reported topographic connections with the belt region, caudal with MGad and rostral with MGpd (see chapter 3; de la Mothe et al., 2006b; Hackett et al., 2007; Molinari et al., 1995).

In the accompanying medial belt study in this thesis, injections into the rostral medial belt area, RM, revealed connections with MGpd, while injections into the caudal medial belt area, both medial and caudal to A1, revealed preferential connetions with MGad. While injections into both the medial and caudal portions of this area revealed prinicipal inputs from MGad, the more caudal of the injections revealed conections that were more distributed in multisensory nuclei. The caudal belt injection in the present study (CM/CL), also located caudal to A1, had connections more concentrated in MGad, not as distributed throughout the multisensory nuclei as was reported in CM. Hackett et al., (2007) reported input to CL mainly from MGpd, but with strong multisensory inputs in the macaque. Thus the main difference between CM and CL in their study arose from the relative distribution of inputs from the MGC, in which CM received input mainly from MGad, and CL received input mainly from MGpd. This is in contrast to results reported here in which CL received inputs mainly from MGad and was less distributed through the multisensory nuclei. The fact that the caudal belt injection straddled the CM/CL border and included both areas (more so CM) may account for the increase in MGad label, but it does not account for the lack of input from the multisensory nuclei. The multisensory input was present from the isolated injection in CM caudal to A1, as well as from one of the CL injections reported by Hackett et al. (2007a). However the

230

other injection in CL from Hackett et al. (2007a) reported few cells in Sg, Lim, and PM consistent with results from the current study. It is possible that the absence of label in multisensory nuclei may have been because the injection was not medial enough. Based on these results the connections of multisensory nuclei with CL remains unclear.

Additional evidence for topography between the lateral belt and the MGC comes from Molinari et al. (1995) in which injections were placed in both rostral and caudal areas of the lateral belt in macaque. The rostral belt injection labeled cells in MGpd and MGm, and the caudal lateral belt injection labeled cells in MGad and MGpd. An additional caudal belt injection that was more caudal and medial labeled cells mainly in MGad. Based on their findings there does appear to be topography in the belt connections from MGpd and MGad.

Topography has been reported by Hackett et al. (1998b), between MGd and the parabelt, where RPB received inputs preferentially from MGpd and CPB was preferentially connected with MGad. Injections into the marmoset parabelt revealed no rostrocaudal topography with MGd (MGad, MGpd) with input almost exlusively from MGpd and few connections with MGad. This lack of input from MGad to either area of the parabelt (specifically CPB) is consistent with the idea that MGad is part of the lemniscal (primary) pathway (discussed in chapter 3) and therefore would not project to what is perceived to be a third level of auditory processing, the parabelt.

Rostrocaudal differences within the parabelt were based mainly on the relative distribution of cells, since injections into both areas involved mainly the same nuclei (MGpd, MGm, Sg, Lim, PM). The distribution of cells shifted from a larger input from MGpd rostrally to increased input of multisensory nuclei (Sg, Lim, Po) caudally. This

preference of multisensory nuclei to be connected with caudal auditory cortex is consistent with what was revealed from injections into the medial belt, and the core regions (see chapter 2; also de la Mothe et al., 2006b; Hackett et al., 2007).

Consistency with the working model of auditory cortex

The lateral belt received input preferentially from one of the dorsal divisions of MGd (MGad, MGpd) as well as MGm, consistent with what has previously been reported (Molinari et al., 1995; Morel and Kaas, 1992; Pandya et al., 1994). In addition rostrocaudal topography was revealed within MGd: rostral areas were preferentially connected with MGpd and caudal areas with MGad consistent with previous findings (Burton and Jones, 1976; Molinari et al., 1995; Morel and Kaas, 1992; Pandya et al., 1994). The parabelt also received input from MGpd and MGm, while there were relatively sparse connections revealed from MGv to either the lateral belt or parabelt. This lack of MGv input, which is characteristic of the primary core areas, is consistent with the hierarchichal model in which the belt is a secondary level of processing and the parabelt is a third. More support for the parabelt position in the hierarchy was revealed from the strong input the parabelt received from the associative thalamic nucleus, PM, which was not present in the lateral belt.

Conclusions

The lateral belt and parabelt regions of auditory cortex have distinct patterns of thalamocortical connections. The lateral belt was almost exclusively connected with the MGC, while the parabelt had strong connections both within and outside of the MGC, in

232

particular with PM. These differnces in regional connection patterns are consistent with

their positions in the hierarchy of auditory cortex. Within each region, rostral and caudal

areas exhibited distinct patterns of thalamocortical connections. Topographic

connections were present between the lateral belt and MGd (MGad, MGpd). The results

of the current study of the thalamocortical connections of the lateral belt and the parabelt

are consistent with the working model of auditory cortex.

CHAPTER VI

DISCUSSION

Our current working model of auditory cortex includes three levels of processing. A primary level, the core region, is surrounded both medially and laterally by a secondary level, the belt region and a third level of processing, the parabelt region. While the model is based on numerous findings, not all of the proposed features have been tested. The medial belt areas in particular have been understudied due, in part, to the difficult location deep within the lateral sulcus. Techniques that allow direct injections of tracers into the medial belt (Hackett et al. 2005) have facilitated the connectional studies presented in this thesis (Figs. 69, 70) and have permitted the identification of connection patterns for this region (Fig. 71). Thus, the work presented in this thesis fills an important void in the anatomical profile of the medial belt, which in combination with recent interest in possible multisensory integration (Fu et al. 2003; Schroeder et al. 2001, 2003) and basic neuron responses (Kajikawa et al. 2005, 2008; Rauschecker et al. 1995, 1997; Recanzone et al., 2000a,b) provides a more complete framework for defining connectional and physiological properties of medial belt areas. In addition, since the model is comprised from studies in New World and Old World monkeys, by injecting the rostral and caudal portions of regions other than the medial belt (core, lateral belt, parabelt) this thesis has provided the opportunity to test the overall model in a single species.

Projections To

Areas	A1	R	RT	CM	MM	RM	RTM	CL	ML	AL	RTL	CPB	RPB	Ri	Pro	STS
A1																
R																
RT																
CM													I			
MM													I			
RM																
RTM																
CL													I			
ML													I			
AL																
RTL																
CPB	I	I														
RPB	I	I		I												
Ri	I	I														
Pro																
STS																

Projections From

Legend:
- ■ Injection site
- ■ Strong connections
- ■ Moderate connections
- ■ Weak connections
- I Infragranular connections
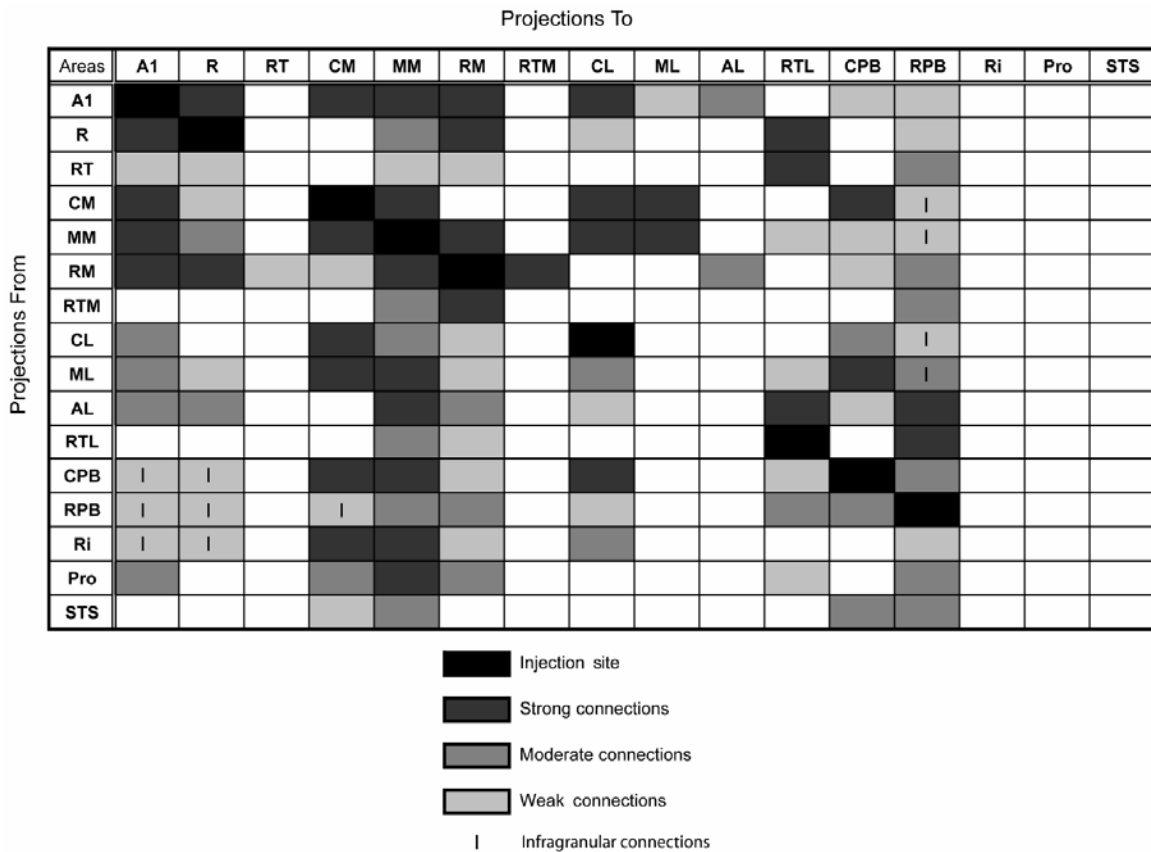
Figure 69. Grid showing a summary of all ipsilateral cortical connections revealed from this study. Areas that are highlighted in a column reflect projections to the field indicated at the top of the column. Areas highlighted in a row reflect areas that the field indicated at the left of the row projects to.

Organization of the Medial Belt

The results of these studies and findings from additional anatomical and physiological studies are reviewed here to provide an overall organization of the medial belt region of auditory cortex.

Architecture of the medial belt

Differences in architecture (cytoarchitecture, myeloarchitecture and

Projections To

Areas	A1	R	RT	CM	MM	RM	RTM	CL	ML	AL	RTL	CPB	RPB
MGv	■	■				*		▨					▨
Mgad	▨	▦		▦	■	▨		■			▨	▨	▨
MGpd	▨	▦		▨	▦	■		▦			■	▦	■
MGm	▦	▦		■	■			■			■	■	■
Sg	▨			▦	▨	▨					▨	■	
Lim	▨			▦	▨							▦	▦
Po	▨			■	▨			▨				■	▨
PM	▨			▦	▨							■	■
PPN					▨	▨					▨		▨
BIC											▨		▨
MD													
PA					▨								
VPI					▨			▨					

Projections From

■ Strong connections

▦ Moderate connections

▨ Weak Connections

* Due to encroachment of the injection into core area R
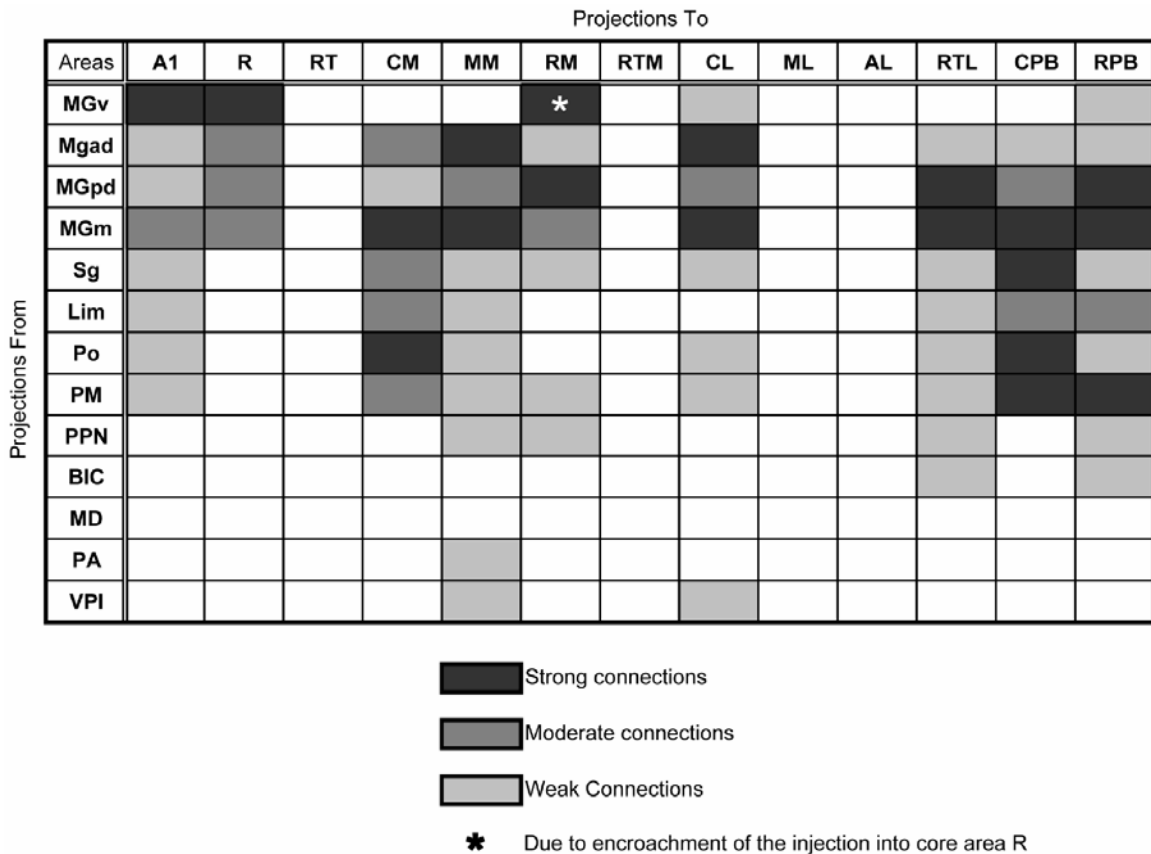
Figure 70. Grid showing a summary of all thalamic projections revealed from this study. Areas that are highlighted in a column reflect projections to the field indicated at the top of the column. Areas highlighted in a row reflect areas that the nucleus indicated at the left of the row projects to.

chemoarchitecture) can be used to identify various regions of auditory cortex (Galaburda and Pandya, 1983; Hackett et al., 1998a, 2001; Imig et al., 1977; Jones et al., 1995; Luethke et al., 1989; Morel et al., 1993; Morel and Kaas, 1992). The medial belt region was easily distinguished from the adjacent core region which was characterized by dense expression of CO in the middle layers, koniocellular cytoarchitecture (high density of small pyramidal cells in layer III, broad granular layer IV, cell sparse layer V) and an
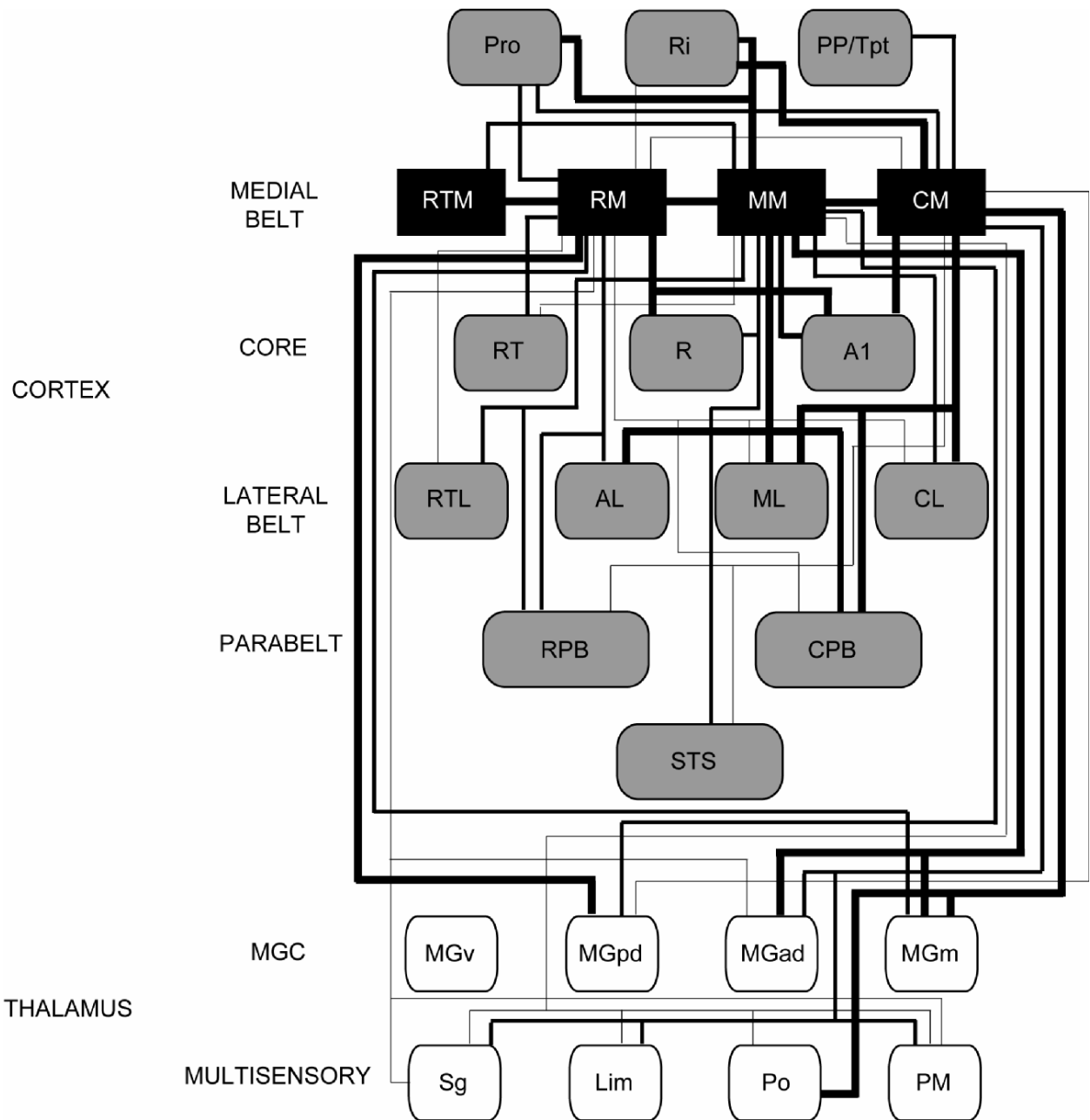
Figure 71. Summary of cortical and thalamic connections of the medial belt areas. Black: medial belt areas; Gray: cortical areas; White: thalamic nuclei. Strength of connections indicated by thickness of line.

astriate pattern of myelination. The medial and lateral regions were revealed in

cytoarchitecture to have a similar narrowing of layer IV compared to adjacent core areas.

The caudal medial and lateral belt areas were similar with a broad layer III and increased

237

columnar spacing in this layer more rostrally. CM was characterized by medium sized cells with poor radial alignment concentrated in the lower half of layer III and reduced overall cortical thickness compared to A1m. RM and RTM were identified in part by their location medial to R and RT. A key feature in distinguishing them from their adjacent core areas (R and RT) was the broad column spacing in RM and RTM, while RTM was identified from RM based on slightly greater cell spacing in RTM. A general caudal to rostral gradient was revealed throughout auditory cortex which resulted in a reduction in overall myelin density and expression of CO and Pv from caudal to rostral areas. Of particular interest were the differences between the caudal and rostral portions of the medial belt in that area CM was revealed to have myeloarchitectonic and chemoarchitectonic features similar to the core areas; whereas the more rostral medial belt areas, RM and RTM, were more similar to the lateral belt than CM. CM exhibited a slight decrease in myelin density from A1, but rostral to CM myelin density was greatly reduced. CM also had a comparable expression of CO in the layer III/IV band to A1, while CO expression was only weakly expressed in the rostral medial belt areas.

Cortical connections of the medial belt

In general the medial belt was revealed to be broadly and topographically connected with auditory cortex (Fig. 69, 71). The medial belt had broad connections with the core, lateral belt, and parabelt consistent with the belt's position as a secondary/intermediate stage in the processing hierarchy. In addition the medial belt exhibited a general trend of rostrocaudal topography in which more rostral areas of the medial belt had stronger connections with rostral areas of the core, lateral belt, and

238

parabelt; and more caudal areas of the medial belt had stronger connections with more caudal areas of the core, lateral belt, and parabelt. The caudal and rostral areas of the medial belt were further distinguished based on somatosensory and multisensory connections which were present in the caudal but absent from the rostral areas (Fig. 71).

The connection of core areas with the medial has been well established (Aitkin et al., 1988; Cipolloni and Pandya, 1989; de la Mothe et al., 2006a; Fitzpatrick and Imig, 1980; Jones et al., 1995; Leuthke et al., 1989; Morel et al., 1993; Morel and Kaas, 1992; Pandya and Sanides, 1973), and in general follows a pattern of rostrocaudal topography (Cipolloni and Pandya, 1989; de la Mothe et al., 2006a; Fitzpatrick and Imig, 1980; Jones et al., 1995; Leuthke et al., 1989; Morel et al. 1993; Morel and Kaas, 1992). In addition to this pattern, direct injections into the medial belt from the current study revealed another pattern of connection between A1 and the medial belt areas (Fig. 71). Injections into RM revealed label in the medial portion of A1 but label was absent from the lateral division, while CM injections labeled cells in the lateral portion of A1. Based on these results it appears that RM is connected with the medial portion of A1 and CM is connected with the lateral portion. This connection pattern supports Pandya and Sanides' (1973) division of the primary auditory cortical area into medial and lateral portions.

The rostrocaudal topography apparent between the core and medial belt fields also extends to the connections between the medial and lateral belt areas and was apparent from injections into both these regions (Fig. 71). An important exception to this rostrocaudal trend was revealed from connection between the medial belt and the parabelt. While labeled cells from injections into RPB were consistent with the expected topographic pattern, with strong connections of RPB with RTM and RM, injections into

CPB did not follow this pattern. CPB injections revealed connections with the caudal portion of CM, a lack of connections with rostral CM (MM) and connections with the more rostral area RM. It is unclear why MM has only a weak, if not completely absent, projection to CPB, when the medial belt areas flanking its rostral and caudal borders have moderate projections, and considering the strong input it receives from CPB. This weak projection is in contrast to the findings from Hackett et al. (1998a), which reported connections between CPB throughout CM, including the rostral portion medial to A1. Like findings from Hackett et al. (1998a), RM appears to be the exception to this rostrocaudal trend, projecting to both CPB and RPB.

RTM as a field requires more extensive investigation as the majority of injections made were not rostral enough to include this area. Even injections made into RM were fairly caudal within the area, and so share strong interconnections with CM and the more rostral area of RM, but not with RTM. Injections into RTL and RPB, both at the rostrocaudal level of RTM, revealed strong projections from RTM with the areas of injection, confirming the topography reported from the rest of the medial belt region. Morel and Kaas (1992), who originally defined the area, did not report any connections to this area from their injections and therefore much is based on location. Direct injections into this most rostral medial belt area would help define both the field and its relation to other auditory areas.

Dense connections to the contralateral hemisphere were present in this study between the medial belt areas and the homotopic area in the contralateral hemisphere, consistent with other findings in auditory cortex (Aitkin et al., 1989: Fitzpatrick and Imig, 1980; Leuthke et al., 1989; Morel et al., 1993). Although the densest connections to the

contralateral side are with the area of injection, areas that connect strongly with the area of injection also appear to connect contralaterally with the injection site, and connections were concentrated in layer 3.

CM also had connections with cortical areas beyond auditory cortex, including projections from the entorhinal cortex, the lower layers of the STS, as well as the posterior parietal cortex. There were strong reciprocal connections between CM and the adjacent somatosensory field Ri, which provides a potential source of somatosensory input to CM, discussed below. Although RM had fewer connections outside of auditory cortex compared to CM, strong reciprocal connections were revealed with Pro, and RM was found to project to the lateral amygdala and the ventral caudate nucleus, but no connection were found with somatosensory areas.

Subcortical connections of the medial belt

In general, the thalamic connections of the medial belt region were similar to those of other belt areas in that the principal input was from MGd (MGad, MGpd) (Fig. 70). The lack of MGv input (characteristic of a primary/core area) and the absence of a strong PM projection (characteristic of parabelt areas) were consistent with the thalamic pattern and hierarchical position of the belt region. Within the medial belt rostral and caudal portions were revealed to have topographic connections with MGd and could be distinguished based on their connections with multisensory nuclei in the thalamus.

Injections into CM and RM revealed two main differences between the thalamic inputs to rostral and caudal portions of the medial belt: 1) the relative inputs from the two divisions of MGd (MGad, MGpd), and 2) input from multisensory nuclei outside of the

MGC. Both CM and RM received projections from MGm; however, CM received

preferential input from MGad, and RM received input preferentially from MGpd (Fig.

71). This is consistent with previous results that the belt areas receive inputs mainly from

the dorsal division of the MGN as well as the magnocellular division (Burton and Jones,

1976; Molinari et al., 1995; Morel and Kaas, 1992; Pandya et al., 1994). The grouping of

the anterior and posterior divisions of the MGd in some studies may have been

responsible for the more general notion that the MGd projects to all belt and parabelt

areas. Separation of MGd into anterior and posterior divisions revealed a different

pattern of input into the medial belt.

Much like the cortical connections, the thalamic connections of CM have a

general pattern, but also more specific ones based on the rostrocaudal location of the

injection within CM (Fig. 71). Caudal CM, in addition to the major inputs from MGad

and MGm, also have stronger connections with multisensory nuclei outside of the MGC

(Sg, Lim, Po, PM) than the more rostral portion CM (MM) (Fig. 71). The more rostral

medial belt area RM had only sparse connections with multisensory nuclei outside of

MGC (Fig. 71). An additional rostrocaudal distinction between the injections of CM was

that caudal CM projected to the pericentral shell of the ventromedial (vm) boundary of

the IC, while rostral CM (MM) projected to the dorsomedial (dm) region of the IC. The

results from this more rostral CM (MM) injection were similar to those from the RM

injections, as RM was also revealed to project to dm of the IC

Functional properties

Although systematic studies of the physiology of the medial belt have been

lacking there have been a few studies have explored this region intermittently. As early as 1973 Merzenich and Brugge reported reversals or discontinuities in the best frequency representation at the boundary of CM and A1: just across the boundary BF decreases abruptly. They also reported that CM was driven over a wide range of frequencies, but that A1 was most excited by tonal frequencies. Their observations have been supported by various studies which also revealed a reversal or disruption in tonotoptic gradient at the border between CM and A1 and that neurons in CM were more broadly tuned (Imig et al.1977; Kajikawa et al., 2005; Kosaki et al. 1997; Merzenich and Brugge, 1973; Rauschecker et al. 1997; Recanzone et al. 2000; Selezneva et al. 2003). This reversal of tonotopic organization at the high frequency border of A1/CM has also been demonstrated in fMRI (Petkov et al., 2006). In addition to supporting the findings of Merzenich and Brugge (1973), Rauschecker et al. (1997), reported an influential study in which neuron responses of the core areas R and A1, as well as CM, were recorded before and after ablation of A1. Following the ablation of A1 responses in R were unaffected; however, responses in CM to tonal stimuli were abolished (though some responses to complex stimuli remained). These results suggest a dependence of CM on A1 for feedforward inputs and have provided support, in conjunction with connectional data, that the belt areas surrounding the core are a second level of processing in auditory cortex. In addition, CM was reported as having a higher proportion of neurons sensitive to spatial location, consistent with findings from Woods et al. (2006).

The notion that CM functions as a typical secondary belt area has recently been challenged from work by Kajikawa et al. (2005), comparing A1 and CM responses to simple acoustic stimuli in which they revealed similarities as well as clear differences

between the two areas. Similarities included: robust onset responses with short response latencies, intensity dependent bandwidths, and largely monotonic BBN rate-level functions. Differences reported were: frequency reversal at the A1 border, shorter minimal response latencies in CM, lower thresholds for tones in CM, and greater expansion bandwidth at higher intensities in CM. In addition a population of broadly tuned units were found in CM, consistent with previous studies of primates (Aitkin et al., 1986; Fu et al., 2003; Imig et al., 1977; Kosaki et al., 1997; Luethke et al., 1989; Merzenich and Brugge, 1973; Rauschecker et al. 1997; Recanzone et al. 2000) and suggest that broader tuning is a feature of CM. Although differences exist between CM and A1 when compared with neuron responses of the lateral belt, which responded poorly under the same anesthetic conditions to tones and noise bursts; CM may overlap more with the core area A1 than with areas of the lateral belt. The belt area CM has been thought to be part of this second level of auditory processing (Rauschecker et al., 1997; Recanzone et al., 2000a), and despite the cortical connections from the current study which supports CM as a belt area, it may in fact be more core-like than belt-like. Response latencies of both tones and noise bursts in CM were found to be core-like in that they were shorter than those found in A1. Scott et al. (2000) reported some short latencies in CM, and additional studies have reported shorter latencies in CM compared to A1 (Bieser and Muller-Preuss, 1996; Lakatos et al., 2005). Recanzone et al. (2000a) found no significant difference in average response latencies between the two areas. Since CM is part of the belt and considered to be a second level of processing (Kaas and Hackett, 2000; Rauscecker et al., 1997; Recanzone et al., 2000a) these shorter than A1 or as short as A1 latencies are unexpected since the belt is suppose to depend on the core for

its activation. The thalamic inputs to the belt come from the MGd (Burton and Jones, 1976; de la Mothe et al., 2006b; Hackett et al., 1998b; Molinari et al., 1995; Morel and Kaas, 1992; Pandya et al., 1994), part of the proposed non-lemniscal pathway (Rouillier et al., 1991). CM, as revealed form the current study however, receives its input preferentially from a division of the MGd, MGad (de la Mothe et al., 2006b; Molinari et al., 1995), which has been suggested as being part of the primary/lemniscal pathway based on architecture and inputs from the ICc (Molinari et al., 1995; Jones, 2003). Possible parallel lemniscal pathways may help to explain the primary-like responses found in CM and should become a direction of future investigations of this area. These results suggest that CM may not function as a typical belt area.

Despite the attention that the caudal medial belt area has received, the same cannot be said for the rostral medial belt. Recently four areas of the medial belt (CM, MM, RM, RTM) have been identified using fMRI based on changes in tonotopic organization (Petkov et al., 2006). The direction of tonotopic organization of RM revealed from this imaging study (low caudally to high rostrally) is consistent with findings from Kosaki et al. (1997). Area MM has also been identified as functionally distinct from caudal belt areas (CM, CL, ML) and with decreased spatial tuning compared to CM (Woods et al., 2006). While there is some functional evidence for defining these medial belt fields, adequate studies of the response properties of neurons in the more rostral medial belt areas (RM and RTM) as well as area MM are lacking, and much about these areas remains uncertain. If the belt area CM is functionally distinct from other belt areas, it is a logical progression to investigate the neighboring medial belt areas to determine if they follow a similar pattern, or if they are consistent with findings

in the lateral belt. Additional studies are needed to better define the neuron response properties of the rostral medial belt areas and fill a void in the data to better address broader issues like the dual streams hypothesis.

Multisensory properties

During the course of data collection in the medial belt, area CM became the focus of multisensory studies when it was discovered that neurons in this area were responsive to both auditory and somatosensory stimulation (Fu et al., 2003; Kayser et al., 2005; Robinson and Burton 1980a,b; Schroeder and Foxe, 2002; Schroeder et al., 2001). As described previously, during their investigation of somatosensory areas, Robinson and Burton reported neurons in area Pa (CM) responsive to cutaneous stimulation, mainly of the upper body (Robinson and Burton 1980a,b). Schroeder and colleagues confirmed the presence of somatosensory responses in the auditory belt area, CM, using electrical stimulation of the median nerve as somatosensory stimuli (Schroeder and Foxe, 2002; Schroeder et al., 2001). In addition, Schroeder and Foxe (2002) revealed that neurons in CM displayed a feedforward pattern of input, with initial activation centered around layer 4, in response to both somatosensory and auditory stimuli. Fu et al. (2003) also reported neurons responsive to auditory and a variety of somatosensory stimulation in CM. Of the neurons responsive to auditory stimulation 72% were also responsive to some form of somatosensory stimulation, and the majority of these somatosensory responses were to cutaneous stimulation of the head and neck. There were no responses to somatosensory stimulation found in A1.

Multisensory integration of auditory and somatosensory modalities has also been demonstrated using fMRI (Foxe et al., 2002; Kayser et al., 2005). Foxe et al. (2002) using auditory, somatosensory, and combined auditory and somatosensory stimulation showed that there was an area of overlap between the auditory stimulation and the somatosensory stimulation. In addition, the activity in response to the auditory and somatosensory stimulation combined exceeded that predicted by summing the auditory and somatosensory unimodal activations, providing evidence for multisensory integration in that particular area of auditory cortex. Due to the location and auditory and somatosensory integration it is thought that the area identified in this study may be the human homologue to area CM in nonhuman primates. Kayser et al. (2005) reported similar results in the macaque caudal belt region.

The finding of neurons responsive to somatosensory stimulation in an area of cortex that was thought to be auditory only presents a question as to the source of the somatosensory input into CM. Injections made directly into the rostral and caudal areas of the medial belt revealed unique thalamocortical connection patterns. RM received inputs mainly from MGpd and MGm, whereas CM received inputs mainly from MGad, MGm, as well as several multisensory nuclei (Po, Sg, Lim, PM). Hackett et al., 2007a, reported similar thalamocortical projections to CM of macaque monkeys. The projections from multisensory nuclei to CM, but not RM, provide a possible source of somatosensory input into CM. Strong reciprocal connections between CM and the adjacent somatosensory field Ri, consistent with findings in macaque (Hackett et al., 2007b; Smiley et al., 2007), provide an additional potential source of somatosensory input to CM. Despite the fact that both CM and A1 receive inputs from multisensory

nuclei, only CM responds to somatosensory stimuli, making these thalamic nuclei an unlikely source of somatosensory input into CM. Based on the current study the most likely source appears to be the cortical area Ri, since A1 does not receive input from multisensory or somatosensory cortical areas.

What versus Where: Dual Streams Hypothesis

The hypothesis of dual streams of processing, "what" versus "where" pathways, have been proposed in both the visual (Mishkin et al., 1983; Ungerleider and Mishkin, 1982) and, to a lesser extent, somatosensory (Mishkin, 1979; Disbrow et al., 2003) systems. Discussion of the possibility of dual streams has extended to the auditory cortex, with a caudal where pathway for processing spatial information, and a rostral what pathway for processing non-spatial information (Alain et al., 2001; Clarke et al., 2002; Colombo et al., 1996; Kaas and Hackett, 1999; Rauschecker and Tian, 2000; Romanski et al., 1999b; Tian et al., 2001). However, evidence has also been reported that the streams are not necessarily completely segregated and that interaction between the two does occur (Kaas and Hackett, 1999; Zatorre et al., 2002). Although this remains a topic of debate, differences in cortical and thalamic connections revealed in the current study as a result of rostrocaudal location within the medial belt were consistent with the proposal of dual streams.

Anatomical support for the segregation of spatial and non-spatial streams was revealed in both the cortical and thalamocortical connections of the medial belt (Fig. 71). Injections into CM revealed connections with somatosensory area Ri, as well as the posterior parietal cortex, which is considered part of the where stream in the visual

system (Ungerleider and Mishkin, 1982), while RM injections resulted in no connections with these caudal areas. Thalamic projections from multisensory nuclei (Sg, Po, Lim, PM) were sparse with RM, but increased strength caudally, with caudal CM receiving strong projections from multisensory nuclei. Thus it appears that somatosensory and multisensory connections are concentrated in the caudal portion of the medial belt, consistent with spatial processing, while RM, proposed as being part of the non-spatial stream, is largely void of these connections. Additional support comes from inputs to CM from entorhinal cortex, which has been reported to be spatially organized (Hafting et al., 2005), and projections from RM to the lateral amygdala, which is involved in emotional processing (Phelps and LeDoux, 2005) and may be related to the emotional significance of sounds. The connectional patterns revealed in the current study are consistent with results from Romanski et al. (1999) which revealed that caudal and rostral areas of the medial belt were connected with functionally distinct regions of prefrontal cortex.

Physiology experiments have reported that neurons in CM are more spatially tuned than those of the core areas (Rauschecker et al., 1997; Recanzone 2000b; Woods et al., 2006) as well as the more rostral area, MM (Woods et al., 2006). Responses to both auditory and somatosensory stimulation have also been reported in CM (Foxe et al., 2002; Fu et al., 2003; Kayser et al., 2005; Robinson and Burton, 1980a,b; Schroeder and Foxe, 2002; Schroeder et al., 2001, 2003). Reported responses to cutaneous stimulation were concentrated in the upper trunk, mainly to the head and neck (Fu et al., 2003; Robinson and Burton, 1980b). Combining these somatosensory responses with auditory may be useful in trying to establish the origin of a sound in which the head turns to locate

a sound or knowing where the head is in space in relation to the sound. In addition to being responsive to both somatosensory and auditory stimuli, neurons in CM are more sensitive to spatial location and so based on physiology there does appear to be support for CM being part of the spatial pathway.

Comparison of the Medial and Lateral Areas of the Belt Region

The medial and lateral belt areas surround the core and combine to form the belt region, a secondary level of processing in auditory cortex. The results of the current study firmly establish the medial belt as part of the larger belt region, though some differences with the lateral belt were revealed. The focus of the current study on the medial belt region fills a void in the anatomical organization of the working model and provides a basis to compare the medial areas with the more established lateral belt areas.

Overall, the current studies of the medial and lateral belt areas revealed a pattern of rostrocaudal topography consistent with findings in auditory cortex (Cipolloni and Pandya, 1989; de la Mothe et al., 2006a; Fitzpatrick and Imig, 1980; Galaburda and Pandya, 1983; Hackett et al., 1998a; Jones et al., 1995; Leuthke et al., 1989; Morel et al. 1993; Morel and Kaas, 1992). In addition, strong connections of medial and lateral regions were revealed with the core and parabelt, consistent with serial processing and the belt as a secondary, intermediate stage (Fig. 69). Topographical patterns were also revealed between the rostral and caudal belt areas and the dorsal divisions of the MGC. MGpd was preferentially connected with the rostral medial and lateral belt areas, and MGad was preferentially connected with the caudal areas of the medial and lateral belt,

similar to findings reported by Molinari et al. (1995) in the lateral belt and Hackett et al. (2007a) in the medial belt (Fig. 70).

Differences between the medial and lateral belt were revealed from somatosensory and multisensory connections. The caudal medial belt areas (CM, MM) were revealed to have strong connections with the somatosensory area Ri, whereas the caudal lateral belt injection had only moderate connections with Ri (Fig. 69). In addition multisensory nuclei of the thalamus had stronger projections to the caudal medial belt, whereas only weak connections were revealed from the caudal lateral belt (Fig. 70). These results are consistent with the root-core-belt model proposed by Galaburda and Pandya (1983) in which the root (medial belt) fields were identified as a separate line/region from the belt (lateral belt) fields. A preference for multisensory thalamic projections to the medial belt region has been reported in previous studies (Burton and Jones, 1976, Pandya et al., 1994) and the root areas have been proposed to have role in multimodal processing (Pandya et al., 1994).

Architectonically the rostral medal belt areas (RM, RTM) were more like the lateral belt areas than the caudal medial belt areas (CM, MM) based on cytoarchitecture (narrowing of layer IV), and attenuation of several robust features in the core (dense myelin, CO, and PV). The caudal medial belt areas appeared to be more core-like, and while there was a slight decrease in density from the adjacent core area, A1, CM and MM still expressed dense myelin, CO, and PV compared to the rostral areas.

Neurons in the belt areas that are more broadly tuned with higher thresholds have been reported in both the medial and lateral belt (Aitkin et al., 1986; Imig et al., 1977; Kosaki et al., 1997; Merzenich and Brugge, 1973; Petkov et al., 2006; Rauschecker and

Tian, 2004; Rauschecker et al., 1995, 1997; Recanzone et al., 2000a,b)as well as tonotopic organization that parallels the core (Imig et al., 1977; Kosaki et al., 1997; Merzenich and Brugge, 1973; Petkov et al., 2006; Rauschecker and Tian, 2004; Rauschecker et al., 1995).

Differences between caudal and rostral lateral belt areas were reported by Tian et al. (2001) in which responses to spatial location vs vocalizations were compared within the lateral belt. The results revealed greater spatial sensitivity in the caudal lateral belt compared with neurons in the rostral lateral belt, which were more selective for the type of call. Although there is not a complementary study in the medial belt, Woods et al. (2006) reported increased spatial tuning in the caudal belt areas CM and CL compared to more rostral areas, consistent with findings in the lateral belt.

Most of the recent attention regarding somatosensory and auditory responses in auditory cortex has focused on the medial belt area CM (Fu et al. 2003; Kayser et al., 2005; Robinson and Burton 1980a,b; Schroeder and Foxe, 2002; Schroeder et al., 2001); however, there is also support for convergence of these modalities in the lateral belt (Kayser et al., 2005). While there is a lack of physiological studies examining somatosensory responses in the caudal lateral belt, it is reasonable to predict based on the similar connection pattern of CL and CM, with input from multisensory nuclei and Ri, that area CL would be responsive to somatosensory stimuli. Additional studies are required to resolve whether the caudal areas of both the medial and lateral belt are responsive to auditory and somatosensory stimulation.

While some differences between the medial and lateral belt were noted, in general the anatomical and functional organization of the medial and lateral belt areas appears to

be similar, comprising a secondary belt region of auditory cortex with connectional and functional topography.

Refinements of the working model

In addition to studying the anatomical profile of the medial belt, injections into other regions of auditory cortex have provided the unique opportunity to test the model in a single species. Given this ability, several revisions to the model have been identified and proposed. A summary of the refinements that should be made to the working model of primate auditory cortex is presented in figure 72.

Identification of the fourth medial belt area, MM

Based on distinct connectional patterns, and limited studies of the functional organization, the medial belt region adjacent to A1 should be recognized as a separate area, MM. The region of cortex medial to A1 has been identified in various models of auditory cortex: proA (Pandya and Sanides, 1973; Galaburda and Pandya, 1983), CM and the caudal portion of area a (Merzenich and Brugge, 1973), CM (Imig et al., 1977, Morel and Kaas, 1992; Morel et al., 1993; Hackett et al., 1998a,b), Pi (Burton and Jones, 1976), with the identification of MM originally proposed by Rauschecker et al. (1998).

Injections into CM made into both rostral (MM) and caudal (CM) portions, shared a general pattern of connections but also revealed distinct connectional patterns more specific to the rostrocaudal location of the injection. Overall, the more rostral CM injection labeled cells farther into rostral auditory cortex and included strong connections with RM, Pro, AL, R. The caudal CM injection had only weak connections with RM and

Figure 72. Revisions to the current working model of primate auditory cortex. Area MM is identified as a distinct auditory cortical area. Dashed white line indicates medial and lateral divisions of A1. Connections between the core and parabelt identified by white lines with arrows indicating direction of projection. The dorsal division of the MGC is divided into MGad and MGpd. Gray line identifies MGad projection to area MM.
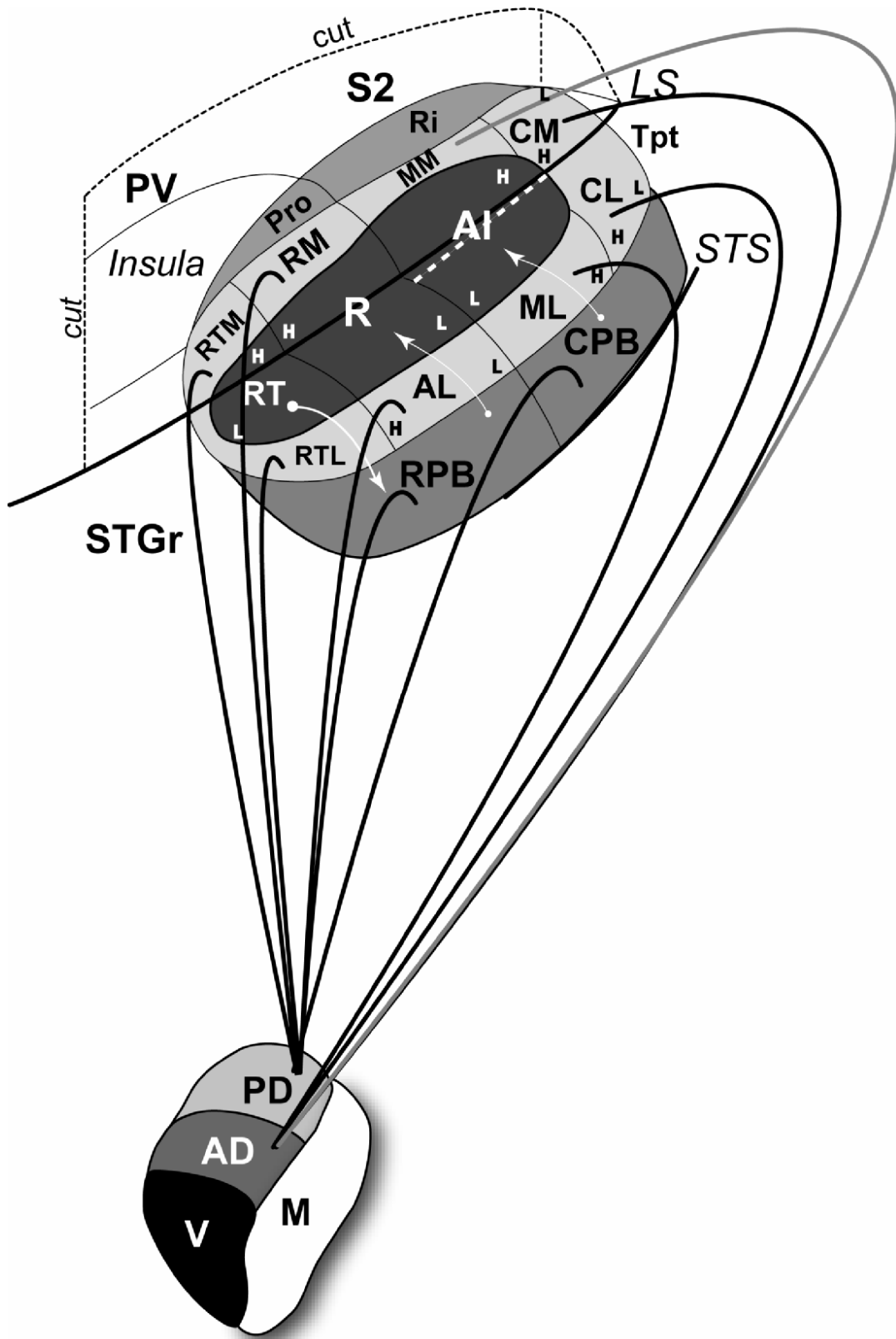
Pro, and most of the connections were confined to the caudal portion of auditory cortex (caudal to A1/R border). In addition, the two portions of CM exhibited distinct connections with the medial and lateral portions of A1, where rostral CM had strong connections with A1m and caudal CM with A1L. While both portions of CM received input preferentially from MGad, the more caudal injection had stronger inputs from the multisensory nuclei. Additional differences were revealed in projections from CM to IC, where rostral CM projected to dm of IC (similar to RM), and caudal CM projected to vm of IC. A unique pattern was also revealed when despite labeling the adjacent medial belt areas RM and CM, labeling after injections into CPB excluded MM. The area MM has also been recently identified using fMRI and revealed to share a low frequency border with RM with higher frequencies represented caudally in the area (Petkov et al., 2006). In addition, Woods et al. (2006) identified MM and reported decreased spatially sensitivity in this area compared to the more caudal CM. Based on these cumulative findings, the model should be revised to reflect the medial belt region adjacent to A1 as a distinct fourth area, MM.

Medial and lateral divisions of A1

    The division of A1 into medial and lateral portions, observed in the present study, was previously proposed by Pandya and Sanides (1973). In addition to the architectonic identification based on a decrease in myelin density laterally, connectional data from injections into the medial belt provide additional support for the division of A1. Injections into RM and rostral CM revealed stronger connections with medial A1 while injections into caudal CM had stronger connections with lateral A1. While no functional

differences have been reported between the medial and lateral portions of A1, a revision of the model to reflect this anatomically-driven division may result in new discoveries in the functional organizations of these subdivisions.

Connections of the core and the parabelt regions

Support for serial processing in the auditory system stems in part from the lack of connections between the core and the parabelt region (Hackett et al., 1998a). While injections into the parabelt revealed a similar lack of connections from core areas A1 and R, injections into the core and parabelt regions revealed two patterns that contrasted with the notion that the core and parabelt shared no significant connections. First, injections into core areas A1 and R revealed weakly labeled infragranular cells in the parabelt, consistent with a feedback projection. Second, core areas A1 and R were mainly void of cells from the parabelt injections, but the core area RT projected to RPB. Since injections revealed that the connections from the parabelt with the core appear to be feedback projections, they are still consistent with serial processing from the core, to the belt, to the parabelt. The lack of projections from A1 and R to the parabelt provides additional support for serial processing in the auditory cortex. Inconsistent with serial processing are the projections from the core area RT to the parabelt. Perhaps RT is a field similar to CM, in that it is a hybrid with core-like and belt-like features, features that will be revealed as additional studies focus on this area. Regardless, the model should be revised to reflect the feedback connections from the parabelt to A1 and R, as well as the projections from RT to RPB.

Division of MGd and the topographical connections with the belt region

A general finding of the auditory belt areas is that they receive input from the dorsal division of the medial geniculate (MGd) (Burton and Jones, 1976; de la Mothe et al., 2006b; Hackett et al., 1998b; Molinari et al., 1995; Morel and Kaas, 1992; Pandya et al., 1994). Over the last number of years several studies have divided MGd into anterior and posterior divisions (Burton and Jones, 1976, Hashikawa et al., 1995; Jones et al., 1995; Jones and Burton, 1976; Molinari et al., 1995), but this has not been consistent in the literature. By identifying the separate divisions of MGd, a connectional pattern emerges with regard to the belt region and supports previous findings of topography between auditory cortex and the MGC. Injections into both rostral (MM) and caudal portions of CM revealed labeled cells predominantly in MGad, whereas RM injections revealed label principally in MGpd. This pattern of rostrocaudal topography was echoed in the lateral belt. RTL was preferentially connected with MGpd, and the caudal belt injection resulted in label predominantly in MGad. While the projections from MGad to CL from the current study, in contrast the results from Hackett et al. 2007a, are consistent with previous results in which projections to the lateral belt shift from MGpd rostrally to MGad caudally (Molinari et al., 1995). Thus there appears to be an overall pattern of rostrocaudal topography, with MGpd projecting preferentially to the rostral belt areas, and MGad projecting preferentially to the caudal belt areas. The model should be amended to reflect the division of MGd into MGad and MGpd, and to reflect the topographical nature of the connections with the belt.

General Conclusions

The work contained in this thesis provides much needed information on the anatomical organization of the medial belt region of auditory cortex. Overall, the marmoset auditory cortex appears to be consistent with the current model of primate auditory cortex, although minor revisions to the model have been identified. Architectonic features established in other species were consistent in marmoset auditory cortex and were useful criteria for identifying areas. The principal focus of this study, the medial belt areas CM, now identified as MM and CM, as well as RM; represent functionally distinct areas of auditory cortex, each with different architectonic and connectional patterns. Evidence for serial and parallel processing was revealed from the general topographic and broad connections of the medial belt with the core, lateral belt, and parabelt, consistent with the medial belt's role as an intermediate stage in processing. However, areas CM and RT have demonstrated both core-like and belt-like features which questions their role in the processing hierarchy. In addition, evidence for "what" and "where" streams of processing was revealed from somatosensory and multisensory connections of the caudal medial belt; connections that were absent from the rostral medial belt, which instead was connected with an emotion related area. Architectonic features and connection patterns also distinguished the core areas A1 and R, the lateral belt areas CL and RTL, and the parabelt areas CPB and RPB. Revisions to the model include MM as a distinct area of the medial belt, division of A1 into medial and lateral portions, feedback connections from the parabelt to the core as well as projections from RT to the parabelt, and division of MGd into MGad and MGpd. The current thesis fills a void in understanding the anatomical organization of the medial belt region and provides

259

a neuroanatomical basis for using the marmoset as a model of the primate auditory

cortex.

REFERENCES

Aggleton JP, Burton MJ, Passingham RE. 1980. Cortical and subcortical afferents to the amygdala of the rhesus monkey (Macaca mulatta). Brain Res 190:347-368.

Aitkin LM, Dickhaus H, Schult W, Zimmermann M. 1978. External nucleus of inferior colliculus: auditory and spinal somatosensory afferents and their interactions. J Neurophysiol 41(4):837-847.

Aitkin LM, Kenyon CE, Philpott P. 1981. The representation of the auditory and somatosensory systems in the external nucleus of the cat inferior colliculus. J Comp Neurol 196(1):25-40.

Aitkin LM, Kudo M, Irvine DR. 1988. Connections of the primary auditory cortex in the common marmoset, Callithrix jacchus jacchus. J Comp Neurol 269(2):235-248.

Aitkin LM, Merzenich MM, Irvine DR, Clarey JC, Nelson JE. 1986. Frequency representation in auditory cortex of the common marmoset (Callithrix jacchus jacchus). J Comp Neurol 252(2):175-185.

Akbarian S, Grusser OJ, Guldin WO. 1992. Thalamic connections of the vestibular cortical fields in the squirrel monkey (Saimiri sciureus). J Comp Neurol 326(3):423-441.

Akbarian S, Grusser OJ, Guldin WO. 1994. Corticofugal connections between the cerebral cortex and brainstem vestibular nuclei in the macaque monkey. J Comp Neurol 339(3):421-437.

Allon N, Yeshurun Y, Wollberg Z. 1981. Responses of single cells in the medial geniculate body of awake squirrel monkeys. Exp Brain Res 41(3-4):222-232.

Anderson, RA, Knight, PL, Merzenich, M.M. 1980. The thalamocortical and corticothalamic connections of AI, AII and the anterior auditory field (AAF) in the cat: evidence for two largely segregated systems of connections. J Comp Neurol 194:663-701.

Bartlett DJK, Hall DA. 2006. Response preferences for "what" and "where" in human non-primary auditory cortex. NeuroImage 32:968-977.

Beck E. 1928. Die myeloarchitektonische Felderung es in der Sylvischen Furche gelegenen Teiles des menschlichen Schläfenlappens. J Psych Neurol 36:1-21.

Bendor D, Wang X. 2005. The neuronal representation of pitch in primate auditory cortex. Nature 436(7054):1161-1165.

Bendor D, Wang X. 2008. Neural response properties of primary, rostral, and rostrotemporal core fields in the auditory cortex of marmoset monkeys. J Neurophysiol. 100:888-906.

Berman AL. 1961a. Interaction of cortical responses to somatic and auditory stimuli in anterior ectosylvian gyrus of cat. J Neurophysiol 24:608-620.

Berman AL. 1961b. Overlap of somatic and auditory cortical response fields in anterior ectosylvian gyrus of cat. J Neurophysiol 24:595-607.

Bieser A, Muller-Preuss P. 1996. Auditory responsive cortex in the squirrel monkey: neural responses to amplitude-modulated sounds. Exp Brain Res 108(2):273-284.

Blum PS, Abraham LD, Gilman S. 1979. Vestibular, auditory, and somatic input to the posterior thalamus of the cat. Exp Brain Res 34(1):1-9.

Blum PS, Gilman S. 1979. Vestibular, somatosensory, and auditory input to the thalamus of the cat. Exp Neurol 65(2):343-354.

Bordi F, LeDoux JE. 1994. Response properties of single units in areas of rat auditory thalamus that project to the amygdala. II. Cells receiving convergent auditory and somatosensory inputs and cells antidromically activated by amygdala stimulation. Exp Brain Res 98(2):275-286.

Borgmann S, Jurgens U. 1999. Lack of cortico-striatal projections from the primary auditory cortex in the squirrel monkey. Brain Res 836:225-228.

Brodmann K. 1909. Vergleichende Lokalisationslehre der Grosshirnrinde. Leipzig: Barth.

Brugge JF. 1982. Auditory cortical areas in primates. In: Woolsey CN, editor. Cortical Sensory Organization, vol 3, Multiple Auditory Areas. Clifton, NJ: Humana Press. p 59-70.

Brunso-Bechtold, J.K., Thompson, G.C., Masterton, R.B. (1981) HRP study of the organization of auditory afferents ascending tot he central nucleus of the inferior colliculus in cat. *Journal of Comparative Neurology*, 197, 705-722.

Burton H, Fabri M, Alloway K. 1995. Cortical areas within the lateral sulcus connected to cutaneous representations in areas 3b and 1: a revised interpretation of the second somatosensory area in macaque monkeys. J Comp Neurol 355(4):539-562.

Burton H, Jones EG. 1976. The posterior thalamic region and its cortical projection in New World and Old World monkeys. J Comp Neurol 168(2):249-301.

Cant NB. 1992. The cochlear nucleus: Neuronal types and their synaptic organization. In DB Webster, AN Popper, RR Fray (Eds.) The Mammalian Auditory Pathway: Neuroanatomy (p. 66-116). New York, Springer-Verlag.

Carreras M, Andersson SA. 1963. Functional properties of neurons of the anterior ectosylvian gyrus of the cat. J Neurophysiol 26:100-126.

Cheung SW, Bedenbaugh PH, Nagarajan SS, Schreiner CE. 2001. Functional organization of squirrel monkey primary auditory cortex: responses to pure tones. J Neurophysiol 85(4):1732-1749.

Cipolloni PB, Pandya DN. 1989. Connectional analysis of the ipsilateral and contralateral afferent neurons of the superior temporal region in the rhesus monkey. J Comp Neurol 281(4):567-585.

Clarke JM. 1994. The Common Marmoset (Callithrix jachhus). Anzccart News 7(2):1-7.

Clemo HR, Stein BE. 1983. Organization of a fourth somatosensory area of cortex in cat. J Neurophysiol 50(4):910-925.

Coleman, J.R., Clerici, W.J. (1987) Sources of projections to subdivisions of the inferior colliculus in the rat. *Journal of Comparative Neurology*, 262, 215-226.

Colombo M, Rodman HR, Gross CG. 1996. The effects of superior temporal cortex lesions on the processing and retention of auditory informationin monkeys (cebus apella). J Neurosci 16(14):4501-4517.

Covey, E., Casseday, J.H. (1986) Connectional basis for frequency representation in the nuclei of the lateral lemniscus of the bat, *Eptesicus fuscus*. *Journal of Neuroscience*, 6, 2926-2940.

Curry MJ. 1972. The exteroceptive properties of neurones in the somatic part of the posterior group (PO). Brain Res 44(2):439-462.

Cusick CG, Wall JT, Felleman DJ, Kaas JH. 1989. Somatotopic organization of the lateral sulcus of owl monkeys: area 3b, S-II, and a ventral somatosensory area. J Comp Neurol 282(2):169-190.

de la Mothe LA, Blumell S, Kajikawa Y, Hackett TA. 2006a. Thalamic connections of auditory cortex in marmoset monkeys: core and medial belt regions. J Comp Neurol 496:27-71.

de la Mothe LA, Blumell S, Kajikawa Y, Hackett TA. 2006b. Thalamocortical connections of core and medial belt auditory cortex in marmoset monkeys. J Comp Neurol 496:72-96.

de la Mothe LA, Blumell S, Kajikawa Y, Hackett TA. 2002. Connections of auditory medial belt auditory cortex in marmoset monkeys. Society for Neuroscience Abstracts:261.266.

deCharms RC, Blake DT, Merzenich MM. 1999. A multielectrode implant device for the cerebral cortex. J Neurosci Methods 93(1):27-35.

deCharms RC, Merzenich MM. 1996. Primary cortical representation of sounds by the coordination of action-potential timing. Nature 381(6583):610-613.

Dehner LR, Keniston LP, Clemo HR, Meredith MA. 2004. Cross-modal circuitry between auditory and somatosensory areas of the cat anterior ectosylvian sulcal cortex: a 'new' inhibitory form of multisensory convergence. Cereb Cortex 14(4):387-403.

Disbrow E, Litinas E, Recanzone GH, Padberg J, Krubitzer L. 2003. Cortical connections of the second somatosensory area and the parietal ventral area in macaque monkeys. J Comp Neurol 462(4):382-399.

Eggermont JJ. 1998. Representation of spectral and temporal sound features in three cortical fields of the cat. Similarities outweigh differences. J Neurophysiol 80(5):2743-2764.

Eliades SJ, Wang X. 2005. Dynamics of Auditory-Vocal Interaction in Monkey Auditory Cortex. Cereb Cortex.

Falchier A, Clavagnier S, Barone P, Kennedy H. 2002. Anatomical evidence of multimodal integration in primate striate cortex. J Neurosci 22(13):5749-5759.

FitzPatrick KA, Imig TJ. 1978. Projections of auditory cortex upon the thalamus and midbrain in the owl monkey. J Comp Neurol 177(4):537-555.

Foxe JJ, Wylie GR, Martinez A, Schroeder CE, Javitt DC, Guilfoyle D, Ritter W, Murray MM. 2002. Auditory-somatosensory multisensory processing in auditory association cortex: an fMRI study. J Neurophysiol 88(1):540-543.

Friedman DP, Murray EA. 1986. Thalamic connectivity of the second somatosensory area and neighboring somatosensory fields of the lateral sulcus of the macaque. J Comp Neurol 252(3):348-373.

Friedman DP, Murray EA, O'Neill JB, Mishkin M. 1986. Cortical connections of the somatosensory fields of the lateral sulcus of macaques: evidence for a corticolimbic pathway for touch. J Comp Neurol 252(3):323-347.

Fu KM, Johnston TA, Shah AS, Arnold L, Smiley J, Hackett TA, Garraghty PE, Schroeder CE. 2003. Auditory cortical neurons respond to somatosensory stimulation. J Neurosci 23(20):7510-7515.

Fu KM, Shah AS, MN OC, McGinnis T, Eckholdt H, Lakatos P, Smiley J, Schroeder CE. 2004. Timing and Laminar Profile of Eye Position Effects on Auditory Responses in Primate Auditory Cortex. J Neurophysiol.

Galaburda A, Sanides F. 1980. Cytoarchitectonic organization of the human auditory cortex. J Comp Neurol 190(3):597-610.

Galaburda AM, Pandya DN. 1983. The intrinsic architectonic and connectional organization of the superior temporal region of the rhesus monkey. J Comp Neurol 221(2):169-184.

Gallyas F. 1979. Silver staining of myelin by means of physical development. Neurol Res 1(2):203-209.

Geneser-Jensen FA, Blackstad TW. 1971. Distribution of acetyl cholinesterase in the hippocampal region of the guinea pig. I. Entorhinal area, parasubiculum, and presubiculum. Z Zellforsch Mikrosk Anat 114(4):460-481.

Glendenning KK, Masterton RB. 1983. Acoustic chiasm:Efferent projections of the lateral superior olive. J Neurosci 3(8):1521-1537.

Gray D, Gutierrez C, Cusick CG. 1999. Neurochemical organization of inferior pulvinar complex in squirrel monkeys and macaques revealed by acetylcholinesterase histochemistry, calbindin and Cat-301 immunostaining, and Wisteria floribunda agglutinin binding. J Comp Neurol 409(3):452-468.

Griffiths TD, Warren JD. 2002. The planum temporale as a computational hub. Trends Neurosci 25(7):348-353.

Groh JM, Trause AS, Underhill AM, Clark KR, Inati S. 2001. Eye position influences auditory responses in primate inferior colliculus. Neuron 29(2):509-518.

Gross NB, Lifschitz WS, Anderson DJ. 1974. The tonotopic organization of the auditory thalamus of the squirrel monkey (Saimiri sciureus). Brain Res 65(2):323-332.

Grusser OJ, Pause M, Schreiter U. 1990a. Localization and responses of neurones in the parieto-insular vestibular cortex of awake monkeys (Macaca fascicularis). J Physiol 430:537-557.

Grusser OJ, Pause M, Schreiter U. 1990b. Vestibular neurones in the parieto-insular cortex of monkeys (Macaca fascicularis): visual and neck receptor responses. J Physiol 430:559-583.

Guldin WO, Akbarian S, Grusser OJ. 1992. Cortico-cortical connections and cytoarchitectonics of the primate vestibular cortex: a study in squirrel monkeys (Saimiri sciureus). J Comp Neurol 326(3):375-401.

Hackett T. 2003. The Comparative Anatomy of the Primate Auditory Cortex (p199-226). In: Ghazanfar A, editor. Primate Audition: Behavior and Neurobiology. Boca Raton: CRC Press.

Hackett, T. A., & Kaas, J. H. (2003). Auditory processing in the primate brain. In M. Gallagher, R. J. Nelson (Eds), Comprehensive handbook of psychology, vol 3, biological psychology. New York: Wiley.

Hackett TA, Karmos G, Schroeder CE, Ulbert I, Sterbing-D'Angelo SJ, D'Angelo WR, Kajikawa Y, Blumell S, de la Mothe L. 2005. Neurosurgical access to cortical areas in the lateral fissure of primates. J Neurosci Methods 141(1):103-113.

Hackett TA, Preuss TM, Kaas JH. 2001. Architectonic identification of the core region in auditory cortex of macaques, chimpanzees, and humans. J Comp Neurol 441(3):197-222.

Hackett TA, de la Mothe LA, Ulbert I, Karmos G, Smiley J, Schroeder CE. 2007b. Multisensory convergence in auditory cortex, II. Thalamocortical connections of the caudal superior temporal plane, J Comp Neurol 502: 924-952.

Hackett TA, Smiley JF, Ulbert I, Karmos G, Lakatos P, de la Mothe LA, Schroeder CE. 2007b. Sources of somatosensory input to the caudal belt areas of auditory cortex, Perception 36:1419-1430.

Hackett TA, Stepniewska I, Kaas JH. 1998a. Subdivisions of auditory cortex and ipsilateral cortical connections of the parabelt auditory cortex in macaque monkeys. J Comp Neurol 394(4):475-495.

Hackett TA, Stepniewska I, Kaas JH. 1998b. Thalamocortical connections of the parabelt auditory cortex in macaque monkeys. J Comp Neurol 400(2):271-286.

Hackett TA, Stepniewska I, Kaas JH. 1999. Prefrontal connections of the parabelt auditory cortex in macaque monkeys. Brain Res 817(1-2):45-58.

Hafting T, Fyhn M, Molden S, Moser M, Moser E. 2005. Microstructure of a spatial map in the entorhinal cortex. Nature 436:801-806.

Hashikawa T, Molinari M, Rausell E, Jones EG. 1995. Patchy and laminar terminations of medial geniculate axons in monkey auditory cortex. J Comp Neurol 362(2):195-208.

Hashikawa T, Rausell E, Molinari M, Jones EG. 1991. Parvalbumin- and calbindin-containing neurons in the monkey medial geniculate complex: differential distribution and cortical layer specific projections. Brain Res 544(2):335-341.

Henkel, C.K., Spangler, K.M. (1983) Organization of the efferent projections of the medial superior olivary nucleus in the cat as revealed by HRP and autoradiographic tracing methods. *Journal of Comparative Neurology*, 221, 416-428.

Henkel, C.K., Brunso-Bechtold, J.K. (1993) Laterality of superior olivary projections to the inferior colliculus in adult and developing ferret. *Journal of Comparative Neurology*, 331, 458-468.

Herzog AG, Van Hoesen GW. 1976. Temporal neocortical afferent connections to the amygdala in the rhesus monkey. Brain Res 115:57-69.

Hopf P. 1954. Die myeloarchitektonic des isocortex temporalis beim menschen. J Hirnforsch 1:208-279.

Imig TJ, Morel A. 1984. Topographic and cytoarchitectonic organization of thalamic neurons related to their targets in low-, middle-, and high-frequency representations in cat auditory cortex. J Comp Neurol 227(4):511-539.

Imig TJ, Morel A. 1985a. Tonotopic organization in lateral part of posterior group of thalamic nuclei in the cat. J Neurophysiol 53(3):836-851.

Imig TJ, Morel A. 1985b. Tonotopic organization in ventral nucleus of medial geniculate body in the cat. J Neurophysiol 53(1):309-340.

Imig TJ, Reale RA. 1980. Patterns of cortico-cortical connections related to tonotopic maps in cat auditory cortex. J Comp Neurol 192(2):293-332.

Imig TJ, Ruggero MA, Kitzes LM, Javel E, Brugge JF. 1977. Organization of auditory cortex in the owl monkey (Aotus trivirgatus). J Comp Neurol 171(1):111-128.

Insausti R, Amaral DG, Cowan WM. 1987. The entorhinal cortex of the monkey: II. Cortical afferents. J Comp Neurol 264(3):356-395.

Jones EG. 1997. The relay function of the thalamus during brain activation. In: Steriade M, Jones E, McCormick D, editors. Thalamus. New York: Elsevier. p 393-531.

Jones EG. 2003. Chemically defined parallel pathways in the monkey auditory system. Ann N Y Acad Sci 999:218-233.

Jones EG, Burton H. 1976. Areal differences in the laminar distribution of thalamic afferents in cortical fields of the insular, parietal and temporal regions of primates. J Comp Neurol 168(2):197-247.

Jones EG, Dell'Anna ME, Molinari M, Rausell E, Hashikawa T. 1995. Subdivisions of macaque monkey auditory cortex revealed by calcium-binding protein immunoreactivity. J Comp Neurol 362(2):153-170.

Jones EG, Powell TP. 1969. Connexions of the somatic sensory cortex of the rhesus monkey. I. Ipsilateral cortical connexions. Brain 92(3):477-502.

Kaas JH, Hackett TA. 1998. Subdivisions of auditory cortex and levels of processing in primates. Audiol Neurootol 3(2-3):73-85.

Kaas JH, Hackett TA. 2000. Subdivisions of auditory cortex and processing streams in primates. Proc Natl Acad Sci U S A 97(22):11793-11799.

Kajikawa Y, de la Mothe LA, Blumell S, Hackett TA. 2005. A comparison of neuron response properties in areas A1 and CM of the marmoset monkey auditory cortex: tones and broad band noise. J Neurophysiol 93:22 - 34.

Kajikawa Y, Hackett TA. 2005. Entropy analysis of neuronal spike train synchrony. J Neurosci Methods 149:90-93.

Kajikawa Y, de la Mothe LA, Blumell S, Sterbing-D'angelo S, D'Angelo W, Camalier C, Hackett T A. 2008. Coding of FM sweep trains and twitter calls in area CM of marmoset auditory cortex. Hearing Research 239(1-2):107-125.

Kayser C, Petkov CI, Augath M, Logothetis NK. 2005. Integration of touch and sound in auditory cortex, Neuron 48:373-384.

Knight PL. 1977. Representation of the cochlea within the anterior auditory field (AAF) of the cat. Brain Res 130(3):447-467.

Kosaki H, Hashikawa T, He J, Jones EG. 1997. Tonotopic organization of auditory cortical fields delineated by parvalbumin immunoreactivity in macaque monkeys. J Comp Neurol 386(2):304-316.

Kosmal A, Malinowska M, Kowalska DM. 1997. Thalamic and amygdaloid connections of the auditory association cortex of the superior temporal gyrus in rhesus monkey (Macaca mulatta). Acta Neurobiol Exp (Wars) 57(3):165-188.

Kowalski N, Versnel H, Shamma SA. 1995. Comparison of responses in the anterior and primary auditory fields of the ferret cortex. J Neurophysiol 73(4):1513-1523.

Krubitzer L, Clarey J, Tweedale R, Elston G, Calford M. 1995. A redefinition of somatosensory areas in the lateral sulcus of macaque monkeys. J Neurosci 15(5 Pt 2):3821-3839.

Krubitzer LA, Kaas JH. 1990. The organization and connections of somatosensory cortex in marmosets. J Neurosci 10(3):952-974.

Kudo, M. (1981) Projections of the nuclei of the lateral lemniscus in the cat. An audoradiographic study. *Brain Research*, 221, 57-71.

Lakatos P, Pincze Z, Fu KG, Javitt DC, Karmos G, Schroeder CE. 2005. Timing of pure tone and noise-evoked responses in macaque auditory cortex. Neuroreport 16(9):933-937.

Lee C, Winer J. 2005. Principles Governing Auditory Cortex Connections. Cerebral Cortex 15:1804-1814.

Lee CC, Imaizumi K, Schreiner CE, Winer JA. 2004. Concurrent tonotopic processing streams in auditory cortex. Cereb Cortex 14(4):441-451.

Leinonen L. 1980. Functional properties of neurones in the parietal retroinsular cortex in awake monkey. Acta Physiol Scand 108(4):381-384.

Leinonen L, Hyvarinen J, Sovijarvi AR. 1980. Functional properties of neurons in the temporo-parietal association cortex of awake monkey. Exp Brain Res 39(2):203-215.

Lewis JW, Van Essen DC. 2000. Corticocortical connections of visual, sensorimotor, and multimodal processing areas in the parietal lobe of the macaque monkey. J Comp Neurol 428(1):112-137.

Liang L, Lu T, Wang X. 2002. Neural representations of sinusoidal amplitude and frequency modulations in the primary auditory cortex of awake primates. J Neurophysiol 87(5):2237-2261.

Linke R, Schwegler H. 2000. Convergent and complementary projections of the caudal paralaminar thalamic nuclei to rat temporal and insular cortex. Cereb Cortex 10(8):753-771.

Lippe WR, Weinberger NM. 1973. The distribution of sensory evoked activity within the medial geniculate body of the unanesthetized cat. Exp Neurol 40(2):431-444.

Love JA, Scott JW. 1969. Some response characteristics of cells of the magnocellular division of the medial geniculate body of the cat. Can J Physiol Pharmacol 47(10):881-888.

Lu T, Liang L, Wang X. 2001a. Neural representations of temporally asymmetric stimuli in the auditory cortex of awake primates. J Neurophysiol 85(6):2364-2380.

Lu T, Liang L, Wang X. 2001b. Temporal and rate representations of time-varying signals in the auditory cortex of awake primates. Nat Neurosci 4(11):1131-1138.

Lu T, Wang X. 2004. Information content of auditory cortical responses to time-varying acoustic stimuli. J Neurophysiol 91(1):301-313.

Luczak A, Hackett TA, Kajikawa Y, Laubach M. 2004. Multivariate receptive field mapping in marmoset auditory cortex. J Neurosci Methods 136(1):77-85.

Luethke LE, Krubitzer LA, Kaas JH. 1989. Connections of primary auditory cortex in the New World monkey, Saguinus. J Comp Neurol 285(4):487-513.

Merchan, M.A., Saldana, E., Plaza, I. (1994) Dorsal nucleus of the lateral lemniscus in the rat: concentric organization and tonotopic projection to the inferior colliculus. *Journal of Comparative Neurology*, 342, 259-278.

Meredith MA, Clemo HR. 1989. Auditory cortical projection from the anterior ectosylvian sulcus (Field AES) to the superior colliculus in the cat: an anatomical and electrophysiological study. J Comp Neurol 289(4):687-707.

Merzenich MM, Brugge JF. 1973. Representation of the cochlear partition of the superior temporal plane of the macaque monkey. Brain Res 50(2):275-296.

Mishkin M. 1979. Analogous neural models for tactual learning and visual learning. Neuropsychologia 17:139-151.

Mishkin M, Ungerleider LG, Macko KA. 1983. Object vision and spatial vision: two cortical pathways. Trends in Neurosci 6:414-417.

Molinari M, Dell'Anna ME, Rausell E, Leggio MG, Hashikawa T, Jones EG. 1995. Auditory thalamocortical pathways defined in monkeys by calcium-binding protein immunoreactivity. J Comp Neurol 362(2):171-194.

Morel A, Garraghty PE, Kaas JH. 1993. Tonotopic organization, architectonic fields, and connections of auditory cortex in macaque monkeys. J Comp Neurol 335(3):437-459.

Morel A, Kaas JH. 1992. Subdivisions and connections of auditory cortex in owl monkeys. J Comp Neurol 318(1):27-63.

Nagarajan SS, Cheung SW, Bedenbaugh P, Beitel RE, Schreiner CE, Merzenich MM. 2002. Representation of spectral and temporal envelope of twitter vocalizations in common marmoset primary auditory cortex. J Neurophysiol 87(4):1723-1737.

Pandya DN, Hallett M, Mukherjee SK. 1969. Intra- and interhemispheric connections of the neocortical auditory system in the rhesus monkey. Brain Res 14(1):49-65.

Pandya DN, Rosene DL. 1993. Laminar termination patterns of thalamic, callosal, and association afferents in the primary auditory area of the rhesus monkey. Exp Neurol 119(2):220-234.

Pandya DN, Rosene DL, Doolittle AM. 1994. Corticothalamic connections of auditory-related areas of the temporal lobe in the rhesus monkey. J Comp Neurol 345(3):447-471.

Pandya DN, Sanides F. 1973. Architectonic parcellation of the temporal operculum in rhesus monkey and its projection pattern. Z Anat Entwicklungsgesch 139(2):127-161.

Petkov CI, Kayser C, Augath M, Logothetis NK.2006. Functional Imaging Reveals Numerous Fields in the Monkey Auditory Cortex. Plos Biology 4(7):e215.

Pfingst BE, O'Connor TA. 1981. Characteristics of neurons in auditory cortex of monkeys performing a simple auditory task. J Neurophysiol 45(1):16-34.

Philibert B, Beitel RE, Nagarajan SS, Bonham BH, Schreiner CE, Cheung SW. 2005. Functional organization and hemispheric comparison of primary auditory cortex in the common marmoset (Callithrix jacchus). J Comp Neurol 487(4):391-406.

Phillips DP, Irvine DR. 1982. Properties of single neurons in the anterior auditory field (AAF) of cat cerebral cortex. Brain Res 248(2):237-244.

Poggio GF, Mountcastle VB. 1960. A study of the functional contributions of the lemniscal and spinothalamic systems to somatic sensibility. Central nervous mechanisms in pain. Bull Johns Hopkins Hosp 106:266-316.

Qi HX, Lyon DC, Kaas JH. 2002. Cortical and thalamic connections of the parietal ventral somatosensory area in marmoset monkeys (Callithrix jacchus). J Comp Neurol 443(2):168-182.

Raczkowski D, Diamond IT, Winer J. 1976. Organization of thalamocortical auditory system in the cat studied with horseradish peroxidase. Brain Res 101(2):345-354.

Rauschecker JP. 1998. Parallel processing in the auditory cortex of primates. Audiol Neurootol 3(2-3):86-103.

Rauschecker JP, Tian B. 2000. Mechanisms and streams for processing of "what" and "where" in auditory cortex. Proc Natl Acad Sci U S A 97(22):11800-11806.

Rauschecker JP, Tian B. 2004. Processing of band-passed noise in the lateral auditory belt cortex of the rhesus monkey. J Neurophysiol 91(6):2578-2589.

Rauschecker JP, Tian B, Hauser M. 1995. Processing of complex sounds in the macaque nonprimary auditory cortex. Science 268(5207):111-114.

Rauschecker JP, Tian B, Pons T, Mishkin M. 1997. Serial and parallel processing in rhesus monkey auditory cortex. J Comp Neurol 382(1):89-103.

Read HL, Winer JA, Schreiner CE. 2002. Functional architecture of auditory cortex. Curr Opin Neurobiol 12(4):433-440.

Reale RA, Imig TJ. 1983. Auditory cortical field projections to the basal ganglia of the cat. Neuroscience 8(1):67-86.

Recanzone GH. 2001. Spatial processing in the primate auditory cortex. Audiol Neurootol 6(4):178-181.

Recanzone GH, Guard DC, Phan ML. 2000a. Frequency and intensity response properties of single neurons in the auditory cortex of the behaving macaque monkey. J Neurophysiol 83(4):2315-2331.

Recanzone GH, Guard DC, Phan ML, Su TK. 2000b. Correlation between the activity of single auditory cortical neurons and sound-localization behavior in the macaque monkey. J Neurophysiol 83(5):2723-2739.

Recanzone GH, Schreiner CE, Sutter ML, Beitel RE, Merzenich MM. 1999. Functional organization of spectral receptive fields in the primary auditory cortex of the owl monkey. J Comp Neurol 415(4):460-481.

Robinson CJ, Burton H. 1980a. Organization of somatosensory receptive fields in cortical areas 7b, retroinsula, postauditory and granular insula of M. fascicularis. J Comp Neurol 192(1):69-92.

Robinson CJ, Burton H. 1980b. Somatic submodality distribution within the second somatosensory (SII), 7b, retroinsular, postauditory, and granular insular cortical areas of M. fascicularis. J Comp Neurol 192(1):93-108.

Robinson CJ, Burton H. 1980c. Somatotopographic organization in the second somatosensory area of M. fascicularis. J Comp Neurol 192(1):43-67.

Rockland KS, Ojima H. 2003. Multisensory convergence in calcarine visual areas in macaque monkey. Int J Psychophysiol 50(1-2):19-26.

Romanski LM, Bates JF, Goldman-Rakic PS. 1999a. Auditory belt and parabelt projections to the prefrontal cortex in the rhesus monkey. J Comp Neurol 403(2):141-157.

Romanski LM, Clugnet MC, Bordi F, LeDoux JE. 1993. Somatosensory and auditory convergence in the lateral nucleus of the amygdala. Behav Neurosci 107(3):444-450.

Romanski LM, Giguere M, Bates JF, Goldman-Rakic PS. 1997. Topographic organization of medial pulvinar connections with prefrontal cortex in the rhesus monkey. J Comp Neurol 379:313-332.

Romanski LM, LeDoux JE. 1993. Information cascade from primary auditory cortex to the amygdala: corticocortical and corticoamygdaloid projections of temporal cortex in the rat. Cereb Cortex 3(6):515-532.

Romanski LM, Tian B, Fritz J, Mishkin M, Goldman-Rakic PS, Rauschecker JP. 1999b. Dual streams of auditory afferents target multiple domains in the primate prefrontal cortex. Nat Neurosci 2(12):1131-1136.

Rouiller EM, Simm GM, Villa AE, de Ribaupierre Y, de Ribaupierre F. 1991. Auditory corticocortical interconnections in the cat: evidence for parallel and hierarchical arrangement of the auditory cortical areas. Exp Brain Res 86(3):483-505.

Sanides F, Krishnamurti A. 1967. Cytoarchitectonic subdivisions of sensorimotor and prefrontal regions and of bordering insular and limbic fields in slow loris (Nycticebus coucang coucang). J Hirnforsch 9:225-252.

Schreiner CE. 1998. Spatial distribution of reponses to simple and complex sounds in the primary auditory cortex. Audiol Neurootol 3:104-122.

Schroeder CE, Foxe JJ. 2002. The timing and laminar profile of converging inputs to multisensory areas of the macaque neocortex. Brain Res Cogn Brain Res 14(1):187-198.

Schroeder CE, Lindsley RW, Specht C, Marcovici A, Smiley JF, Javitt DC. 2001. Somatosensory input to auditory association cortex in the macaque monkey. J Neurophysiol 85(3):1322-1327.

Schwartz IR. 1992. The superior olivary complex and lateral lemniscal nuclei. In DB Webster, AN Popper, RR Fray (Eds.) The Mammalian Auditory Pathway: Neuroanatomy (pp. 66-116). New York, Springer-Verlag.

Scott BH, Malone BJ, Semple MN. 2000. Physiological delineation of primary auditory cortex in the alert rhesus macaque. 2000 Abstract Viewer/Itinerary Planner. Washington, DC: Society for Neuroscience.

Stepniewska I, Kaas JH. 1997. Architectonic subdivisions of the inferior pulvinar in New World and Old World monkeys. Vis Neurosci 14(6):1043-1060.

Stepniewska I, Ql HX, Kaas JH. 2000. Projections of the superior colliculus to subdivisions of the inferior pulvinar in New World and Old World monkeys. Vis Neurosci 17(4):529-549.

Sweet RA, Dorph-Petersen KA, Lewis DA. 2005. Mapping auditory core, lateral belt, and parabelt cortices in the human superior temporal gyrus. J Comp Neurol 491(3):270-289.

Tian B, Rauschecker JP. 1994. Processing of frequency-modulated sounds in the cat's anterior auditory field. J Neurophysiol 71(5):1959-1975.

Tian B, Rauschecker JP. 2004. Processing of frequency-modulated sounds in the lateral auditory belt cortex of the rhesus monkey. J Neurophysiol 92(5):2993-3013.

Tian B, Reser D, Durham A, Kustov A, Rauschecker JP. 2001. Functional specialization in rhesus monkey auditory cortex. Science 292(5515):290-293.

Turner BH, Mishkin M, Knapp M. 1980. Organization of the amydalopetal projections from modality-specific cortical association areas in the monkey. J Comp Neurol 191:515-543.

Ungerleider LG and Mishkin M. 1982. Two cortical visual systems. In *Analysis of Visual Behavior*, Ingle DJ, Goodale MA and Mansfield RJW eds. Cambridge, Mass: MIT Press, pp. 549-586.

Van Hoesen GW, Pandya DN. 1975. Some connections of the entorhinal (area 28) and perirhinal (area 35) cortices of the rhesus monkey. I. Temporal lobe afferents. Brain Res 95(1):1-24.

Vogt C, Vogt O. 1919. Allgemeinere Ergebnisse unserer Hirnforschung. J Psych Neurol 24:279-462.

von Economo C, Koskinas G. 1925. Die Cytoarchitectonik der Hirnrinde des erwachsenen menschen. Berlin: Julius-Springer.

Wallace MN, Kitzes LM, Jones EG. 1991. Intrinsic inter- and intralaminar connections and their relationship to the tonotopic map in cat primary auditory cortex. Exp Brain Res 86(3):527-544.

Wang X, Kadia SC. 2001. Differential representation of species-specific primate vocalizations in the auditory cortices of marmoset and cat. J Neurophysiol 86(5):2616-2620.

Wang X, Merzenich MM, Beitel R, Schreiner CE. 1995. Representation of a species-specific vocalization in the primary auditory cortex of the common marmoset: temporal and spectral characteristics. J Neurophysiol 74(6):2685-2706.

Werner-Reiss U, Kelly KA, Trause AS, Underhill AM, Groh JM. 2003. Eye position affects activity in primary auditory cortex of primates. Curr Biol 13(7):554-562.

Wepsic JG. 1966. Multimodal sensory activation of cells in the magnocellular medial geniculate nucleus. Exp Neurol 15(3):299-318.

Winer JA. 2005. Decoding the auditory corticofugal systems. Hearing Research 207(1-2):1-9.

Winer JA, Chernock ML, Larue DT, Cheung SW. 2002. Descending projections to the inferior colliculus from the posterior thalamus and the auditory cortex in rat, cat, and monkey. Hear Res 168(1-2):181-195.

Winer JA, Morest DK. 1983. The medial division of the medial geniculate body of the cat: implications for thalamic organization. J Neurosci 3(12):2629-2651.

Wong-Riley M. 1979. Changes in the visual system of monocularly sutured or enucleated cats demonstrable with cytochrome oxidase histochemistry. Brain Res 171(1):11-28.

Woods TM, Lopez SE, Long JH, Rahman JE, Recanzone GH. 2006. Effects of stimulus azimuth and intensity on the single-neuron activity in the auditory cortex of the alert macaque monkey. J Neurophys 96:3323-3337.

Yeterian EH, Pandya DN. 1998. Corticostriatal connections of the superior temporal region in rhesus monkeys. J Comp Neurol 399(3):384-402.

Yukie M. 2002. Connections between the amygdala and auditory cortical areas in the macaque monkey. Neuroscience Research 42:219-229.

Zatorre RJ, Bouffard M, Ahad P and Belin P (2002) Where is "where" in the human auditory cortex. Nat. Neurosci. 5:905-909.